Shahriar Emami

UWB Communication Systems: Conventional and 60 GHz

Principles, Design and Standards

Springer

UWB Communication Systems: Conventional and 60 GHz

Shahriar Emami

UWB Communication Systems: Conventional and 60 GHz

Principles, Design and Standards

Springer

Shahriar Emami
Samsung R&D
San Jose, CA
USA

ISBN 978-1-4614-6752-6 ISBN 978-1-4614-6753-3 (eBook)
DOI 10.1007/978-1-4614-6753-3
Springer New York Heidelberg Dordrecht London

Library of Congress Control Number: 2013932772

Printed on acid-free paper

Springer is part of Springer Science+Business Media (www.springer.com)

To my parents, our memories
and
To my brothers

Preface

Ultra wideband (UWB) technology is at least 50-years old. However, up until roughly a decade ago its use was limited to the military. FCC through its landmark ruling dated 14 February 2002 authorized the use of UWB for commercial applications on unlicensed basis. A decade of intense research and development on commercial applications of UWB followed the ruling. The end result is not only a published standard and working prototypes, but capable silicon and some other products.

Since the beginning of the new millennium, a significant amount of spectrum, around 60 GHz, has been allocated for unlicensed use around the world. The vast amount of spectrum, its unlicensed nature, propagation characteristics at 60 GHz, and a few other factors make this band ideal for developing high throughput short-ranged WPANs. The vision to support WPANs with Gigabit transmission capability at 60 GHz has led to publication of five standards and working chipsets. Above and beyond that, the first wave of 60 GHz products is on the store shelves. A snapshot of the two technologies is provided below.

Technology	UWB	60 GHz UWB
Standard	WiMedia	IEEE 802.15.3c IEEE 802.11ad ECMA 387 WirlessHD WiGig
MAC	IEEE 802.15.3 MAC WiMedia MAC	IEEE 802.15.3c MAC ECMA 387 MAC
Modulation	MB-OFDM	SC (GMSK, DAMI, BPSK, QPSK, 8-PSK, 16-QAM, 64-QAM) OFDM
Coding	Convolutional coding	RS Convolutional coding LDPC
Bandwidth	3×528 MHz	2 GHz
Data Rate	480 Mbps	7 Gbps
Range	10 m	10 m
Band Allocation	Unlicensed	Unlicensed
Environment	Indoor	Indoor

UWB and 60 GHz technology have a great deal in common. Both are unlicensed WPAN technologies used for high throughput indoor communications.[1] Consequently their band allocation type, application domain, operating environment, ranges, and data rates are roughly the same. The similarities do not end there. 60 GHz technology can be viewed as UWB as well, because its respective bandwidth is greater than 500 MHz.[2] In fact, we will refer to 60 GHz technology as 60 GHz UWB (in contrast to the conventional UWB). In conclusion, UWB and 60 GHz UWB are two very similar technologies applied to the same application domain. It is most appropriate to introduce, compare, and contrast them side-by-side in a single text.

To that end this book is divided into nine chapters.

Chapter 1 introduces UWB concepts and technology. A short history is provided first. Then the regulatory authorization process and the details of the FCC First Report and Order are described. The applications of UWB technology, emission masks, and restrictions on its usage are detailed. The differences between regulations in the US and other countries are discussed. Lastly, properties and characteristics of UWB signal are described and the sweet spots for UWB technology are identified.

UWB channel models are described in Chap. 2. Initially, channel sounding techniques are introduced. Then components of IEEE 802.15.3 channel model, an enhanced version of IEEE 802.15.3 channel model and IEEE 802.15.4a channel models are detailed. The shortcomings of models are identified and their differences are pointed out.

Chapter 3 focuses on impulse radio (IR). A working definition is provided and transceiver block diagram is illustrated. Various pulse shaping techniques as well as a pulse shape custom tailoring technique are presented. Modulation schemes are described, their performances are compared, and time hopping multiple access scheme is elaborated.

Advanced techniques for power spectral density and modulation schemes are the topic of Chap. 4. PSDs of IR modulation schemes are examined and various ways to mitigate PSDs are presented. Techniques to deal with multipath such as rake receiver and T-R scheme are introduced. Then dual format modulation (DFM) is justified and its performance is evaluated. Finally, IEEE 802.15.4a standard is described in detail.

Chapter 5 presents a couple of alternative UWB modulation schemes. Multi-band OFBM (MB-OFDM) and direct sequence UWB (DS-UWB) are defined and their transmitter architectures are shown. The modulation, coding, scrambling, and spreading operations are illustrated. Then other specific issues related to each modulation scheme such as time frequency codes for MB-OFDM and M-BOK codes for DS-UWB are discussed in detail.

---

[1] UWB can be used in low data rate applications with longer ranges as well.

[2] As per FCC First Report and Order a signal is considered UWB if either the signal bandwidth is larger than 500 MHz or its fractional bandwidth is 0.2 or larger.

Selected UWB topics including MAC, ranging, chipsets, test equipment, and products are the subject of Chap. 6. Medium access control of IEEE 802.15.3, IEEE 802.15.4a and WiMedia as well as their operations are described. A fundamental lower bound for ranging known as Cramer-Rao lower bound (CRLB) is introduced and is used to compare the performance of UWB with that of narrowband systems. Then time of arrival ranging scheme and its variations are detailed and compared. Following a description of UWB chipset evolution examples of available chipsets are presented. Finally, evaluation kits, reference design kits, and existing test equipment are described and the UWB products in the market are listed.

Chapter 7 is dedicated to introducing 60 GHz communications. A working definition for 60 GHz band is established, the 60 GHz regulations in various countries are described, and their differences are highlighted. Characteristics and properties of this band are discussed and listed, hence pointing to the class of applications that could take advantage of this technology. Capacity analysis and link budget study are conducted to reveal the technology potentials. Directional antenna feature of 60 GHz UWB and antenna training procedure are elaborated. MAC attributes and unequal error protection feature are discussed and their benefits are highlighted. At the end, landscape for chipset process technology is drawn, existing and potential developers are identified, and first wave of 60 GHz technology products are listed.

The objective of Chap. 8 is to introduce the existing/upcoming IEEE 60 GHz UWB standards. Operational modes of IEEE 802.15.3c, IEEE 802.11ad are explored; their supported data rates and their applications are highlighted. Various transmitter components such as modulation, coding, scrambler, spreading, and interleaving are detailed. Band plan and emission mask applicable to each standard are described as well.

Chapter 9 introduces and reviews the remaining 60 GHz standards such as ECMA 387, WirelessHD and WiGig. Initially, the transmitter block diagrams for ECMA 387 are presented. Then the various transmitter components such as modulation, coding, scrambler, spreading, and interleaving are detailed. Band plan and emission mask are described as well. Finally, industry alliance standards, WirelessHD, and WiGig are introduced and their unique features are described.

The material presented in this book can be used to offer any of the following graduate-level courses.

- UWB Communications.
- WPAN High Data Rate Standards.
- Conventional and 60 GHz UWB.

The text can also be used to offer an undergraduate senior-level course on UWB communications. Practicing engineers and technical managers can benefit from this text as well. It can also serve as a technical reference on the subject. The suggested chapters in the order of presentation for each course are listed below.

Introduction to UWB	Chapters 1, 3–6
WPAN Standards (graduate level)	Chapters 1–5, 8 and 9
UWB (graduate level)	Chapters 1 through 6
Conventional and 60 GHz UWB (graduate level)	Chapters 1 through 9
Short/long course Industry Course	Chapters 1, 3, 5, 8 and 9

Problems and simulation projects are placed at the end of the chapters to master the material. While problems would be more helpful to undergraduate students, simulation projects are geared towards graduate studies.

I am hopeful that this text would be beneficial to students, engineers, and interested parties in understanding, designing, implementing, and/or researching various UWB systems.

Shahriar Emami

Contents

Abbreviations and Acronyms

AAS	Asymmetric antenna system
ADC	Analog-to-digital converter
AGC	Automatic gain control
AOA	Angle of arrival
ASIC	Application specific integrated circuit
ASK	Amplitude shift keying
AV	Audio visual
AWG	Arbitrary waveform generator
AWGN	Additive white Gaussian noise
BAN	Body-area network
Blk-ACK	Block acknowledgement
Blk-NAK	Block negative acknowledgement
BOK	Bi-orthogonal keying
BOM	Bill of materials
BPM	Bi-phase modulation
BPM	Burst position modulation
BPSK	Binary phase shift keying
CAP	Contention access period
CC	Convolutional code
CFP	Contention free period
CIR	Channel impulse response
CLT	Central limit theorem
CMOS	Complementary metal oxide semiconductor
CMS	Common mode signaling
CP	Cyclic prefix
CRLB	Cramer-Rao lower bound
CSMA/CA	Carrier sensing multiple access/carrier avoidance
CTA	Channel time allocation
CTAP	Channel time access period
CES	Channel estimation sequence
DAA	Detect and avoid
dBi	dB over isotropic
DAMI	Dual alternate mark inversion

DARPA	Defense Advanced Research Project Agency
DBPSK	Differential BPSK
DCM	Dual carrier modulation
DEV	Device
DHS	Double helical scan
DMF	Dual format modulation
DPO	Digital phosphor oscilloscope
DQPSK	Differential QPSK
DRP	Distributed reservation protocol
DSA	Dynamic spectrum access
DSO	Digital sampling scope
DSP	Digital signal processing
DS-UWB	Direct sequence-UWB
DTCP	Digital transmission content protection
EBK	Evaluation board kit
ECMA	European Computer Manufacturers Association
EEP	Equal error protection
EGC	Equal gain combining
EIRP	Equivalent isotropic radiated power
EVK	Evaluation kit
FCC	Federal Communications Commission
FEC	Forward error correction
FFD	Full function devices
FFT	Fast Fourier transform
FOE	Frequency offset estimation
GaAs	Gallium arsenide
Gbps	Giga bits per second
GMSK	Gaussian minimum shift keying
GPS	Global positioning system
GPR	Ground penetration radar
GTS	Guaranteed time slot
GUI	Graphical user interface
HD	High definition
HDMI	High definition media interface
HEX	Hexadecimal
HRP	High-rate PHY
HSI	High-speed interface
IC	Integrated circuit
IEEE	Institute of Electrical and Electronics Engineers
IFFT	Inverse FFT
InP	Indium phosphide
IR	Impulse radio
ISO	International Standards Organization
LDPC	Low density parity check code
LFSR	Linear feedback shift register

LNA	Low noise amplifier
LOS	Line of sight
LRP	Low-rate PHY
LS	Least squares
LSB	Least significant bit
MAC	Medium access control
MB-OFDM	Multi band-OFDM
M-BOK	M-ary BOK
MCTA	Management CTA
MMSE	Minimum mean square error
mmW	Millimeter wave
MPSK	M-ary phase shift keying
MQAM	M-ary QAM
MRC	Maximal ratio combining
MSB	Most significant bit
MSK	Minimum shift keying
MUX	Multiplex
NLOS	None line of sight
NPRM	Notice of proposed rule making
NOI	Notice of inquiry
NTIA	National Telecommunication Information Agency
OFDM	Orthogonal frequency division multiplexing
OOK	On-off keying
OWR	One way ranging
OWR-TOA	One way ranging time of arrival
TWR-TOA	Two-way ranging time of arrival
PAM	Pulse amplitude modulation
PAN	Personal area network
PAPR	Peak-to-average power ratio
PCA	Prioritized channel access
PCI	Peripheral component interconnect
PDP	Power delay profile
PG	Processing gain
PHY	Physical layer
PN	Psuedo noise
PNC	Piconet controller
PPM	Pulse position modulation
PRF	Pulse repetition frequency
PSD	Power spectral density
PSM	Pulse shape modulation
PSNR	Peak signal-to-noise ratio
QAM	Quadrature amplitude modulation
QOS	Quality of service
QPSK	Quadrature phase shift keying
RDK	Reference design kit

RFIC	Radio frequency integrated circuit
RFD	Reduced function device
RLS	Recursive least squares
RRC	Root raised cosine
RS	Reed-Solomon
SAS	Symmetric antenna system
SC	Single carrier
SCBT	Single carrier block transmission
SDS-TWR	Symmetric double sided-TWR
SFD	Start frame delimiter
SIFS	Short interframe space
SiGe	Silicon germanium
SNR	Signal-to-noise ratio
SQPSK	Spread QPSK
SS	Spread spectrum
Sync	Synchronization
TCM	Trellis coded modulation
TDMA	Time domain multiple access
TDOA	Time difference of arrival
TFC	Time frequency code
TH	Time hopping
TOA	Time of arrival
TR-IR	Transmitter reference IR
TWR	Two way ranging
TWR-TOA	Two-way ranging time of arrival
UEP	Unequal error protection
UNII	Unlicensed national information infrastructure
UWB	Ultra wideband
VNA	Vector network analyzer
VQM	Video quality metric
WiMAX	Worldwide interoperability for microwave access
WirelessHD	Wireless high definition consortium
WiGig	Wireless gigabit alliance
WLAN	Wireless local area network
WPAN	Wireless personal area network
ZF	Zero forcing

Chapter 1
UWB Preliminaries

The chapter starts with the definitions for ultra wideband (UWB). A short history of the technology is presented and pioneers of the field are introduced. We then turn to UWB regulatory history and discuss Federal Communications Commission (FCC) first report and order. The dynamic spectrum access (DSA) is introduced and UWB is viewed as a way to implement DSA. Main attributes of UWB systems including transmit power, transmission capacity, link budget, resilience to multi-path fading, and extremely large spreading factor are elaborated in the following sections. The chapter concludes with a discussion of the sweet spots for the UWB technology.

1.1 UWB Definition

Between 1950 and 1990 a number of unconventional communication systems were introduced. They were referred to as carrier-less radios, impulse radio (IR), non-sinusoidal transceivers, or baseband modulation. In addition to having no carrier frequency, these unconventional systems had extremely large bandwidths. The efforts to find commonalities between these systems have led to two definitions.

The first definition was provided by the Defense Advanced Research Project Agency (DARPA[1]). In 1989, a study panel from DARPA defined a new term, known as UWB [1]. As per DAPPA definition, signals with a fractional bandwidth B_f equal to or larger than 0.25 are classified as UWB signals. Fractional bandwidth is the ratio of 3 dB signal bandwidth to center frequency [2], or

$$B_f = \text{Bandwidth}\,(3\,\text{dB})/\text{Center frequency}.$$

In February 2002, FCC in its First Report and order updated UWB signal definition [3]. A signal is considered UWB if either the -10 dB bandwidth of the signal is larger than 500 MHz or its fractional bandwidth is at least 0.2. The fractional bandwidth was defined as

[1] DARPA was established in 1958. Since then it has funded the development of many vital technologies such as GPS and the Internet.

S. Emami, *UWB Communication Systems: Conventional and 60 GHz*,
DOI: 10.1007/978-1-4614-6753-3_1,

$$B_f = \text{Bandwidth (10 dB)/center frequency} = 2(f_H - f_L)/(f_H + f_L)$$

where f_L and f_H are the lower and upper 10 dB frequencies of the power spectrum relative to the PSD peak.

These definitions brought the unconventional communication systems under one UWB umbrella. The FCC definition, in fact, encompasses a number of other signals. As such, since its introduction a number of other UWB signals and modulation types have been reported in the literature. References [1, 4] provide excellent reviews of the UWB technology, as well as its history.

Now let us examine the power spectrum of two signals A and B shown in Fig. 1.1. The lower and upper 3 dB frequencies of signal A shown in Fig. 1.1a are $f_L = 0.471$ GHz and $f_H = 1.600$ GHz, respectively. Signal bandwidth and the center frequency are

$$\text{Bandwidth} = 1.6 - 0.471 = 1.129\,\text{GHz}$$

and

$$\text{Center frequency} = \frac{(f_L + f_H)}{2} = 1.0355\,\text{GHz}.$$

Fractional bandwidth becomes $B_f = 1.129\text{e}9/1.0355\text{e}9 = 1.0903$. Signal A is considered a UWB signal per DARPA definition.

The fractional bandwidth of signal A as per FCC definition is

$$B_f = 2(2.16\text{e}9 - 0.19\text{e}9)/(2.16\text{e}9 + 0.19\text{e}9) = 1.6766\,\text{GHz}$$

since $f_L = 0.19$ GHz and $f_H = 2.16$ GHz, respectively. Both definitions classify signal A as a UWB signal.

Now let us compute the fractional bandwidth for signal B. The lower and upper 3 dB frequencies of signal B is shown in Fig. 1.1b are $f_L = 6.67$ GHz and $f_H = 7.60$ GHz, respectively. Signal bandwidth, center frequency, and fractional bandwidth are

$$\text{Bandwidth} = 7.6 - 6.67 = 0.93\,\text{GHz},$$

$$\text{Center frequency} = \frac{(f_L + f_H)}{2} = 7.135\,\text{GHz}$$

and

$$B_f = 0.93\text{e}9/7.135\text{e}9 = 0.1303\,\text{GHz}.$$

As per DARPA definition, signal B is not a UWB signal as its fractional bandwidth is below 0.25.

The fractional bandwidth of signal B as per FCC definition is

$$B_f = 2(8.16\text{e}9 - 6.19\text{e}9)/(8.16\text{e}9 + 6.19\text{e}9) = 0.2746\,\text{GHz}$$

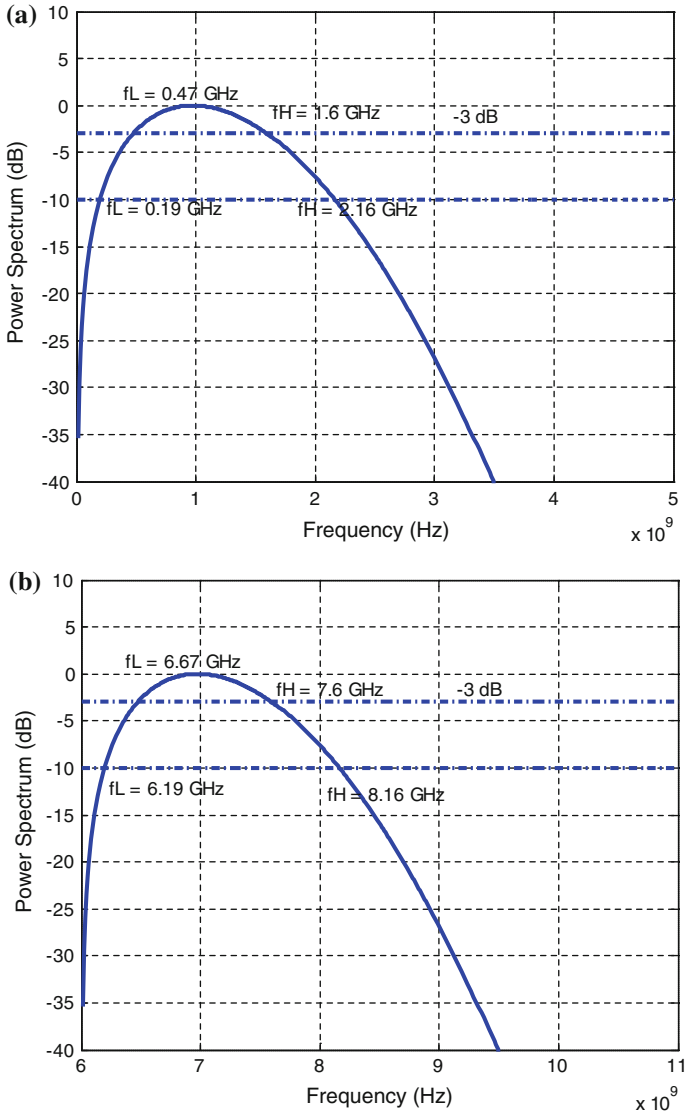

Fig. 1.1 **a** Power spectrum of signal A and **b** Power spectrum of signal B

since $f_L = 6.19$ GHz and $f_H = 8.16$ GHz, respectively. The FCC definition, contrary to DARPA definition, regards signal B as a UWB signal.

There are a couple of differences between the two definitions. First, the FCC definition of bandwidth, unlike DARPA definition, is based on -10 dB frequency points.

Second, FCC has a lower threshold for UWB fractional bandwidth (0.2 as opposed to 0.25 for DARPA). Consequently, the FCC definition is more inclusive.

1.2 UWB Technology History

The work on IR and carrier-free transmission started in the 1940s and 1950s. Radar was the primary application area [2]. Applications to data communication did not start until the late 1960s [1]. Harmuth, a faculty at Catholic University of America, worked on electromagnetic properties of nonsinusoidal signals and authored several books [5–7]. Ross conducted his dissertation research on what is considered UWB today in the early 1960s [8–9]. Throughout the 1970s and 1980s, Ross, Robins, Bennett, as well as other engineers from Sperry Research worked on applications of baseband radio technology.

By the late 1980s, patents and publications on unconventional communications had become widespread. Unconventional communication schemes were grouped together and labeled as UWB by DARPA. UWB proponents envisioned commercial applications of this technology and shared their vision with FCC. Among the applications was the potential to deliver very large amounts of information over short distances without requiring a dedicated band. The interactions with FCC continued in the 1990s and finally led to legalization of UWB for commercial applications in 2002 [4].

1.3 UWB Pioneers

Over the past 60 years a number of engineers and researchers have worked on what we know as UWB technology today. Their work resulted in many articles and patents. The first books on UWB were written by Harmuth, a faculty at Catholic University of America. The first dissertation on UWB and an instrumental patent on UWB belong to Ross [10]. Among the UWB researchers Harmuth, Ross, Robbins, Van Etten, and Morey are the true pioneers [1].

1.4 UWB Regulatory History

The vision behind legalization of UWB was to allocate a frequency range to unlicensed UWB devices on nonexclusive basis in which their radiation level would be on par with unintentional radiators (limited to −41.3 dBm/MHz). In 1998, the FCC motivated by the enthusiasm and work of UWB proponents issued a notice of inquiry (NOI) [11]. It was basically an inquiry from interested parties to voice their opinion, whether or not they were in favor of legalizing UWB.

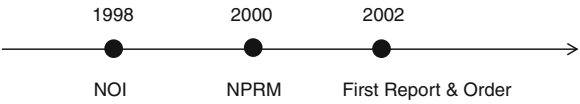

Fig. 1.2 The sequence of events that led to legalization of UWB in the US

About 1,000 submissions, some in favor and others against UWB, were made to FCC. They consisted of reports, studies, recommendations, and some prototypes. Together with NTIA,[2] FCC examined the evidence and weighted the benefits of legalizing UWB against the interference potential of UWB to the existing radio services. A primary concern was the interference potential to GPS, as the GPS signal is weak. In 2000, FCC signaled the beginning of UWB era with the release of Notice of Proposed Rule Making (NPRM). Eventually, on February 14, 2002, UWB was made legal in the US. The restrictions associated with the use of UWB are spelled out in the First Report and Order. The sequence of events is shown in Fig. 1.2

1.5 FCC First Report and Order [3]

As per First Report and Order UWB devices would have to operate in-between 3.1 and 10.6 GHz with a PSD limited to −41.3 dBm/MHz.[3] For communication application, an indoor and an outdoor emission mask are provided (Fig. 1.3a–b). Only handheld UWB devices can operate outdoors. In both cases, much smaller radiation is required in GPS band. Sufficient protection for cellular, PCS, and satellite TV services has also been provided. The outdoor mask is somewhat more stringent[4] in regard to protecting these services.

In addition to data communications, the first report and order also authorized the use of UWB for other applications such as imaging devices and vehicular radars. Some of these applications are for civilian and commercial while others are for military purposes. Similar to the data communications case, a radiation mask is specified for each application (Fig. 1.3c–d).

---

[2] In US, FCC regulates the use of air waves for nongovernment users. On the other hand, National Telecommunication Information Agency (NTIA) is in charge of spectral issues for federal government entities.

[3] As per FCC Part 47 Sect. 15, the radiated emissions from an intentional radiator operating above 960 MHz must be limited to electric field strength of 500 μV/m at 3 m away from the radiator in every 1 MHz. The radiated power is given by

$$P = E_o^2 \, 4\pi R^2 / \eta$$

where E_o, R and η denote the electric field, the radius of the sphere at which field strength is measured and characteristic impedance of vacuum ($\sim 377\ \Omega$), respectively. Upon substitution into the radiated power equation, we end up with an emitted power of roughly 75 nW or $10\log(75e{-}9/0.001) = -41.3$ dBm/MHz.

[4] An additional 10 dB compared to the indoor mask.

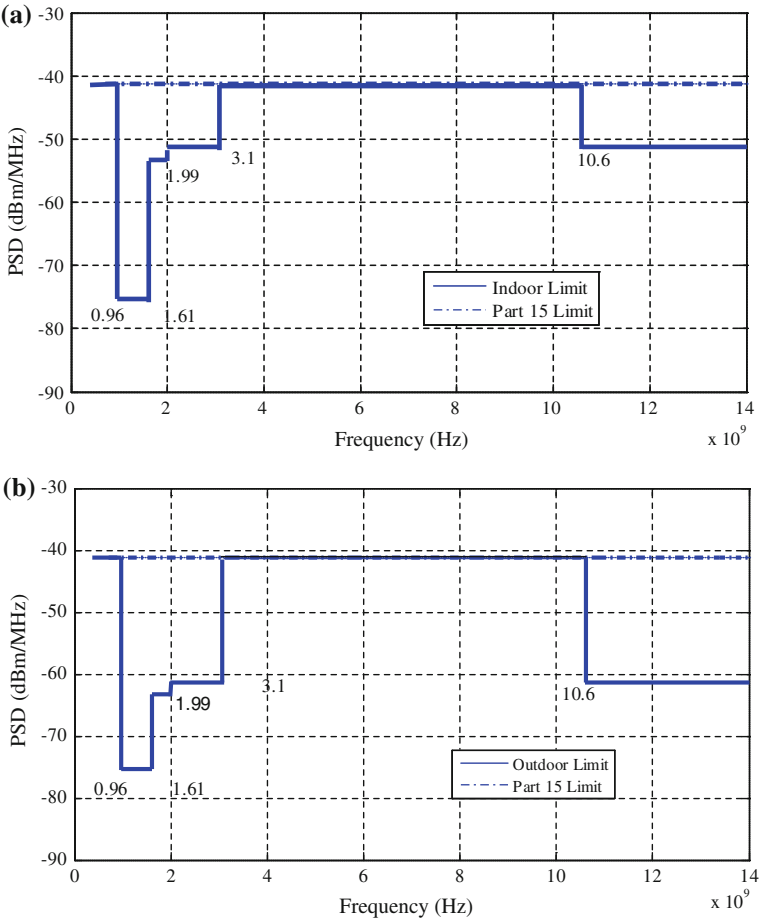

Fig. 1.3 FCC UWB masks: **a** indoor; **b** outdoor; **c** imaging; and **d** vehicular

Automotive or vehicular radars monitor the space in the vicinity of an automobile. They can be used to either provide feedback to the driver or activate brakes, if collision is unavoidable. In addition to collision avoidance, it can be used for cruise control, airbag activation, and roadside assistance. Note that unlike other UWB systems, automotive radar systems operate in 22–29 GHz range.

UWB imaging systems can be divided into ground penetration radars (GPR), wall imaging, through-wall imaging, and medical imaging. The emission limits for these imaging systems are listed in Table 1.1. The goal of GPR is to search for and locate the objects underneath the ground. The objects inside or behind a wall are revealed in wall imaging. The GPR and wall imaging usage is limited to public safety, research community, and commercial mining. Through-wall imaging, as the name implies, allows one to examine the adjacent rooms to look for people or objects of interest. Its usage is licensed and is limited to law enforcement,

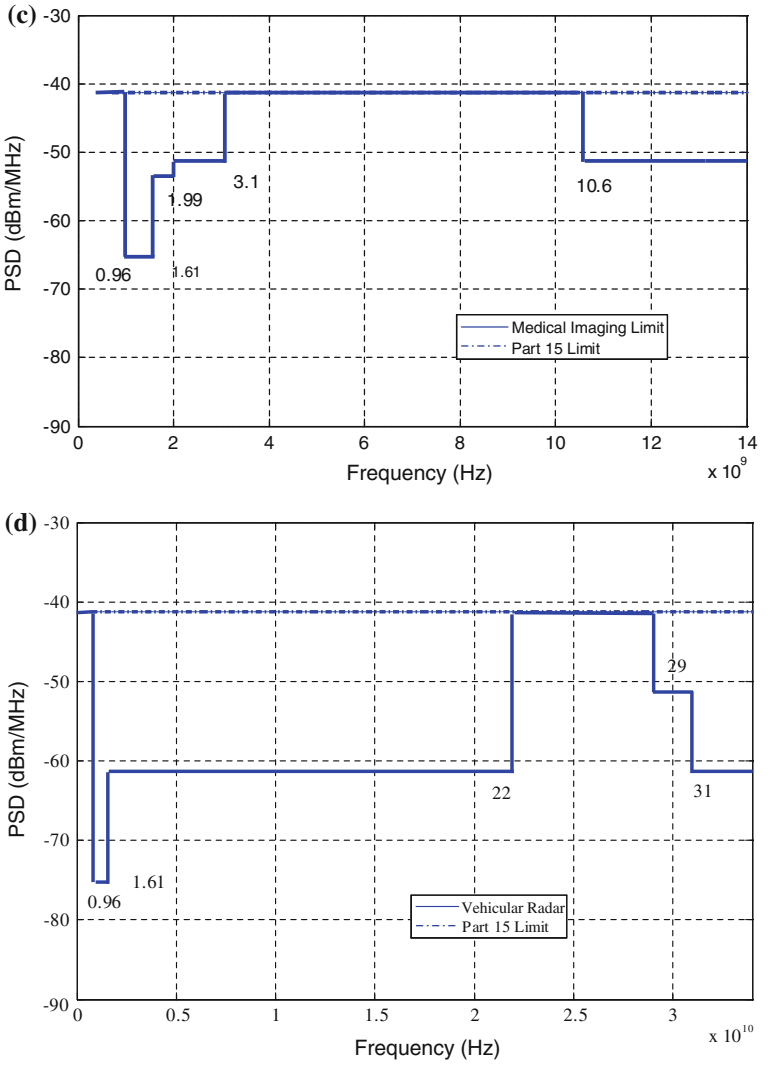

Fig. 1.3 continued

emergency rescue, and fire fighters. A related application is surveillance in which an RF perimeter is monitored. The technology must operate in 1.9–10.6 GHz range and its use is limited to public safety, emergency rescue organizations, manufacturing, and petroleum licensed users. Imaging systems must operate between 3.1 and 10.6 GHz. This technology requires a license and can only be used by healthcare practitioners.

Table 1.1 Emission limits (dBm) for various UWB applications

Frequency range (MHz)	960–1,610	1,610–1,990	1,990–3,100	3,100–10,600	Above 10,600	1,164–1,240[a] 1,559–1,610[a]
GPR	−65.3	−53.3	−51.3	−41.3	−51.3	−75.3
Through-wall imaging (below 960 MHz)	−65.3	−53.3	−51.3	−51.3	−51.3	−75.3
Through-wall imaging (1.99–10.6 GHz range)	−46.3	−41.3	−41.3	−41.3	−51.3	−56.3
Surveillance systems	−53.3	−51.3	−41.3	−41.3	−51.3	−63.3

[a] These emissions are to be measured with a resolution bandwidth of no less than 1 kHz while all others are to be measured with a resolution bandwidth of 1 MHz

1.6 Dynamic Spectrum Access

In conventional spectrum allocation regime, the spectrum is allocated exclusively to a certain service. Others have to stay away from the allocated spectrum. Studies have shown that the conventional allocation scheme leads to congestion and inefficient use of spectrum. It is desirable to bring in secondary users to utilize the unused spectrum. DSA offers schemes that improve the efficiency of spectrum usage through accommodation of secondary users.

DSA can be divided into three access models. Among them the hierarchical access model is most compatible with the wireless systems of today's and FCC's vision. The concept behind hierarchical access model is to share the licensed bands with the secondary users, while limiting the interference to primary users. The hierarchical access consists of two spectrum sharing approaches namely spectrum overlay and spectrum underlay. In spectrum overlay[5] there are two types of users known as primary and secondary users. Primary users have priority over the secondary users in terms of spectrum access. Secondary users can only use the spectrum when primary users are absent. As soon as a primary is detected, secondary has to leave the band within a short time. In underlay scheme, the secondary user transmits at all times but it has a very low emission profile. Because of the low emission profile, the impact of the secondary on primary's performance is negligible. In conclusion, in spectrum overlay only the unused spectral regions are targeted while spectrum underlay takes advantage of underused regions.

1.7 UWB Regulations in Other Countries

UWB spectrum covers a large swath of frequencies that have been home to a number of different wireless systems and services. They include services such as WiMAX, 3G/4G, satellite communications, various types of radars, and radiolocation. The incumbent users of spectrum feel somewhat uneasy about sharing their resources with UWB for a couple of reasons. First, they are accustomed to traditional paradigms of exclusive spectrum assignment. Second, spectrum sharing based on primary/secondary assignment (or spectrum overlay/underlay) is somewhat of uncharted territory.

In the United States, the First Report and order FCC allocated the spectrum from 3.1 to 10.6 GHz for UWB communications. FCC feels that provisions in the First Report and Order provide adequate protection for the existing services. Above and beyond that, the regulations will be revisited if any unforeseen issues arise.

Regulators around the world have had more conservative views with respect to UWB and spectrum overlay/underlay. European and far-eastern regulators have proposed a couple of protection mechanisms for incumbent users of spectrum.

[5] Also known as opportunistic spectrum access.

Detect and avoid (DAA) is the primary protection mechanism. It essentially means that upon detection of a primary user, the secondary user would need to either leave the band or lower its emission level to a predetermined amount. The other mechanism is low duty cycle (LDC). To qualify as an LDC device (a) the transmission time within each second would have to be upper bounded by 5 %, (b) the transmission time within each hour has to be less than 0.5 %, and (c) duration of each transmission would have to be limited to 5 ms. In what follows, we review the UWB regulatory status in Europe, Japan, Korea, China, and Singapore at the time of this writing [12, 13]. Changes and updates to the regional rules are quite likely.

Japan—UWB devices in Japan can only operate indoors in the following range:

$$\text{UWB Spectrum}_{\text{Japan}} = [(3.4 - 4.8)U(7.25 - 10.25)]\,\text{GHz}.$$

For operation in the low band, namely 3.4–4.8 GHz, DAA functionality is a requirement. The requirement can be waived, if the emission level is lowered from the usual -41.3 to -70 dBm/MHz. Unlike in the US, Japanese law requires conducted emission tests as opposed to radiated testing. Operation in the high band, namely 7.25–10.25 GHz, requires the emission limit of -41.3 dBm/MHz and no DAA. In Japan, UWB devices are required to have a minimum data rate of 50 Mbps.

Korea—Korean allocated UWB spectrum is defined as

$$\text{UWB Spectrum}_{\text{Korea}} = [(3.1 - 4.8)U(7.2 - 10.2)]\,\text{GHz}.$$

DAA capability or LDC is only a requirement while UWB devices operate in 3.1–4.8 GHz band. Similar to Japanese regulations, with the emission limit of -70 dBm/MHz, the DAA requirement can be waived. UWB devices operating in the high band, namely 7.2–10.2 GHz, require the emission limit of -41.3 dBm/MHz. UWB devices in Korea can only operate indoors.

China—Chinese allocated UWB spectrum consists of union of a low band, 4.2–4.8 GHz, and a high band or 6–9 GHz. In other words,

$$\text{UWB Spectrum}_{\text{China}} = [(4.2 - 4.8)U(6 - 9)]\,\text{GHz}.$$

The lower portion of UWB band is for indoor use only, while the upper portion of band can be utilized for both indoor and outdoor use. Only UWB devices operating in the low band are required to implement DAA. However, the DAA requirement can be waived upon lowering of emission to -70 dBm/MHz. Operation in 6–9 GHz is subject to the emission limit of -41.3 dBm/MHz. The Chinese UWB regulations are not finalized yet and are subject to change.

Europe—The allocated UWB spectrum in Europe is

$$\text{UWB Spectrum}_{\text{Europe}} = [(3.1 - 4.8)U(6 - 9)]\,\text{GHz}.$$

UWB devices operating in 3.1–4.8 GHz range and subject to emission level of -41.3 dBm/MHz should be DAA or LDC capable. The requirement can be

dropped, if the limit is lowered to −80 dBm/MHz for 3.4–3.8 GHz range and to −70 dBm/MHz for 3.1–3.4 and 3.8–4.2 GHz ranges. As we stand today, 6–8.5 GHz band is open to UWB devices with no DAA requirement and subject to the limit of −41.3 dBm/MHz. DAA or LDC is required for operation in 8.5–9 GHz range. However, if the emission level is lowered to −65 dBm/MHz DAA requirement can be dropped. A minimum utilized bandwidth of 50 MHz for UWB devices is required in Europe.

Singapore—Following a period of public consultation IDA[6] established the regulations for UWB consumer and business data communication systems. As per these regulations UWB systems operating in 3.4–4.8 GHz range must utilize a mitigation technique such as DAA. However, UWB devices can operate in 6–9 GHz band with no DAA requirement. In either case, the emissions are limited to −41.3 dBm/MHz.

1.8 Spectrum Overlay/Underlay Classification

We have so far described UWB signal, the UWB regulations in a number of countries, as well as DSA. The question before us is whether UWB can be considered as spectrum overlay or spectrum underlay. It turns out that the answer depends not only on UWB signal definition but on the frequency band of operation, PSD level and specific country/region.

The situation is clear cut in US, as UWB devices are authorized to operate simultaneously with the primary user in 3.1–10.6 GHz range, subject to emission limit of −41.3 dBm/MHz. Clearly, in the US spectrum underlay approach is applicable to UWB devices. Unfortunately, situation elsewhere is not nearly as clear. For instance in Japan as long as a UWB device stays in the upper band, it can operate simultaneously in primary user band. As such spectrum underlay is applicable. However, while operating in the lower band, PSD becomes a key parameter. If PSD stays below −70 dBm/MHz, UWB device can operate simultaneously in primary user band. This falls within spectrum underlay regime. But if −70 dBm/MHz $<PSD<$ −41.3 dBm/MHz, then we are dealing with the opportunistic access or spectrum overlay. The classification for a number of countries and a region are provided in Table 1.2A and B. In summary, regulators in Europe, Japan, Korea, and China authorize spectrum underlay subject to (1) a very low emission limit (at least −70 dBm/MHz) or (2) operation in a high frequency band (above 6 GHz).

[6] IDA stands for Infocomm Development Authority.

Table 1.2 Overlay/Underlay classification

A

Country	Lower band	Upper band
Japan	3.4–4.8 GHz: if -70 dBm/MHz $< PSD < -41.3$ dBm/MHz OVERLAY if $PSD < -70$ dBm/MHz UNDERLAY	7.25–10.25 GHz: UNDERLAY
Korea	3.1–4.8 GHz: if -70 dBm/MHz $< PSD < -41.3$ dBm/MHz OVERLAY if PSD < -70 dBm/MHz UNDERLAY	7.2–10.2 GHz: UNDERLAY
China	4.2–4.8 GHz: if -70 dBm/MHz $< PSD < -41.3$ dBm/MHz OVERLAY if $PSD < -70$ dBm/MHz UNDERLAY	6–9 GHz: UNDERLAY
Singapore	3.4–4.8 GHz: OVERLAY	6–9 GHz: UNDERLAY

B

Region	3.1–3.4 GHz	3.4–3.8 GHz	3.8–4.2 GHz	6–8.5 GHz	8.5–9 GHz
Europe	if -70 dBm/MHz $< PSD < -41.3$ dBm/MHz OVERLAY if $PSD < -70$ dBm/MHz UNDERLAY	if -80 dBm/MHz $< PSD < -41.3$ dBm/MHz OVERLAY if $PSD < -80$ dBm/MHz UNDERLAY	if -70 dBm/MHz $< PSD < -41.3$ dBm/MHz OVERLAY if $PSD < -70$ dBm/MHz UNDERLAY	UNDERLAY	if -65 dBm/MHz $< PSD < -41.3$ dBm/MHz OVERLAY if $PSD < -65$ dBm/MHz UNDERLAY

1.9 UWB Properties

1.9.1 Transmit Power

Let's consider a UWB transmitter occupying the 3.1–10.6 GHz frequency range. The total power in the band is

$$P = \mathrm{PSD}\left(\frac{\mathrm{dBm}}{\mathrm{MHz}}\right) + 10\log(\text{Bandwidth in MHz})$$

$$P = -41.25 + 10\log(7500) = -2.55\,\mathrm{dBm}\,\text{or}\,0.55\,\mathrm{mW}.$$

In practice, a UWB device will utilize only a fraction (1/3 to 1/5) of the spectrum. The total transmitted power will then be a fraction of a milli-watt (0.1–0.2 mW).

Table 1.3 PSD of some wireless systems [12]

Wireless system	Transmit power spectral density (dBm/MHz)
WCDMA	18
WLAN	[7 17]
Bluetooth 2.0	[−29.20 −15.23]
UWB	−41.25

Two UWB modulation schemes, known as multiband-OFDM (MB-OFDM)[7] and DS-UWB,[8] will be introduced in Chap. 4. Let us compare their transmit power. Multiband-OFDM utilizes slightly over 1.5 GHz of bandwidth, or 3×528 MHz to be exact [14]. The total transmit power is

$$P = -41.25 + 10\log(3 \times 528) = -9.25\,\text{dBm}.$$

DS-UWB, the other UWB technology, offers two options [15]. Low band option is 1.75 GHz wide while the high band option is 3.5 GHz wide. The power associated with the two options can be computed in the following way:

$$P = -41.25 + 10\log(1750) = -8.82\,\text{dBm} \quad \text{(low band option)}$$
$$P = -41.25 + 10\log(3500) = -5.81\,\text{dBm} \quad \text{(high band option)}.$$

Let us compare PSD level associated with UWB with that of other services such as WLAN and WCDMA. As per Table 1.3, there is roughly 60 and 50 dB differential in PSD levels between UWB and WCDMA and WLAN, respectively. Thus, the PSD associated with UWB is considerably less than that of GSM and WCDMA. The low PSD level associated with UWB in comparison with that of narrowband systems demonstrate that UWB can peacefully coexist with other narrowband systems (Fig. 1.4).

1.9.2 Capacity

Shannon-Hartley capacity theorem [16] states the relationship between the capacity, signal-to-noise ratio (SNR), and bandwidth (B).

$$C = B\log_2\left(1 + \frac{S}{N}\right)$$

Capacity can be improved by increasing the bandwidth or the SNR. As seen the relationship between capacity and bandwidth is linear, while the relationship

[7] MB-OFDM is the basis for WiMedia UWB technology as well as ECMA-368 and ISO/IEC 26907 standards.

[8] DS-UWB Physical Layer Submission to 802.15 Task Group 3a, IEEE 802.15.3a Working Group, P802.15.03/0137r0, 2004.

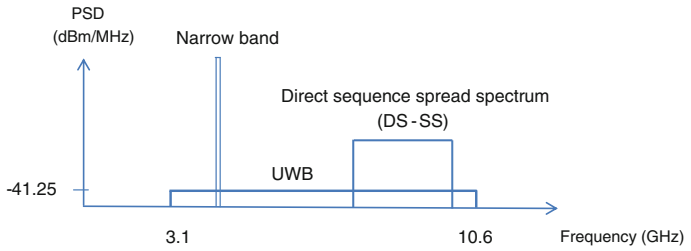

Fig. 1.4 PSD of various systems

between the capacity and SNR is logarithmic. Linear relationships grow much faster compared to the logarithmic relationships. UWB technology increases the capacity linearly through bandwidth increase.

Capacity of UWB system in terms of UWB system parameters can be computed in the following fashion. Let S and N denote the received power at the receiver and noise floor, respectively. Both signal and noise power are expressed in dB. By definition

$$\mathrm{SNR}_{\mathrm{dB}} = S - N.$$

The received signal power at the transmitter site is given as

$$S = P_T + G_T + G_R - L - I$$

where P_T, G_T, G_R, L, and I denote transmitted power, transmitter gain, receiver gain, path loss, and implementation loss, respectively. Path loss is specified by the following well-known expression [16]:

$$L = 20\log(4\pi \mathrm{d} f_c/c).$$

where d and fc represent the transmitter/receiver spacing and the center frequency, respectively. Noise power is defined as

$$N = 10\log(\mathrm{KT}) + 10\log(B) + 10\log(F)$$

where 10log(KT) and F are -174 dBm/Hz and noise figure, respectively. Finally we get

$$\mathrm{SNR}_{\mathrm{dB}} = P_T + G_T + G_R - L - I - N.$$

A convenient form of capacity is obtained upon converting $\mathrm{SNR}_{\mathrm{dB}}$ to linear scale and substitution into the Shannon-Hartley equation

$$C = B\log_2\left(1 + 10^{(P_T+G_T+G_R-L-I-N)/10}\right).$$

Consider a UWB system with a bandwidth of 1,500 MHz and omnidirectional antennas at both transmitter and receiver. Various parameters of the system are specified in Table 1.4.

Table 1.4 System parameters

Parameter	Values
Transmit power (P_T)	−9.25 dBm
Center frequency (fc)	4 GHz
Noise figure (F_{dB})	7 dB
Implementation loss (I)	3 dB

Let us compare UWB and 802.11g[9] in terms of capacity at various distances. In 802.11g channels are 20 MHz wide, center frequency is at 2.4 GHz, and the maximum transmit power is 30 dBm. Figure 1.5 shows a capacity comparison between the two systems. It is evident that UWB offers an extremely large capacity at short distances.

1.9.3 Link Budget

Let us answer a question: is UWB high speed communications possible. We shall consider a few scenarios first, namely 100 Mbps @ 10 m, 200 Mbps @ 4 m, and finally 500 Mbps @ 2 m. Then, we shall make some assumptions. Subject to the 1.5 GHz of bandwidth, the transmitted power will be −10 dBm. The transmit/receive antenna gains are assumed to be 0 dBi as they are omnidirectional. The SNR values [with strong forward error correction codes (FEC)] are 4, 5, and 6 dB depending on the FEC rate. Finally, implementation loss due to non-ideal filtering, mixing, etc., is assumed to be limited to 3 dB.

We will take away the losses and signal strength requirement at the receiver from the transmit power. Whatever margin is left will be used to combat multipath fading and shadowing. Consequently,

$$M = P_T + G_T + G_R - L - N - \text{SNR} - I,$$

where M, N, and L denote margin, noise power, and path loss, respectively. The expressions for noise power and path loss are

$$N = -174 + 10\log(R) + 10\log(F)$$

with $R = 100$, 200, and 500 Mbps and $F = 7$ dB,

$$L = 20\log(4\pi \mathrm{d} f_c/c)$$

with $f_c = 3{,}850$ MHz.

[9] IEEE 802.11g is a wireless protocol for wireless local area networks implemented using direct sequence spread spectrum (DSSS) and orthogonal frequency division multiplexing (OFDM) signaling methods in 2.4 GHz ISM band. In the United States IEEE 802.11g operates under FCC Part 15 regulations.

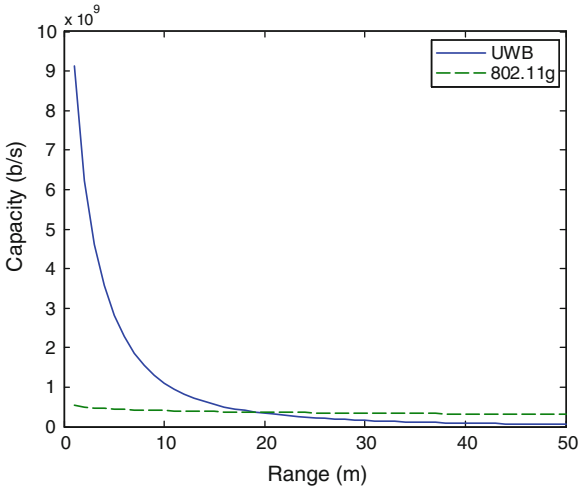

Fig. 1.5 Capacity versus range

Table 1.5 Margin for the three scenarios

Data rate	100 Mbps	200 Mbps	500 Mbps
M (dB)	5.8	9.8	10.8

The computed margins for different data rates are listed in Table 1.5. There is, clearly, adequate margin to combat multipath and shadowing in each of the three scenarios.

1.9.4 Resilience to Multipath Fading

The spectral notch created by destructive multipath fading could take away the spectrum of a narrowband system. This phenomenon results in serious performance degradation. However, the same spectral notch removes only a small percentage of UWB signal as the signal bandwidth is much larger compared to a narrow band system. Consequently, UWB is resilient to multipath fading and requires a smaller fading margin compared to narrowband systems. The scenario is illustrated in Fig. 1.6.

1.9.5 Excellent Temporal Resolution

Short pulses and high resolution of UWB signal make them ideal for ranging. Ranging is treated in Chap. 5. Cramer-Rao lower bound (CRLB) for ranging error

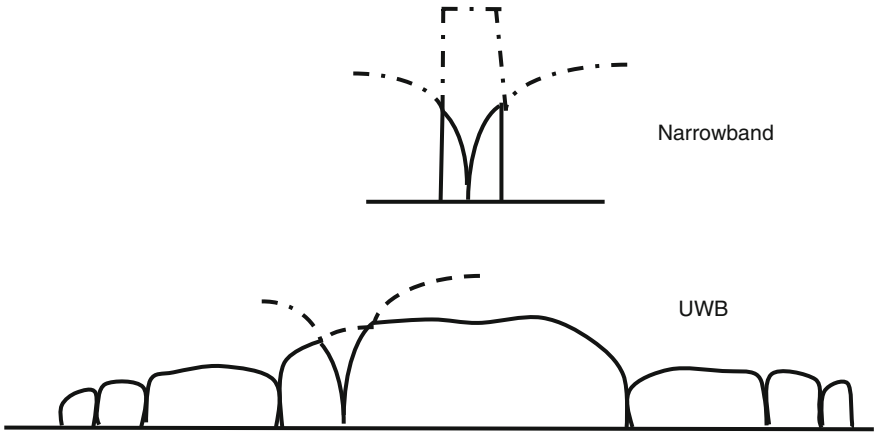

Fig. 1.6 Spectra of narrowband and UWB signals in presence of multipath fading

will be introduced enabling us to compare ranging systems. As we will see at SNR of 10 dB, a 500 MHz UWB signal achieves a lower bound of approximately 2 cm while a 802.11a/g signal with a bandwidth of 20 MHz has a lower bound of roughly 50 cm. The temporal resolutions gained by UWB signals are far superior to those of narrowband systems.

1.9.6 Extremely Large Spreading Factor

The link budget analysis revealed that high data rates are achievable at short ranges. UWB systems could have very large spreading ratio due to having extremely large bandwidths. By spreading the signal one can gain range at the expense of reducing the data rate. Both extremes offer commercial applications. While high data rate systems can deliver high definition content around home, low-throughput systems, such as IEEE 802.15.4a,[10] offer range for applications such as sensing and automation.

1.9.7 Non-exclusive Spectral Allocation

Typically, when new wireless services/technologies are established they are given spectrum of their own. The cost of spectrum acquisition is passed on to the consumer in one form or another. One of the main attractions of UWB systems is

[10] This standard is covered in Chap. 3.

that they do not require exclusive spectrum allocation. UWB is essentially a spectrum underlay/overlay technology. As such they share the spectrum with the primary users.

1.10 UWB Over Cable

Often one associates UWB with wireless transmission, but UWB signals can be transmitted over coaxial cable as well. Splitters, couplers, and coaxial cable attenuate UWB signal. However, it has been shown that a properly designed coaxial home network can support high data rates (up to 600 Mbps) between 3 to 5 GHz up to a range of 300 ft [17, 18].

Both existing and newly constructed homes vary in size significantly. As such it is difficult to cover the entire home with wireless UWB transmission only. The exiting coaxial backbone can be used to deliver content to individual rooms. Then, UWB wireless transmission provides coverage within each room. Pulselink[11] and Sigma Designs[12] both offer UWB over cable solutions. The technology behind Pulelink's is proprietary CWave Technology while Sigma Designs advocates its WiMedia-based solution.

1.11 UWB Sweet Spots

Each wireless technology shines in some application space (Fig. 1.7). For instance, ZigBee's forte is in low data rate throughput applications of up to 250 kbps and ranges upto 10 m. WiFi shines in Internet delivery applications with rates in tens of megabits per second and ranges upto 100 m. From what we have seen here so far, it appears that UWB will be a great candidate in short ranges for very high-throughputs upto perhaps 1 Gbps. UWB is also a good candidate for low data rate applications (up to 3 Mbps) with longer ranges (30–50 m).

What We Learned

- The two definitions of UWB signal and their differences.
- The regulatory history of UWB and FCC First Report and Order.
- Various applications of UWB technology; corresponding spectral limits; and the usage restrictions.
- Differences between UWB regulations in the US and other countries.
- Relationship between DSA and UWB as well as overlay/underlay classification of UWB.

[11] http://pulselink.com/

[12] http://www.sigmadesigns.com/. It appears that UWB-based solutions are not offered any longer.

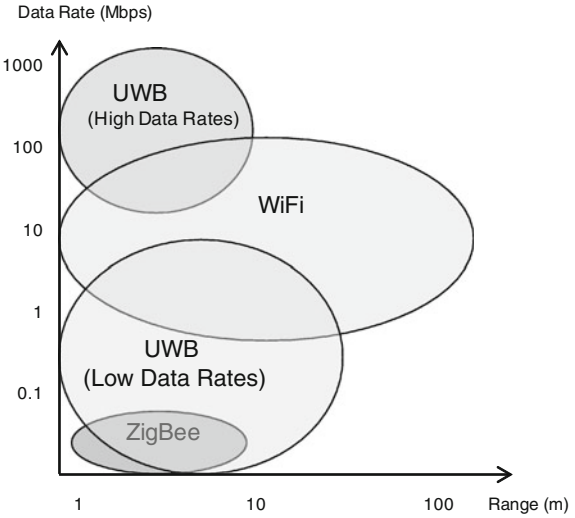

Fig. 1.7 Wireless systems position

- Link budget and capacity calculations for UWB systems.
- Fine resolution capability and multipath resilience properties of UWB systems.
- The sweet spots for UWB technology.

Problems

1. The mathematical definition for the Gaussian pulse and Gaussian monocycle pulse is given as

$$g_0(t) = \frac{1}{\sqrt{2\pi}\sigma} e^{-\frac{t^2}{2\sigma^2}}$$

and

$$g_1(t) = -\frac{t}{\sqrt{2\pi}\sigma^3} e^{-\frac{t^2}{2\sigma^2}}.$$

Find the 10 dB bandwidth and fractional bandwidth of the two pulses when $\sigma = 0.0353$ ns.

2. Does either of the two pulses in problem 1 fit the FCC indoor mask?
3. Find the capacity of a UWB system that utilizes the band ranging from 3.1 to 5.1 GHz. Compare the system capacity with that of another UWB system that operates between 5.1 and 7.1 GHz. Can you draw any conclusions?
4. A UWB system utilizes the spectrum ranging from 4 to 5 GHz. Can this system support a range of 4 m with a data rate of 300 Mbps? Justify any assumptions that you make.

5. Compare the transmission range of low-band and high-band options of DS-UWB systems.
6. A UWB communication system occupies the frequency range from 3.1 to 4.6 GHz. Another UWB system with 4 GHz of bandwidth is devised to have a transmission range identical to that of the other system. Determine the lower/upper 10 dB frequencies of this system.

References

1. T.W. Barrett, History of Ultra Wideband communications and Radar: Part I, UWB communications. *Proceedings Progress In Electromagnetics Symposium 2000* (*PIERS 2000*), Cambridge, MA July 2000
2. I. Oppermann, M. Hamalainen, J. Iinatti, *UWB theory and applications*. (Wiley, New York, 2004)
3. Federal Communications Commission (FCC), Revision of Part 15 of the Commission's Rules Regarding Ultra Wideband Transmission Systems, First Report and Order, ET Docket 98–153, FCC 02–48, Adopted February 2002, Released April, 2002
4. K. Siwiak, D. McKeown, *Ultra-wideband radio technology*. (Wiley, New York, 2004)
5. H.F. Harmuth, *Transmission of Information by Orthogonal Functions*, 1st edn. (Springer, New York, 1969)
6. H.F. Harmuth, *Nonsinusoidal Waves for Radar and Radio Communication* (Academic Press, New York, 1981)
7. H.F. Harmuth, *Antennas and waveguides for nonsinusoidal waves* (Academic Press, New York, 1984)
8. G.F. Ross, The transient analysis of multiple beam feed networks for array systems, Ph.D. Dissertation, Polytechnic Institute of Brooklyn, Brooklyn, NY, 1963
9. G.F. Ross, The transient analysis of certain TEM mode Four-Port networks. IEEE Trans. Microw. Theory Tech., **MTT**(11), 528–547 (November 1966)
10. G.F. Ross, Transmission and reception system for generating and receiving base-band duration pulse signals without distortion for short base-band pulse communication systems. U.S. Patent 3,728,632, issued 17 Apr 1973
11. Federal Communications Commission (FCC), Rules regarding ultra-wideband transmission systems, Notice of inquiry, FCC 98–208, ET Docket 98–153, Technical report, 1998
12. G. Heidary, *WiMedia UWB: Technology of choice for wireless USB and Bluetooth*. (Wiley, New York, 2008)
13. IDA Singapore, *Proposed IDA's Decision and Explanatory Memorandum on the Regulatory Framework for Devices Using Ultra-Wideband Technology*, September 2007
14. J. Balakrishnan, A. Batra, A. Dabak, A multi-band OFDM system for UWB communication, *Proceedings IEEE Conference on Ultra Wideband Systems and Technologies*, pp. 354–358, 2003
15. DS-UWB Physical Layer Submission to 802.15 Task Group 3a, IEEE 802.15.3a Working Group, P802.15.03/0137r0, 2004
16. J.G. Proakis, *Digital communications*, 3rd edn. (McGraw-Hill, Inc., New York, 1995)
17. [online]. Available at: <http://www.pulselink.net>
18. [online]. Available at: <http://www.sigmadesigns.com>

Chapter 2
UWB Channel Modeling

The channel modeling objectives are listed and two schemes for channel sounding known as frequency sweeping and time domain are introduced. We then review the 802.15.3a channel model, aimed for high-throughput UWB applications with a range of up to 10 meters, in detail. Some of the weaknesses of 802.15.3a are addressed in another work. The modeling differences are revealed, enhancements are emphasized, and new parameter sets for three different environments are provided. Finally IEEE 802.15.4a channel model targeted for low throughput, longer range ultra wideband applications such as sensing, RFID, and automation is described. Model parameters are defined, generation process is explained, and differences with 802.15.3a are listed.

2.1 Channel Modeling Goals

There are two main objectives in developing channel modeling for a particular application. First, channel modeling exercise leads to valuable findings in reference to characteristics of a channel. With an insight into the channel, PHY parameters can be selected properly. Second, in the process of PHY definition and well before a communication system is actually built, it is desirable to get a feel for system performance in realistic scenarios. System simulation with the use of channel models enables us to evaluate the PHY reliably.

2.1.1 Channel Sounding Measurements

Channel models are mathematical definitions of channel behavior. To validate a channel model one needs to resort to channel measurements. From these channel measurements, channel model parameters are extracted. Oftentimes channel measurements are referred to as channel sounding.

S. Emami, *UWB Communication Systems: Conventional and 60 GHz*,
DOI: 10.1007/978-1-4614-6753-3_2,

Two channel measurement (or channel sounding) techniques known as frequency sweeping and time domain methods are introduced here. Frequency sweeping [1] is perhaps the most popular technique for UWB sounding mainly due to implementation simplicity. Vector network analyzer (VNA) generates a chirp signal (frequency varying sinusoid) to sweep the spectrum in hundreds of steps. Temporal resolution and the impulse response duration are given as

$$\text{Temporal esolution} = \frac{1}{N\Delta f}$$

$$\text{Impulse Respone Duration} = \frac{N-1}{N\Delta f}$$

where N, Δf are the number of steps and frequency step, respectively.

The received signal, estimated transfer function of the channel, is amplified and recorded through the receiver port of the VNA. Once the sweep is complete, the data are transported to a personal computer (PC) for post-processing. The IFFT of the data are taken to obtain the channel impulse response (Fig. 2.1).

The measured channel should remain stationary while the channel measurement is in progress. The UWB signals are typically in the other few GHz. As such, channel should remain stationary around 10 s. The other limitation of this technique is the transmitter receiver spacing. Because of losses in the cable, one should limit the transmitter/receiver spacing to around 20 m.

In time domain channel sounding method [1], the signal generated by the pulse generator is transmitted over the channel. While the transmitted pulse is not exactly an impulse, it is a short duration (picosecond long) signal. The receive antenna picks up the signal and forwards it onto the digital sampling scope (DSO) after amplification. Since the transmitted signal is known, channel impulse response can be recovered through deconvolution process (Fig. 2.2).

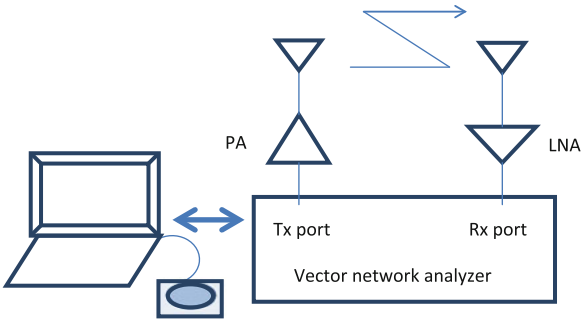

Fig. 2.1 Frequency sweeping method

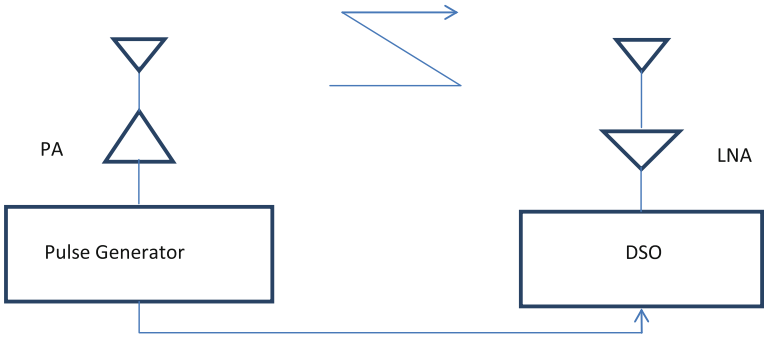

Fig. 2.2 Time domain method

2.2 UWB Channel Models

In this section channel models for IEEE 802.15.3a, which was developed for high-throughput applications, is examined first. We then present an enhanced channel model that proposes and implements some modifications to this channel mode. Lastly, the IEEE channel model for IEEE 802.15.4a, targeting low data rate systems, is presented.

2.2.1 IEEE 802.15.3a UWB Channel Model

There is an extensive literature on UWB channel modeling. The most comprehensive effort was undertaken by IEEE 802.15.3a in 2002–2003 time frame. A summary is presented in [2]. Here we review this work. There are three components to channel model namely, path loss, large-scale fading, and small-scale fading.

2.2.1.1 Large-Scale Fading

The path loss is based on free space model given as

$$L = 20\log(4\pi f_c d/c)$$

where

$$fc = \sqrt{f_L f_H}$$

and f_L and f_H are -10 dB lower and upper frequencies, respectively. Shadowing is found to be lognormally distributed with a standard deviation of 3 dB.

2.2.1.2 Small-Scale Fading

As for small-scale fading, the IEEE 802.15.3a channel modeling group examined a larger number of measurements and considered three channel models namely tap delay line, Δ–K, and Saleh–Valenzuels (S–V) model. Among the three models, both Δ–K and S–V models are cluster based. The following three metrics were selected for comparison purposes: (1) RMS delay spread, (2) Mean excess delay, and (3) Number of significant paths within 10 dB of the main ray.

The original S–V model utilizes Rayleigh multipath gain. It was found that in the case of UWB, S–V channel model with lognormal amplitude (modified S–V) provides the best fit to the measurement data. This can be explained as follows. In the case of narrowband signal, there are a large number of multipath components within the receiver resolution time and central limit theorem (CLT) can be invoked. That, however, is not the case with UWB. Since the spacing between the samples is small, the number of multipath components is typically small and the CLT cannot be invoked.

2.2.1.3 Environments

Three different environments were picked. Each channel model has two components, LOS/NLOS component and the spacing between the transmitter and receiver. The channel modeling scenarios are known as CM1, CM2, CM3, and CM4 as follows:

CM1 LOS 0–4 m
CM2 NLOS 0–4 m
CM3 NLOS 4–10 m
CM4 NLOS (25 ns of RMS delay severe multipath and above).

2.2.1.4 The S–V Model

A clustering structure is present in the channel impulse response and there are a number of rays within each cluster (Fig. 2.3).

In mathematical terms, the S–V model is given as

$$h(t) = X \sum_{l=0}^{L} \sum_{k=0}^{K} a_{k,\,l}(t - T_l - \tau_{k,\,l})$$

where $a_{k,l}$, T_l, $\tau_{k,l}$, and X denote multipath channel coefficient, delay of the first ray of lth cluster, delay of the kth ray of the lth cluster, and lognormal shadowing, respectively [3].

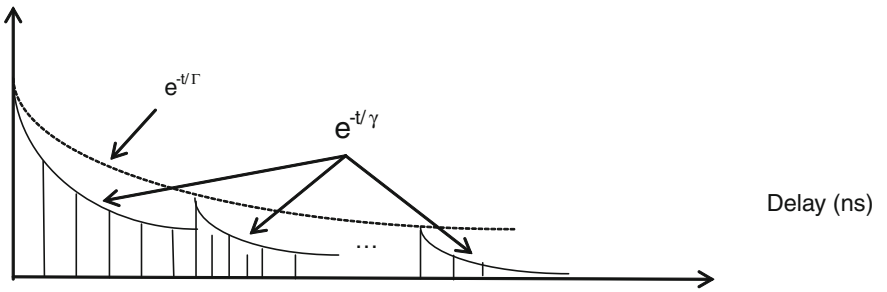

Fig. 2.3 Saleh–Valenzuels (S–V) model

The S–V parameters are listed below:

- Λ Cluster arrival rate (1/ns)
- λ Ray arrival rate (1/ns)
- Γ Cluster decay factor (dB/ns)
- γ Ray decay factor (dB/ns)
- σ_1 Standard deviation of lognormal variable for cluster fading (dB)
- σ_2 Standard deviation of lognormal variable for ray fading (dB)
- σ_x Standard deviation of lognormal shadowing of entire impulse response (dB).

The conditional distributions of cluster and ray arrival times are

$$p(T_l|T_{l-1}) = \Lambda e^{-\Lambda(\tau_l - \tau_{l-1})}$$
$$p\left(\tau_{k,\,l}|\tau_{(k-1),\,l}\right) = \lambda e^{-\lambda\left(\tau_{k,\,l} - \tau_{(k-1),\,l}\right)} \quad k > 0.$$

The channel coefficients definition is

$$\alpha_{k,\,l} = p_{k,\,l}\xi_l\beta_{k,\,l}$$

where $p_{k,\,l}$ accounts for signal inversion due to reflections (+1/−1 equally likely), ξ_l reflects the fading associated with the lth cluster, and $\beta_{k,\,l}$ corresponds to the fading associated with the kth ray of the lth cluster.

The distribution of $\left|\xi_l\beta_{k,\,l}\right|$ is lognormal with mean of $\mu_{k,\,l}$ and variance of $(\sigma_1^2 + \sigma_2^2)$ where σ_1^2 and σ_2^2 are variances of cluster and ray fading, respectively. We also have

$$E\left[\left|\xi_l\beta_{k,\,l}\right|^2\right] = \Omega_0 e^{-T_l/\Gamma} e^{-t_{k,\,l}/\gamma}$$
$$\mu_{k,l} = \frac{10\ln(\Omega_0) - 10^{T_l/\Gamma} - 10^{\tau_{k,\,l}/\gamma}}{\ln(10)} - \frac{(\sigma_1^2 + \sigma_2^2)\ln(10)}{20}$$

where Ω_0 is the mean energy of the first path of the first cluster.

Table 2.1 Model parameters for CM1, CM2, CM3, and CM4 [2]

Model parameters	CM1	CM2	CM3	CM4
Λ (1/ns)	0.0233	0.4	0.0667	0.0667
λ (1/ns)	2.5	0.5	2.1	2.1
Γ	7.1	5.5	14.00	24.00
γ	4.3	6.7	7.9	12
σ_1 (dB)	3.3941	3.3941	3.3941	3.3941
σ_2 (dB)	3.3941	3.3941	3.3941	3.3941
σ_x (dB)	3	3	3	3

2.2.1.5 Computed Model Parameters

The model parameters for CM1, CM2, CM3, and CM4 have been extracted by matching some parameters of the model to the data, the measurement set and are given in Table 2.1. Parameters consisted of mean excess delay, RMS delay spread, and number of significant paths within 10 dB of the peak.

A realization for each environment is provided below. Note that CM4 has the most number of multipath components (Fig. 2.4).

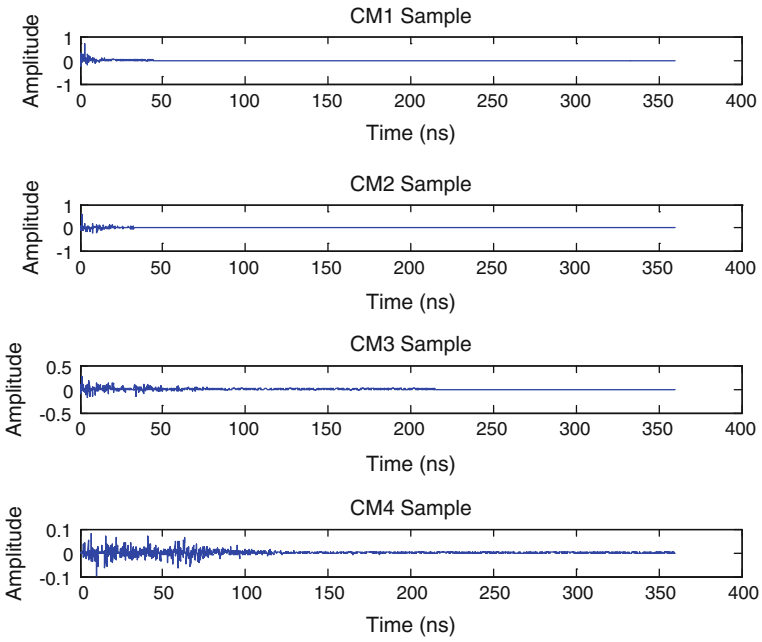

Fig. 2.4 Channel model realizations

Table 2.2 A comparison between the model and data

RMS delay spread	CM1 (ns)	CM2 (ns)	CM3 (ns)	CM4 (ns)
Target	5.28	8.03	14.28	25
Actual	5	8	15	25

2.2.1.6 Comparison

Once all realizations are obtained, a number of parameters including cluster and ray arrival rates, cluster and ray decay factors, standard deviation of cluster and ray, as well as standard deviation of lognormal shadowing can be estimated. A comparison between RMS delay spread of the model (actual) versus data (target) is given in Table 2.2. Results indicate a good match between the two.

2.2.2 An Enhanced UWB Channel Model

IEEE 802.15.3a channel model has a few shortcomings. For instance, in channel model the impact of human body and handheld devices were ignored. In a later study [4], realistic handheld devices were employed and walking speeds of up to 1 m/s were considered. Similar to IEEE 802.15.3a S–V channel model was utilized with some modifications. Detailed modeling of cluster and ray decay factors (dual power decay) and Weibull distribution for ray power were among the modifications.

2.2.2.1 Model Parameters

The channel model parameters are as follows:

- Λ Cluster arrival rate (1/ns)
- λ Ray arrival rate (1/ns)
- Γ_1, Γ_2 Cluster decay factors (dB/ns)
- γ Ray decay factor (dB/ns)
- γ Ray decay factor for the tail cluster (dB/ns)
- σ_r, η_r Weibull distribution scale and shape factor
- σ_1 Standard deviation of lognormal variable for cluster fading (dB)
- σ_x Standard deviation of lognormal shadowing (dB).

2.2.2.2 Differentiators

The key differences between 802.15.3a and this model are:

- The last cluster is known as the tail cluster. The ray decay factor associated with this cluster (γ_τ) is different from that of the other clusters (γ).

- There is no overlap between successive clusters.
- Cluster decay factor is excess delay dependent. As such, instead of having a fixed decay factor (Γ) two decay factors (Γ_1 and Γ_2) are utilized. They are used when the excess delay is less than 50 ns and above 50 ns, respectively.
- Ray power within each cluster is modeled as having Weibull distribution given as

$$\frac{\eta_r}{\sigma_r}\left(\frac{|\beta|^2}{\sigma_r}\right)^{\eta_r-1} e^{-\left(\frac{|\beta|^2}{\sigma_r}\right)^{\eta_r}}$$

where σ_r and η_r are the distribution parameters.

2.2.2.3 Environments

To validate the simulation results, a measurement campaign was conducted. The measurement environments consisted of a Laboratory (LAB), a conference room (CAN), and a Hallway (HAA). The environment's physical dimensions as well as the measured ranges were the following:

LAB	8 × 14 × 2.3 m	2–7 m
CAN	15 × 17 × 2.3 m	2–7 m
HAA	12 × 17 × 6 m	6–17 m.

The signal bandwidth, center frequency, and effective resolution were 2.5, 4.5 GHz, and 0.4 ns, respectively.

2.2.2.4 Estimated Channel Parameters

The estimated model parameters in absence of human movement and presence of movement are given in Table 2.3. Standard deviation of shadowing and cluster fading are larger in presence of human body and movement.

A comparison between the RMS delay spread and 90 % energy capture window of the simulated and measured data revealed a close match between the two [4].

Table 2.3 Model parameters in absence/presence of human movement [4]

Model parameters	LAB	CAN	HAA
Λ (1/ns)	0.060/.068	0.056/0.056	0.056/0.06
λ (1/n)	0.6/0.6	0.6/0.6	0.6/0.6
Γ_1, Γ_2 (dB/ns)	0.31,0.27/0.35,0.27	0.18, 0.13/0.21, 0.13	0.12, 0.1/0.13, 0.1
γ (dB/ns)	0.83/1	0.85/0.95	0.8/0.98
γ_t (dB/ns)	0.3/0.3	0.2/0.2	0.2/0.2
(σ_r, η_r)	(1.8, 1)/(1.8, 0.9)	(2,0.8)/(2, 0.8)	(2, 0.8)/(2, 0.8)
σ_1 (dB)	NA	NA	NA
σ_2 (dB)	3.8/5.6	3.8/4	4/4.5
σ_x (dB)	0.2/4.5	0.1/1.7	0.2/2.3

2.2.3 IEEE 802.15.4a UWB Channel Model

IEEE 802.15.4a channel modeling committee has developed a UWB channel model for low data rate application. The findings have been captured in [5]. A summary of the approach is presented in this section.

2.2.3.1 Large-Scale Fading

Large-scale path loss is expressed as

$$PL = PL_0 + 10n \log\left(\frac{d}{d_0}\right) + s$$

where d, d_0, PL_0, n, and s are distance, reference distance, path loss at reference distance, path loss exponent, and shadowing respectively. Path loss exponent in LOS, soft NLOS (obstructed LOS), and NLOS vary from 1 to 2 (1 in a corridor and 2 in an office), 3 to 4, and 4 to 7, respectively. Shadowing is modeled as a zero mean Gaussian random variable with standard deviation of σ.

Here path loss is modeled as being both distance and frequency dependent. To make the model simpler, these dependencies are assumed to be separable. In other words,

$$PL(d, f) = PL(d)PL(f)$$

where

$$PL(f) \propto \left(\frac{f}{f_c}\right)^{-2\kappa}.$$

2.2.3.2 The Channel Model

The complex baseband impulse response of the channel based on S–V model is given as

$$h(t) = \sum_{l=0}^{L} \sum_{k=0}^{K} a_{k,\,l} e^{j\phi_{k,\,l}} (t - T_l - \tau_{k,\,l})$$

where

$a_{k,\,l}$ Multipath gain coefficient
$\emptyset_{k,\,l}$ Multipath phase (it is a uniform random variable in [0, 2π] range)
T_l Delay of the first ray of l th cluster
$\tau_{k,\,l}$ Delay of the k th ray of the l th cluster.

Parameter L is Poisson distributed as

$$\frac{(\bar{L})^L}{L!} e^{-\bar{L}}$$

with a mean of $\bar{L}$.

Cluster arrival times follow a Poisson Process as in 802.15.3a channel model. However, ray arrival times are modeled as a mixture of Poisson processes as

$$p\left(\tau_{k,\,l} | \tau_{(k-1),\,l}\right) = \beta\lambda_1 e^{-\lambda_1(\tau_{k,\,l} - \tau_{(k-1),\,l})} + (\beta - 1)\lambda_2 e^{-\lambda_2(\tau_{k,\,l} - \tau_{(k-1),\,l})}$$

where β denotes the mixture probability and λ_1, λ_2 are the ray arrival rates.

Within each cluster power associated with different clusters is exponential. In other words,

$$E\left\{\left|\alpha_{k,\,l}\right|^2\right\} = \Omega_l \frac{1}{\gamma_l[(1-\beta)\lambda_1 + \beta\lambda_2 + 1]} e^{-\frac{\tau_{k,\,l}}{\gamma_l}}$$

where Ω_l and γ_l denote the energy of the lth cluster and cluster decay rate. For some NLOS environments an alternate PDP exists with Y_{rise} (rate of PDP increase to its local maxima), γ_1, and χ (attenuation of the first component) as parameters

$$E\left\{\left|\alpha_{k,\,l}\right|^2\right\} = \left(1 - e^{-\frac{\tau_{k,\,l}}{\gamma_{\text{rise}}}}\right) e^{-\frac{\tau_{k,\,l}}{\gamma_l}} \frac{\gamma_1 + \gamma_{\text{rise}}}{\gamma_l} \frac{\Omega_l}{\gamma_l + \gamma_{\text{rise}}(1-\chi)}.$$

Intra-cluster decay rate is related to the cluster arrival time in the following manner:

$$\gamma_{l=k_\gamma T_l + \gamma_0}.$$

Mean power of lth cluster is of exponential decay form given in

$$10\log\,\Omega_l = 10\log\left(e^{-\frac{T_l}{\Gamma}}\right) + M_{\text{cluster}}$$

where M_{cluster} is a Gaussian variable with a standard deviation of σ_{cluster}.

2.2.3.3 Small-Scale Fading

The small-scale amplitude is modeled as Nakagami distribution given by

$$\frac{2}{\Gamma(m)}\left(\frac{m}{\Omega}\right)^m x^{2m-1} e^{-\frac{m}{\Omega}x^2}$$

where m ($m \geq 1/2$, $\Gamma(m)$ and Ω denote Nakagami-m factor, gamma function, and mean power. The m factor has a lognormal distribution with mean and standard deviation of μ_m and σ_m, respectively. The mean and standard deviation of m in terms of τ are

$$\mu_m(\tau) = m_0 - k_m\tau$$
$$\sigma_m(\tau) = \hat{m}_0 - \hat{k}_m\tau.$$

The first component of each cluster is deterministic and is specified by

$$m = \tilde{m}_0.$$

2.2.3.4 Environments

A number of different environments were considered based on intended applications of IEEE 802.15.4a.

They included:

1. Residential LOS and NLOS (CM1, CM2)
2. Office LOS and NLOS (CM3, CM4)
3. Outdoor LOS and NLOS (CM5, CM6)
4. Industrial environments LOS and NLOS (CM7, CM8)
5. Agricultural areas/farms (CM9).

2.2.3.5 Model Parameters

The model parameters are listed below:

$\bar{L}$	Mean number of clusters
Λ	Cluster arrival rate
λ_1, λ_2, β	Ray arrival rates and mixture probability (mixed Poisson model parameters)
Γ	Cluster decay constant

k_γ, γ_0	Intra cluster decay time constant parameters
σ_c	Cluster shadowing variance
σ	Shadowing standard deviation
m_0, k_m	Nakagami-m factor mean parameters
$\hat{m}_0$, $\hat{k}_m$	Nakagami-m factor standard deviation parameters
$\tilde{m}_0$	Nakagami-m factor for the first component of each cluster
γ_{rise}, γ_1, and χ	Alternative PDP shape parameters for some NLOS environments.

Channel model parameters for different environments are provided in Tables 2.4, 2.5, 2.6, and 2.7.

Table 2.4 Model parameters for CM1 and CM2 [5]

Parameter	CM1	CM2
PL_o (dB)	43.9	48.7
n	1.79	4.58
σ (dB)	2.22	3.51
κ	1.12	1.53
$\bar{L}$	3	3.5
Λ (1/ns)	0.047	0.12
λ_1, λ_2 (1/ns), β	1.54, 0.15, 0.095	1.77, 0.15, 0.045
Γ (ns)	22.61	26.27
k_γ	0	0
γ_0 (ns)	12.53	17.5
σ_c (dB)	2.75	2.93
m_0 (dB)	0.67	0.69
$\hat{m}_0$ (dB)	0.28	0.32
$\tilde{m}_0$	NA	NA

Table 2.5 Model parameters for CM3 and CM4 [5]

Parameter	CM3	CM4
PL_o (dB)	35.4	59.9
n	1.63	3.07
σ (dB)	1.9	3.9
κ	0.03	0.71
$\bar{L}$	5.4	1
Λ (1/ns)	0.016	NA
λ_1, λ_2 (1/ns), β	0.19, 2.97, 0.0184	NA
Γ (ns)	14.6	NA
k_γ	0	NA
γ_0 (ns)	6.4	NA
σ_c (dB)	3	NA
m_0 (dB)	0.42	0.5
$\hat{m}_0$	0.31	0.25
$\tilde{m}_0$	NA	NA
χ	NA	0.86
γ_{rise}	NA	15.21
γ_l	NA	11.84

2.2.3.6 Differentiators

There are some key differences between IEEE 802.15.3a and IEEE 802.15.a channel models. First, IEEE 802.15.4a models the channel impulse response as a complex baseband process, while IEEE 802.15.3a uses a real model. Second, ray arrival times in 802.15.4a are mixed Poisson as opposed to plain Poisson in IEEE 802.14.3a. Third, intra-cluster decay factor depend on cluster arrival time. Fourth, small-scale amplitudes of 802.15.4a have a Nakagami distribution as opposed to lognormal in 802.15.3a.

2.2.3.7 Procedure

The steps taken to generate channel model for IEEE 802.15.4a, in a nutshell, are as follows:

- Generate number of clusters
- Generate cluster arrival times
- Generate ray arrival times within each cluster
- Compute mean power for each component
- For each component compute Nakagami distributed amplitude using the mean power
- Generate phase for each component from $[0, 2\pi]$ uniform distribution.

Table 2.6 Model parameters for CM5, CM6, and CM9 [5]

Parameter	CM5	CM6	CM9
PL_o (dB)	45.6	73	48.96
n	1.76	2.5	1.58
σ (dB)	0.83	2	3.96
κ	0.12	0.13	0
$\bar{L}$	13.6	10.5	3.31
Λ (1/ns)	0.0048	0.0243	0.0305
λ_1, λ_2 (1/ns), β	0.27, 2.41, 0.0078	0.15, 1.13, 0.062	0.0225, NA, 1
Γ (ns)	31.7	104.7	56
k_γ	0	0	0
γ_0 (ns)	3.7	9.3	0.92
σ_c (dB)	3	3	3
m_0 (dB)	0.77	0.56	4.1
$\hat{m}_0$ (dB)	0.78	0.25	2.5
$\tilde{m}_0$	NA	NA	0

Table 2.7 Model parameters for CM7 and CM8 [5]

Parameter	CM7	CM8
PL_o (dB)	56.7	56.7
n	1.2	2.15
σ (dB)	6	6
κ	−1.103	−1.427
$\bar{L}$	4.75	1
Λ (1/ns)	0.0709	NA
λ (1/ns)	NA	NA
Γ (ns)	13.47	NA
k_γ	0.926	NA
γ_0 (ns)	0.651	NA
σ_c (dB)	4.32	NA
m_0 (dB)	0.36	0.36
$\hat{m}_0$ (dB)	1.13	01.15
$\tilde{m}_0$	12.99	
χ	NA	1
γ_{rise}	NA	17.35
γ_l	NA	85.36

What We Learned

- Channel sounding techniques.
- Procedures for generating UWB channel models.
- S–V model and the rationale for its use in UWB channels.
- The differences between UWB channel amplitude distribution and that of narrowband channel.
- The weaknesses of IEEE 802.15.3a channel model.
- The differences between the environments of IEEE 802.15.3a and IEEE 802.15.4a channel model.
- The differences between the modeling elements of IEEE 802.15.3a and IEEE 802.15.4a channel model.

Simulation Projects

1. Use 100 realizations of IEEE 802.15.3a CM1 channel model to determine:
   (a) Average RMS delay spread
   (b) Minimum RMS delay spread
   (c) Maximum RMS delay spread
   (d) CDF of RMS delay spread.
2. Rework problem 1 for CM2, CM3, and CM4 channel models.
3. Use 100 realizations of IEEE 802.15.4a CM1 channel model to determine:
   (a) Average RMS delay spread
   (b) Minimum RMS delay spread

(c) Maximum RMS delay spread
(d) CDF of RMS delay spread.

4. Rework problem 3 for CM2, CM3, CM4, CM5, CM6, CM7, CM8, and CM9 channel models.

References

1. I. Oppermann, M. Hamalainen., J. Iinatti, UWB *Theory and Applications* (Wiley, 2004)
2. A.F. Molisch, J.R. Foerster., M. Pendergrass, Channel models for ultra wideband personal area networks, *IEEE Pers. Commun. Mag.* **10**, 14–21 (2003)
3. A.A.M. Saleh, R.A. Valenzuela, A statistical model for indoor multipath propagation. IEEE J. Select. Areas Commun. **5**(2), 128–137 (1987)
4. I. Kovacs et al., Enhanced UWB radio channel model for short range communication scenarios including user dynamics, 14th IST Mobile and Wireless Communications Summit (2005)
5. A.F. Molisch, K. Balakrishnan, C.C. Chong, D. Cassioli, S. Emami, A. Fort, J. Karedal, J. Kunisch, H.Schantz, K. Siwiak., M.Z. Win, A comprehensive model for ultra wideband propagation channels, *IEEE Trans. Antennas Prop*, 3151–3166 (2006)

Chapter 3
Modulation Schemes and Multiple Access for Impulse Radio

This chapter is dedicated to impulse radio as it is a very prominent form of UWB. Initially, impulse radio (IR) is introduced and generic transceiver architecture for IR is presented. Then, common and custom tailored pulse shapes for impulse radios are discussed. Various IR modulation techniques are presented and their performance is analyzed. To enable multiple accesses, a technique known as time hopping (TH) is introduced and it is integrated into various modulation techniques. Finally, the impact of the various antenna types on the transmitted and received UWB signal is investigated.

3.1 Impulse Radio[1] Basics

3.1.1 Impulse Radio Definition

Transmitted impulse radio signal is a stream of pulses with a low duty cycle [1]. Each bit is represented by one or more pulses. The typical range for the duty cycle varies from 1/10 to 1/1,000.

The IR waveform is constructed in the following fashion. Bits or symbols are mapped into N frames. We refer to N frames as a frame block (FB). Each frame consists of a pulse with a low duty cycle. FBs representing bits are then concatenated to form the UWB signal. IR parameters are as follows:

T Bit period
N Number of pulses representing a bit
T_f Frame duration

$$T = N\,\mathrm{T}_f$$

[1] As it was established in Chap. 1, impulse radio is a subset of UWB systems.

S. Emami, *UWB Communication Systems: Conventional and 60 GHz*,
DOI: 10.1007/978-1-4614-6753-3_3,

T_p Pulse duration

$$T_f = M\,T_p$$

$1/T_f$ Pulse repetition frequency (PRF)
$1/M$ Duty cycle

An FB made of three frames ($N = 3$) with a duty cycle of 1/10 is shown in Fig. 3.1. As such

$$T = 3\,T_f$$

and

$$T_f = 10\,T_p.$$

3.1.2 Processing Gain

IR by definition is an intermittent source. As such, it does not see the interference all the time and can suppress (or ignore) interference. This capability is reflected in the processing gain. The processing gain in dB for IR is given by [2]

$$PG = PG_1 + PG_2$$

where

$$PG_1 = 10\log(N) \quad \text{(repetition PG expressed in dB)}$$

$$PG_2 = 10\log\left(T/T_p\right) \quad \text{(duty cycle PG expressed in dB)}$$

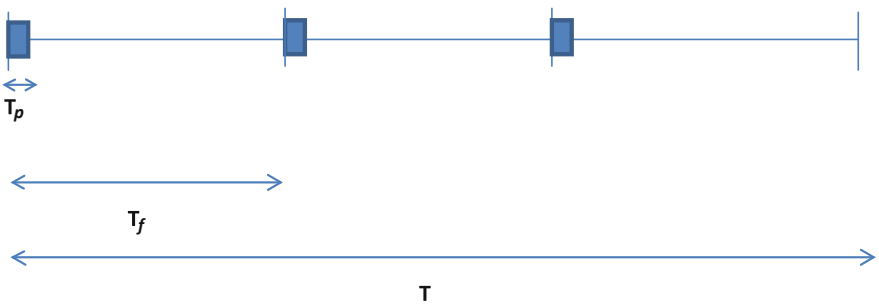

Fig. 3.1 Illustration of a frame block

N Number of pulses representing a bit
T Bit period
T_p Pulse duration.

Transmitted waveform from an IR transmitter is depicted in Fig. 3.2, where there is a single frame per FB and bit stream is {1 0 1}. Note that the middle pulse is the flipped version of the first (or the last) pulse. As we will see later, this signal is modulated using BPSK technique.

3.1.3 Transceiver Block Diagram

The IR transmitter/receiver block diagram is provided in Fig. 3.3 [1]. A modulated stream out of the modulator is pulse shaped. It is then filtered and transmitted

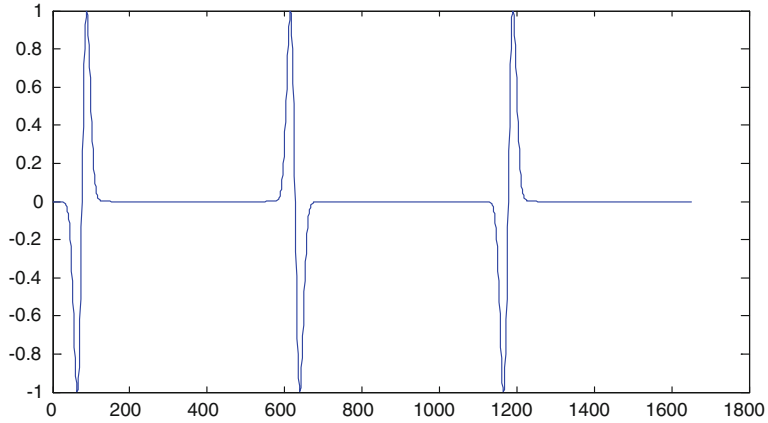

Fig. 3.2 An impulse radio waveform

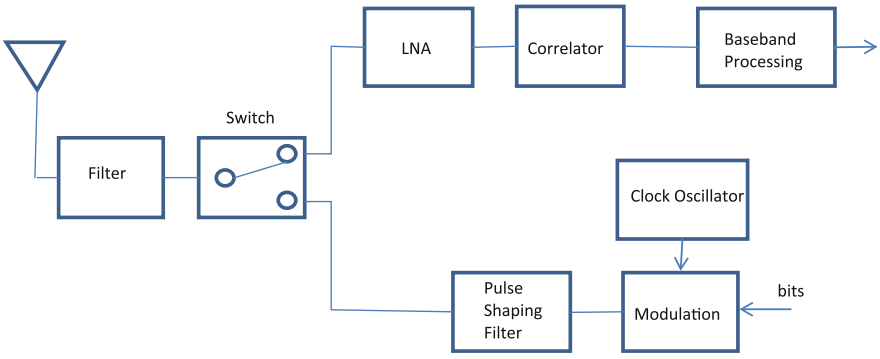

Fig. 3.3 Block diagram of impulse radio transceiver

via antenna. The received signal is passed through the select filter and routed to the LNA when the switch is in the correct position. LNA amplifies the signal and inputs it to the correlator. The correlator (or matched filter) detects the pulse and passes the results to baseband processor to make a decision.

3.2 Pulse Shape Options

There are a number of options for pulse shaping. Laplacian [3] and Hermitian pulses (or Hermites) [4, 5] have been utilized before. However, in UWB applications Gaussian pulses are the most popular. Next, we introduce Gaussian pulses of different orders. Hermites will be introduced in a later section.

3.2.1 Gaussian Pulse Family

The mathematical definition for the Gaussian pulse is given as [6]

$$g_0(t) = \frac{1}{\sqrt{2\pi}\sigma} e^{-\frac{t^2}{2\sigma^2}}$$

where σ^2 is the variance parameter of the pulse. Gaussian pulse has an infinite extent. However, in practice pulse duration is limited to

$$T_p = 4\sqrt{\pi}\sigma.$$

The first derivative of the Gaussian pulse, also known as the Gaussian monocycle, has the following form:

$$g_1(t) = -\frac{t}{\sqrt{2\pi}\sigma^3} e^{-\frac{t^2}{2\sigma^2}}.$$

Higher order derivatives of Gaussian pulse have been used in UWB systems. Table 3.1 lists the first five derivatives of the Gaussian pulse and their spectrum. A 0.5 ns Gaussian pulse and its first three derivatives are depicted in Fig. 3.4. The normalized power spectra of these pulses are shown in Fig. 3.5. The center frequency of each Gaussian derivative is found by determining the peak of its respective spectrum. The end result is

$$f_c = \frac{\sqrt{n}}{T_p} \quad \text{for} \quad n = 1, 2, 3, \ldots$$

Note that the center frequency goes up as the derivative order increases.

Table 3.1 The first five derivatives of Gaussian pulse

n	g(t)	G(f)
1	$-\frac{t}{\sqrt{2\pi\sigma^3}}e^{-\frac{t^2}{2\sigma^2}}$	$2j\pi fe^{-2(\pi\sigma f)^2}$
2	$-\frac{1-\frac{t^2}{\sigma^2}}{\sqrt{2\pi\sigma^3}}e^{-\frac{t^2}{2\sigma^2}}$	$-4(j\pi f)^2e^{-2(\pi\sigma f)^2}$
3	$\frac{3t-\frac{t^3}{\sigma^2}}{\sqrt{2\pi\sigma^5}}e^{-\frac{t^2}{2\sigma^2}}$	$-8j(\pi f)^3e^{-2(\pi\sigma f)^2}$
4	$\frac{3-6\frac{t^2}{\sigma^2}+\frac{t^4}{\sigma^4}}{\sqrt{2\pi\sigma^5}}e^{-\frac{t^2}{2\sigma^2}}$	$16(\pi f)^4e^{-2(\pi\sigma f)^2}$
5	$\frac{-15+10\frac{t^3}{\sigma^2}-\frac{t^5}{\sigma^4}}{\sqrt{2\pi\sigma^7}}e^{-\frac{t^2}{2\sigma^2}}$	$32j(\pi f)^5e^{-2(\pi\sigma f)^2}$

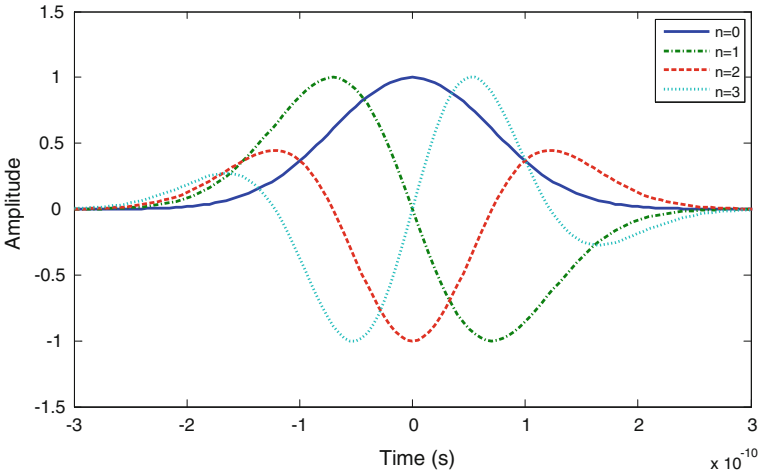

Fig. 3.4 Temporal representation of Gaussian pulse and its first three derivatives

A Gaussian doublet is composed of two reversed Gaussian pulses with some gap between them [7]. In other words

$$s(t) = g_n(t) - g_n(t - t_d)$$

where t_d is the spacing between the two pulses. The spectrum of the pulse of the pulses can be expressed as

$$S(f) = \left(1 - e^{-2\pi j t_d f}\right) G_n(f)$$

where $G_n(f)$ is the spectrum of $g_n(t)$. An example of doublet spectrum is shown in Fig. 3.6 where the duration of the Gaussian pulse and the gap between the pulses are 0.5 and 2 ns long, respectively. The spectrum of these pulses exhibits periodic nulls and their spacing is the inverse of the temporal gap between the reversed pulses (500 MHz in this case). They are clearly useful in applications when one desires to have nulls in certain spots in the spectrum.

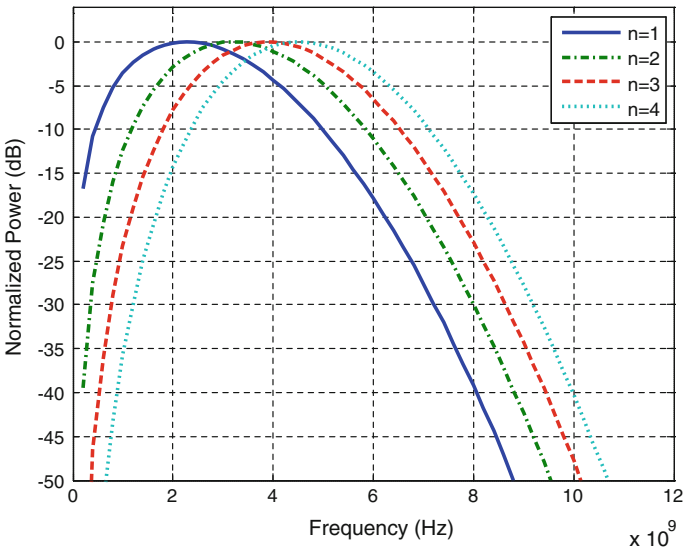

Fig. 3.5 The spectra of the first four derivatives of the Gaussian pulse

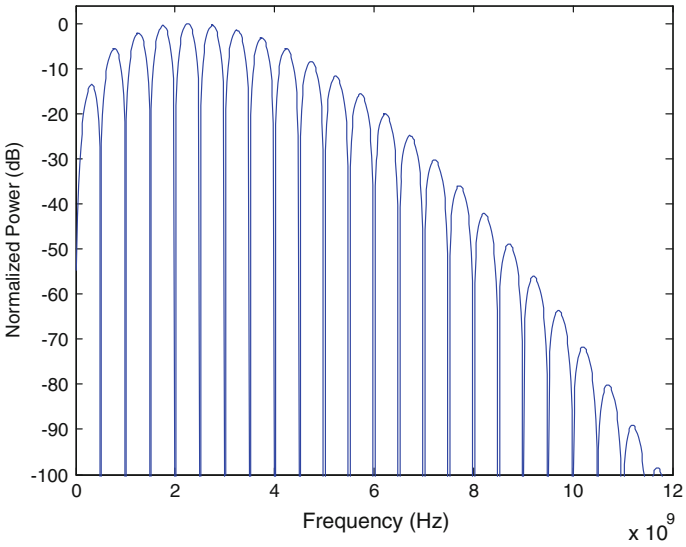

Fig. 3.6 The spectrum of a Gaussian doublet

Linear combination of various orders of Gaussian derivatives can be used to obtain an FCC compliant emission mask.

3.3 Custom Tailored Pulse Shapes

Canned pulse shapes like the one we have introduced so far are not sufficient for all UWB applications. More specifically, a desired canned pulse may not occupy the entire required band or may not meet a desired mask. For instance, first order Hermitian pulse does not meet the FCC mask without upconversion. A systematic approach to pulse design for ultra-wideband applications is discussed in [8]. Let $H(f)$ and $h(t)$ denote the frequency mask[2] and its impulse response, respectively. The objective here is to design a pulse $\psi(t)$ that is limited in time to T_m seconds and is not distorted as a result of the mask filtering operation. Mathematically speaking we have

$$\lambda\psi(t) = \int_{-\infty}^{+\infty} \psi(\tau)h(t-\tau)\mathrm{d}\tau = \int_{-\frac{T_m}{2}}^{+\frac{T_m}{2}} \psi(\tau)h(t-\tau)\mathrm{d}\tau$$

where λ is an attenuation factor. Upon discretization of the continuous time one gets

$$\lambda\psi(n) = \sum_{m=-N/2}^{N/2} \psi(m)h(n-m)\, n = -\frac{N}{2}, \ldots, \frac{N}{2}$$

as the pulse duration T_m is sampled N times. If expressed in matrix notation, the resulting equation is

$$\lambda \begin{bmatrix} \psi\left(-\frac{N}{2}\right) \\ \vdots \\ \psi(0) \\ \cdot \\ \vdots \\ \psi\left(\frac{N}{2}\right) \end{bmatrix} = \begin{bmatrix} h(0) & \cdots & h(-N) \\ \vdots & \ddots & \vdots \\ h(N) & \cdots & h(0) \end{bmatrix} \begin{bmatrix} \psi\left(-\frac{N}{2}\right) \\ \vdots \\ \psi(0) \\ \cdot \\ \vdots \\ \psi\left(\frac{N}{2}\right) \end{bmatrix}$$

or

$$\lambda\Psi = H\Psi.$$

Consequently Ψ is the eigenvector of H. The eigenvalue decomposition technique from linear algebra can be used to compute the eigenvalues of H and their corresponding eigenvectors. It turns out that the largest eigenvectors provides the best fit to the mask.

[2] Examples of spectral masks are FCC masks presented in Chap. 1.

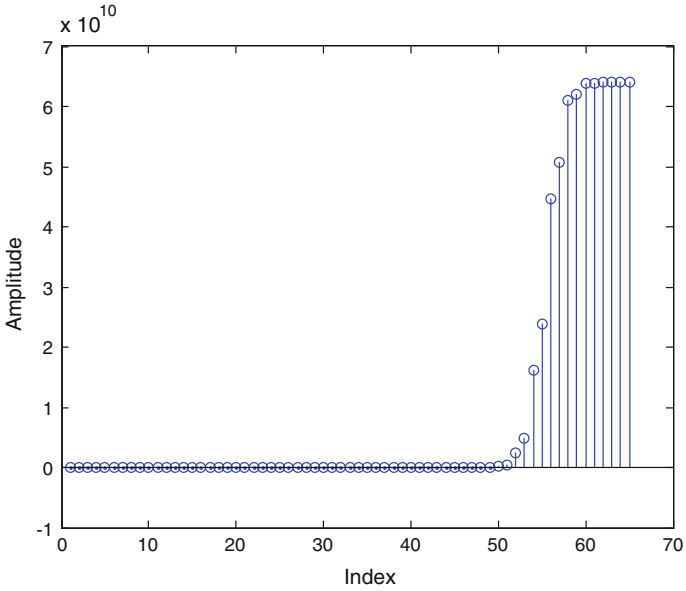

Fig. 3.7 H eigenvalues in ascending order

Let us design a UWB pulse to occupy the spectrum between 3.1 and 5.1 GHz. We select the number of samples and pulse duration to be $N = 64$ and $Tm = 1$ ns. The impulse response of the mask is represented as

$$h(t) = 2f_U \text{sinc}(2f_U t) - 2f_L \text{sinc}(2f_L t)$$

where $f_L = 3.1\,\text{GHz}$ and $f_H = 8.1\,\text{GHz}$. The eigenvalues of the matrix H are computed and are shown in Fig. 3.7 in ascending order. The eigenvectors corresponding to the two largest eigenvalues of matrix H are shown in Figs. 3.8 and 3.9. The PSD of these pulses overlaid on the top of the indoor FCC are plotted in Figs. 3.10 and 3.11. The designed UWB pulses clearly comply with the FCC mask.

There is a clear tradeoff between the pulse width and axacent channel interference. In other words, if we choose 0.5 ns instead of 1 ns, the peak to sidelobe ratio reduces considerably. The situation is illustrated in Fig. 3.12. As such pulse duration must be carefully selected to be short enough while having an acceptable PSD. Another interesting property is that the pulses corresponding to the eigenvectors are orthogonal. The cross-correlation between the eigenvectors corresponding to the two largest eigenvalues of matrix H is computed in Fig. 3.13. Lastly, the utility of this technique is not limited to bandpass type spectrum shapes. Any spectral shape is supported by this technique.

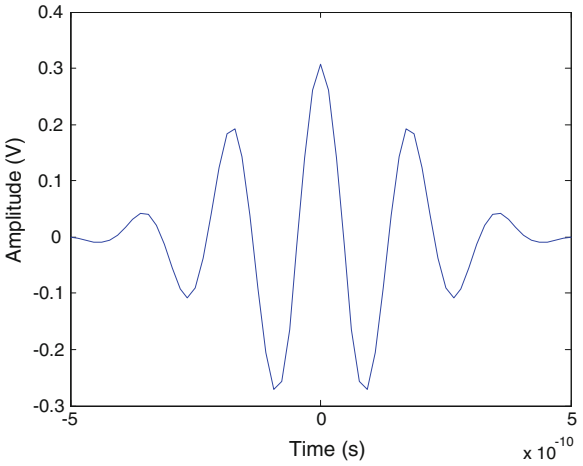

Fig. 3.8 UWB pulse corresponding to the largest eigenvalue

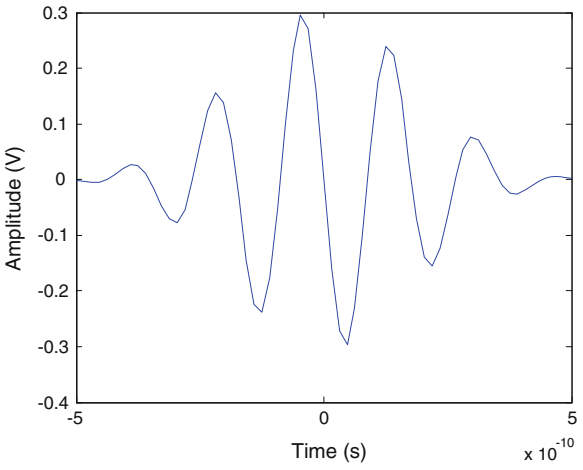

Fig. 3.9 UWB pulse corresponding to the second largest eigenvalue

3.4 IR Pulse Generating Circuits

The IR pulses have a couple of unusual attributes such as short duration and fast rise time that make them exotic. Conventional radio transmitters cannot generate these exotic pulses. On the other hand, similar pulses have been used in radar technology for a long time. However, the pulse generation technology used in radars is not suitable for handheld devices envisioned for IR as they lead to bulky and expensive form factors.

Over the past decade, many different techniques have been proposed in the literature. Here, we mention a few pulse generation techniques appropriate for CMOS process technology. These designs offer not only good performance but also low consumption power [9–11, 17–20]. A CMOS-based circuit for generating Scholtz's monocycle was proposed by Kim et al. [9]. A low power

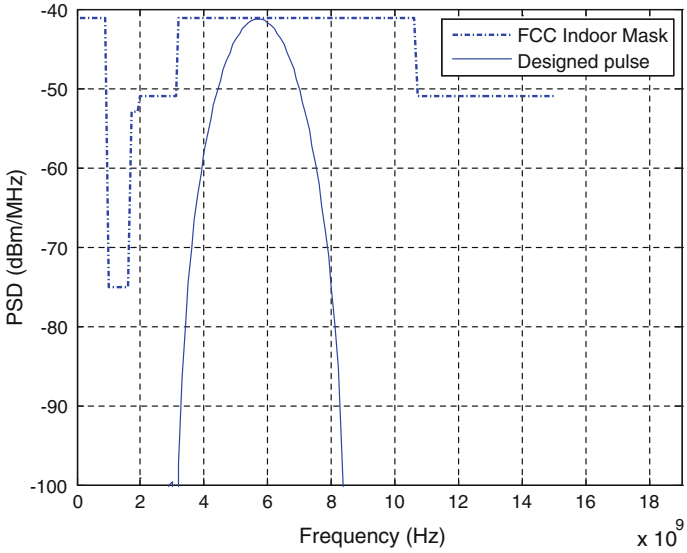

Fig. 3.10 PSD corresponding to the largest eigenvalue

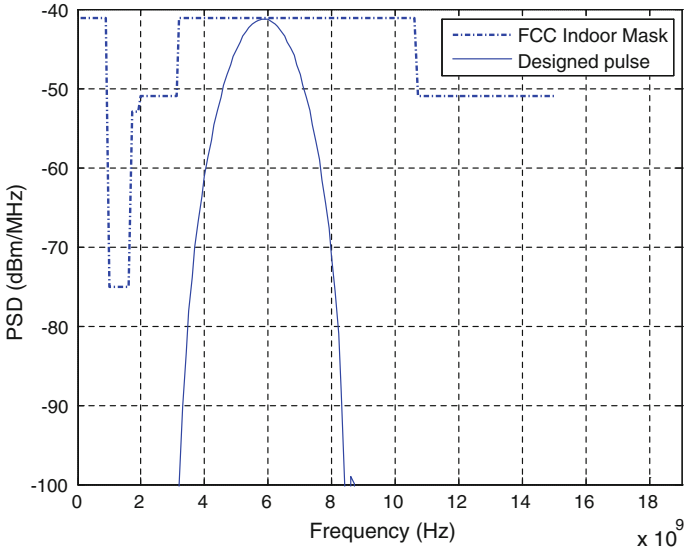

Fig. 3.11 PSD corresponding to the second largest eigenvalue

CMOS-based programmable design for generating various pulse forms is provided in [10]. Another CMOS-based design, known as distributed waveform generator (DWG), has been introduced in [11]. The 180 nm low power design supports arbitrary waveforms as well as integrated OOK and PPM.

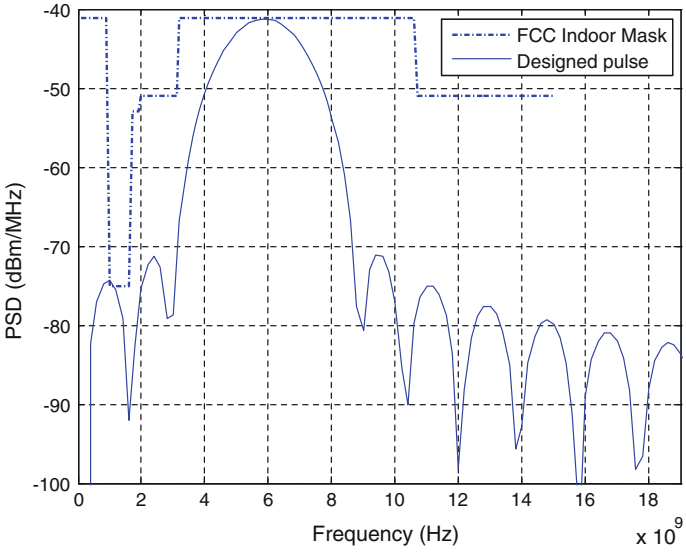

Fig. 3.12 PSD corresponding to the largest eigenvalue when $Tm = 0.5$ ns

Fig. 3.13 Cross correlation between the eigenvectors corresponding to the largest eigenvalues of H

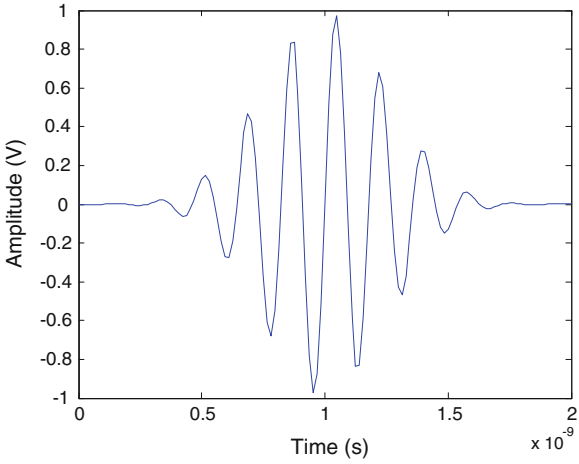

3.5 Modulation Options

Classical modulation schemes such as OOK, BPSK, PAM, PPM, and PPM-BPSK can be modified to accommodate IR format. FB associated with the source alphabet[3] is defined first. FB corresponding to the individual alphabets in the stream are then concatenated to form the IR transmitted stream.

[3] "0" and "1" in case of a binary sources.

3.5.1 PPM

In PPM information is inserted in the pulse delay. Subject to source inputs of "0" and "1" the associated FB are $\sum_{k=0}^{N-1} w\left(t - k\mathrm{T}_f\right)$ and $\sum_{k=0}^{N-1} w(t - k\mathrm{T}_f - \delta)$, respectively. As such, the transmitted stream is given as

$$y(t) = \sum_{j=-\infty}^{\infty} \sum_{k=0}^{N-1} w(t - jT - k\mathrm{T}_f - \delta \mathrm{d}_j)$$

where $w(t)$, δ, d_j, and T are the pulse shape, fixed delay, the binary data, and the bit period, respectively. If there is one frame per FB ($N = 1$), the transmitted waveform reduces to

$$y(t) = \sum_{j=-\infty}^{+\infty} w(t - \delta \mathrm{d}_j - jT).$$

An example is shown in Fig. 3.14.

In presence of AWGN, the received signal is

$$r(t) = y(t) + n(t)$$

where $n(t)$ is the AWGN with zero mean and variance of σ^2. The decision variables and the decision rules are defined by [12]

$$z_0 = \int_o^{T_b} r(t + nT_b) w(t) \mathrm{d}t$$

$$z_1 = \int_o^{T_b} r(t + nT_b) w(t - \delta) \mathrm{d}t$$

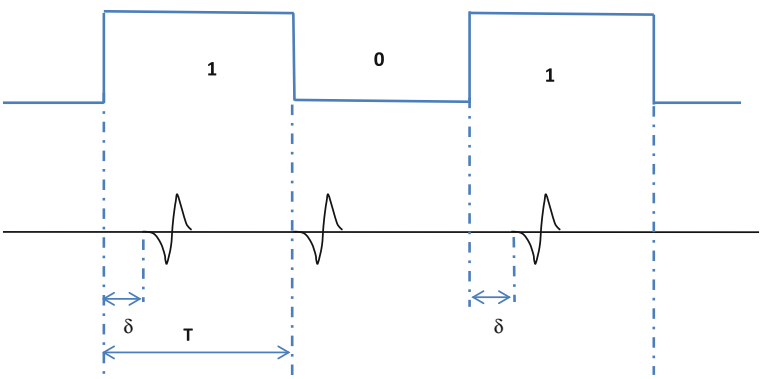

Fig. 3.14 Illustration of PPM

and

$$d_i = \begin{cases} 0 & \text{if } |z_0| \gg |z_1| \\ 1 & \text{if } |z_0| < |z_1|. \end{cases}$$

A closed form for probability of error of this non-coherent scheme has been found [12]

$$P = Q\left(\sqrt{(1+\rho)\gamma_b}\right) + Q\left(\sqrt{(1-\rho)\gamma_b}\right) \quad \textit{if } \gamma_b > 8\,\text{dB}$$

where γ_b denotes the SNR per bit ρ is the autocorrelation function of the w(t) and Q is the well-known Q function. The mathematical forms of ρ and Q are

$$\rho = \frac{\int_0^{T_b} w(t)w(t-\delta)\mathrm{d}t}{\int_0^{T_b} w^2(t)\mathrm{d}t}$$

and

$$Q(x) = \left(1\Big/\sqrt{2\pi}\right) \int_x^{\infty} e^{-(t^2/2)}\mathrm{d}t.$$

Clearly, the PPM error performance is a function of the utilized pulse shape.

Let us consider an example. The PPM pulse shape is assumed to be the first derivative of the Gaussian monocycle

$$w(t) = \left[1 - (t/\sigma)^2\right] e^{-\frac{1}{2}(t/\sigma)^2}$$

The normalized autocorrelation of the PPM pulse can be computed as

$$\rho = \left[1 - (\delta/\sigma)^2 + \left(\frac{1}{12}\right)(\delta/\sigma)^4\right] e^{-\frac{1}{4}(\delta/\sigma)^2}.$$

The probability of bit error in PPM is minimized when $\rho = 0$. That happens when δ/σ equals 1.04 or 3.30. The situation is illustrated in Fig. 3.15.

Alternatively, one can utilize modified Hemitian pulses (MHP) of first, second, and third orders (as listed in Table 3.3). The optimum value for δ/σ to minimize PPM bit error rate can be determined in a similar manner. Figure 3.16 shows the autocorrelation function as a function of δ/τ. The optimum δ/τ values for first, second, and third order modified Hemitian pulses are listed in Table 3.2.

Let us compare the performance of optimum PPM ($\rho = 0$) with a PPM system corresponding to a local maxima of correlation function where $\rho = 0.31$. The performance is plotted in Fig. 3.17. There is a theoretical difference of about 1.5 dB between the optimum and non-optimum PPM systems based on the choice of fixed delay δ.

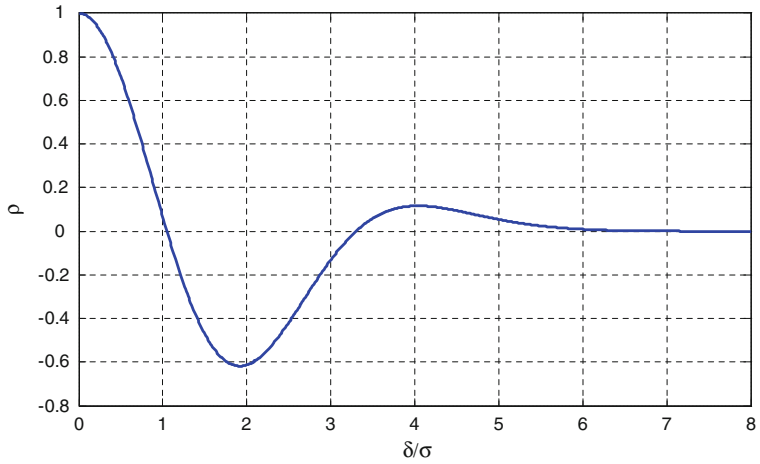

Fig. 3.15 Normalized autocorrelation for first derivative of the Gaussian monocycle

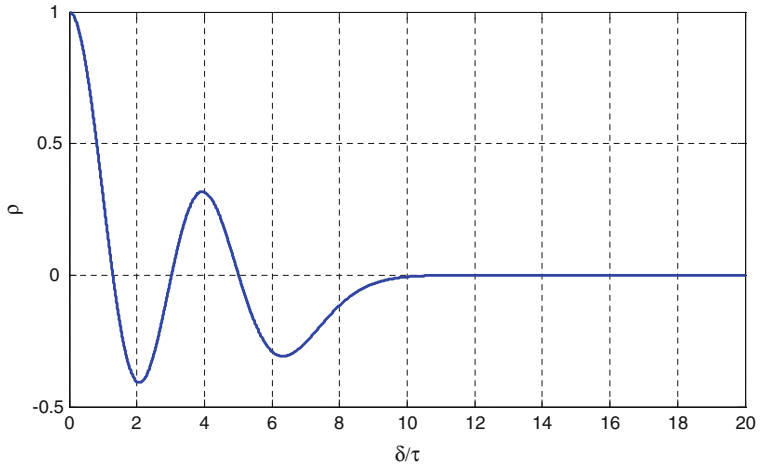

Fig. 3.16 Normalized autocorrelation for a third order MHP

Table 3.2 Optimum delay versus pulse order

n (MHP order)	$(\delta/\tau)_{\text{optimum}}$
1	2
2	1.53, 3.69
3	1.28, 3.02, 5.01

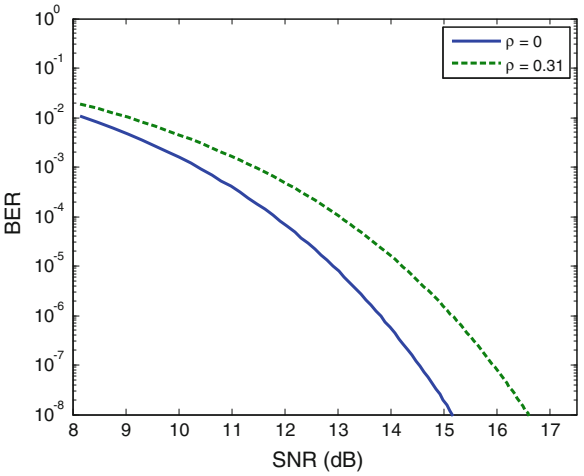

Fig. 3.17 Probability of bit error versus SNR for optimum and non-optimum PPM systems

Table 3.3 MHP pulses and their respective spectra

n	h(t)	H(f)
0	$\sqrt{\frac{E_0}{\tau\sqrt{2\pi}}}e^{-\frac{t^2}{4\tau^2}}$	$\sqrt{\frac{E_0}{\tau\sqrt{2\pi}}}2\sqrt{\pi}\tau e^{-(2\pi f\tau)^2}$
1	$\sqrt{\frac{E_1}{\tau\sqrt{2\pi}}}e^{-\frac{t^2}{4\tau^2}}\left(\frac{t}{\tau}\right)$	$\sqrt{\frac{E_1}{\tau\sqrt{2\pi}}}(-j4\pi f\tau)2\sqrt{\pi}\tau e^{-(2\pi f\tau)^2}$
2	$\sqrt{\frac{E_2}{2\tau\sqrt{2\pi}}}e^{-\frac{t^2}{4\tau^2}}\left[\left(\frac{t}{\tau}\right)^2-1\right]$	$\sqrt{\frac{E_2}{2\tau\sqrt{2\pi}}}(1-(4\pi f\tau)^2)2\sqrt{\pi}\tau e^{-(2\pi f\tau)^2}$
3	$\sqrt{\frac{E_3}{6\tau\sqrt{2\pi}}}e^{-\frac{t^2}{4\tau^2}}\left[\left(\frac{t}{\tau}\right)^3-3\left(\frac{t}{\tau}\right)\right]$	$\sqrt{\frac{E_3}{6\tau\sqrt{2\pi}}}(-j12\pi f\tau+j(4\pi f\tau)^3)2\sqrt{\pi}\tau e^{-(2\pi f\tau)^2}$

3.5.2 BPSK (BPM)

Binary phase shift keying (BPRK) is also known as bi-phase modulation (BPM). Here, information is placed in signal sign. As such, source symbols "1" and "0" are mapped into $\sum_{k=0}^{N-1} w(t-k\mathrm{T}_f)$ and $-\sum_{k=0}^{N-1} w(t-k\mathrm{T}_f)$ FB, respectively. Thus, the transmitted waveform is then given as

$$y(t) = (2d_j - 1)\sum_{j=-\infty}^{\infty}\sum_{k=0}^{N-1} w(t - jT - k\mathrm{T}_f)$$

where $w(t)$, T, and d_j represent the pulse shape, bit period, and binary data, respectively. The waveform reduces to

$$y(t) = (2d_j - 1)\sum_{j=-\infty}^{\infty} w(t - jT)$$

when there is only a single frame per FB. An example is depicted in Fig. 3.18.

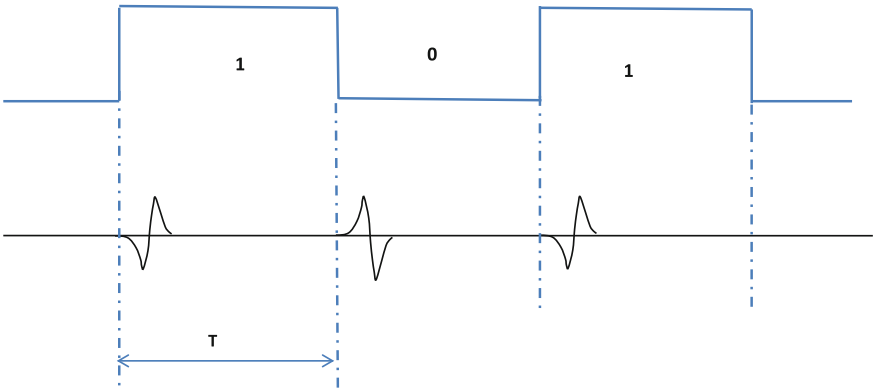

Fig. 3.18 Illustration of BPSK

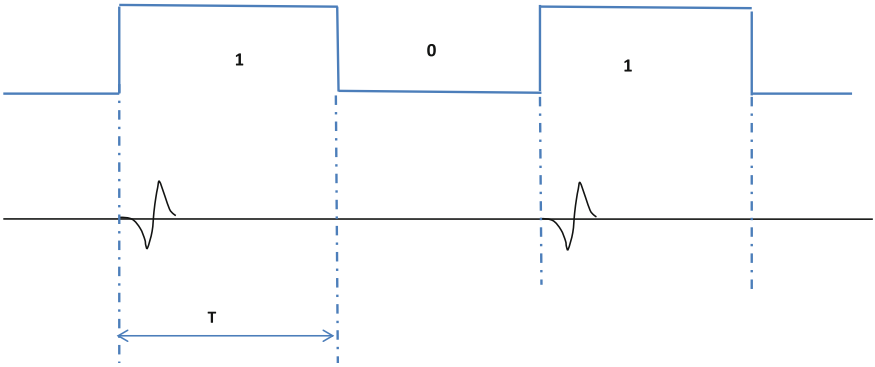

Fig. 3.19 Illustration of OOK

The probability of bit error associated with antipodal signaling in presence of AWGN is [13]

$$P = Q\left(\sqrt{2\gamma_b}\right)$$

where γ_b denotes the SNR per bit. The decision variable and the decision rule are given as

$$z = \int_o^{T_b} r(t + nT_b)w(t)\mathrm{d}t$$

and

$$d_j = \begin{cases} 1 & \text{if } z \gg 0 \\ 0 & \text{if } z < 0. \end{cases}$$

3.5.3 OOK

On–Off Keying (OOK) carries the information in the presence or absence of pulses. FB corresponding to source bits "0" and "1" are 0 and $\sum_{k=0}^{N-1} w(t - k\mathrm{T}_f)$, respectively. Consequently, OOK transmitted signal is then given as

$$y(t) = \sum_{j=-\infty}^{\infty} \sum_{k=0}^{N-1} w\big(t - jT - k\mathrm{T}_f\big)\mathrm{d}_j$$

where $w(t)$, T and d_j represent the pulse shape, bit period, and binary data, respectively. If each FB consists of a single frame, we have

$$y(t) = \sum_{j=-\infty}^{\infty} w(i - jT)\mathrm{d}_j.$$

An example is shown in Fig. 3.19.

OOK is a polar modulation scheme. The probability of bit error associated with such scheme in the presence of AWGN is [13]

$$P = Q\big(\sqrt{\gamma_b}\big)$$

where γ_b denotes the SNR per bit.

3.5.4 M-ary PAM

In M-ary PAM signal amplitude carries the information in signal amplitude levels. The transmitted signal is then defined as

$$y(t) = \sum_{j=-\infty}^{\infty} \pm a_j \sum_{k=0}^{N-1} w\big(t - jT - k\mathrm{T}_f\big)$$

where $w(t)$, T, and a_j represent the pulse shape, symbol period, and M-ary data which come from $\{\pm a_1, \pm a_2, \ldots, \pm a_{M/2}\}$, $a_1 < a_2 < \ldots < a_{M/2}$ respectively.[4]

[4] The frame blocks corresponding to di-bit symbol $\boldsymbol{d^1 d^0}$ (such as 11,10, 00,01) are given by

$$\pm a_i \sum_{k=0}^{N-1} w(t - kT_f)$$

where

$$a_i = 2\big(2d^1 - 1\big) + 2d^0 - 1 \quad 1 \le i \le M/2$$

The transmitted waveform reduces to

$$y(t) = \sum_{j=-\infty}^{\infty} \pm ajw(t - jT)$$

when every FB has only one frame in it. Figure 3.20 shows a 4-ary PAM waveform. When $M = 2$ M-ary PAM degenerates to BPSK.

The symbol and bit error probability are expressed as [13]

$$P_s = 2\left(1 - \frac{1}{M}\right) Q\left(\sqrt{\frac{6\log_2 M}{M^2 - 1}\gamma_b}\right)$$

and

$$P = \frac{2}{\log_2 M}\left(1 - \frac{1}{M}\right) Q\left(\sqrt{\frac{6\ \log_2 M}{M^2 - 1}\gamma_b}\right)$$

where γ_b denotes the SNR per bit.

(Footnote 4 continued)
for M = 4.

Similarly, frame blocks corresponding to tri-bit symbol $\boldsymbol{d^2 d^1 d^0}$ are given by

$$\pm a_i \sum_{k=0}^{N-1} w(t - kT_f)$$

where

$$a_i = 4\left(2d^2 - 1\right) + 2\left(2d^1 - 1\right) + 2d^0 - 1 \quad 1 \le i \le M/2$$

for $M = 8$.

As an example, the di-bit to amplitude mapping for $M = 4$ is shown below.

$\boldsymbol{d^1 d^0}$	a_i
00	−3
01	−1
10	1
11	3

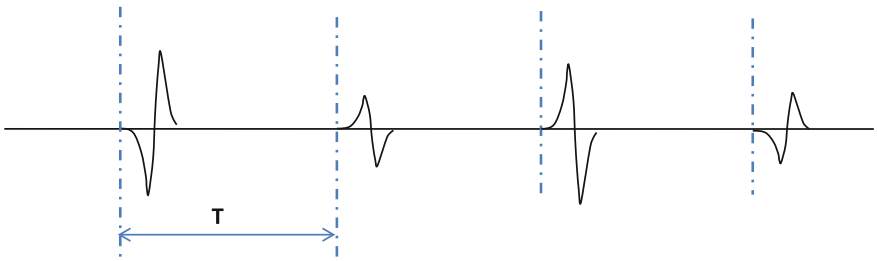

Fig. 3.20 Illustration of 4-ary PAM

3.5.5 PPM-BPSK Hybrid

PPM-BPSK is a non-binary modulation scheme that carries two bits per symbol. More specifically, information is inserted into signal sign and delay. The FB associated with 00, 01, 10, and 11 are $-\sum_{k=0}^{N-1} w(t-k\mathrm{T}_f)$, $\sum_{k=0}^{N-1} -w(t-k\mathrm{T}_f-\delta)$, $\sum_{k=0}^{N-1} w(t-k\mathrm{T}_f)$ and $\sum_{k=0}^{N-1} w(t-k\mathrm{T}_f-\delta)$, and, respectively. The transmitted stream is given by

$$y(t)=\left(2d_j^1-1\right)\sum_{j=-\infty}^{\infty}\sum_{k=0}^{N-1} w\left(t-jT-k\mathrm{T}_f-\delta d_j^0\right)$$

where $w(t)$, δ, $\{d_j^1, d_j^0\}$, and T are the pulse shape, fixed delay, the binary data, and the bit period, respectively.

In presence of AWGN, the received signal is

$$r(t)=y(t)+n(t)$$

where $n(t)$ is the AWGN with zero mean and variance of σ^2. The decision variables and the decision rule are defined as [12]

$$z_0=\int_o^{T_b} r(t+nT_b)w(t)\mathrm{d}t$$
$$z_1=\int_o^{T_b} r(t+nT_b)w(t-\delta)\mathrm{d}t$$

and

$$d_j^1=\begin{cases}1 & \text{if } z_0 \gg -z_1\\ 0 & \text{if } z_0 < -z_1\end{cases}$$
$$d_j^0=\begin{cases}0 & \text{if } |z_0|\geq|z_1|\\ 1 & \text{if } |z_0|<|z_1|.\end{cases}$$

The average probability of error is determined by [12]

$$P = Q\left(\sqrt{(1+\rho)\gamma_s}\right) + \frac{1}{2}Q\left(\sqrt{(1-\rho)\gamma_s}\right) \quad if\ \gamma_b > 8\text{dB}$$

where γ_s denotes the SNR per symbol, ρ is the autocorrelation function of the $w(t)$. Comparatively speaking, hybrid PPM-BPSK with the same SNR achieves the same performance as PPM. Thus, hybrid modulation is 3 dB more efficient than PPM, as it transmits two bits instead of one.

3.5.6 Pulse Shape Modulation

In pulse shape modulation (PSM), alphabet symbols are represented by orthogonal pulses. One popular family of orthogonal pulses is modified Hermitian pulses (MHP).[5] The mathematical expression for modified Hermitian (or Hermite) pulses (MHP) of various orders is as follows [4, 5]:

$$h_n(t) = \sqrt{\frac{E_n}{\tau n!\sqrt{2\pi}}} e^{-\frac{t^2}{4\tau^2}} n! \sum_{i=0}^{\left[\frac{n}{2}\right]} \left(-\frac{1}{2}\right)^i \frac{\left(t/\tau\right)^{n-2i}}{(n-2i)!i!}$$

where n, $\left[\frac{n}{2}\right]$, τ and E_n denote pulse order, integer part of $n/2$, a scaling factor, and the energy associated with the nth order pulse. In practice, τ is chosen to be $T_p/10$ where T_p is the pulse duration. Hermitian pulses of zeroth, first, second, and third together with their spectra are given in Table 3.3.

It can be shown that the set of Hermitian pulses form an orthogonal set. In other words, any two pulses from the set are orthogonal to each other. Another interesting property of the MHP is that pulse duration as well as pulse bandwidth does not vary much between two successive orders. Lower order MHP are shown in Fig. 3.21.

3.5.7 Frame Block Expressions

A summary of FB expressions for various modulation schemes are provided here. Once the FB expressions corresponding to '1' and '0' are known, we can easily write down the FB corresponding to an arbitrary bit. Mathematical expression for the UWB signal can be obtained by concatenating the FB.

The FB corresponding to bits '1', '0', and arbitrary bit d[6] are listed for binary OOK, BPSK and PPM in Table 3.4A. The FB corresponding to '00', '01', '10',

[5] Hermitian pulses unlike modified Hermitian pulses (MHP) are not orthogonal.

[6] Could be either '1' or '0'.

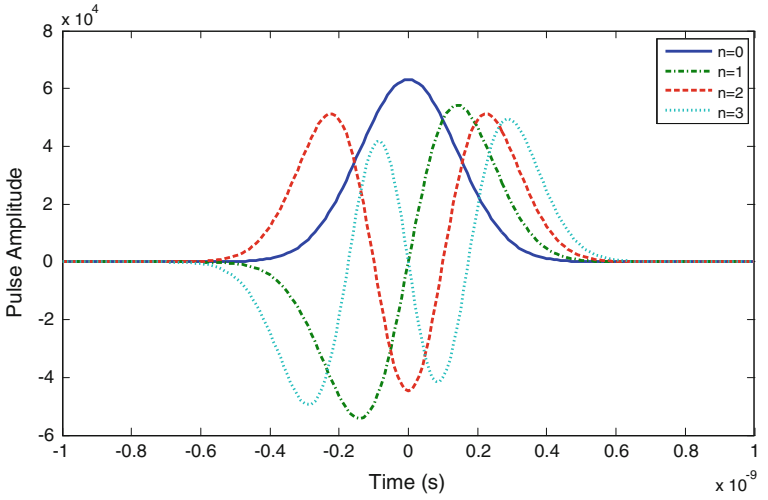

Fig. 3.21 MHP of various orders

Table 3.4 (A) Frame blocks (FB) expressions; (B) Frame blocks (FB) expressions for PPM-BPSK hybrid modulation; (C) a_i for M-ary PAMPAM

(A)

Modulation	FB '0'	FB '1'	FB 'd'
OOK	0	$\sum_{k=0}^{N-1} w(t-k\mathrm{T}_f)$	$d\sum_{k=0}^{N-1} w(t-k\mathrm{T}_f)$
BPSK	$-\sum_{k=0}^{N-1} w(t-k\mathrm{T}_f)$	$\sum_{k=0}^{N-1} w(t-k\mathrm{T}_f)$	$(2d-1)\sum_{k=0}^{N-1} w(t-k\mathrm{T}_f)$
PPM	$\sum_{k=0}^{N-1} w(t-k\mathrm{T}_f)$	$\sum_{k=0}^{N-1} w(t-k\mathrm{T}_f-\delta)$	$\sum_{k=0}^{N-1} w(t-k\mathrm{T}_f-\mathrm{d}\delta)$

(B)

FB '00'	$-\sum_{k=0}^{N-1} w(t-k\mathrm{T}_f)$
FB '01'	$-\sum_{k=0}^{N-1} w(t-k\mathrm{T}_f-\delta)$
FB '10'	$\sum_{k=0}^{N-1} w(t-k\mathrm{T}_f)$
FB '11'	$\sum_{k=0}^{N-1} w(t-k\mathrm{T}_f-\delta)$
FB '$\mathrm{d}^1\mathrm{d}^0$'	$(2d^1-1)\sum_{k=0}^{N-1} w(t-k\mathrm{T}_f-\mathrm{d}^0\delta)$

(C)

M	a_i
4	$2(2d^1-1)+2d^0-1 \quad i=1,2$
8	$4(2d^2-1)+2(d^1-1)+2d^0-1 \quad i=1,2,3,4$

and '11' are given in Table 3.4B. For non-binary modulation PPM-BPSK hybrid, the amplitude levels for $M = 4$ and $M = 8$ are provided in Table 3.4C.

3.6 Multiple Access

Since radios in an IR network are not synchronized with each other, signals from multiple sources could arrive at the destination at the same time. Poor SNR due to pulse collisions leads to unsatisfactory system performance. The situation can be remedied if each user imposes a different pseudo random delay on every transmitted pulse. In this way, collisions become very infrequent and as such multiple access capability is achieved. This technique is known as time hopping [1].

Digital implementation of a pseudo noise (PN) sequence of length N renders 2^N-1 outcomes. The outcomes of a PN are mapped into equidistance delays. The delay gets imposed on pulse onset after modulation. A Linear Feedback Shift Register (LFSR) can be used to generate PN sequences [13]. One starts with some initial state excluding all zeros state. With every clock, the shift register contents are pumped in and out of a shift register. Register content at a given time is known as the state. One ends up with a finite number of states that are repeated after 2^N-1 clocks. The generated states can be mapped into delay. Then, the resulting delays are added to signal onset. A PN code of length three is implemented in Fig. 3.22. As seen, there are a total of 7 states. The mapper (from PN sequence states to delay) is given in Table 3.5.

3.7 Time Hopped Modulations

Time hopping can be incorporated into the modulation scheme to enable multiple access. In this section, we incorporate time hopping into BPSK and PPM. The approach can be applied to other modulation schemes as well.

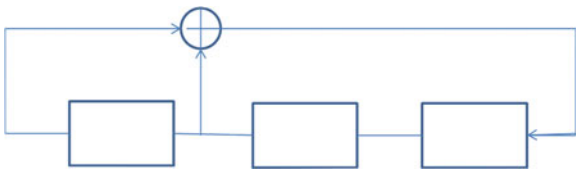

Fig. 3.22 A LFSR is used to generate a PN sequence

Table 3.5 Generated PN sequence

Clock	LFSR State	Delay
0	100	3
1	001	0
2	010	1
3	101	4
4	011	2
5	111	6
6	110	5

3.7.1 TH-BPSK

TH-BPSK is very similar to BPSK with the exception that the onset of each pulse is determined by a PN sequence. The modulated waveform when there are N repetitions per bit is given as

$$y(t) = \sum_{j=-\infty}^{\infty} \sum_{k=0}^{N-1} w(t - jT - k\mathrm{T}_f - c(j,k)\mathrm{T}_c)\,(2\mathrm{d}j - 1)$$

where $c(j, k) = \{0, 1, 2,\ldots, p\}$, $w(t)$, T_f, T_c, and d_j denote PN code, pulse waveform, frame duration, time slot, and binary data, respectively (Fig. 3.23).

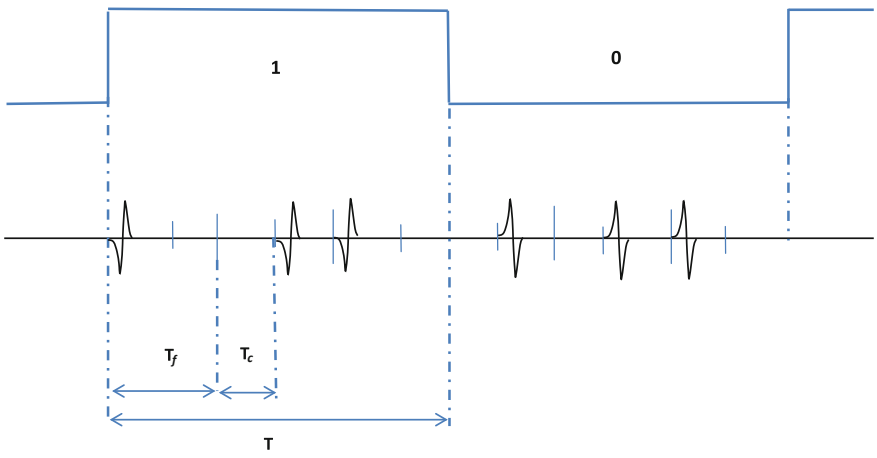

Fig. 3.23 An illustration of TH-BPSK

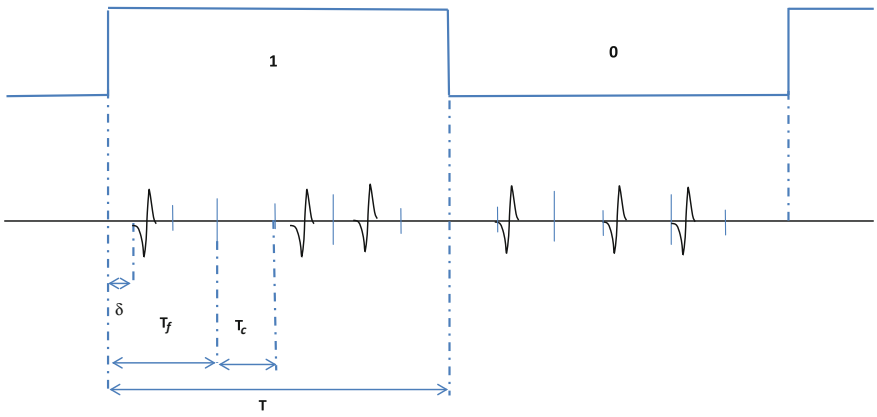

Fig. 3.24 An illustration of TH-PPM

3.7.2 TH-PPM

TH-PPM is similar to PPM with the exception that the onset of each pulse is determined by a PN sequence. The modulated waveform when there are N repetitions per bit is given as

$$y(t) = \sum_{j=-\infty}^{\infty} \sum_{k=0}^{N-1} w(t - jT - kT_f - c(j,k)T_c - \delta d_j)$$

where $c(j, k) = \{0, 1, 2,\ldots, p\}$, $w(t)$, T_f, T_c, δ, and d_j denote PN code, pulse waveform, frame duration, time slot, fixed delay, and binary data, respectively (Fig. 3.24).

3.8 Multiple Access with TH-PPM

In a TH-PPM, a frame is divided into Nu slots. In other words $T_f = Nu\ T_c$. A maximum of Nu users can be accommodated with no collision. The situation is illustrated in Fig. 3.25. TH-PPM processing gain (in dB) has three additive components PG_1, PG_2, and PG_3 as [2]

$$PG = PG_1 + PG_2 + PG_3$$

where

Fig. 3.25 An illustration of multiple access with TH-PPM

$$\begin{aligned} \mathrm{PG}_1 &= 10\log(N) \\ \mathrm{PG}_2 &= 10\log\left(\mathrm{T}_f/\mathrm{T}_c\right) = 10\log(Nu) \\ \mathrm{PG}_3 &= 10\log\left(\mathrm{T}_c/\mathrm{T}_p\right) \end{aligned}$$

T_p Pulse duration
T_c Slot duration
T_f Frame duration.

Let us consider an example. The number of pulses per bit and the processing gain of a TH-PPM are 100 and 34 dB, respectively. (a) Determine the maximum number of users supported by this system subject to PPM delay of $\mathrm{T}_p/4$. (b) Compute the duty cycle when maximum number of users is supported.

(a) Since $N = 100$ PG=10 log (100) = 20 dB

Processing gain is given by

$$\mathrm{PG} = \mathrm{PG}_1 + \mathrm{PG}_2 + \mathrm{PG}_3$$

Solving for PG_2, we get

$$10\log(Nu) = \mathrm{PG} - \mathrm{PG}_1 - \mathrm{PG}_3$$

To maximize *Nu*, *PG3* must be minimized.

$$\mathrm{PG}_3 = 10\log\left(\mathrm{T}_c/\mathrm{T}_p\right).$$

At the minimum, T_c should contain the pulse wide and fixed delay of $\mathrm{T}_p/4$. As such

$$\mathrm{PG}_3 = 10\log\left(\left(\mathrm{T}_p + \mathrm{T}_p/4\right)/\mathrm{T}_p\right) = 2.23\,\mathrm{dB}$$

Substituting back into *Nu* equation we get

$$10\log(Nu) = 34 - 20 - 2.23$$

And finally $Nu = 15$.

(b)

$$\begin{aligned}\text{Duty cycle} &= \left(\mathrm{T}_p/\mathrm{T}_c\right)x\left(\mathrm{T}_c/\mathrm{T}_f\right)\\ &= \left(T4/\left(\mathrm{T}_p + \mathrm{T}_p/4\right)\right)x(1/Nu)\\ &= (1/(1+1/4))x(1/15) = 0.053\end{aligned} \quad .$$

3.9 Antenna Effect

Unlike narrowband systems, UWB systems can shape the transmitted signal. Some authors have modeled both transmit and receive antennas as differentiators (or high pass filters) [14].

In another study various combinations of transmit and receive antennas were considered [18]. Utilized antennas consisted of Ridged-Horn antenna (RDH), Vivaldi antenna (VVD), TEM-Horn antenna (TEM), Disc-Cone antenna (DSC), Biconical antenna (BCN). Gaussian pulses were employed as excitation signals. The outcomes were as follows. A BCN/BCN combination where transmitter and receiver antennas are both Biconical antennas resulted in integration of the excitation signal. A BCN used with any other antenna as transmit or receive antenna, did not impact the shape of the excitation at the receiver end. Any other combination of antennas led to the differentiation of the excitation signal at the receiver.

Yet in another study [16], conical, TEM horn, D*dot probe (extremely short monopole), and monopole antennas were analyzed and tested. The results are summarized in Table 3.6. It is seen that reciprocity does not hold. In other words, a given antenna type behaves quite differently in transmission versus reception modes. In fact, the transmit mode functionality of an antenna is proportional to the derivative of the receive mode functionality of the same antenna [20]. The output could be identical to the input, its first derivative, its second derivative, or its integral depending on the antenna type and whether it is used as a transmitting or receiving antenna. As for monopole antenna, when used as a receiving antenna it acts as an integrator. The modeling of the receiver antenna as a differentiator in [14] is in contrast to the findings reported in [15, 16]. A summary is presented in Table 3.6.

What We Learned

- Definition and elements of IR communication systems.
- Gaussian family pulse shaping, Gaussian doublets, and Hermite pulse shaping.
- Limitations of predefined pulse shapes such as Gaussian pulse shapes and custom tailored pulse shape generation.
- UWB modulation/demodulation techniques and tradeoffs.

Table 3.6 Antenna function on the basis of antenna type and transmit/receive mode

Mode	Conical	TEM horn	D*dot probe
Transmitting antenna	No change	Der[b]	Second der[c]
Receiving antenna	Int[a]	No change	Der

[a] integral
[b] derivative
[c] second derivative

- Enabling multiple access through time hopping.
- Impact of antennas on transmitted/received UWB signal.

Problems and Simulation Project

1. A Gaussian monocycle is 0.25 ns long. Draw the pulse spectrum and determine the center frequency and 10 dB bandwidth of the pulse.
2. A Gaussian pulse is 0.4 ns long. Determine the center frequency, 10 dB bandwidth, and fractional bandwidth of the first four derivatives of the pulse.
3. Design a UWB pulse to satisfy both of the following requirements:
   (a) to occupy the frequency range from 3.1 to 6 GHz.
   (b) to avoid interference with narrowband users located at 5,100 and 5,400 MHz.
4. Design a UWB pulse to satisfy both of the following requirements:
   (a) to extend from 3.1 to 6 GHz in frequency spectrum
   (b) to avoid the frequency range from 5 to 5.5 GHz.
5. Plot the BER performance of a PPM system versus the transmitter/receiver separation distance.

References

1. I. Oppermann, M. Hamalainen, J. Iinatti, *UWB Theory and Applications*, (Wiley, USA, 2004)
2. Time Domain Corporation, Comments of time domain corporation, In the matter of revision of part 15 of the FCC's rules regarding ultra wideband transmission systems, Docket, pp. 98–154 (1998)
3. J.T. Conroy, J.L. LoCicero, D.R. Ucci, Communication techniques using Monopulse waveforms. IEEE Mil. Commun. Conf. Proc. **2**, 1181–1185 (1999)
4. M. Ghavami, L.B. Michael, S. Haruyama, R. Kohno, A novel UWB pulse shape modulation system. Kluwer Int. J. Wireless Pers. Commun. **23**(1), 105–120 (2002)
5. M. Herceg, T. Matic, T. Svedek, Performances of hybrid amplitude shape modulation for UWB communication systems over AWGN channel in a single and multi-user environment. Radio Eng. **18**(3), 265–271 (2009)
6. L. De Nardis, G. Giancola, M.G. Di Benedetto, Power limits fulfillment and MUI reduction based on pulse shaping in UWB networks, IEEE Int. Conf. Commun. pp. 3576–3580 (2004)

7. M. Hamalainen, V. Hovinen, J. Iinatti, M. Latva-aho, In-band interference power caused by different kinds of UWB signals at UMTS/WCDMA frequency bands, in *Proceedings of the 2001 IEEE Radio and Wireless Conference, RAWCON2001*, Waltham-Boston, Massachusetts, pp. 97–100, August 2001
8. B. Parr, B.L. Cho, K. Wallace, Z. Ding, A novel ultra-wideband pulse design algorithm. IEEE Commun. Lett. pp. 219–221 (2003)
9. H. Kim, D. Park, Y. Joo, *Design of CMOS Scholtz's monocycle pulse generator* (IEEE Conf. Ultra Wideband Syst. Technol., Reston, VA, 2003)
10. K. Marsden, H.J. Lee, D.S. Ha, H.S. Lee, Low power CMOS reprogrammable pulse generator for UWB systems. IEEE Conf. Ultra Wideband Syst. Technol. Reston, VA, pp. 443–447 (2003)
11. Y. Zhu, Ultra-wideband pulse generation, detection and filtering using distributed Architectures and Circuits, Ph.D. Dissertation, 2008
12. X. Huang, Y. Li, Performance of impulse-train-modulated ultra-wideband systems. IEEE Trans. Commun. **54**(11), 1933–1936 (2006)
13. J.G. Proakis, *Digital Communications*, 3rd edn. (McGraw-Hill, Inc., New York, 1995)
14. F. Ramirez-Mireles, R.A. Scholtz, System performance analysis of impulse radio modulation. Radio Wirel. Conf. pp. 67–70, Colorado Springs (1998)
15. K. Rambabu, E.C.A. Tan, K.M.K. Chan, M.Y.W. Chia, Study of antenna effect on UWB pulse shape in transmission and reception, in *Proceedings IEEE International symposium on Antennas and Propagation,* Singapore, November 2006
16. J.R. Andrews, UWB sources, antennas and propagation, picosecond pulse labs, Application Note AN-14a, August 2003
17. D. D. Wentzloff, A. P. Chandrakasan, A 47pJ/pulse 3.1 to 5 GHz all-digital UWB transmitter in 90 nm CMOS. IEEE Int. Sol. State Circ. Conf. 2007
18. J. Ryckaert, et al., Ultra-wide-band transmitter for low-power wireless body area networks: Design and evaluation. IEEE Trans. Circ. Sys. **52**(12) 2005
19. T. Norimatsu, et al., A novel UWB impulse-radio transmitter with all-digitally-controlled pulse generator. in European Solid-State Circuits Conference, pp. 267–270, Sep. 2005
20. C.-F. Liang, S.-T. Liu and S.-I. Liu, A calibrated pulse generator for impulse-radio UWB applications. IEEE J Sol. State Circ. **41**(11) 2006

Chapter 4
Advanced Impulse Radio Techniques

In Chap. 3 impulse radio was defined and various modulations and a multiple access scheme were described. There are, however, a few shortcomings associated with these schemes. First, the power spectral density (PSD) of IR could be undesirable. For instance, TH-OOK spectral spikes could interfere with other spectrum users. Secondly, the IR performance in multipath fading could be poor. Multi-path fading channel model can be incorporated into the receiver to improve performance. Thirdly, the existing schemes do not provide a trade-off between performance and complexity. To address these issues some advanced techniques are introduced here. Initially, power spectrum of IR signal is determined and techniques to mitigate PSD are discussed. Then for operation in multipath environments rake receiver and transmitted reference (TR) modulation are proposed and studied. Next a scheme known as dual format modulation (DFM) that accommodates both simple and complex demodulators is described and its performance is evaluated. Lastly, three IEEE 802.15.4a, IEEE 802.15.6 and IEEE 802.15.4f standards that utilize various forms of impulse radio are described in some details.

4.1 Power Spectral Density

Consider TH-PPM, TH-OOK, and TH-BPSK modulation schemes. Let $x(t)$ be the pulse shape in all three modulation schemes. Additionally, assume that the duration of the utilized time hopping code is equal to that of the symbol. The PSD of these modulations are given below [1–3].

PPM:

$$G(f) = \frac{1}{4T^2}\sum_{n=-\infty}^{\infty}\left[\left|X\left(\frac{n}{T}\right)\right|^2\left|\sum_{k=0}^{N-1}e^{j2\pi(T_f k+c_k T_c)\frac{n}{T}}\right|^2\left(1+\cos\left(\frac{2\pi n\delta}{T}\right)\right)\delta\left(f-\frac{n}{T}\right)\right]$$
$$+\frac{1}{2T}|X(f)|^2\left|\sum_{k=0}^{N-1}e^{j2\pi\left(T_f k+c_k T_c\right)f}\right|^2(1-\cos(2\pi f\delta))$$

S. Emami, *UWB Communication Systems: Conventional and 60 GHz*,
DOI: 10.1007/978-1-4614-6753-3_4,

OOK:

$$G(f) = \frac{1}{2T^2}\sum_{n=-\infty}^{\infty}\left[\left|X\left(\frac{n}{T}\right)\right|^2\left|\sum_{k=0}^{N-1} e^{j2\pi(T_f k + c_k T_c)\frac{n}{T}}\right|^2 \delta(f-\frac{n}{T})\right] + \frac{1}{2T}|X(f)|^2\left|\sum_{k=0}^{N-1} e^{j2\pi\left(T_f k + c_k T_c\right)f}\right|^2$$

BPSK:

$$G(f) = \frac{1}{T}|X(f)|^2\left|\sum_{k=0}^{N-1} e^{j2\pi\left(T_f k + c_k T_c\right)f}\right|^2$$

where $X(f)$ is the Fourier transform of $x(t)$.

Spectrum of TH-PPM and TH-OOK consist of both continuous and discrete parts. The discrete part is made up of stream of delta functions with the spacing of $1/T$. These spectral lines (or delta functions) interfere with the other spectrum users. Contrary to TH-PPM and TH-OOK, TH-BPSK has a pure continuous PSD and does not have any spectral lines as evident in [1]

$$G(f) = \frac{1}{T}|X(f)|^2\left|\sum_{k=0}^{N-1} e^{j2\pi\left(T_f k + c_k T_c\right)f}\right|^2.$$

Spectral lines appear in PSD when (1) a non-antipodal modulation such as PPM and OOK is used or (2) symbols are not equiprobable in an antipodal modulation such as BPSK. The spectral lines can be eliminated, if symbol-based polarity randomization is introduced. Then the resulting PSD for both TH-PPM and TH-OOK becomes

$$G(f) = \frac{1}{T}|X(f)|^2\left|\sum_{k=0}^{N-1} e^{j2\pi\left(T_f k + c_k T_c\right)f}\right|^2.$$

Even in the absence of the spectral lines, PSD has a peak-to-average ratio due to variations. The penalty is paid in power back off. In the end, the transmission range of UWB device is shortened. It can be shown that infinite duration pulse-based polarity randomization eliminates the peak-to-average ratio. The resulting PSD would be [1]

$$G(f) = \frac{1}{T}|X(f)|^2.$$

Consequently, PSD is defined by the pulse spectrum alone. However, polarity randomization of infinite length is not practical. It has been demonstrated that pulse-based parity randomization over a finite number of symbols leads to mitigation of peak-to-average ratio and smoothing of the PSD [1].

In summary, pulse-based polarity randomization can eliminate spectral lines. Above and beyond that, if the utilized code is long, PSD approaches that of the used pulse. As for symbol-based polarity randomization, it too can eliminate spectral lines. Additionally, if it is deployed in conjunction with a long TH code (or a few short TH codes) it can mitigate peak-to-average ratio.

4.2 Rake Receiver

In multipath scenarios, signal reflections travel through different paths and arrive at the receiver end in different times with different gains.

$$r(t) = \sum_{k=1}^{N} a_k e^{j\phi_k} s(t - \tau_k) + n(t)$$

If the signal resolution far exceeds that of the channel, multipath signal components can be added up to improve performance [4]. Channel is estimated first, thus delays t_1, t_2, …, t_L and the gains associated with them are known. Then a correlation receiver is implemented for each path. At the end, these components are added up after proper weighting. The components can be added using EGC (equal gain combining) or MRC (maximal ratio combining). The rake receiver is shown in Fig. 4.1 in which each parallel path is called a finger.

In severe multipath environments, rake receiver might require a large number of fingers. As such, implementing a rake receiver might be too costly. In these

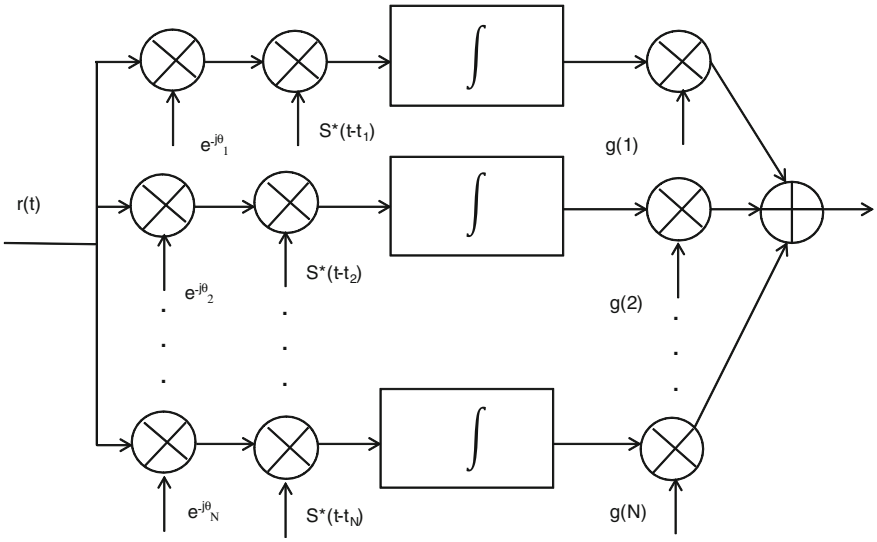

Fig. 4.1 Rake receiver structure

Table 4.1 Rake receiver variations

Rake type	Implemented fingers
All rake	All fingers
First L rake	The first L fingers
Best L rake	The L largest finger
Threshold rake	Fingers above a threshold

scenarios, one could use variations of rake receiver such as *all rake, first L rake, best L rake, or threshold rake*. All rake implements a full fledge rake receiver. In *first L rake*, the first L fingers of rake receiver are combined. *Best L rake* combines the fingers corresponding to the L largest samples of CIR. *Threshold rake* combines only the fingers that correspond to the CIR samples above a threshold. Note that rake variations require some processing upfront to select the finger that would be combined. However, at the end they reduce complexity. The rake receiver variations are listed in Table 4.1.

4.3 Transmit Reference Impulse Radio

Impulse radio collects the multipath energy and improves its performance through the utilization of Rake receiver. The number of multipath components in a rich multipath environment could be large (over 100 components). That leads to a large number of fingers in the rake structure. As such a Rake receiver implementation could be costly. The alternative is to deploy other variations of rake receiver such as selective Rake. However, the performance would be inferior to the Rake receiver. Transmit reference impulse radio (TR-IR), originally proposed by Hector and Tomlinson [5], harvests the multipath channel energy without resorting to channel estimation and the complex rake receiver structure.

The transmitter block diagram is shown in Fig. 4.2. Each bit is represented by two pulses, the reference pulse and the data pulse. The reference pulse is fixed throughout the transmission process. The actual data is contained in the data pulse. The main assumption is that channel does not change during a bit interval. Thus, both reference and data pulses experience the same channel in a bit interval.

In terms of performance, TR-IR is at least 6 dB inferior to the IR with an ideal Rake receiver. Since each bit is conveyed by two pulses, there is a 3 dB loss compared to conventional IR. The other 3 dB is due to noise in the reference signal. At the receiver, the data and reference pulse are multiplied by each other. The decision variable examines the sign of the product to make a decision.

Each frame of every bit is represented by one reference pulse and a data pulse separated by a delay of T_d. A TR-IR transmitted waveform is shown in Fig. 4.3. The transmitted waveform can be expressed as

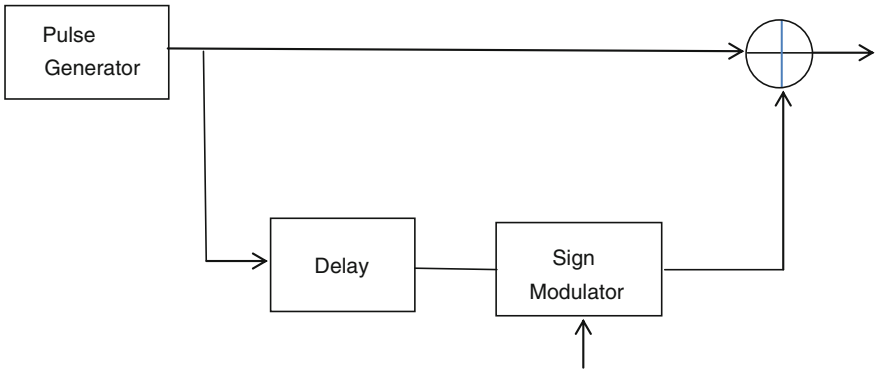

Fig. 4.2 TR-IR Transmitter block diagram

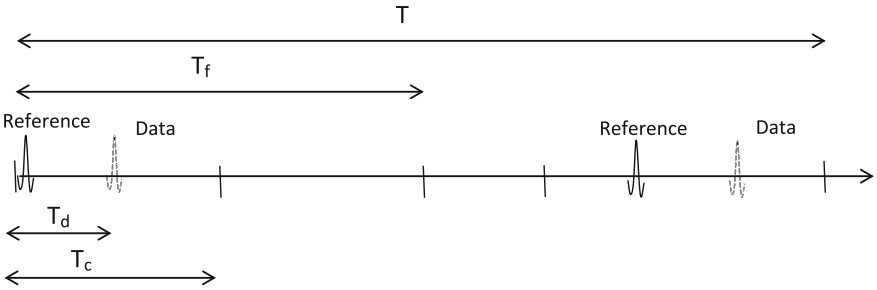

Fig. 4.3 In this TR-IR example there are two frames per bit and two chips per frame

$$s(t) = \sum_{i=0}^{\infty} \sum_{j=0}^{N_f - 1} \left[p(t - iT - jT_f - c_j T_c) + b_i p(t - iT - jT_f - c_j T_c - T_d) \right]$$

where b_i, c_j, and $p(t)$ are the ith modulation symbol, jth value of the PN sequence, and a UWB pulse, respectively. 0 and 1 are mapped into -1 and 1, respectively. The channel impulse response is given by

$$h(t) = \sum_{k=0}^{K} a_k \delta(t - \tau_k).$$

The received signal is modeled as

$$r(t) = s(t) * h(t) + n(t)$$

where $n(t)$ and * denote the zero mean noise AWGN with variance of σ^2 and convolution operation, respectively.

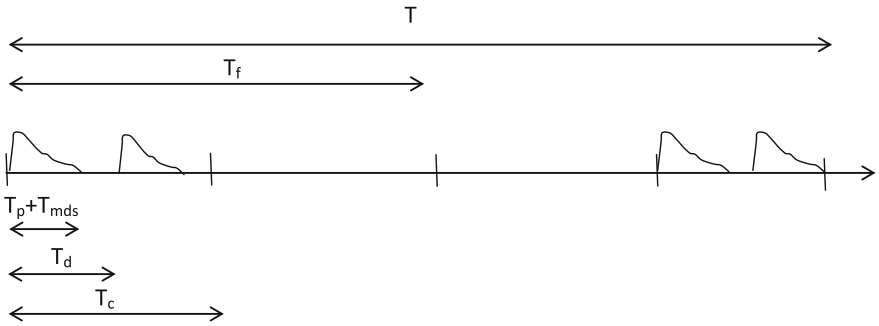

Fig. 4.4 The received TR-IR signal after going through the channel

Upon substitution for $s(t)$, we get

$$r(t) = \sum_{i=0}^{\infty} \sum_{j=0}^{N_f-1} \left[p(t - iT - jT_f - c_j T_c) * \sum_{k=0}^{K} a_k \delta(t - \tau_k) \right.$$
$$\left. + b_i p(t - iT - jT_f - c_j T_c - T_d) * \sum_{k=0}^{K} a_k \delta(t - \tau_k) \right] + n(t).$$

After some algebra, we end up with

$$r(t) = \sum_{i=0}^{\infty} \sum_{j=0}^{N_f-1} \left[g(t - iT - jT_f - c_j T_c) + b_i g(t - iT - jT_f - c_j T_c - T_d) \right] + n(t)$$

where

$$g(t) = \sum_{k=0}^{K} a_k p(t - \tau_k).$$

The length of $g(t)$ is equal to $T_p + T_{\text{mds}}$ where T_{mds} is the maximum delay spread of the channel. In a properly designed TR-IR system we need to make sure that

$$T_p + T_{\text{mds}} \leq T_d.$$

The situation is illustrated in Fig. 4.4.
At the receiver, the decision variable is given by

$$z_i = \sum_{j=0}^{N_f-1} \int_{iT+jT_f+c_j T_c+T_d}^{iT+jT_f+c_j T_c+T_d+T_I} r(t) r(t - T_d) \mathrm{d}t$$

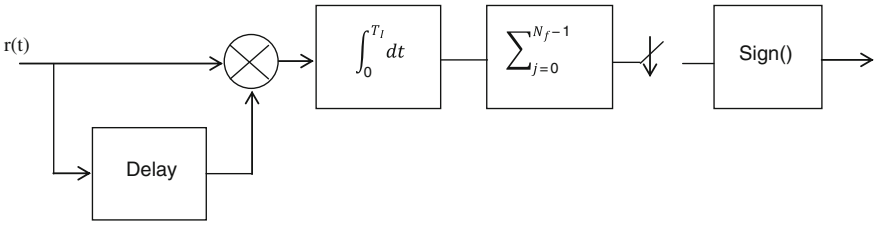

Fig. 4.5 TR-IR receiver block diagram

where T_I is greater than $T_p + T_{mds}$. Based on the sign of z_i, receiver decides whether 1 or 0 was transmitted (Fig. 4.5).

The received noisy reference signal limits the performance of TR-IR. However, it has been shown that performance can be improved when a cleaner estimate for reference signal is available [6]. Such a reference signal is obtained by averaging the reference signal over a bit interval. The approach is valid, if the channel remains invariant over bit duration.

4.4 Dual Format Modulation

With the aid of a rake receiver, the performance of IR in multipath approaches performance in AWGN. The flip side rake structures could be too complex to build. TR-IR has a simple structure, but suffers from a performance loss compared to conventional IR. The complexity that can be afforded depends on the usage scenarios. There are scenarios where receivers with different levels of complexity can be employed based on cost and service expectation. Thus, it is desirable to have a modulation scheme that can be demodulated either with a rake or a TR structure. Clearly, rake receiver delivers better performance.

The DFM scheme is a modulation that can be demodulated with either a TR-IR or a receiver equipped with Rake structure. In the remainder of this section we present the approach taken in [7]. The transmitted DFM-UWB signal is given by

$$s(t) = \sum_{i=0}^{\infty} \sum_{j=0}^{N_f-1} \left[b_{i-1} p\left(t - iT - jT_f - c_j T_c\right) + \left(\overline{b_{i-1} + b_i}\right) p\left(t - iT - jT_f - c_j T_c - T_d\right) \right]$$

where b_i, c_j, and $p(t)$ are the ith modulation symbol, jth value of the PN sequence, and a UWB pulse, respectively. Logics 0 and 1 are mapped into -1 and 1, respectively (Fig. 4.6).

An examination of Table 4.2 demonstrates that is similar to TR-IR, phase difference between the reference and data pulse determines the current bit. Thus, a TR-IR correlation receiver can be utilized to demodulate the stream.

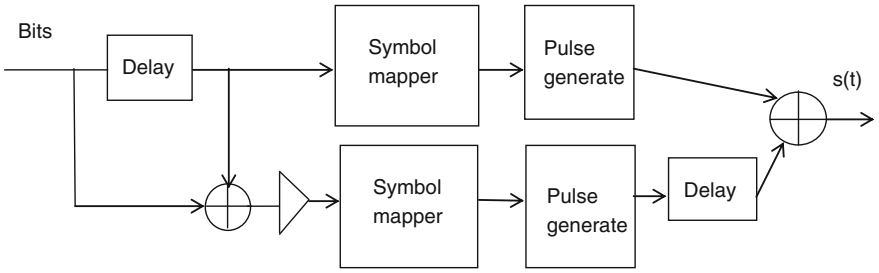

Fig. 4.6 Dual format transmitter block diagram

Table 4.2 Phase difference between the reference and data pulse

Previous bit	Current bit	Reference pulse b_{i-1}	Data pulse $\overline{b_{i-1} + b_i}$	Phase difference (degrees)
0	0	−1	1	180
0	1	−1	−1	0
1	0	1	−1	180
1	1	1	1	0

Within each frame, one of the following signals is transmitted:

$$s_0(t) = -1\left(\frac{p(t)}{\sqrt{2N_f E_p}}\right) + 1\left(\frac{p(t-T_d)}{\sqrt{2N_f E_p}}\right)$$

$$s_1(t) = -1\left(\frac{p(t)}{\sqrt{2N_f E_p}}\right) - 1\left(\frac{p(t-T_d)}{\sqrt{2N_f E_p}}\right)$$

$$s_2(t) = 1\left(\frac{p(t)}{\sqrt{2N_f E_p}}\right) - 1\left(\frac{p(t-T_d)}{\sqrt{2N_f E_p}}\right)$$

$$s_3(t) = 1\left(\frac{p(t)}{\sqrt{2N_f E_p}}\right) + 1\left(\frac{p(t-T_d)}{\sqrt{2N_f E_p}}\right)$$

where is E_p the energy associated with pulse $p(t)$. Since $p(t)$ and $p(t - T_d)$ are orthogonal pulses, the above signals are two-dimensional signals and can be represented as the following vectors:

$$s_0 = [-1 \quad 1]$$
$$s_1 = [-1 \quad -1]$$
$$s_2 = [1 \quad -1]$$
$$s_3 = [1 \quad 1]$$

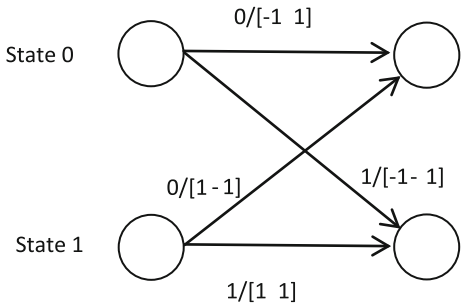

Fig. 4.7 Two-state Trellis

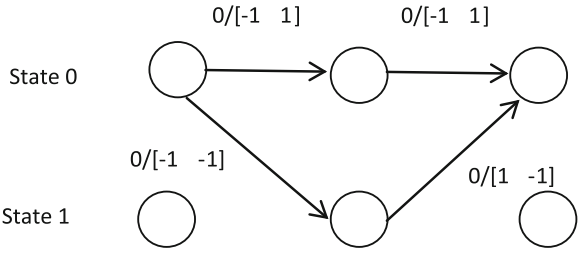

Fig. 4.8 Euclidean distance calculation

These vectors define a two-state trellis diagram as shown in Fig. 4.7. A state indicates the value of the previous bit. The signals in BPSK and TR-IR constellations can be represented by $\{-\sqrt{E}, \sqrt{E}\}$ and $\left\{-\sqrt{E/2}, \sqrt{E/2}\right\}$ (E = 2Ep), respectively. As such they have the Euclidean distance of $d_{\text{BPSK}} = 2\sqrt{E}$ and $d_{TR} = \sqrt{2E}$. In the trellis, the minimum Euclidean distance between any two signals that depart from a state and merge again at the same state is given by $\sqrt{d_{\text{BPSK}}^2 + d_{\text{TR}}^2} = \sqrt{6E}$ as illustrated in Fig. 4.8.

Consequently, this hybrid scheme is 4.76 dB superior to TR-IR or 1.76 dB superior to uncoded BPSK.

4.5 IEEE 802.15.4a

The original IEEE 802.15.4, released in 2003, is based on direct sequence spread spectrum DS-SS technology and operates in 868 MHz (Europe), 915 MHz (US), and 2.4 GHz (worldwide) bands. Ranging operation and data rates beyond 250 kbps are not supported in IEEE 802.15.4. These shortcomings led to the development of IEEE 802.15.4a. Two different physical layers namely chirp spread spectrum and UWB are supported by IEEE 802.14.4a [8]. Chirp spread spectrum is beyond our scope. Here we will focus on the UWB piece of the PHY.

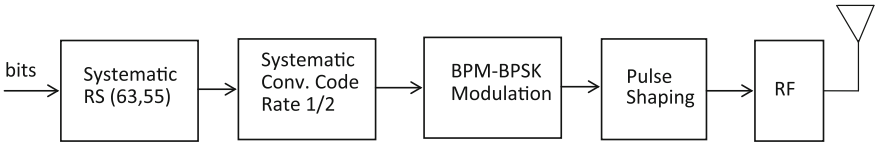

Fig. 4.9 Transmitter block diagram

4.5.1 The Transmitter

The transmitter block diagram is drawn in Fig. 4.9. The forward error correction scheme is a concatenated code made of an outer Reed-Solomon (RS) code and an inner convolutional code. Both codes are systematic. The bit stream is encoded using rate 0.873 RS (63, 55) and rate ½ convolutional codes. The encoded stream is then passed on to the modulation block. Finally, the modulated block output is pulse shaped and transmitted over the channel.

The systematic RS (63, 55) code takes a block of $55 \times 6 = 330$ bits (as each symbol is 6 bits long) and attaches 48 bits to the block. Then, the systematic rate ½ convolutional encoder, with the generator polynomials of $g_0 = [010]$ and $g_1 = [101]$, attaches another $330 + 48$ bits to the stream. The information bit and the redundancy bits are mapped into burst position and polarity, respectively.

4.5.2 Modulation

The standard utilizes an IR scheme for modulation which is a combination of BPM (burst position modulation) and BPSK. There is a small difference between BPM and the conventional PPM. In BPM, unlike PPM, each bit is represented by a pulse burst as opposed to a single pulse. A data symbol is shown in Fig. 4.10. Low peak voltages preferred in CMOS can be accommodated when utilizing a pulse burst as opposed to a single pulse.

If a burst is transmitted in the first half of the symbol it represents "0". Otherwise, if the burst is sent during the second half of the symbol it represents "1". The sign (polarity) of the pulse burst carries another bit of information. However, this information bit is redundant and it is obtained from a systematic convolutional of rate ½. As such both coherent and non-coherent demodulators can be used. A non-coherent demodulator receives just the burst position information. Coherent demodulator recovers the sign of the pulse burst as well. Clearly, coherent modulator will be superior in terms of performance.

The transmitted signal is given by the following mathematical expression:

$$x(t) = (1 - 2b_1) \sum_{n=0}^{N_{cpb}-1} (1 - 2s_n)\, p(t - b_0 T_{BPM} - cT_{burst} - nT_c)$$

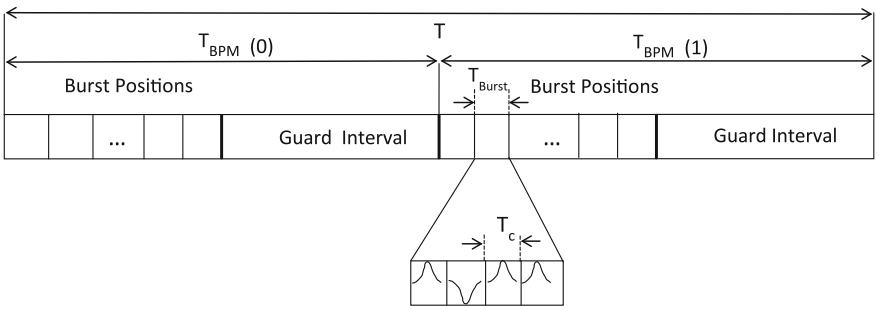

Fig. 4.10 IEEE 802.15.4a data symbol details

where b_0, b_1, s_n, and c denote the bit that determines the burst position, the bit that determines burst polarity, random scrambling code, and the burst hopping position, respectively. The scrambling code (sn) and the burst hopping position (c) belong to $\{0, 1\}$ and $\{0, 1, 2,\ldots, N_{\text{hop}} - 1\}$, respectively.

Each symbol is divided into T_{BPM} intervals. To enable multiple access via time hopping, each T_{BPM} interval is further divided into a number of slots or burst positions. Each burst represents a symbol and is made of a number of chips. Within a chip a single pulse is placed. Each chip is 2.003 ns long. The guard intervals are there to eliminate ISI.

4.5.3 Pulse Shape

A reference pulse is defined as

$$r(t) = -\frac{4\beta}{\pi\sqrt{T_p}} \frac{\cos[(1+\beta)\pi t/T_p] + \frac{\sin[(1-\beta)\pi t/T_p]}{4\beta(t/T_p)}}{\left(4\beta t/T_p\right)^2 - 1}$$

where T_p is the pulse length and $\beta = 0.6$. The normalized cross-correlation between $r(t)$ and any other waveform $p(t)$ is

$$\varphi(\tau) = \frac{1}{\sqrt{E_r E_p}} \int_{-\infty}^{\infty} r(t) p^*(t+\tau)$$

where E_r and E_p are the energies associated with $r(t)$ and $p(t)$, respectively. Pulse $p(t)$ is considered standard compliant, if it satisfies two conditions. First, the main lobe of the (absolute value of) cross-correlation function remains larger than 0.8 for at least T_w ns. Second, the (absolute value of) cross-correlation side lobes should be smaller than (or equal to) 0.3. Parameters are channel dependent and are listed in Table 4.3.

Table 4.3 Parameters of the reference and compliant pulse shapes

Channel number	T_p (ns)	T_w (ns)
0,1,2,3,5,6,8,9,10,12,13,14	2	0.5
7	0.92	0.2
4, 11	0.75	0.2
15	0.74	0.2

Table 4.4 IEEE 802.15.4a band plan

Channel number/type	Center frequency (MHz)	Bandwidth (MHz)
0/sub-gigahetrz	499.2	499.2
1/Low	3494.4	499.2
2/Low	3993.6	499.2
3/Low	4492.8	499.2
4/Low	3993.6	1331.2
5/High	6489.6	499.2
6/High	6988.8	499.2
7/High	6489.6	1081.6
8/High	7488.0	499.2
9/High	7987.2	499.2
10/High	8486.4	499.2
11/High	7987.2	1331.2
12/High	8985.6	499.2
13/High	9484.8	499.2
14/High	9984.0	499.2
15/High	9484.8	1354.97

4.5.4 Band Plan

There are a total of 16 channels in the band plan. They are divided into three bands, namely the sub-gigahertz band, the low band, and the high band. The ranges associated with these three bands are 249.6–748.8, 3,244.8–4,742.4, and 5,948.8–1,023.4 MHz, respectively.

Channels, band types, their center frequencies, and 3-dB bandwidth are listed in Table 4.4. Out of 16 channels, 12 are roughly 500 MHz wide. The remaining channels (4, 7, 11, and 15) are 1,331.2, 1,081.6, 1,331.2, and 1,354.97 MHz wide. A graphical representation of the band plan is provided in Fig. 4.11.

UWB devices can choose to implement any one of the three bands. If a device chooses to implement sub-gigahertz band, support for channel 0 is mandatory. If a device chooses to implement the low band, support for channel 3 is mandatory. If a device chooses to implement the high band, support for channel 9 is mandatory. All other bands are considered optional. There are a total of 32 complex channels. A device would be standard compliant if the two complex channels in a mandatory band are implemented.

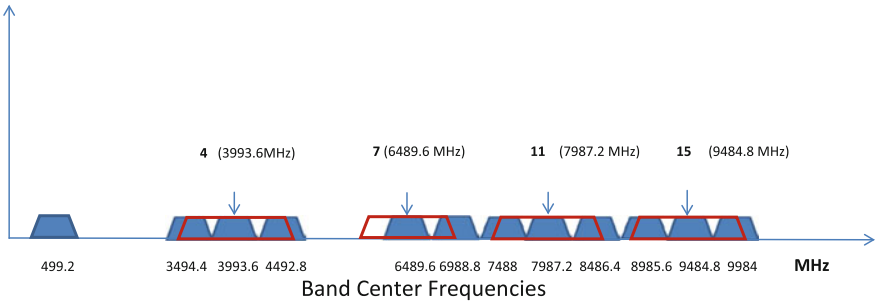

Fig. 4.11 Graphical representation of 802.15.4a band plan

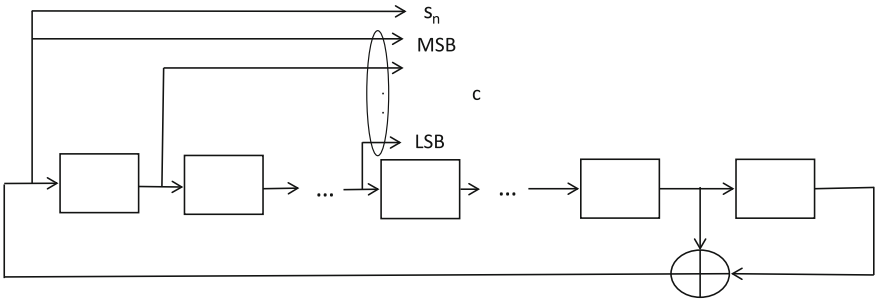

Fig. 4.12 The LFSR structure, the scrambling code, and the hopping position code

The 500 MHz wide channels are expected to provide range measurements with the accuracy of about 1 m. Higher level of accuracy can be obtained by utilizing one of the four wider channels (4, 7, 11, and 15). If used for data communications, these wider bands offer larger ranges compared to 500 MHz wide channels.

4.5.5 Scrambling and Hopping Codes

A common scrambler with the generator polynomial

$$g(D) = 1 + D^{14} + D^{15}$$

can be used to generate both the scrambling code and hopping position code as shown in Fig. 4.12. While polarity scrambling code is only a bit long, the hopping sequence picks up as many bits as required by the selected data rate (1, 3, or 5 bits) from the LFSR.

4.5.6 Data Rates

Let us examine Fig. 4.10 again. Symbol period consists of N_c chips

$$T = N_c T_c$$

where N_c and T_c denote number of chips per symbol and chip duration, respectively. BPM period is by definition

$$T_{\text{BPM}} = {}^{T}/_{2}.$$

Each pulse burst consists of N_{cpb} back-to-back chips or in other words,

$$T_{\text{burst}} = N_{\text{cpb}} T_{c.}$$

The total number of burst positions is computed in the following fashion:

$$N_{\text{burst}} = {}^{T}/_{T_{\text{burst}}}.$$

The number of hops is related to the total number of burst positions through

$$N_{\text{hop}} = {}^{N_{\text{burst}}}/_{4}$$

as only a quarter of the symbol duration can accommodate time hopping.

Finally, IEEE 802.15.4a data rates can be computed using the following expression:

$$\text{Data Rate} = 2 \times \text{RS code rate} \times \text{Convolutional code rate} \times \left(\frac{1}{T}\right).$$

In some cases convolutional coding is bypassed. In these situations we substitute 1 for the rate. Table 3.8 lists the data rates for different channels.

For instance, let us compute the data rates for channel 7 as follows:

$$\begin{aligned}
\text{Data rate} &= 2 \times 0.873 \times 0.5 \times (1/(2.003\text{e} - 9 \times 4096)) \sim 0.11 \text{ Mbps} \\
\text{Data rate} &= 2 \times 0.873 \times 0.5 \times (1/(2.003\text{e} - 9 \times 512)) \sim 0.85 \text{ Mbps} \\
\text{Data rate} &= 2 \times 0.873 \times 0.5 \times (1/(2.003\text{e} - 9 \times 64)) \sim 6.81 \text{ Mbps} \\
\text{Data rate} &= 2 \times 0.873 \times 0.5 \times (1/(2.003\text{e} - 9 \times 16)) \sim 27.24 \text{ Mbps} \\
\text{Data rate} &= 2 \times 0.873 \times 1 \times (1/(2.003\text{e} - 9 \times 32)) \sim 27.24 \text{ Mbps.}
\end{aligned}$$

It is evident from Table 4.5 that most data rates (such as 0.11 Mbps option in channel 7) can be implemented with more than one set of parameters. However, these options have different characteristics. The option with larger N_{cpb} leads to a longer operating range. On the other hand, more users can be supported with the option with smallest N_{cpb}. Furthermore, larger N_{cpb} option is appropriate for coherent receivers operating in high delay spread environments. Non-coherent receivers operating in environments with high delay should use smallest N_{cpb} option.

Table 4.5 IEEE 802.15.4a data rates

Channel number	Data rate (Mbps)	FEC	N_c, N_{cpb}, N_{hop}
0,1,2,3,5,6,8,9,10,12,13,14	0.11	RS, Conv.	4096,128,8
		RS, Conv.	4096,32,32
		RS, Conv.	4096,512,2
0,1,2,3,5,6,8,9,10,12,13,14	0.85	RS, Conv.	512,16,8
		RS, Conv.	512,4,32
		RS, Conv.	512,64,2
0,1,2,3,5,6,8,9,10,12,13,14	6.81	RS, Conv.	64,2,8
		RS	128,1,32
		RS, Conv.	64,8,2
0,1,2,3,5,6,8,9,10,12,13,14	1.7	RS, Conv.	256,2,32
0,1,2,3,5,6,8,9,10,12,13,14	27.24	RS	32,1,8
		RS, Conv.	16,2,2
4,11	0.11	RS, Conv.	4096,128,8
		RS, Conv.	4096,512,2
4,11	0.85	RS, Conv.	512,16,8
		RS, Conv.	512,64,2
4,11	6.81	RS, Conv.	64,2,8
		RS, Conv.	64,8,2
4,11	27.24	RS	32,1,8
		RS, Conv.	16,2,2
7	0.11	RS, Conv.	4096,128,8
		RS, Conv.	4096,512,2
7	0.85	RS, Conv.	512,16,8
		RS, Conv.	512,64,2
7	6.81	RS, Conv.	64,2,8
		RS, Conv.	64,8,2
7	27.24	RS	32,1,8
		RS, Conv.	16,2,2
15	0.11	RS, Conv.	4096,128,8
		RS, Conv.	4096,512,2
15	0.85	RS, Conv.	512,16,8
		RS, Conv.	512,64,2
15	6.81	RS, Conv.	64,2,8
		RS, Conv.	64,8,2
15	27.24	RS, Conv.	32,1,8
		RS	16,2,2

4.6 IEEE 802.15.6

There are two operational modes in the standard known as the default and high quality of service (QoS) modes. While the default mode is targeted for medical and non-medical applications, high QoS mode is intended for high priority medical applications. The standard defines both UWB and narrow band PHYs. Here our coverage is limited to the UWB PHY option. Table 4.6 defines mandatory and optional modulations for the two modes of 802.15.6 PHY [9].

Table 4.6 IEEE 802.15.6 UWB PHY

Mode	Mandatory modulation	Optional modulation
Default	Impulse radio (IR) with on–off signaling	FM
High QoS	Impulse radio (IR) with DBPSK/DQPSK	NA

4.6.1 Transmitter Components

The scrambler, the error correction codes, and the interleaver used in the standard are described here.

4.6.1.1 Scrambler

A scrambler with the following generator polynomial:

$$g(D) = 1 + D^2 + D^{12} + D^{13} + D^{14}$$

is utilized where D is a single bit delay element. Scrambler and descrambler should both start from the same state. The scrambler seed value is specified in the PHY header of the received frame.

4.6.1.2 Error Correction Codes

The default and high QoS modes utilize BCH (63, 51) and BCH (126, 63) codes, respectively. The generator polynomial for the systematic BCH codes (63, 51) is given by

$$g(x) = 1 + x^3 + x^4 + x^5 + x^8 + x^{10} + x^{12}.$$

BCH (126, 63) code is a shortened code and is implemented from BCH (127, 64) with the generator polynomial specified by

$$\begin{aligned} g(x) = 1 &+ x^2 + x^5 + x^{15} + x^{18} + x^{19} + x^{21} + x^{22} + x^{23} + x^{24} + x^{25} + x^{26} + x^{30} \\ &+ x^{31} + x^{32} + x^{33} + x^{35} + x^{36} + x^{38} + x^{40} + x^{47} + x^{48} + x^{49} + x^{51} \\ &+ x^{53} + x^{55} + x^{56} + x^{61} + x^{63}. \end{aligned}$$

To implement the shortened code, a single zero bit is appended to 63 bits of information to construct a 64 bit message block. The message is encoded using BCH (127, 64) block code. The one bit in the systematic portion of the codeword is removed and the remaining 126 encoded bits are transmitted.

Table 4.7 Defined mapping ($K = 4$)

(b_0, b_1, b_2, b_3)	$(d_0, d_1, \ldots, d_7)$
0000	00001111
0001	00010111
0010	00110011
0011	00011011
0100	01011010
0101	00111100
0110	01010101
0111	01100110
1000	01101001
1001	10011001
1010	10010110
1011	10100101
1100	10101010
1101	11000011
1110	11001100
1111	11110000

4.6.1.3 Bit Interleaver

The standard uses an algebraic interleaver to minimize the impact on complexity and latency. The new position to which index n is permuted is defined following modulo-N arithmetic expression

$$\Pi(n) = nb \; mod \; N$$

where N is the interleaver length, $\Pi(n)$ is an integer between 0 and $N - 1$ (inclusive), b is a relative prime to N, $N = 192$, and $b = 37$. If the total number of bits at the input to the interleaver (N_T) is not an integer multiple of N, then in the last block we set $N = rem(N_T, N)$, where *rem* represents the remainder of the integer division.

4.6.2 Modulation Choices

IEEE 802.15.6 UWB PHY supports IR and FM-UWB modulations. IR is implemented with (1) on–off signaling and (2) DBPSK/DQPSK modulations. Unlike IR, FM-UWB is a continuous signal. The on–off signaling IR here has a structure

Table 4.8 Defined mapping ($K = 1$)

b_0	(d_0, d_1)
0	10
1	01

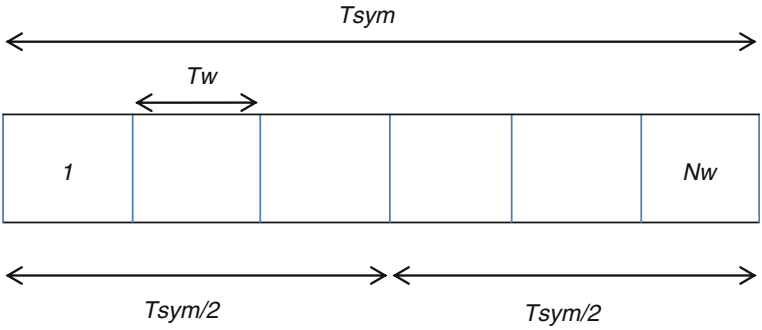

Fig. 4.13 The symbol structure for on–off signaling impulse radio

similar to BPM-BPSK IR in IEEE 802.15.4a. All three modulation choices are described here.

4.6.2.1 On–Off Signaling Impulse Radio

A mapping from groups of K information bits denoted as $(b_0, b_1,\ldots, b_{K-1})$ from an alphabet of size $M = 2^K$ into groups of $2K$ bits denoted as $(d_0, d_1, \ldots, d_{2K-1})$ of the same alphabet size is defined such that the minimum Hamming distance between the resulting bit group members is maximized. The mapping for $K = 4$ and $K = 1$ are provided in Tables 4.7 and 4.8. Note that $K = 1$ mapping is optional.

The resulting bit groups are encoded using the symbol structure shown in Fig. 4.13. To accommodate on–off signaling, similar to IEEE 802.15.4a the symbol interval is divided into two equal segments. Only one single slot is used at a time. The extra slots are there to support time hopping required for multi-user operation. As such the associated duty cycle is given by T_w/T_{sym} ratio and to be kept around 3 %.

The mth symbol of the transmitted IR with on–off signaling modulation using the burst pulse option, when input bit is one, is given by

$$x^m(t) = \sum_{n=0}^{2K-1} d_n^m w_{2Km+n}\left(t - n\left(\frac{T_{\text{sym}}}{2}\right) - mKT_{\text{sym}} - h^{2Km+n}T_w\right)$$

where d_n^m is the nth component of the mth symbol, $h^{(j)}$ is the time hopping sequence, s_i denotes static scrambling of the burst pulse and the burst pulse is defined as

$$w_n(t) = \sum_{i=0}^{\text{Ncpb}-1} (1 - 2s_i)p\left(t - iT_p\right).$$

Table 4.9 DBPSK bit onto ϕ_M mapping

g_m	ϕ_{M+1}
0	0
1	π

Table 4.10 DQPSK bits onto ϕ_M mapping

g_m	g_m	ϕ_{M+1}
1	1	$\pi/2$
0	1	π
0	0	$-\pi/2$
1	0	0

4.6.2.2 DBPSK/DQPSK Impulse Radio

The differentially encoded symbols are given by

$$c_m = c_{m-1}\exp(j\emptyset_m)$$

where c_m denotes the mth differentially encoded BPSK or QPSK symbol and $m = (1, 2,\ldots, N)$. Symbol c_0 with amplitude of unity and an arbitrary phase value is used as the reference symbol in the encoder. The bit onto ϕ_M mappings are defined in Tables 4.9 and 4.10.

Once the differential symbols are generated, they are encoded using the symbol structure shown in Fig. 4.14. Only one single slot is used at a time. The extra slots are there to support time hopping required for multi-user operation. The duty cycle, given by T_w/T_{sym} ratio, is kept around 3 %.

The transmitted IR signal with DBPSK/DQPSK modulation is described by

$$x(t) = \sum_{m=0}^{N-1} c_m w(t - mT_{\text{sym}} - h_m T_w)$$

and

$$w(t) = \sum_{i=0}^{N_{\text{cpb}}-1} (1 - 2s_i)p(t - iT_p)$$

where h_m and s_i denote time hopping sequence, and static scrambling of the burst pulse, respectively.

4.6.2.3 FM-UWB

Analog FM signal with a wide modulation index can be used to generate UWB signals. The bandwidth of FM signal depends not only on bandwidth of the

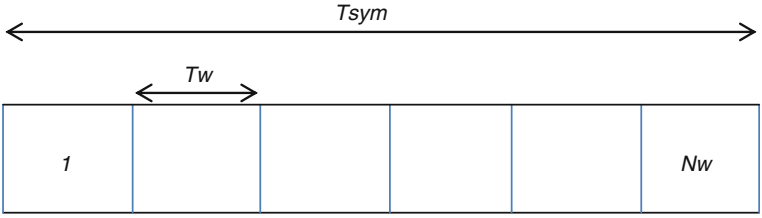

Fig. 4.14 The symbol structure for DBPSK/DQPSK impulse radio

modulating signal but on the FM modulation index as well. As such a large modulation index ($\beta \gg 1$) can be used to occupy an ultrawide bandwidth.

To generate the transmitted signal, FM-UWB concatenates CP-FSK with wideband FM to generate the transmitted signal. Initially, the bit stream (g_0, g_1,…, g_{P-1}) is converted to $b(t)$ waveform using

$$b(t) = \sum_m (1 - 2g_m) p(t - mT_{\text{sym}})$$

where $p(t)$ is a Gaussian pulse with time bandwidth product of 0.8. The subcarrier signal is given by

$$s(t) = VS\left[2\pi f_{\text{sub}} t + 2\pi \Delta f_{\text{sub}} \int_{-\infty}^{t} b\left(t'\right) dt' + \emptyset_0\right]$$

where V, $S(t)$, β_{sub}, T_{sym}, Δf_{sub}, and ϕ_0 denote the amplitude, modulating carrier, modulation index, symbol time, peak frequency deviation, and the initial carrier phase, respectively. The carrier can be triangular. Sinusoidal and sawtooth carriers are acceptable as well.

Subsequently, FM-UWB signal is specified by

$$V(t) = A\sin\left[2\pi f_c t + 2\pi \Delta f \int_{-\infty}^{t} s\left(t'\right) \mathrm{d}t'\right]$$

where Δf, $\mathrm{K_o}$, $\mathrm{f_m}$, β denote peak frequency deviation, RF oscillator sensitivity (in rad/v), highest present in $s(t)$ and modulation index, respectively. Note that $\beta = \Delta f / f_m$ and $\Delta f = \mathrm{K_o}.\mathrm{V}$.

Standard utilizes subcarrier frequency of 1.5 MHz, subcarrier bandwidth of 800 kHz, subcarrier modulation index of unity, and FM modulation index of 130.5 to support data rate of 202.5 kbps.

4.6.3 Pulse Shaping

Here, the pulse choices for on–off signaling and DBPSK/DQPSK IR options are defined. One can either use a single pulse denoted by $p(t)$ with duration of $T_w = T_p$. Alternatively, a pulse burst can be utilized denoted by

$$\sum_{i=0}^{\text{Ncpb}-1} p(t - iTw)$$

where $T_w = Ncpb\, T_p$.

As for the pulse shape, there is no mandatory one. Instead the standard provides a few options consisting of short pulse, chirp pulse, and chaotic pulse.

4.6.3.1 Short Pulse Shape

Pulse $p(t)$ is considered standard compliant, if the normalized cross correlation of it with a reference pulse is larger than 0.8 in the main lobe. The normalized cross correlation between $r(t)$, reference pulse, and a pulse $p(t)$ is

$$\varphi(\tau) = \frac{Re}{\sqrt{E_r E_p}} \left\{ \int_{-\infty}^{\infty} r(t) p^*(t+\tau) \right\}$$

where E_r and E_p are the energies associated with $r(t)$ and $p(t)$, respectively. The reference (root raised cosine) is given by

$$r(t) = \begin{cases} 1 - \beta + 4\frac{\beta}{\pi} & t = 0 \\ \frac{\beta}{\sqrt{2}} \left[\left[1 + \frac{2}{\pi}\right] \sin\left(\frac{\pi}{4\beta}\right) + \left[1 - \frac{2}{\pi}\right] \cos\left(\frac{\pi}{4\beta}\right) \right] & t = \pm\frac{T}{4\beta} \\ \frac{\sin[(1-\beta)\pi t/T] + 4\beta\left(\frac{t}{T}\right)\cos[(1+\beta)\pi t/T]}{\pi\frac{t}{T}\left[1-\left(4\beta\frac{t}{T}\right)^2\right]} & \textit{elsewhere} \end{cases}$$

where $\beta = 0.5$ and $T = 1/499.2$ MHz.

4.6.3.2 Chirp Pulse Shape

Chirp pulse shape in baseband complex representation is specified by

$$p(t) = \Psi(t) \exp[j(2\pi \int_{-Tw/2}^{t} f_i(t')dt' + \theta_0)]$$

Table 4.11 UWB PHY low band allocation

Channel number	Central frequency (MHz)	Bandwidth (MHz)	Channel attribute
1	3494.4	499.2	Optional
2	3993.6	499.2	Mandatory
3	4492.8	499.2	Optional

Table 4.12 UWB PHY high band allocation

Channel number	Central frequency (MHz)	Bandwidth (MHz)	Channel attribute
4	6489.6	499.2	Optional
5	6988.8	499.2	Optional
6	7488.0	499.2	Optional
7	7987.2	499.2	Mandatory
8	8486.4	499.2	Optional
9	8985.6	499.2	Optional
10	9484.8	499.2	Optional
11	9984.0	499.2	Optional

where θ_0 and $\psi(t)$ and $f_i(t)$ are an arbitrary constant phase, a window function defined for $-\frac{T_w}{2} \leq t \leq \frac{T_w}{2}$ and instantaneous chirp frequency given by $K_c t + f_{\text{error}}(t)$, respectively. If the instantaneous frequency error function ($f_{\text{error}}(t)$) is set to zero where one ends up with a linear up chirp given by

$$p(t) = \Psi(t) \exp\left(2\pi j\left(\frac{K_c}{2}t^2 + \Theta_0\right)\right)$$

where $K_c = \Delta f / T_w$ is the chirp slope, θ_i is an initial phase shift, $\Delta f = 520$ MHz is the chirp frequency sweep, and $T_w = 64$ nsec is the pulse duration.

4.6.3.3 Chaotic Pulse Shape

Chaotic signal in baseband complex representation is specified by

$$p(t) = \exp[2\pi j \int_{-Tw/2}^{t} f_i\left(t'\right) dt']$$

where $f(t)$, instantaneous frequency sweep, consists of the sum of a number of sawtooth or triangular waveforms and T_w is the pulse waveform duration. These pulses are constant envelope type as they are obtained through frequency modulation.

Table 4.13 Data rates for on–off signaling

PRF (MHz)	N_w	N_{hop}	T_w (ns)	T_{sym} (ns)	FEC rate	Bit rate (MHz)	N_{cpb}
0.487	32	16	64.103	2051.300	0.81	0.3948	32
0.975	32	16	32.051	1025.600	0.81	0.7897	16
1.950	32	16	16.026	512.820	0.81	1.579	8
3.900	32	16	8.012	256.410	0.81	3.159	4
7.800	32	16	4.006	128.210	0.81	6.318	2
15.600	32	16	2.003	64.103	0.81	12.636	1

Table 4.14 Data rates for DBPSK/DQPSK

PRF (MHz)	N_w	N_{hop}	T_w (ns)	T_{sym} (ns)	Spreading factor	FEC rate	Bit rate (MHz)	N_{cpb}
0.487	32	32	64.103	2051.300	1	0.5	0.243	32
0.975	32	32	32.051	1025.600	1	0.5	0.457	16
1.950	32	32	16.026	512.820	1	0.5	0.975	8
3.900	32	32	8.012	256.410	1	0.5	1.950	4
7.800	32	32	4.006	128.210	1	0.5	3.900	2
7.800	32	32	4.006	128.210	1	0.5	7.800	2
3.906	32	32	8.012	1794.900	7	0.5	0.278	4
3.906	32	32	8.012	1794.900	7	0.5	0.557	4

4.6.4 Band Plan

Band plan consists of 499.2 MHz wide channels in both low and high bands. There are three channels in the low band and eight channels in the high band. There is one mandatory channel in each band, while others are optional. The UWP PHY low and high band channel definitions are given in Tables 4.11 and 4.12.

4.6.5 Data Rates

Data rates for on–off signaling and DBPSK IR can be computed using the following expression:

$$\text{Data Rate} = \text{FEC code rate} \times \left(\frac{1}{T_{\text{sym}}}\right).$$

On the other hand, data rate for DQPSK IR option is given by

$$\text{Data Rate} = \text{FECcode rate} \times \left(\frac{2}{T_{\text{sym}}}\right).$$

For instance, let us compute the data rates for on–off signaling

$$\begin{aligned}
\text{Data rate} &= 0.81 \times (1/(2048\text{e}-9)) \sim 0.3955 \text{ Mbps} \\
\text{Data rate} &= 0.81 \times (1/(1024\text{e}-9)) \sim 0.791 \text{ Mbps} \\
\text{Data rate} &= 0.81 \times (1/(512\text{e}-9)) \sim 1.58 \text{ Mbps} \\
\text{Data rate} &= 0.81 \times (1/(256\text{e}-9)) \sim 3.16 \text{ Mbps} \\
\text{Data rate} &= 0.81 \times (1/(129\text{e}-9)) \sim 6.3281 \text{ Mbps} \\
\text{Data rate} &= 0.81 \times (1/(64\text{e}-9)) \sim 12.656 \text{ Mbps.}
\end{aligned}$$

Data rates for on–off signaling and DBPSK/DQPSK are provided in Tables 4.13 and 4.14.

4.7 IEEE 802.15.4f

The UWB PHY in IEEE 802.15.4f, low rate PRF UWB (LRP-UWB), strives to enable transmitters with very little complexity. Features such as simple modulations, no scrambling, simple pulse shaping, no dithering, low pulse repetition frequency (PRF), and relaxed temporal requirements have been incorporated into the standard [10].

4.7.1 Transmitter Components

4.7.1.1 Scrambler

In an attempt to make the standard very simple, no scrambling is implemented in the standard.

4.7.1.2 Error Correction Codes

Error correction coding is not utilized in the base and the long-range modes. However, the extended mode deploys a convolutional code rate ¼ with the octal generator representation (5,7,7,7) and constraint length ($k = 3$).

4.7.1.3 Bit Interleaver

In an attempt to make the standard very simple, no interleaving is implemented in the standard.

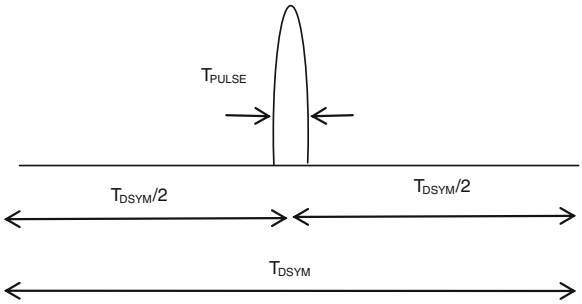

Fig. 4.15 Base mode LRP UWB PHY symbol structure

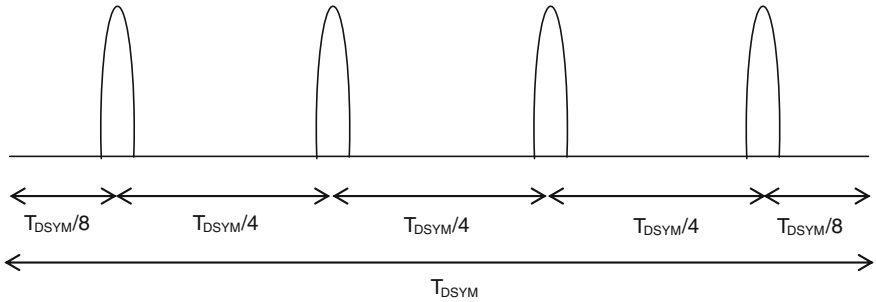

Fig. 4.16 Extended mode LRP UWB PHY symbol structure

4.7.2 Modulation Choices

The UWB, PHY, LRP-UWB consists of three modes. These modes implement IR with different modulations.

4.7.2.1 Base Mode

The base mode utilizes an IR with OOK. One bit of information is communicated by the virtue of presence or absence of a narrow pulse in the middle of symbol time. To encode a binary 1, a single pulse is transmitted. On the contrary, no pulse is transmitted to encode binary 0. The symbol structure is depicted in Fig. 4.15. Symbol and pulse durations are denoted by T_{DSYM} and T_{CHIP}, respectively. Among all the modes, base mode provides the highest data rate.

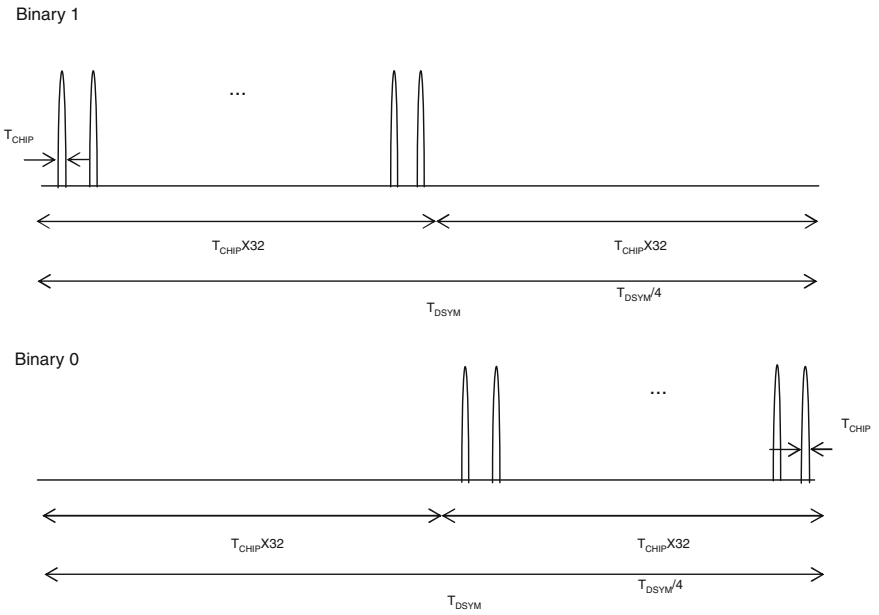

Fig. 4.17 Long-range mode LRP UWB PHY symbol structure

4.7.2.2 Extended Mode

Information bit stream is encoded using rate ¼ convolutional code with constraint length of three ($k = 3$) and octal generator polynomial representation of (5,7,7,7). The symbol structure is shown in Fig. 4.16. Similar to the base mode, IR with OOK is utilized here. However, this mode trades data rate for extra sensitivity. As such it provides a lower data rate compared to the base mode at the expense of increased sensitivity.

4.7.2.3 Long-Range Mode

Impulse radio with 2PPM is used in the long-range mode. Binary symbol structure is presented in Fig. 4.17. Each symbol is 64 chips long. In other words $T_{\mathrm{DSYM}} = 64\ T_{\mathrm{CHIP}}$ where T_{DSYM} and T_{CHIP} denote the symbol period and chip duration, respectively. Unlike the other two modes, a single pulse burst of 32 pulses are used. Each pulse, when present is placed in the chip center. This modulation is similar to that of IEEE 802.15.4a. Among all three modes long-range mode provides the lowest data rate and the best sensitivity.

Table 4.15 LRP UWB PHY spectral mask

PSD limit (dBr)	−18	−10	0	−10	−18
Band 0	Below 5624.32 MHz	5624.32 to 5786.56 MHz	5786.56 to 7192.64 MHz	7192.64 to 7354.88 MHz	Above 7354.88 MHz
Band 1	Below 6090.24 MHz	6090.24 to 6165.12 MHz	6165.12 to 8311.68 MHz	8311.68 to 8386.56 MHz	Above 8386.56 MHz
Band 2	Below 6922.24 MHz	6922.24 to 7121.92 MHz	7121.92 to 8852.48 MHz	8852.48 to 9052.16 MHz	Above 9052.16 MHz

Table 4.16 Data rates for LRP UWB PHY

Mode	PRF (MHz)	T_{sym} (μs)	FEC	Modulation	Data rate
Base	1.0	1	None	OOK	1 Mbps
Extended	1.0	4	None	OOK	250 kbps
Long-range	2.0	32	Convolutional	PPM	31.25 kbps

4.7.3 Pulse Shaping

There is no mandatory pulse shape but the pulse spectrum should satisfy one of the three masks described in Table 4.15.

4.7.4 Band Plan

Band plan consists of three channels (0–2) and occupies the 6.2896 to 9.1856 GHz frequency range. The bands are described in Table 4.15.

4.7.5 Data Rates

Data rates for base and long-range modes are given by

$$\text{Data Rate} = \left(\frac{1}{T_{\text{sym}}}\right).$$

For the extended mode, however, the data rate expression is

$$\text{Data Rate} = \text{FEC code rate} \times \left(\frac{1}{T_{\text{sym}}}\right).$$

The calculated rates are provided in Table 4.16.

What We Learned

- The undesirable spectral property of OOK and PPM and the remedy.
- The peak-to-average reduction of BPSK PSD.
- Rake receiver justification and implementation options.
- T-R modulation scheme and its advantages/disadvantages.
- The advantage and implementation of DFM.
- IEEE 802.15.4a transmitter description, offered rates, applications, and band plan.
- IEEE 802.15.4f transmitter description, offered rates, applications, and band plan.
- IEEE 802.15.6 transmitter description, offered rates, applications, and band plan.

Problems and Simulation Project

1. A PPM modulator employs Gaussian monocycle pulses. Compare the spectrum of the PPM modulator with that of the Gaussian monocycle pulse. Propose a technique to mitigate the spectrum of the PPM modulator. Apply your proposed technique and compare the resulting spectrum with the original PPM spectrum.
2. An UWB channel has three components. The middle component is the strongest. The earlier and later components arrive 1.5 and 3 ns before and after the main components, respectively, and are 10 and 3 dB weaker compared to the middle component, respectively. Draw the block diagram of a rake receiver for an UWB BPSK transmitter operating over this communication channel.
3. Simulate the BER performance of an IEEE 802.15.4a system occupying channel number 1 and providing the lowest data rate in AWGN as well as in CM1.

References

1. Y.P. Nakache, A.F. Molisch, Spectral shape of UWB signals—influence of modulation format, multiple access scheme and pulse shape. in *Proceedings of 57th IEEE Semiannual Vehicular Technology Conference* (*VTC'03*), vol. 4, pp. 2510–2514, Apr 2003
2. J. Romme, L. Piazzo, On the power spectral density of time-hopping impulse radio. in *Proceedings of IEEE Conference on Ultra Wideband Systems and Technologies* (*UWBST'02*), Baltimore, Md, 2002, pp. 241–244
3. N. Lehmann, A.M. Haimovich, The power spectral density of a time hopping UWB signal: a survey. in *Proceedings of IEEE Conference on Ultra Wideband Systems and Technologies* (*UWBST'03*), Reston, Va, USA, Nov 2003, pp. 234–239
4. R. Price, P.E. Green, A communication technique for multipath channels. in Proceedings of IRE, March 1958, pp. 555–570
5. R.T. Hoctor, H.W. Tomlinson, An overview of delay-hopped transmitted-reference RF communications. in *Technical Information Series*, G.E. Research and Development Center, Jan 2002, pp. 1–29
6. J.D. Choi, W.E. Stark, Performance of ultra-wideband communications with suboptimal receiver in multipath channels. IEEE J. Sel. Areas Commun. **20**(9), 1754–1766 (2002)
7. P.V. Orlik, S. Zhao, A. Molisch, A hybrid UWB modulation design compatible for both coherent and noncoherent receivers. Proc. IEEE ICC **10**, 4741–4745 (2006)
8. IEEE P802.15.4a/D7, Jan 2007, Part 15.4: Wireless medium access control (MAC) and physical layer (PHY) Specifications for low-rate wireless personal area networks (LRWPANs)
9. IEEE P802.15.6, Feb 2012, Part 15.6: wireless body area networks
10. IEEE P802.15.4f, April 2012, PART 15.4: low-rate wireless personal area networks (LR-WPANs). Amendment 2: active radio frequency identification (RFID) system physical layer (PHY)

Chapter 5
UWB Modulation Schemes

To be considered ultra wideband (UWB) per FCC definition, a signal must satisfy one of the two frequency domain requirements as stated in Chap. 1. One family of signals that satisfy the UWB requirements are impulse radios. There are, however, a number of others. Impulse radios were treated in Chaps. 3 and 4. In this chapter, we introduce other UWB modulation types such as frequency hopping (also known as multiband) and direct sequence approaches.

5.1 Main Approaches to UWB Modulation

As we saw in Chap. 1, either its bandwidth or its relative bandwidth defines a UWB signal. As per FCC definition if the bandwidth is beyond 500 MHz or the relative bandwidth is above 0.2, the signal is considered UWB. Therefore, there are many different ways to synthesize UWB signals. Impulse radio (IR) is one of the oldest forms of UWB. In addition to impulse IR, other classes of UWB signals exist. The two main classes are known as frequency hopping and direct sequence.

Frequency hopping or multiband approaches can be divided into two main categories, parallel and serial multiband transmission schemes. A summary of the approaches in provided in Ref. [1]. Serial schemes are further divided into predetermined (known) and information bearing sequences. Predetermined sequences are found apriori to provide isolation between piconets. Multiband OFDM (MB-OFDM) is a serial transmission scheme with predetermined sequences. Information bearing sequences are used in multiband transmission schemes (such as spectral keying) to convey information to the receiver. As such, demodulation requires implementation of multiple parallel receivers.

Direct sequence UWB can be implemented using either binary or ternary sequences. A summary of both types are provided in Ref. [1]. Direct sequence binary codes comprise Walsh codes, Barker, m-sequences, Kasami sequences, and Gold codes. It has been shown that perfect autocorrelation property for binary codes, in the sense of obtaining a delta function for autocorrelation function, is not achievable. Promising forms of ternary codes have been developed by Ipatov [2]

S. Emami, *UWB Communication Systems: Conventional and 60 GHz*,
DOI: 10.1007/978-1-4614-6753-3_5,

as well as Hoholdt, and Justesen [3]. These ternary codes are superior to binary codes in two ways. First, perfect autocorrelation property is achievable. Secondly, ternary codes exist for many more lengths than do binary codes.

5.2 Multiband OFDM

Multiband OFDM (MB-OFDM), by definition, is a serial frequency hopping signal with OFDM transmission scheme in each band [4]. It was originally submitted as a proposal for IEEE 802.15.3a physical layer. Later an entity known as MB-OFDM alliance special interest group (MBOA-SIG) was formed to promote the PHY solution. In 2005 MBOA-SIG and WiMedia alliance merged into WiMedia. WiMedia's work led to a complete set of PHY, MAC, and the MAC-PHY interface specifications and was submitted to Ecma, a non-profit industry association. Ecma International selected MB-OFDM as their UWB technology of choice. There are two pieces to the standard, namely ECMA-368 (High Rate Ultra Wideband PHY and MAC) and ECMA-369 (MAC-PHY Interface for ECMA-368) [5, 6]. ECMA-368 is also ETSI TS 102 455 standard. International Organization for Standardization (ISO) has also published ECMA-368 and ECMA-369 under ISO/IEC 26907and ISO/IEC 26908.[1]

5.2.1 MB-OFDM Definition and Parameters

The baseband MB-OFDM Signal is given by

$$x(t) = \sum_{n=0}^{N-1} d(n) e^{j2\pi n \Delta f t}$$

where d(n), N and Δf denote the data, number of subcarriers and subcarrier spacing, respectively. The transmitted RF signal is described by

$$s(t) = \sum_{k} Re\{x_k(t - kT_{\mathrm{SYM}}) e^{j2\pi f_k t}\}$$

where T_{SYM} and f_k represent OFDM symbol duration and carrier frequency, respectively.

There are three bands associated MB-OFDM, each is 528 MHz wide resulting in a total bandwidth of slightly over 1.5 GHz. The OFDM scheme deploys QPSK signaling for individual subcarrier. There are 128 subcarriers out of which 100 are data tones. FFT period, cyclic prefix (CP) and guard interval as well as other

[1] http://www.iso.org/iso/iso_catalogue/catalogue_tc/catalogue_detail.htm?csnumber=53426

Table 5.1 WiMedia parameters

MB-OFDM parameter	Value
Modulation	OFDM/QPSK (or DCM)
FFT size	128
Data tones	100
FFT length	242.42 ns
Cyclic prefix	60.61 ns
Guard interval	9.47 ns
Symbol interval	312.5 ns
Bandwidth	3 × 528 MHz
FEC	Convolutional rate 1/3 (g0 = 133, g1 = 165, g2 = 171) (K = 7) Rates 1/2, 5/8, 3/4 are obtained through puncturing

system parameters are listed Table 5.1. A standard convolutional code rate 1/3 with constraint length of 7 is used to protect source bits. This is the mother code. Rates ½, ¾ and 5/8 are easily obtained by puncturing the mother code with a puncturing mask.

5.2.2 Data Rates

Supported data rates are listed in Table 5.2. As seen, the lowest and highest data rates are 53.3 and 480 Mbps, respectively. Time and frequency spreading are used for some data rates. Note that rates 320 Mbps and higher deploy dual carrier modulation or DCM. This modulation scheme will be reviewed in a later section.

Let us compute the data rates from system parameters. OFDM symbol length is 312.5 ns long. OFDM symbol rate is the inverse of that. In other words, symbol rate becomes $1/(312.5 \times 10^{-9}) = 3.2 \times 10^6$ Hz. Each OFDM symbol carries 100 data tones and utilizes QPSK for individual subcarriers. Thus, the raw data-rata rate equals $3.2 \times 10^6 \times 100 \times 2 = 640$ Mbps. The highest data rate deploys convolutional code rate ¾ and no time/frequency spreading. As such the data rate becomes $640 \times (3/4) = 480$ Mbps.

Table 5.2 WiMedia data rates

Data rate (Mbps)	Time spreading	Frequency spreading	Modulation
53.3 (FEC rate 1/3)	Y	Y	QPSK
80 (FEC rate 1/2)	Y	Y	QPSK
106.7 (FEC rate 1/3)	Y	N	QPSK
160 (FEC rate 1/2)	Y	N	QPSK
200 (FEC rate 5/8)	Y	N	QPSK
320 (FEC rate 1/2)	N	N	DCM
400 (FEC rate 5/8)	N	N	DCM
480 (FEC rate 3/4)	N	N	DCM

In general,
Symbol rate = 1/(OFDM symbol duration),
Raw bit rate = symbol rate x Number of subcarriers x bits per constellation, and
Data rate = Raw bit rate x FEC rate x Frequency spread. x Time spread. Consequently the various data rates are computed as follows:

$$\begin{aligned}
\text{Data rate} &= 640 \times (1/3) \times (1/2) \times (1/2) = 53.3 \quad \text{Mbps} \\
\text{Data rate} &= 640 \times (1/2) \times (1/2) \times (1/2) = 80 \quad \text{Mbps} \\
\text{Data rate} &= 640 \times (1/3) \times (1/2) = 106.7 \quad \text{Mbps} \\
\text{Data rate} &= 640 \times (1/2) \times (1/2) = 160 \quad \text{Mbps} \\
\text{Data rate} &= 640 \times (5/8) \times (1/2) = 200 \quad \text{Mbps} \\
\text{Data rate} &= 640 \times (1/2) = 320 \quad \text{Mbps} \\
\text{Data rate} &= 640 \times (5/8) = 400 \quad \text{Mbps} \\
\text{Data rate} &= 640 \times (3/4) = 480 \quad \text{Mbps.}
\end{aligned}$$

5.2.3 Time and Frequency Spreading

In frequency spreading the negative side of spectrum is filled with the conjugate of the positive side. That results in a frequency spreading factor of two. Frequency spreading as we described results in a real transmit signal. As such, data rates 53.3 and 80 Mbps put out real signals.

Time spreading repeats the signal in time. The time spreading factor is two. The total spreading factor is the product of time and frequency spreading factors. Consequently, the two lowest rates have a combined spreading factor of four, while the highest three rates have no spreading whatsoever.

5.2.4 Subcarrier Types

There are four types of subcarriers or tones, namely data, pilot, guard, and null. As we mentioned, there are 100 subcarriers or tones. There are also 12 pilots used to assist receiver in the demodulation process (tracking and other receiver functions). The 10 guard tones can either carry data or be used to meet the regional spectral masks. Lastly, there are 6 null tones that remove symbol DC and sculpt band edges.

5.2.5 OFDM PHY Parameters

Typically an OFDM system is designed in the following manner. Initially CP is selected to eliminate ISI based on the channel delay spread. Then the OFDM

symbol period is chosen such that symbol power efficiency due to CP is maintained.[2] Next, subcarrier spacing is found by inverting the IFFT symbol duration.[3] Within each subcarrier, channel should be flat. Finally, total number of subcarriers is computed upon dividing the total bandwidth by the subcarrier spacing.

Let us go over the rationale behind selection of PHY parameters of MB-OFDM. The CP should be long enough to avoid ISI. The maximum delay spread is about 30 ns. The CP would have to be at least twice the maximum delay spread. Thus, one arrives at a CP of 60 ns. IFFT portion of the symbol has to be selected such that loss associated with CP is small. For this loss to remain less than 1 dB, the IFFT symbol length should be four times the CP length or around 240 ns

$$10\log_{10}\left(\frac{5}{4}\right) \sim 1 \text{ dB}.$$

The guard interval should provide enough time for frequency hopping circuits to switch. 9 ns is quite reasonable considering the circuit limitations. The OFDM symbol becomes 309 ns if we tally up all the pieces

$$60 + 240 + 9 = 309\ ns.$$

Subcarrier spacing becomes around 4 MHz wide. With a bandwidth of 500 MHz about 125 subcarriers can be deployed. Rounding up to the nearest power of two, we get

$$N = \frac{500}{4} \sim 128.$$

The exact parameters values are slightly different to simplify the implementation.

5.2.6 Time Frequency Codes

Frequency hopping is conducted according to periodic frequency hopping pattern. These patterns are referred to as TFCs or time frequency codes. Figure 5.1 demonstrates the transmitted signal in time frequency space according to [1 2 3 1 2 3] TFC.

TFCs are listed in Table 5.3. The length of each TFC is 6 OFDM symbols long. Some TFCs use all three bands, some use two bands and others use a single band.

The first four TFCs are three band type and the last three are the single band type. Single band type is used when the other two bands are experiencing interference. However, there is a penalty of 10log3 = 4.7 dB in their transmit power.

---

[2] The OFDM symbol period must be significantly less than coherence time of the channel to avoid ICI.

[3] Subcarrier bandwidth must be much larger than the channel Doppler spread.

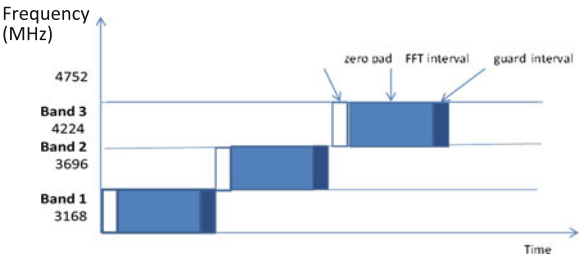

Fig. 5.1 Illustration of time frequency codes

Regulators want the spectrum to be spread and balanced. As such there is a power incentive when hopping is used. Single band type TFCs are also known as fixed frequency interleaving (FFI).

Later in the process two band TFCs were introduced. They are used when one out of three bands is experiencing interference. Compared to single band TFCs, there is a $10\log 2 = 3$ dB power advantage in using two band TFCs. However, there is a 1.7 dB penalty compared to three band TFCs. Multiple band type TFCs are also known as time frequency interleaving (TFI) (Table 5.4).

5.2.7 WiMedia Band Plan

The band plan for WiMedia is shown in Fig. 5.2. The UWB spectrum from 3.1 to 10.7 GHz is divided into 14 equal pieces. Each band is 528 MHz and the center frequency of each band is shown under the frequency axis. The lowest center frequency corresponds to band 1 and the highest center frequency corresponds to band 14. Each three adjacent bands form a band group. Band groups 1 through 4 are constructed this way. The last two bands, namely 13 and 14 are placed in band

Table 5.3 List of TFCs

TFC	Band ID
1	123123
2	132132
3	112233
4	113322
5	111111
6	222222
7	333333

Table 5.4 New TFCs

TFC	Band ID
8	1 2 1 2 1 2
9	1 3 1 3 1 3
10	2 3 2 3 2 3

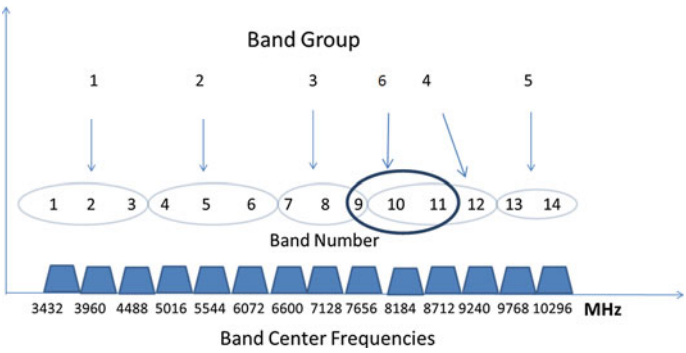

Fig. 5.2 WiMedia band plan

group 5. Band group 6, consisting of bands 9, 10, and 11, was added later on to provide a useable band group for Japan, Korea, and China. Thus, there are a total of 6 band groups. Each band group, with the exception of band group 5, consists of 3 bands. All TFCs can be implemented in each band group excluding band group 5. Since band group 5 consists of two bands, it can only accommodate single and double band TFCs.

5.2.8 Scrambler

To whiten the bit stream prior to the transmission, the standard practice is to XOR data with a PN sequence. A standard PN sequence for scrambling is described by the following binary difference equation:

$$x(n) = x(n-14) \; + \; x(n-15)$$

which is based on primitive polynomial generator

$$g(D) = 1 + D^{14} \; + \; D^{15}.$$

Pseudo random sequences are typically generated by an LFSR (linear feedback shift register). We start with some initial condition and clock the circuit. Register contents change with every clock and a new output bit is generated. The source bits are combined with the PN sequence using binary arithmetic (modulo two) according to

$$y(n) = d(n) \; + \; x(n).$$

The descrambler combines the scrambled signal with the PN sequence to recover the source data

$$s(n) = y(n) + x(n).$$

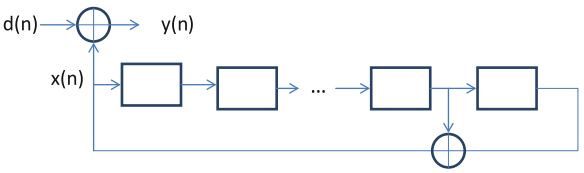

Fig. 5.3 LFSR Implementation of the scrambler

Note that both scrambler and descrambler should start from the same state. The scrambler block diagram is depicted in Fig. 5.3.

5.2.9 WiMedia Transmitter

A block diagram for WiMedia transmitter is shown below. Source bits are randomized using a randomizer to break any long sequence of 1 s or 0 s. The output bits are encoded using convolutional codes. The code polynomial is a standard convolutional code with K = 7. For some rates coded bits are punctured. The bits are then interleaved across multiple OFDM symbols to make the burst error look random. The resulting bits are then mapped into QPSK constellations. OFDM symbols are formed and IFFT is taken. The quadrature components are then passed to the DAC. The analog waveform is then upconverted and transmitted (Fig. 5.4).

5.2.10 Zero Padding

Guard time results in spectral ripples. In a power limited scenario such as UWB, one would have to back off the power by the ripple depth. That reduces transmitter range. To eliminate the problem, guard time is replaced with zeros. This technique is referred to as zero padding.

5.2.11 DCM

At higher data rates (320 Mbps and above) where FEC is weak, performance can be improved through the use of dual carrier modulation (DCM[4]). Here the idea is to transmit the same information twice on two different subcarriers subject to independent fading. If one copy is destroyed by fading, chances are the other one is still available to decode.

The bit stream is divided into groups of four bits denoted by

$$\left[b_{a(n)}\ b_{a(n)+1}\ b_{a(n)+50}\ b_{a(n)+51}\right]$$

[4] DCM is a four-dimensional modulation scheme.

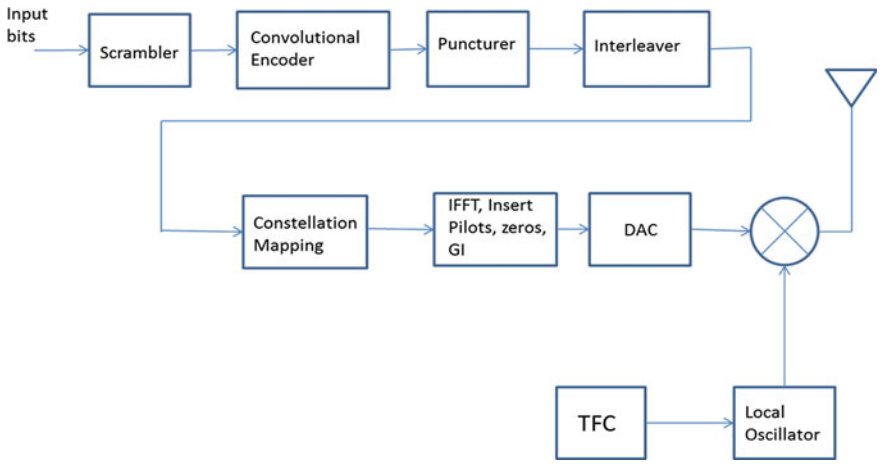

Fig. 5.4 WiMedia transmitter block diagram

where

$$a(n) = \begin{cases} 2k & k \in [0, 24] \\ 2k + 50 & k \in [25, 49] \end{cases}$$

and are consequently are mapped into QPSK constellations defined by

$$\left[x_{a(n)} + jx_{a(n)+50}\right] = \left[2b_{a(n)} - 1 \quad 2b_{a(n)+1} - 1\right]$$

$$\left[x_{a(n)+1} + jx_{a(n)+51}\right] = \left[2b_{a(n)+50} - 1 \quad 2b_{a(n)+51} - 1\right].$$

These QPSK constellations are then mapped, using a linear transformation, into two 16-QAM signals through

$$\begin{bmatrix} y_n \\ y_{n+50} \end{bmatrix} = \frac{1}{\sqrt{10}} \begin{bmatrix} 2 & 1 \\ 1 & -2 \end{bmatrix} \begin{bmatrix} x_{a(n)} + jx_{a(n)+50} \\ x_{a(n)+1} + jx_{a(n)+51} \end{bmatrix}.$$

The resulting signals $[y_n y_{n+50}]$ are placed on two OFDM subcarriers that are 50 subcarriers apart. Performance wise, DCM is superior to QPSK in multipath channels.

5.2.12 Spectrum Availability

The UWB regulatory status in US, Europe, Japan, Korea, and China was provided in Chap. 1. In US, UWB unlicensed devices can operate in all WiMedia 14 bands

Table 5.5 A. Europe, B. Japan, C. Korea, D. China

Band	Requirement
A. Europe	
Bands 1and 2	Requires DAA
Band 3	Under consideration whether DAA is required or not
Bands 7 through 10	UWB operation is permitted
Band 11	Under consideration for UWB operation
B. Japan	
Band 2 and 3	DAA required
Bands 9 through 13	UWB operation is permitted
C. Korea	
Bands 1, 2 and 3	DAA required
Band 9 through 13	UWB operation is permitted
D.China	
Band 3	DAA required
Band 7 through 11	UWB operation permitted

and 6 band groups. As for others, the regulations are mapped into WiMedia band plan and requirements for individual bands are provided in Table 5.5a–d, [7].

Europe: As seen in Chap. 1, 6–8.5 GHz band is open to UWB devices in Europe. Consequently, WiMedia bands 7 through 10 can operate without DAA. On the other hand, WiMedia bands 1 and 2 can be used only with DAA functionality. The jury is still out on the faith of bands 3 and 11. Band group 3 is the only available band group. A summary of the UWB bands status is given in Table 5.5a.

Japan: Out of the 14 WiMedia bands, only bands 2, 3, 9, 10, 11, 12, and 13 can be used. The first two bands, 2 and 3, can only be used with DAA functionality. The DAA requirement can be waived, if the emission level is lowered from −41.3 to −70 dBm/MHz. As for band groups, only band group 6 is available in Japan.

Korea: WiMedia bands 1, 2, 3, 9, 10, 11, 12, and 13 can be used only. Implementation of DAA in bands 1 and 2 is required, while DAA implementation in band 3 is waived until 2010. DAA requirement for bands 1, 2 and 3 can be waived upon lowering of emission level from the usual −41.3 to −70 dBm/MHz. Band groups 1, 4, and 6 are available for operation in Korea.

China: WiMedia bands 3, 7, 8, 9, 10, 11, as well as band groups 3 and 6 are available for operation in China. Operation in band 3 is subject to DAA implementation. However, the DAA requirement for band 3 can be waived upon lowering of emission to −70 dBm/MHz.

5.2.13 WiMedia 1.5

The latest version of the standard, WiMedia 1.5, that was released in 2009 introduces higher data rates. The new rates are 640, 800, 960, and 1024 Mbps,

Table 5.6 WiMedia 1.5 data rates

Data rate (Mbps)	Modulation	FEC	Time spreading	Frequency spreading
640	MDCM	LDPC rate 1/2	N	N
800	MDCM	LDPC rate 5/8	N	N
960	MDCM	LDPC rate 3/4	N	N
1,024	MDCM	LDPC rate 4/5	N	N

respectively. The modulation, coding, and spreading details of the new rates are presented in Table 5.6.

The higher data rates (640 Mbps and above) take advantage of a modulation scheme known as modified dual carrier modulation (MDCM). This scheme is also known as 256DCM. Conceptually it is similar to the DCM mode in the original WiMedia except that larger constellations are used. The modulation procedure is described below.

The bit stream is divided into groups of eight bits denoted by

$$[b_{8k}\ b_{8k+1}\ b_{8k+2}\ b_{8k+3}\ b_{8k+4}\ b_{8k+5}\ b_{8k+6}\ b_{8k+7}]$$

where

$$k \in [0, 49].$$

Each eight bit groups is divided into the first four bits and the last four bits represented by $[b_{8k}\ b_{8k+1}\ b_{8k+2}\ b_{8k+3}]$ and $[b_{8k+4}\ b_{8k+5}\ b_{8k+6}\ b_{8k+7}]$ respectively. Each four bit partition is mapped into 16QAM constellation as depicted in Fig. 5.5. Then pairs of 16QAM constellations points denoted by

$$x_{\mathrm{ai}} + jx_{\mathrm{aq}}$$

and

$$x_{\mathrm{bi}} + jx_{\mathrm{bq}}$$

are mapped, using a linear transformation, defined by $\begin{bmatrix} y_n \\ y_{n+50} \end{bmatrix} = \frac{1}{\sqrt{170}} \begin{bmatrix} 4 & 1 \\ 1 & -4 \end{bmatrix} \begin{bmatrix} x_{\mathrm{ai}}+jx_{\mathrm{aq}} \\ x_{\mathrm{bi}}+jx_{\mathrm{bq}} \end{bmatrix}$. into two 256QAM constellation points y_n and y_{n+50}. These points are placed on two OFDM subcarriers that are 50 subcarriers apart.

The raw bit rate is given by

$$3.2 \times 10^6 \times 100 \times (8/2) = 1280 \text{ Mbps}$$

as each subcarrier is modulated by a 256QAM and half of the subcarriers are redundant.

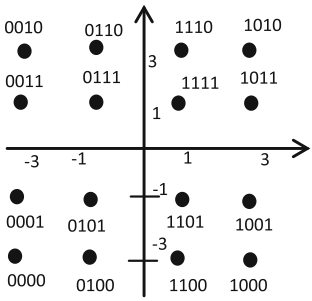

Fig. 5.5 WiMedia constellation diagram

The various data rates are computed as follows:

$$\begin{aligned}
\text{Data rate} &= 1280 \times (1/2) = 640 \text{ Mbps} \\
\text{Data rate} &= 1280 \times (5/8) = 800 \text{ Mbps} \\
\text{Data rate} &= 1280 \times (3/4) = 960 \text{ Mbps} \\
\text{Data rate} &= 1280 \times (4/5) = 1024 \text{ Mbps.}
\end{aligned}$$

5.3 Direct Sequence UWB

By definition, DS-UWB is an application of direct sequence spread spectrum in UWB [8]. If it was not for its large fractional bandwidth, this system would simply be a direct sequence spread spectrum (DS-SS) system.

5.3.1 DS-UWB Parameters

DS-UWB system parameters are listed in Table 5.7.

Table 5.7 DS-UWB parameters

DS-UWB parameter	Value
Modulation	BPSK
Spread spectrum code	Ternary codes length 2, 3, 6, 12 and 24
FEC	Convolutional (k = 7) Rates 1/2 and 3/4 (through puncturing)
Band plan	−Low band (3.1−4.9 GHz) required −High band (6.2−9.7 GHz) optional
Bands	− 1.75 GHz (low band) −3.5 GHz (high band)
Pulse shape	Root raised cosine (RRC)

Bits are spread using ternary spread spectrum codes of different lengths. The ternary codes are as follows:

Supported ternary codes

L	Ternary code
1	1
2	1,0
3	1,0,0
4	1,0,0,0
6	1,0,0,0,0,0
12	0, −1,−1,−1, 1, 1, 1,−1, 1, 1,−1, 1
24	−1, 0, 1, −1, −1, −1, 1, 1, 0, 1, 1, 1, 1, −1, 1, −1, 1, 1, 1, −1, 1, −1, −1, 1

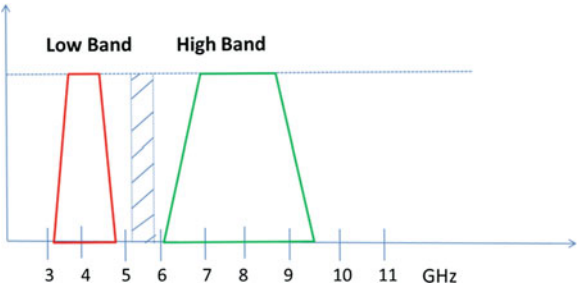

Fig. 5.6 DS-UWB band plan

Convolutional codes of rates ½ and ¾ codes with constraint length K = 7 are used. The low band system is 1.5 GHz wide while the high band one is 3.5 GHz long. The band plan is provided in Fig. 5.6.

5.3.2 DS-UWB Data Rates

The offered data rates are presented in Table 5.8. Rates vary from 24 to 1320 Mbps. Different data rates are obtained through interplay of FEC and spread spectrum codes.

System chipping rate is fixed (1320 MHz) while the code length varies with data rate. Symbol rate is derived by dividing the chip rate by code length. Data rate is obtained by multiplying the symbol rate by the FEC rate.

$$1320/12 = 110 \text{ MHz} \quad 110 \times (1/2) = 55 \text{ Mbps}$$

The data rate can be computed in terms of system parameters as given in

$$\textbf{Data Rate} = \textbf{Chip rate} \times \textbf{FEC rate} \times (\textbf{1}/\textbf{Code length}).$$

The individual data rates are obtained as follows:

$$\begin{aligned}
\text{Data Rate} &= 1320 \times 1/2 \times 1/24 &&\sim 28\text{Mbps}\\
\text{Data Rate} &= 1320 \times 1/2 \times 1/12 &&= 55\text{Mbps}\\
\text{Data Rate} &= 1320 \times 1/2 \times 1/6 &&= 110\text{Mbps}\\
\text{Data Rate} &= 1320 \times 1/2 \times 1/3 &&= 220\text{Mbps}\\
\text{Data Rate} &= 1320 \times 3/4 \times 1/2 &&\sim 500\text{Mbps}\\
\text{Data Rate} &= 1320 \times 1 \times 1/2 &&= 660\text{Mbps}\\
\text{Data Rate} &= 1320 \times 3/4 \times 1 &&\sim 1000\text{Mbps}\\
\text{Data Rate} &= 1320 \times 1 \times 1 &&= 1320\text{Mbps}.
\end{aligned}$$

5.3.3 DS-UWB Transmitter

Block diagram of a DS-UWB transmitter is shown in Fig. 5.7. The information bits are fed through a scrambler to break any long runs of 1's or 0's. The output bits are then convolutionally coded and punctured if necessary. Interleaving is utilized to turn burst errors into random errors in the receiver. The bits are then mixed by the ternary codes, pulse shaped. The waveform is then converted to analog, upconverted and transmitted over the channel via the antenna.

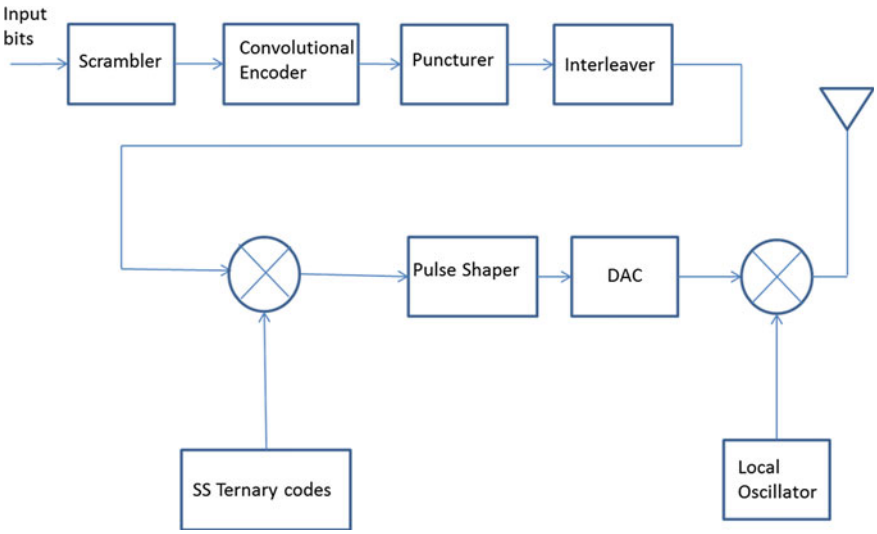

Fig. 5.7 DS-UWB transmitter block diagram

Table 5.8 DS-UWB data rates

Data rate (Mbps)	Spread spectrum code length
28 (FEC rate of ½)	24
55 (FEC rate of ½)	12
110 (FEC rate of ½)	6
220 (FEC rate of ½)	3
500 (FEC rate of 3/4)	2
660 (No FEC required)	2
1,000 (FEC rate of 3/4)	1
1,320 (No FEC required)	1

5.3.4 Puncturing Convolutional Codes

Wireless communication standard typically provide a few rates. That is achieved by using convolutional codes with different rates. As such the transceiver would require more than one set of encoders and decoders. This is a costly proposition. Instead, with punctured codes one could have N different rates but with only one encoder/decoder set. Performance wise, punctured code rates perform well, but they are not optimal.

DS-UWB utilizes a mother code of rate ½. Rather ¾ punctured code can be obtained the following way. The encoded bit stream out of rate ½ coder is divided into 6 bit segments. Then a puncturing mask is applied to the stream. The masks just discards bit 4 and 5 in the sequence of 6 bits. Thus, one ends up with 4 bits for every 3 input bits.

$$b_0b_1b_2\mathbf{b_3b_4}b_5|b_6b_7b_8\mathbf{b_9b_{10}}b_{11}|b_{12}b_{13}b_{14}\mathbf{b_{15}b_{16}}b_{17}$$

As such, the punctured rate is ¾. A comparison between the coding gain of the optimum rate ¾ and the punctured rate ¾ is shown in Table 5.9. As seen, the punctured code, though not optimal, performs quite well.

5.3.5 M-BOK Mode

M-ary Bi-Orthogonal modulation places its symbols $s_1, s_2,\ldots, s_{M/2}$ on M/2 orthogonal axis. The other M/2 symbols are $-s_1, -s_2,\ldots, -s_{M/2}$. The modulation performance improves as M becomes larger and in the limit, it approaches the Shannon limit of −1.59 dB. We can think of M-ary Bi-Orthogonal Keying (M-BOK) code words as the M-BOK modulation symbols. As such the code words can be represented by $\{c_1, c_2,\ldots, c_{M/2}, -c_1, -c_2,\ldots, -c_{M/2}\}$.

Table 5.9 DS-UWB data rates

Code	Coding gain (dB)
Optimum	6.5
Punctured	5.7

Table 5.10 4-BOK code words

Input bits	4-BOK codewords
00	1 1
01	1 −1
11	−1 −1
10	−1 1

For instance, Walsh-Hadamard matrices can be used to form codewords. M-BOK codes of length 2 are the rows of the matrix

$$\begin{bmatrix} W_2 \\ -W_2 \end{bmatrix}$$

where $W_2 = \begin{bmatrix} 1 & 1 \\ 1 & -1 \end{bmatrix}$ is the Walsh-Hadamard matrix of size 2×2. Upon substitution we get

$$\begin{bmatrix} W_2 \\ -W_2 \end{bmatrix} = \begin{bmatrix} 1 & 1 \\ 1 & -1 \\ -1 & -1 \\ -1 & 1 \end{bmatrix}.$$

For DS-UWB the mapping from input bits to the 4-BOK is provided in Table 5.10.

In addition to the ternary codes listed earlier, DS-UWB supports M-BOK codes. First the bit stream is divided into 2 bit segments. Then the 2 bit words are replaced by their corresponding code word from Table 5.11. As an example, let us spread the gray coded bit stream {1 0 0 1 1 1} using 4-BOK codes of length L = 4.

Using Table 5.11, the spread stream will be 0 0 −1 0 0 0 1 0 −1 0 0 0.

The data rate for the lower and upper bands are given by

Data Rate = Chip rate x bit per symbol x FEC rate x (1/Code length) and are listed in Tables 5.12 and 5.13.

What We Learned

- MB-OFDM modulation, coding, data rates, time frequency codes, and band plan
- MB-OFDM parameter selection
- MB-OFDM band availability in various countries
- MB-OFDM transmitter architecture
- DS-UWB modulation, coding, data rates, and band plan
- DS-UWB transmitter architecture
- M-BOK codes.

Table 5.11 4-BOK code words for $L = 2$, 4, 6, and 12 subject to natural and Gray coding

Input data: gray coding (First in time on left)	Input data: natural coding (First in time on left)	$L = 12$	$L = 6$	$L = 4$	$L = 2$
00	00	1,0,0,0,0,0,0,0,0,0,0,0	1,0,0,0,0,0	1,0,0,0	1,0
01	01	0,0,0,0,0,0,1,0,0,0,0,0	0,0,0,1,0,0	0,0,1,0	0, 1
11	10	−1,0,0,0,0,0,0,0,0,0,0,0	−1,0,0,0,0,0	−1,0,0,0	−1, 0
10	11	0,0.0,0,0,0,−1,0,0,0,0,0	0,0,0,−1,0,0	0,0,−1,0	0, −1

Table 5.12 Lower band data rates

Data rate (Mbps)	FEC rate	Code length
110	½	L = 12
220	½	L = 6
500	¾	L = 4
660	1	L = 4
1,000	¾	L = 2
1,320	1	L = 2

Table 5.13 Upper band data rates

Data rate (Mbps)	FEC rate	Code length
220	½	L = 12
660	¾	L = 6
1,000	¾	L = 4
1,320	1	L = 4

Problems and Simulation Projects

1. Draw the receiver block diagram for WiMedia transmitter.
2. Simulate the BER performance of WiMedia system in AWGN, CM1, CM2, CM3, and CM4. Operate in band 1 and select the lowest data rate.
3. Repeat the above exercise for the highest data rate.
4. Draw the receiver block diagram for DS-UWB transmitter.
5. Simulate the BER performance of DS-UWB system in AWGN, CM1, CM2, CM3, and CM4. Operate in the low band and utilize the lowest data rate.
6. Repeat the above exercise for the highest data rate.
7. A WiMedia-based product with no DAA functionality is being planned for both European and Japanese markets. Propose available bands and TFCs for this product. Compare the transmission range of this product to that of another product made for the US market that operates in band 1. Justify any assumptions that you need to make.

References

1. R. Aiello, A. Batra, *Ultra Wideband Systems: Technologies and Applications* (Elsevier, Amsterdam, 2006)
2. V.P. Ipatov, Ternary Sequences with Ideal Autocorrelation Properties. Radio Eng. Electron. Phys. **24,** pp. 75–79, Oct 1979
3. T. Hoholdt, J. Justesen, Sieves for Low Autocorrelation Binary Sequences. IEEE Trans. Inf. Theory, **29**(4), pp. 597–600, July 1983
4. J. Balakrishnan, A. Batra, A. Dabak, A multi-band OFDM system for UWB communication, in *Proceedings of IEEE Conference on Ultra Wideband Systems and Technologies*, pp. 354–358, 2003
5. Ecma International standard ECMA-368, High Rate UltraWideband PHY and MAC Standard, 2nd ed. http://www.ecma-international.org/publications/standards/Ecma-368.html, Dec 2007
6. Ecma International standard ECMA-369, MAC-PHY Interface for ECMA-368, 2nd ed. http://www.ecma-international.org/publications/standards/Ecma-369.html, Dec 2007
7. G. Heidary, *WiMedia UWB: Technology of Choice for Wireless USB and Bluetooth*, Wiley, London, 2008
8. DS-UWB Physical Layer Submission to 802.15 Task Group 3a, IEEE 802.15.3a Working Group, P802.15.03/0137r0, 2004

Chapter 6
Miscellaneous UWB Topics: MAC, Ranging, Chipsets and Products

Miscellaneous UWB topics such as MAC, ranging and silicon are addressed in this chapter. Medium access control (MAC) layers of UWB standards such as IEEE 802.15.3, IEEE 802.15.4a as well as WiMedia are briefly reviewed. Shared features and the differentiators are pointed out. Then the case for UWB application in ranging is made by comparing its performance against that of a narrowband system. A few variations of time of arrival (TOA) ranging scheme known as one-way ranging time of arrival (OWR-TOA), two-way ranging time of arrival (TWR-TOA) and symmetric double-sided two-way ranging (SDS-TWR) are described. The error performance of TWR-TOA and SDS-TWR are compared. We then turn our attention to UWB silicon. The evolution path for UWB silicon is described, evaluation kits and reference design kits are introduced and UWB test equipment is reviewed. The chapter concludes with a description of UWB products in the market.

6.1 Medium Access Control

6.1.1 IEEE 802.15.3 MAC

IEEE 802.15.3 MAC [1] defines a piconet as a group of devices consisting of a piconet controller (PNC) and many devices (DEV) as shown in Fig. 6.1. This MAC protocol is considered a centralized MAC protocol since PNC node is in charge of channel allocations.

A piconet is typically formed around a person or object. PNC manages the resources based on requests and provides quality of service (QOS) as well. To exchange data with other devices, a DEV needs to join a piconet. Once a DEV is associated with a piconet, it can exchange data directly with the other devices without going through the PNC.

The procedure to join a piconet is as follows. Every PNC puts out a beacon. A DEV searches for a beacon. If a beacon is found, it sends a request to join and

S. Emami, *UWB Communication Systems: Conventional and 60 GHz*,
DOI: 10.1007/978-1-4614-6753-3_6,

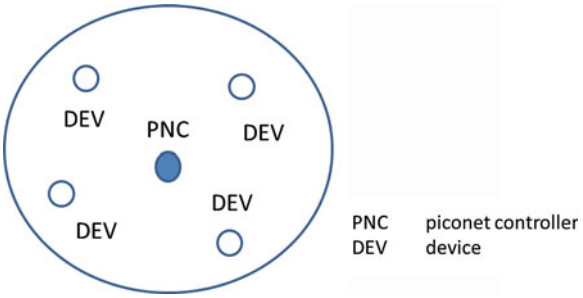

Fig. 6.1 Illustration of the piconet concept

becomes associated with the piconet. If no beacon is found and DEV has PNC capability, it can form a piconet and start putting out a beacon. An example is provided below. All devices receive PNC beacon and join the piconet. Then one device exchanges data directly with PNC, while two other device pairs exchange data directly. The situation is illustrated in Fig. 6.2.

Time is divided into many periods known as superframes. A superframe structure is shown in Fig. 6.3. One can see three fields named beacon, CAP and CTAP, if a superframe is put under the microscope. Either CAP or CTAP can be used by each device to access the channel. Contention access period (CAP) is CSMA/CA (carrier sensing multiple access/carrier avoidance) based, while CTAP is TDMA based. CAP is used by the DEVs to send their association requests to PNC. Channel time access period (CTAP) has two fields known as management CTA (MCTA) and channel time allocation (CTA). MCTA is utilized for sending commands to or from PNC, while CTA is used for data communications.

Consider a scenario in which device 1 has some data to send to device 2. The sequence of the events is described below and the corresponding frame field for each event is indicated in parenthesis:

– device 1 requests association (CAP)
– device 2 requests association (CAP)
– device 1 requests a channel to communicate with device 2 (CAP)

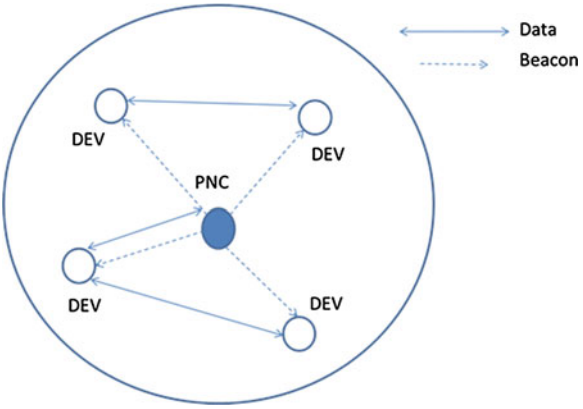

Fig. 6.2 Information exchange in a piconet

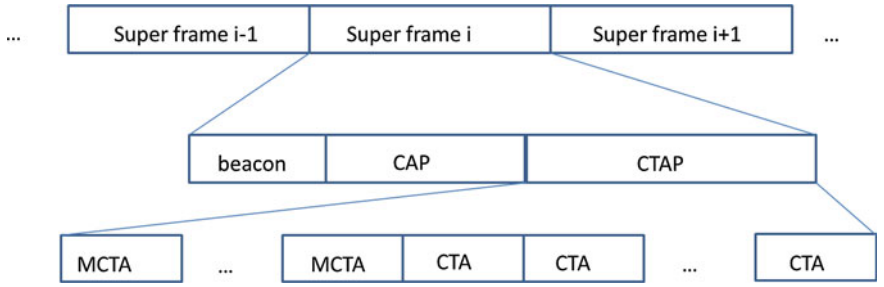

Fig. 6.3 The 802.15.3c superframe

– PNC broadcasts the CTA information in the beacon (beacon)
– devices 1 and 2 communicate with each other (CTA)
– device 1 sends release request (CAP)
– PNC honors the request (beacon)
– device 1 disassociates itself (CAP)
– device 2 disassociates itself (CAP)

Note that CAP provides only a best effort service. On the other hand, QOS is provided in CTAP. As for supported ARQ options, they include No ACK, Immediate ACK, and Delayed ACK.

6.1.2 WiMedia MAC

Unlike IEEE 802.15.3 MAC, this protocol is a distributed MAC [2]. Only one type of device exists and all active devices transmit beacons. A cluster of connected DEVs are referred to as a beacon group as opposed to piconet in IEEE 802.15.3 MAC.

The WiMedia MAC superframe is made of a beacon period and a data access period and lasts 65,536 us. The access scheme is a combination of DRP (distributed reservation protocol) and PCA (prioritized channel access). Essentially, DRP and PCA denote TDMA and CSMA-CA, respectively. Beacon period contains coordination information with other devices, while data access period is used for data transfer and control purposes.

When a device begins operation, it scans the channel and looks for beacons for a period of at least one superframe. If a beacon is found, it then joins the beacon group and stays tuned to beacon period. If no beacon is found, the device can transmit its own beacon and define its superframe start time. Channel access can be set up through the use of beacon slots within a beacon period. Requests, responses, reservations, and neighborhood information are conveyed in beacons.

Reservations are either hard or soft. In hard reservation, the time slot is to be used by the reservation owner. However, the time slots in soft reservation are available for contention. Priority access is provided for the reservation owner, in the event he needs to access the time slot.

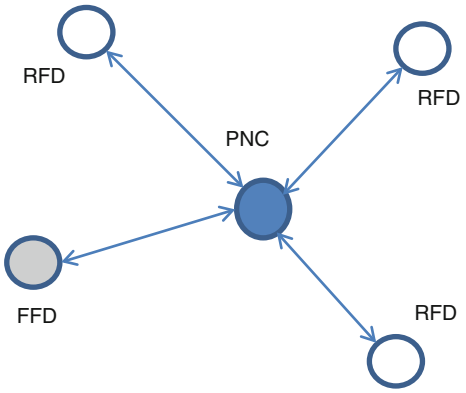

Fig. 6.4 Star topology

Three are types of acknowledgments known as No Acknowledgment, Immediate Acknowledgment, and Block Acknowledgment that are supported. No Acknowledgment and Immediate Acknowledgment lead to highest and lowest throughput levels. Block Acknowledgment falls somewhere in-between. No Acknowledgment and Immediate Acknowledgment are suited for delay sensitive and content sensitive applications, respectively.

Protocol supports power management. To save power, an inactive device can turn off its beacon and go to hibernation state. A notice to other devices as well as the return time is posted in the beacon.

6.1.3 IEEE 802.15.4a MAC

Two types of devices namely full function devices (FFD) and reduced function devices (RFD) are supported in IEEE 802.15.4a [3, 4]. An FFD can act as a personal area network (PAN) controller (PNC), while an RFD can join a PAN, but cannot function as a PAN coordinator.

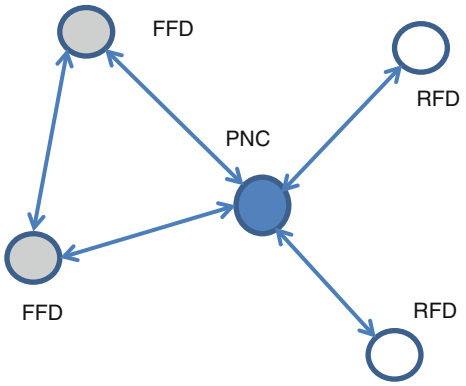

Fig. 6.5 Peer-to-peer topology

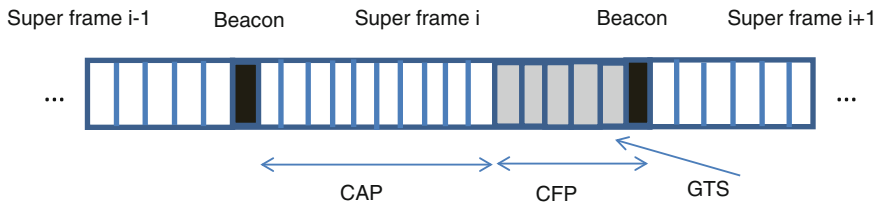

Fig. 6.6 Superframe structure

As for topologies, both peer-to-peer and star topologies shown in Figs. 6.4 and 6.5 are supported in the standard. In star topology nodes (FFDs or RFDs) directly communicate with the PAN coordinator. In contrast to the star topology, FFDs can communicate directly with each other in peer-to-peer topology, while RFDs can only communicate with the PAN coordinator.

A beacon is broadcast by the PAN coordinator in the star topology. Superframe is the interval from onset of one beacon to that of the next beacon and is divided into 16 slots. With the exception of the first slot which is a beacon, all other slots are used for data transmission from PAN coordinator to a node or vice versa. The details of superframe structure are shown in Fig. 6.6.

Data transfer phase from PAN coordinator to a node starts when the PAN coordinator addresses the desired node in the transmitted beacon. Then the intended node transmits a data request command using CSMA/CA to the coordinator to start its transmission. Coordinator sends the acknowledgment followed by the data. Upon the receipt of the data, the node sends an acknowledgement command. For low latency applications, PAN coordinator can reserve some slots to allocate to such applications. These slots are known as guaranteed time slots (GTS) and are made available to a desired node. Contention free period (CFP) is composed of GTSs, the remaining slots make up the contention access period (CAP).

If a node has some data to send to the coordinator, it has to listen to the beacon. If it has been assigned a GTS, it can send the data in the assigned time slot. Otherwise, it has to send the data during CAP using CSAMA/CA. The coordinator, after receiving the data, sends an acknowledgement command to the node to complete the procedure.

The CSMA-CA scheme in 802.15.4a can be summarized as follows. When a node has some data to send, it picks a random multiple of back-off delay. Once the delay is expired, the device listens to the channel and transmits if the channel is idle. Otherwise, it selects a larger back-off delay and repeats the procedure.

One of the key differences between the IEEE 802.15.4a and previous IEEE standards is the provisions for ranging functionality. Even so, support for ranging by a vendor is optional. The packet used for ranging is a standard packet with just a specific bit set in the packet header. Some packet exchanges between the two nodes are necessary for ranging calculation. Positioning (as opposed to ranging) can be derived from ranging data by implementers, but is not part of the standard itself.

6.2 Ranging Accuracy of UWB Versus Narrowband Systems

Let τ, $\hat{\tau}$ and $E[\,]$ denote TOA, its estimate and expectation operation, respectively. By definition, error variance of TOA is

$$\sigma_{\hat{\tau}}^2 = E\left[(\hat{\tau} - \tau)^2\right].$$

Cramer-Rao lower bound (CRLB) provides the low bound for the mean squared error (MSE) of any unbiased estimate of the TOA [5]. It can be shown that CRLB for TOA has the following mathematical form [6]:

$$\sigma_{\hat{\tau}}^2 \geq \frac{1}{8\pi^2\beta^2 \mathrm{SNR}}$$

where $\sigma_{\hat{\tau}}^2$, β and SNR denote variance of $\sigma_{\hat{\tau}}^2$, signal bandwidth and Eb/No. The ranging error CRLB is given by $c\sigma_{\hat{\tau}}$ where c is the speed of light. CRLB does not account for any errors due to multipath. In fact, the only source of error considered is AWGN.

A comparison between the ranging capability of a UWB signal with that of a narrowband signal is made when SNR ranges between -10 dB and 10 dB in Fig. 6.7. The narrowband signal is an 802.11 a/g with a bandwidth of 20 MHz. There is a significant difference between the ranging accuracy of the UWB and a narrowband system, particularly when SNR is low. While the error associated with the CRLB of UWB is 20 cm, the CRLB of the narrowband system is close to 5 m.

The CRLB of three UWB systems with bandwidths of 500 MHz, 1 GHz, and 3 GHz are presented in Fig. 6.8. Very accurate ranging can be obtained with UWB

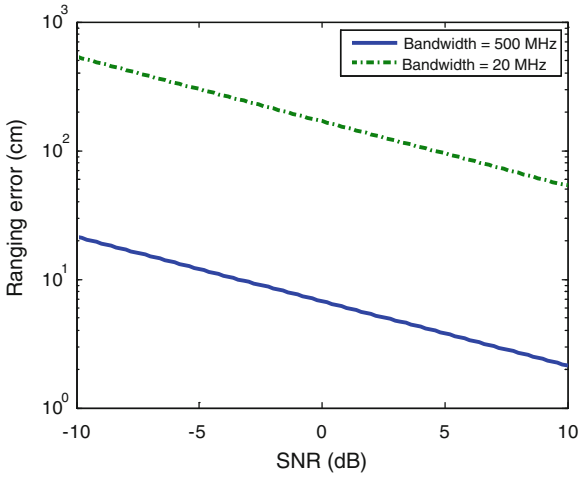

Fig. 6.7 CRLB of the ranging error

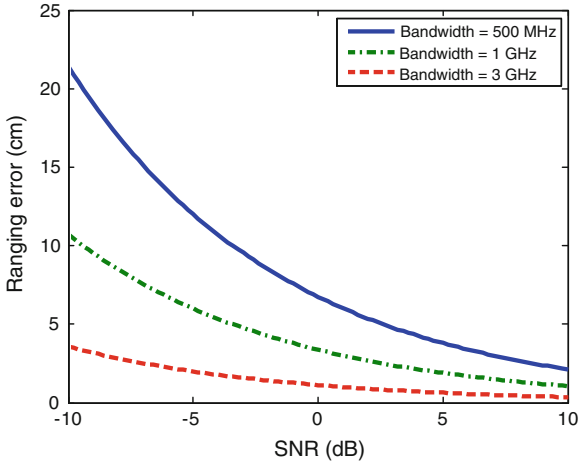

Fig. 6.8 CRLB of the ranging error

signals. The bounds are less than 22, 12, and 5 cm for 0.5, 1 and 3 GHz systems, respectively.

6.3 TOA Ranging Techniques

In TOA methods one or more ranging transactions take place. A ranging transaction is defined as transmission of a token by the initiator node and the reception of it by the target node. Range is determined by combining the departure instance, arrival instance, and/or flight times. In what follows the most popular variations of TOA namely one-way ranging (OWR), two-way ranging (TWR), and SDS-TWR are described. IEEE 802.15.4a has selected TWR and SDS-TWR as its mandatory and optional ranging protocols, respectively [3].

The transmitted token for ranging consists of multiple repetition of a sequence with good auto and cross-correlation properties. In IEEE 802.15.4a ternary sequences of length 31 with perfect autocorrelation properties have been utilized. These sequences have perfect periodic autocorrelation. As such, multipath components in the arriving signal can be easily identified.

6.3.1 One-Way Ranging Time of Arrival

In TOA OWR node A sends a token to the target node B. The elapsed time between departure from node A (T_1) and arrival at the target node B (T_2) is the propagation time and is given by $t_p = T_2 - T_1$ as seen in Fig. 6.9. One-way ranging (OWR) requires perfect synchronization between the originator and the

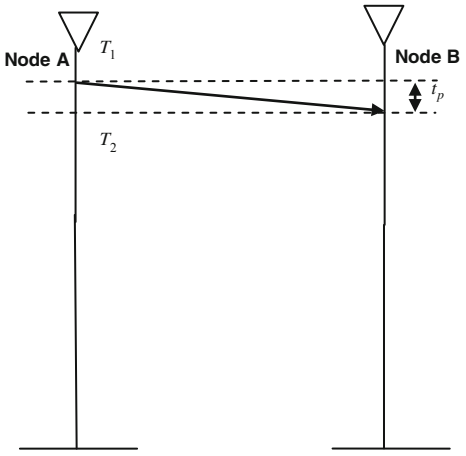

Fig. 6.9 Timing diagram for OWR

recipient nodes. Achieving perfect synchronization is not easy and as such is considered a limitation of this approach.

6.3.2 Two-Way Ranging Time of Arrival

One popular and well-known method of ranging is TWR [7]. Node A transmits a token to node B. Upon reception, node B sends the token back to node A. The timing diagram for this method is shown in Fig. 6.10. It is clear that

$$2t_p + t_{\text{reply}B} = t_{\text{round}A}$$

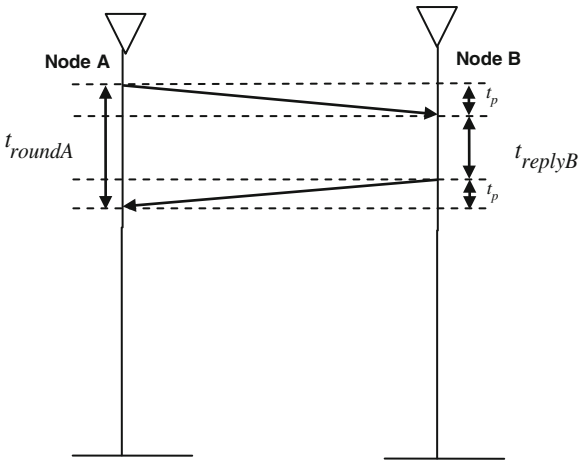

Fig. 6.10 Timing diagram for TWR

where $t_{\text{round}A}$, $t_{\text{reply}B}$ and t_p are turn around associated with node A, reply time associated with node B, and the propagation time from node A to node B (also known as time of flight), respectively. Upon solving for t_p we get

$$t_p = \frac{t_{\text{round}A} - t_{\text{reply}B}}{2}$$

In practice these two quantities, $t_{\text{round}A}$ and $t_{\text{reply}B}$, are measured with two different clocks with different drifts. The estimated value for t_p can be determined from

$$\hat{t}_p = \frac{t_{\text{round}A}(1 + e_A) - t_{\text{reply}B}(1 + e_B)}{2}$$

where e_A and e_B are tolerances associated with nodes A and B crystals, respectively. For instance, $e_A = 10^{-6}$ for a 1 ppm crystal.

Upon substitution for $t_{\text{round}A} = 2t_{\text{p}} + t_{\text{reply}B}$ we get

$$\hat{t}_p = \frac{(2t_p + t_{\text{reply}B})(1 + e_A) - t_{\text{reply}B}(1 + e_B)}{2}.$$

After some algebra one ends up with

$$\hat{t}_p - t_p = \frac{2t_p e_A + t_{\text{reply}B} e_A - t_{\text{reply}B} e_B}{2}$$

In practice t_p is significantly smaller than $t_{\text{reply}B}$ and, therefore

$$\hat{t}_p - t_p \approx \frac{1}{2} t_{\text{reply}B}(e_A - e_B).$$

6.3.3 *Symmetric Double-Sided Two-Way Ranging Time of Arrival*

In Symmetric Double-Sided Two-Way Ranging Time of Arrival (SDS-TWT-TOA), the TWT is essentially repeated twice [8]. However, nodes take turns initiating TWR. Process is depicted in Figs. 6.11 and 6.12. The straightforward implementation of this method requires four messages (Fig. 6.11); the efficient implementation of it is accomplished with only three ranging messages (Fig. 6.12). From Fig. 6.11 we have

$$2t_p + t_{\text{reply}B} = t_{\text{round}A}$$

$$2t_p + t_{\text{reply}A} = t_{\text{round}B}$$

where $t_{\text{round}A}$, $t_{\text{round}B}$, $t_{\text{reply}A}$ and $t_{\text{reply}B}$ are round trip time measured by node A, round trip time measured by node B, node A reply time and node B reply time, respectively.

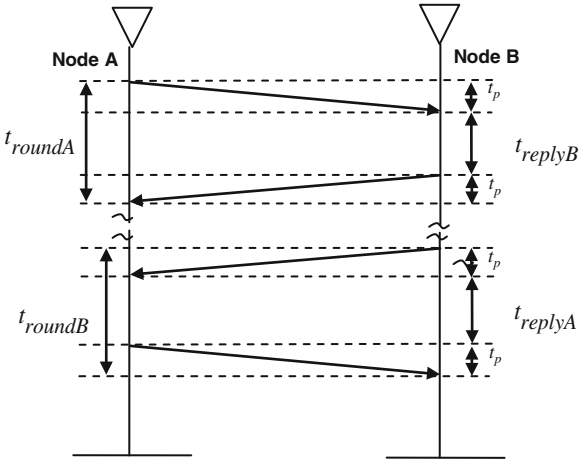

Fig. 6.11 Timing diagram for straightforward implementation of SDS-TWR

If we add the two equations and solve for t_p we get

$$t_p = \frac{t_{\text{roundA}} - t_{\text{replyA}} + t_{\text{roundB}} - t_{\text{replyB}}}{4}.$$

In practice ($t_{\text{round}A}$, $t_{\text{reply}A}$) pair and ($t_{\text{round}B}$, $t_{\text{reply}B}$) pair are measured with two different clocks with different drifts. The estimated value for t_p can be determined from

$$\hat{t}_p = \frac{\left(t_{\text{roundA}} - t_{\text{replyA}}\right)(1 + e_A) + \left(t_{\text{roundB}} - t_{\text{replyB}}\right)(1 + e_B)}{4}.$$

After some algebra we get

$$\hat{t}_p - t_p = \frac{e_A\left(t_{\text{roundA}} - t_{\text{replyA}}\right) + e_B\left(t_{\text{roundB}} - t_{\text{replyB}}\right)}{4}.$$

Let us define

$$t_{\text{replyB}} = t_{\text{replyA}} + \delta_{\text{reply}}.$$

We then substitute for $t_{\text{roundA}} = 2t_p + t_{\text{replyB}}$ and $t_{\text{roundB}} = 2t_p + t_{\text{replyA}}$ into the error equation

$$\hat{t}_p - t_p = \frac{e_A\left(t_{\text{roundA}} - t_{\text{replyA}}\right) + e_B\left(t_{\text{roundB}} - t_{\text{replyB}}\right)}{4}.$$

After simplifications we end up with

$$\hat{t}_p - t_p = \frac{1}{2}t_p(e_A + e_B) + \frac{1}{4}\delta_{\text{reply}}(e_A - e_B).$$

Since t_p is significantly smaller than δ_{reply}, then

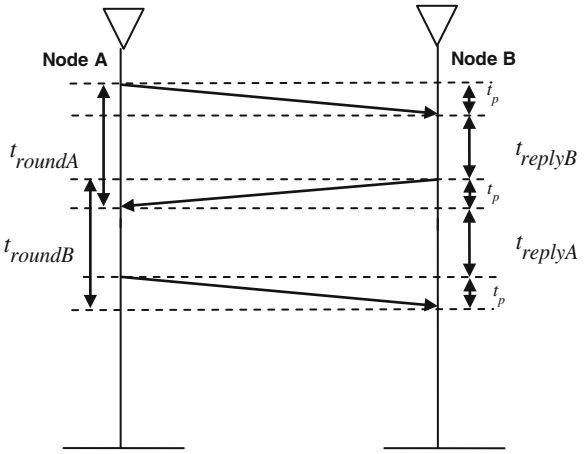

Fig. 6.12 Timing diagram for efficient implementation of SDS-TWR

$$\hat{t}_p - t_p \approx \frac{1}{4}\delta_{\text{reply}}(e_A - e_B).$$

As δ_{reply} is typically a small fraction of the reply time (t_{replyA} or t_{replyB}), the measurement error due to SDS-TWT-TOA is much smaller compared to that of TWR-TOA.

6.4 UWB Chipsets

Historically speaking, the very first UWB chipset was made by Aether Wire and Location,[1] Inc in 1993 [1]. A few other companies such as Time Domain[2] followed suit. However, the numbers remained quite low as the application domain at the time was limited to defense. Consumer electronics-related IC development took off in early 2000 following the release of the FCC First Report and order. In the coming years, many fabless semiconductor companies[3] developed silicon. However, a majority of them pursued WiMedia-based ICs.

First generation chipsets were composed of multiple chips to accommodate PHY, MAC, RF, and LNA functionalities. Two chip solutions that integrated the PHY and MAC into one and LNA and RF into another chip soon replaced the first generation ICs. The latest trend is to accommodate all the functionalities in a single chip. From process point of view, the first generation ICs were mainly

[1] http://www.aetherwire.com/.

[2] http://www.timedomain.com/.

[3] Chipset manufacturing requires huge amount of investment. As such a fabless semiconductor company designs chipsets, but the fabrication is outsourced to a semiconductor company. Over the past 15 years, the fabless model has turned into the preferred business model for the semiconductor industry.

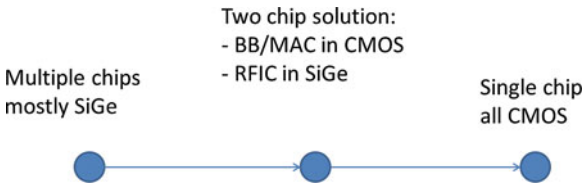

Fig. 6.13 UWB chip set evolution path

implemented in SiGe. Two chip solutions implemented baseband chip in CMOS and RFIC in SiGe. The single chip solutions in the market are in CMOS. The evolution path is depicted in Fig. 6.13.

Among UWB vendors, both Alereon[4] and Sigma Designs[5] offer two chip solutions. Among proprietary solutions, Pulse Link[6] offers a three chip solution namely baseband, RFIC and LNA. More details are provided in Tables 6.1 and 6.2.

6.5 Evaluation Board Kit and Reference Design Kit

By definition an EVK consists of a pair of transceivers controlled by a windows based GUI installed on a PC (or laptop). The link from the PC to the transceivers can be wired or wireless. One can send packets back and forth between the transceivers and gather link statistics. As such EVKs can be used for demo purposes, evaluation, and/or testing. Vendors offer EVKs to their potential customers, partners, and interested parties. In the following configuration (Fig. 6.14), EVK's application in wireless video streaming is shown.

Some companies offer an encoder board and a decoder board instead. The encoder and decoder evaluation boards serve as a transmitter/receiver pair. In this case each board is considered an evaluation board kit (EBK).

While EVK and EBK demonstrate capabilities of a technology, they are not adequate for product purposes. The RDK, on the other hand, is a turnkey solution which enables rapid development of a specific product. Included in the kit are typically board schematics, PCB layouts, bill of materials (BOM), firmware, test routines, and a user guide.

Sigma Designs, Pulse Link, and Alereon offer RDK. A mini PCI and an Ethernet over coax bridge reference designs are available from Sigma Designs. Pulse Link and Alereon offer a number of reference designs for wireless and coax applications. Tables 6.3, 6.4 list Aleron and Pulse link RDKs.

[4] http://www.alereon.com/.

[5] http://www.sigmadesigns.com/. It appears that UWB-based solutions are not offered any longer.

[6] http://www.pulselink.com/.

Table 6.1 WiMedia-based chipset developers

WiMedia company	Chipset	Comments
Alereon	BB/MAC (AL 6301)	All data rates, band groups 1, 3, 4, 5, 6 (3.1–10.6 GHz)
	RFIC (AL 5100)	RFIC in SiGe BiCMOS BB/MAC in CMOS130 nm
Sigma designs	BB/MAC (BW 401) RFIC (BW 110)	All data rates, band group 1 only

Table 6.2 A proprietary chipset developer

Company	Chipset	Comment
Pulse link	BB/MAC (PL3130), RFIC (PL3120), low noise amplifier (PL3110)	up to 1.35 Gbps RFIC and LNAin SiGe 180 nm BB/MAC in CMOS 130 nm

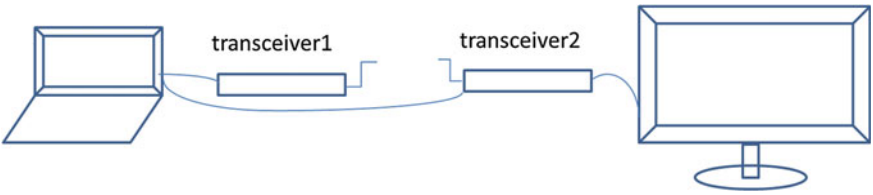

Fig. 6.14 UWB EVK concept

Table 6.3 Alereon RDKs

RDK number	Functionality
AL5750-RDK-00	1080p wireless UWB A/V adapter
AL6622-RDK-00	Wireless monitor/docking station
AL6624-RDK-00	Wireless docking station

Table 6.4 Pulse link RDKs

RDK number	Functionality
PL3301-RDK	Mini PCI card
PL3302-RDK	Ethernet over coax
PL3303-RDK	1394 over coax
PL3304-RDK	Wireless HDMI transmitter and receiver
PL3305-RDK	HDMI over coax transmitter and receiver

6.6 UWB Test Equipment

A number of UWB signal characteristics such as the small pulse width, huge bandwidth, and small (near noise floor) power spectral density presented a challenge to the existing test equipment. Having witnessed that, test equipment

Table 6.5 Tektronix

Equipment	Functionality	Application
AWG7000 series	Generates WiMedia signal for all bands	Waveforms can be created using RFXpress software
	Band groups 1 and 2 with no external components	Waveform can also be imported from MATLAB, Mathcad or Excel
	Band groups 3-6 using an external upconverter	Impairments can be added to the waveform
DPO 70000 series	Captures UWB signals	Comes with a report generatorand determines pass/fail based on WiMedia 1.2 test spec
	Conducts a set of measurements	

manufacturers offered equipment suitable for the UWB market. In the remainder of this section we review some of the available UWB test equipment (Tables 6.4, 6.5, 6.6, 6.7, and 6.8).

Tektronix[7] offers arbitrary waveform generators (AWGs) with large sampling rates such as AWG 7000 [9]. RFXress software, a window-based application that runs on the AWG 7000 series, can be used to generate WiMedia or any other UWB signals. As for WiMedia waveforms, band group 1 and 2 signals are generated in RF form, while band group 3 to 6 signals require external upconverters for RF conversion. DPO70000 series can capture UWB signals and conduct a number of measurements. The report generator software could determine whether a signal passes/fails WiMedia 1.2 spec.

Agilent's[8] N7916A Studio Signal Software can be used to generate WiMedia signals, when it is run on Agilent's N6030A AWG [10]. To convert the baseband signal to RF, one can drive Agilent E8267 D PSG vector signal generator with quadrature signal originated from N6030A AWG.

Ellisys[9] WiMedia Explorer 300 generator (WEX300G) and analyzer (WEX300A) can put out WiMedia compliant RF waveform and capture WiMedia traffic for analysis and debugging purposes, respectively [12, 13]. Wired version is available for regions/countries where regulations are not established yet or regulations require conducted tests. Lecroy's[10] UWB trainer transmits WiMedia packets, while tracer captures, analyzes, and decodes WiMedia UWB signals [11]. Within the trainer, bit level content of packet, as well as its timing and frequency can be modified by the user. Lecroy's system can be used to test UWB system functions as well as protocol level compliance. Both Ellisys WiMedia explorer and Lecroy's tracer/trainer need to be used in conjunction with a desktop or a laptop, as they do not have any display capabilities.

[7] http://www.tek.com/.

[8] http://www.home.agilent.com/agilent/home.jspx?cc=IR&lc=eng.

[9] http://www.ellisys.com/.

[10] http://www.lecroy.com/.

Table 6.6 Agilent

Agilent equipment	Functionality
Agilent's N7619A signal studio software	WiMedia baseband waveforms can be specified Impairments can be added
N6030A (or N6031A) AWG	Baseband MB-OFDM signal can be synthesized
Agilent E8267 D PSG vector signal generator	RF signal can be generated by driving Agilent E8267 D PSG vector signal generator with the quadrature signals
Agilent DS080000 series	Capture MB-OFDM signal and analyze it using 89600 vector signal analysis software

Table 6.7 Ellisys

Equipment	Functionality	Application
Ellisys WiMedia Explorer 300 analyzer & generator (WEX300A, WEX300G and WEX300DUO)	Generates WiMedia-compliant waveform Capture UWB traffic over the air to assist development of Wireless USB devices	An aid for design, analysis, and debugging

Table 6.8 LeCroy

Equipment	Functionality
LeCroy UWB tracer/trainer (UW005APA-X)	Transmit WiMedia packets with full control of data stream protocol analyzer captures, analyzes, and decodes WiMedia traffic

6.7 UWB Products

A vast majority of UWB products in the market are devices that transport high definition content from laptop or desktop environments to flat panel displays, speakers, or projectors. They include wireless HDMI, wireless docking stations, and wireless multimedia adapters. Some support 1080p while others support 720p format. The offered kits have either three or two pieces from factors. The three-piece kits consist of the receiver base, the receiver adapter, and the transmitter adapter while the two-piece ones are made of the receiver adapter and the transmitter adapter. Truelink wireless USB to HDMI kit,[11] Toshiba wireless dynadock,[12] Icreon wireless audio/video docking station[13] and Imation Link wireless A/V extender[14] are just a few examples of UWB products on the shelves.

[11] http://www.cablestogo.com/product.asp?cat_id=3810&sku=29354.

[12] http://us.toshiba.com/accessory/PA3686U-1SET.

[13] http://www.alereon.com/demos/demo-video-1.

[14] http://www.imation.com/Global/ImationLinkInfoSheet_82710.pdf.

Another envisioned application of UWB is in ranging, location and positioning. Zebra[15] technologies offers a UWB based real time location system (RTLS) solution known as Dart UWB technology. The RTLS consists of sensors (UWC-1300-A-00AA), tags (UWT-1100-A-00AB), readers (UWD-1000-A- 03AA), hubs (UWH-1100-A-00AA) and wands (WND-3100-A-00AA). Dart UWB solution is IEEE 802.14.4f compliant and provides a location accuracy of better than 1 foot and a range of up to 200 m. Ubisense[16] offers RTLS solutions based on UWB for various application such as asset management and assembly control systems. The indoor/outdoor location accuracy is limited to 1 foot. PLUS Location Systems[17] provides UWB RTLS products and services. Array of RTLS products include tags and readers. Sub-meter location system accuracy is claimed.

Wireless sensor networks are another application area for UWB technology. Decawave[18], a fabless semiconductor, offers a single chip CMOS based single chip transceiver (ScenSor1) supporting IEEE 802.15.4a standard.

Lastly UWB has been applied to miscellaneous applications. Uraxs[19], an UWB system and solution company, has developed a communication/geo-location system for parents and their children. Children wear wrist watch like devices (RUMS4c) and that enables them to send a message to their parents when they are in danger. The plan is to add voice/video delivery capabilities over UWB. MNN MotionGrid, a portable position aiding system utilizing UWB technology, is developed by XSENS[20]. It can be used in training, simulation, sport science and on-set motion capture.

What We Learned

- IEEE 802.15.3 fundamentals
- Superframe structure and functionality
- Device admission sequence of events
- WiMedia MAC and IEEE 802.15.3 MAC differentiators
- IEEE 802.15.4a MAC and IEEE 802.15.3 MAC differentiators
- Ranging performance lower bound
- OWR-TOA, TWR-TOA, and SDS-TWR ranging schemes
- Comparing the performance of OWR-TOA, TWR-TOA, and SDS-TWR
- UWB chipset evolution
- EVK, EBK, and RDK and their differences
- Available UWB test equipment
- MB-OFDM signal generators and analyzers
- Existing UWB products in the market.

---

[15] http://www.zebra.com/us/en.html.

[16] http://www.ubisense.net/en/.

[17] http://pluslocation.com/.

[18] http://www.decawave.com/.

[19] http://www.uraxs.com/Index.aspx.

[20] http://www.xsens.com/.

Problems

1. Compare the location accuracy of ECMA-368 vs. that of DS-UWB.
2. What are the differences between IEEE 802.15.3a MAC and WiMedia MAC?
3. Consider the scenario where a UWB transmitter is placed 20 m away from an IEEE 802.11a compliant transmitter. The UWB transmitter details are as follows:

   - Modulation: BPSK
   - Coded rate: 1Mbps
   - Coding: convolutional rate ½ coding with $K = 4$
   - UWB spectrum range from 3.1 to 4.1 GHz

   A UWB receiver is placed on the straight line connecting the two transmitters and will be staying on this line throughout the experiment. Plot receiver BER versus UWB transmitter/receiver spacing as the spacing is increased from 3 m to 10 m.

4. Take two UWB chipsets from two vendors. Present a thorough comparison between them.

References

1. IEEE 802.15.3, PART 15.3: wireless medium access control (MAC) and physical layer (PHY) specifications for high-rate wireless personal area networks (WPANs), 2003
2. European Computer Manufacturing Association, UWB: high rate ultra wideband PHY and MAC standard, Technical report, www.ecma-international.org, 2005
3. IEEE P802.15.4a/D7, PART 15.4: wireless medium access control (MAC) and physical layer (PHY) specifications for low-rate wireless personal area networks (LRWPANs), 2007
4. L. De Nardis, M.G. Di Benedetto, Overview of IEEE 802.15.4/4a standards for low data rate wireless personal data networks, in *Proceedings of WPNC'07*, (Hannover, Germany, 2007), pp. 285–289
5. H.L.V. Trees, *Detection, estimation, and modulation theory: Part I*, 2nd edn. (Wiley, New York, 2001)
6. H. Urkowitz, *Signal theory and random processes* (Artech House, Norwood, 1983)
7. W.C. Lindsey, M.K. Simon, *Phase and Doppler measurements in two-way phase coherent tracking systems* (Dover, New York, 1991)
8. R. Hach, Symmetric double sided two-way ranging, in *Proceedings of IEEE P802.15 Working Group for Wireless Personal Area Networks (WPAN), Doc. IEEE P.802.15-05-0334-00-004a*, 2005
9. Tektronix Arbitrary Waveform Generator. Available at: <http://www.tek.com/datasheet/signal-generator/awg7000-arbitrary-waveform-generator-arbitrary-waveform-generators>
10. Agilent Technologies Solutions for MB-OFDM Ultra-Wideband Application Note. Available at: http://readpdf.net/file/agilent-technologies-solutions-for-mb-ofdm-ultra-wideband.html
11. LeCroy UWB Tracer/Trainer. Available at: http://www.lecroy.com/
12. WiMedia Explorer 300 Analyzer. Available at: <http://www.ellisys.com/>
13. WiMedia Explorer 300 Generator. Available at: http://www.ellisys.com/, http://www.wirelesshd.org/. Accessed 26 Dec 2010

Chapter 7
Communications Via 60 GHz Band

A working definition for 60 GHz band is provided and the available 60 GHz spectral allocations in many countries around the globe are described. Then the unique characteristics and capabilities of 60 GHz are discussed, the case for 60 GHz technology is made, and the potential applications are listed. Topics such as system capacity, link budget, and various modulation options are addressed in detail. Finally, IC process technologies are compared, chipset makers are introduced, and products in the market are listed.

7.1 60 GHz Band Definition

The electromagnetic spectrum is divided into a number of frequency bands. Millimeter wave[1] (mmW) and V-band[2] are two widely familiar bands that include 60 GHz. By definition, the frequency range from 30 to 300 GHz is called the mmW, as the wavelengths associated with this interval vary from 10 to 1 mm. V band occupies the range from 50 to 75 GHz. The other two frequency bands around 60 GHz known as U and E bands[3] are as follows (Fig. 7.1).

U band: ranges from 40 to 60 GHz.

E band: ranges from 60 to 90 GHz.

The band of interest to us is a subset of both mmW and V bands. Roughly speaking, the range from 50 to 60 something GHz is considered to be the 60 GHz band. There is a significant amount of unlicensed allocated spectrum available worldwide in this band. However, the specifics of the band such as upper frequency edge, lower frequency edge, bandwidth as well as emission limits vary from country to country.

The 60 GHz band allocated spectra (such as bandwidths and band edges) in different countries are listed in Table 7.1 and Fig. 7.2. The following observations are noteworthy. First, the available spectrum in the 60 GHz band is quite large.

[1] Per ITU's nomenclature this band is known as Extremely High Frequency (EHF) [1].
[2] This definition is provided by Radio Society of Great Britain [2].
[3] These definitions are provided by Radio Society of Great Britain [2].

S. Emami, *UWB Communication Systems: Conventional and 60 GHz*,
DOI: 10.1007/978-1-4614-6753-3_7,

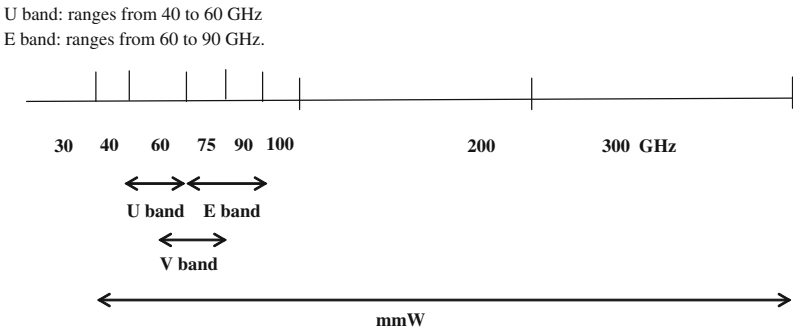

Fig. 7.1 Illustration of frequency bands in the neighborhood of 60 GHz

Table 7.1 60 GHz band specifics [3–10, 34]

Country or region	Band edges (GHz)
USA	57, 64
Canada	57, 64
Europe	57, 66
United Kingdom	57.1, 63.9
Australia	59.4, 62.9
Japan	59, 66
China	59, 64
Korea	57, 64
New Zealand	59, 64
Brazil	57, 64
South Africa	59, 64

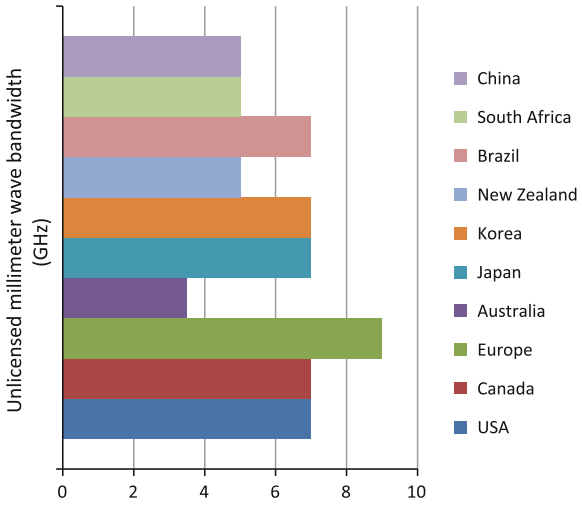

Fig. 7.2 Available unlicensed 60 GHz bandwidth in different countries (or regions) [4–34]

The allocations vary from 3.5 to 9 GHz depending on region or country. Second, 60 GHz allocations are unlicensed. Radio operation in the unlicensed spectrum[4] (or license-free spectrum) does not incur any cost to the consumer. Third, since 60 GHz is available in many countries across the world,[5] one can launch products for the global markets as opposed to just regional ones. The end result is availability of affordable products for huge markets.

7.2 60 GHz Spectral Allocations

The 60 GHz regulations across the world are relatively recent and have been established mainly over the past 10 years. A listing of the regulatory documents of each country together with their publication date is provided in Table 7.2. Technical specifications such as the transmitted power, equivalent isotropic radiated power (EIRP)[6] and antenna gain limitation for various countries/regions are provided in Table 7.3.

Japan Ministry of Public Management, Home Affairs, Posts and Telecommunication (MPHPT) introduced their 60 GHz regulations in 2000 [3]. As per regulations maximum bandwidth and power are constrained to 2,500 MHz and 10 dBm, respectively. In the US, FCC finalized the 60 GHz rules in 2004. As per FCC rule, 7 GHz worth of unlicensed spectrum (between 57 and 64 GHz) was made available for 60 GHz applications [4]. In 2005, Canada published its regulations. Canada's 60 GHz regulations released by Industry Canada Spectrum Management and Telecommunications (IC-SMT) are identical to that of the US [5]. Australian regulations were also released in 2005 as well [6]. So far, Australia's 60 GHz allocated band is the smallest among all. Korea's allocation established by the Ministry of Information and Communication (MIC) came in 2006 [7]. The 7 GHz allocated band is at par with most of the industrial world. ETSI proposal, unveiled in 2006, requires a minimum bandwidth of 500 MHz with transmit power of upto 20 dBm [8]. The European regulations will be finalized upon ECC approval. In the UK, Ofcom[7] has allocated 6.8 GHz of frequency in 60 GHz band on license exempt basis [9]. In 2011, following a period of public consultation, Singapore's IDA[8] opened 57–66 GHz band with the maximum EIRP

[4] As per FCC definition (http://www.Fcc.gov) users can operate without a license in unlicensed spectrum, but they must comply with requirements and rules including FCC's Part 15. Note that these users do not have exclusive use of the spectrum and are subject to interference.

[5] Countries listed in Table 7.1 account for less than half the world population. However, they are among nations with the highest gross domestic product (GDP). With their purchasing power, they are the most likely customers for new products.

[6] By definition, equivalent isotropic radiated power (EIRP) is the product of power (P) and antenna gain (G). In other words $EIRP = PG$.

[7] Ofcom is the entity in charge of UK's communication industries and spectrum usage.

[8] IDA stands for Infocomm Development Authorithy.

Table 7.2 Regulatory documents relevant to 60 GHz band [4–10]

Country/region	Regulatory body	Document	Years
USA	FCC	CFR Title 47 Part 15.255	2004
Canada	IC-SMT	RSS-210	2005
Europe	ETSI	DTR/ERM-RM-049	2006
Japan	MPHPT	Regulations for the enforcement of radio law, 6–4.2 specified low power radio station (17) 59–66 GHz band	2000
Korea	Ministry of Information and Communication	Frequency allocation comment of 60 GHz band	2006
Australia	ACMA	Radiocommunications (Low interference potential devices) class license variation 2005 (No. 1)	2005
Singapore	IDA	IDA's decision and explanatory memorandum on the regulatory framework for 60 GHz frequency	2011
United Kingdom	ofcom	Release of 59–64 GHz band	2009

Table 7.3 60 GHz limits across the world [4–34]

Country or region	Transmit power (mW)	Mean EIRP (dBm)	Max EIRP (dBm)	Maximum antenna gain (dBi)
USA and Canada	500	40	43	33*
Europe	20	NA	57	37
United Kingdom	10	NA	55	30
Australia	10	NA	51.7	41.8
Japan	10	NA	58	47
Korea	10	NA	27	17
New Zealand	500	40	43	33*
China	10	44	47	–

*subject to 10 dBm transmit power

of 40 dBm for unlicensed operation [10]. Under this decision, a license must be acquired for larger EIRP levels in 57–63 GHz.

7.3 60 GHz Characteristics

The 60 GHz signal is impacted by different phenomena such as oxygen absorption, rainfall, material attenuation, and path loss to name a few. Below is a summary:

– at 60 GHz signal is absorbed by oxygen molecules to much higher extent compared to other frequencies. More specifically, the high oxygen absorption at 60 GHz leads to significant signal attenuation of up to 17 dB/km [11]. However, in short range communication (less than 50 m), this effect is not much of a factor;
– rainfall attenuates the 60 GHz signal as well. In fact, the attenuation due to rain could be twice to three times that of the oxygen absorption. Clearly, rain does not impact indoor communications;
– signal attenuation at 60 GHz due to dry wall, white board, and wall studs has been compared to that of lower frequencies such as 2.5 GHz [12]. Typically, larger attenuations at 60 GHz have been observed;
– Friis free space path loss indicates that path loss differential between 60 GHz and 2.5 GHz is significant because

$$20 \log\left(\frac{60e9}{2.5e9}\right) = 27.6 \text{ dB}.$$

– the main mechanisms of signal propagation at 60 GHz are LOS as well as the first- and second-order reflection paths [13]. There is very little diffraction at 60 GHz as the signal wavelength is smaller than most objects. However, there is more reflection off the objects that would diffract at lower frequencies for the same reason;
– since antenna length is proportional to the signal wavelength, 60 GHz antennas are smaller compared to antennas at lower frequencies. Consequently, lesser power is picked up at 60 GHz by a single antenna;
– antenna size at 60 GHz is small (60 GHz wavelength is only 5 mm long). Consequently, implementation of multiple antenna solutions on portable devices becomes feasible. On the other hand, the transceiver chain (antenna included) can be integrated into a chip enabling a small form factor.

The signal 60 GHz signal does not travel very far due to the aforementioned attenuation factors. It is therefore suitable for high throughput indoor data delivery. The significant signal attenuation at 60 GHz limits the coverage, but at the same time results in higher frequency reuse. Furthermore, 60 GHz communications would have to utilize directional antennas with narrow beams as we will see later. However, narrow beams feature of directional antennas as well as attenuation factors result in secure communications and limited interference.

7.4 Capacity

A useful form of Shannon–Hartley capacity expression was derived in Chap. 1 as

$$C = B \log_2\left(1 + 10^{(P_T + G_T + G_R - L - I - N)/10}\right)$$

Table 7.4 Parameters list

Parameter	Value
Center frequency	60 GHz
Bandwidth	2 GHz
Transmit power	10 dBm
Noise figure	10
Implementation loss	8
Path loss exponent	2.5

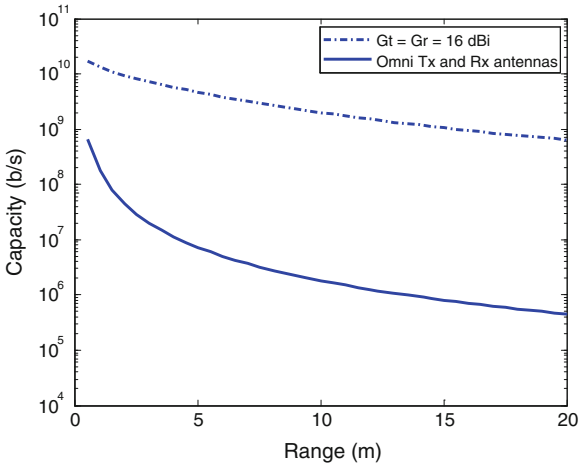

Fig. 7.3 60 GHz band capacity with and without directional antennas

where P_T (dBm), G_T (dB), G_R (dB), L(dB), I (dB), N (dBm), and B (Hz) denote transmit power, transmit antenna gain, receive antenna gain, path loss, implementation loss, noise floor, and bandwidth, respectively.

Here, two 60 GHz scenarios are considered and Shannon–Hartley transmission capacity for each scenario is computed. In one scenario, omni antennas are deployed at both transmitter and receiver ends. In the other scenario, directional antennas with antenna gains of 16 dBi are utilized at the transmitter and receiver.

The parameters are listed in Table 7.4. We consider a 2 GHz wide channel with 10 dBm transmit power similar to the 802.15.3c vision. The path loss is chosen to be 2.5, as we are interested in NLOS type channels. As per the capacity plot shown in Fig. 7.3, the omni directional setup is incapable of supporting gigabit data rates. On the other hand, the directional antenna setup supports multi-gigabit rates up to a range of roughly 20 m. Above and beyond that, capacity reduction as a function of range is rather drastic for the omni setup. In the first 5 m, the capacity drops by two orders of magnitude. However, for the directional antenna setup, the capacity reduces quite gracefully.

This example demonstrates that Giga bit transmission rates cannot be achieved with omnidirectional antennas but requires the use of directional antennas at both transmit and receive ends. Antenna directivity gain depends on the exact application geometry. Typically, antenna gains are at least 10 dBi.

7.5 Link Budget

In what follows we consider two specific links, namely 2 Gbps @ 5 m and 2 Gbps @10 m. A number of assumptions are also made to carry out the required analysis. Transmit power is set at 10 dBm with the antenna gain of 30 dBi (below maximum gain of 33 dBi). The signal bandwidth of 2 GHz is used to achieve a 2 Gbps data rate. The SNR of 14 dB is needed, if a single carrier QPSK modulation with FEC is used.

As we saw in Chap. 1, the link margin is given by

$$M = P_T + G_T + G_R - L - N - SNR - I,$$

where P_T, G_T, G_R, SNR, I, L, and N denote transmit power, transmit antenna gain, receiver antenna gain, signal-to-noise ratio at the receiver, implementation loss,

$$L = 20\log(4\pi \mathrm{d} f_c/c)$$

and

$$N = -174 + 10\log(B) + 10\log(F).$$

The link margins for the two links are listed in Table 7.5. The link margins are above the 10 dB that is required to combat shadowing and body obstructions.

7.6 Modulation Options

There are a few modulation classes that one can consider such as multi-carrier (or OFDM), single carrier (linear) systems, and constant envelope schemes (such as GMSK). These modulations are suitable choices as they are well understood, offer performance compromises, and have been used in a number of other existing standards. In the remainder of this section, some important attributes of these modulations are listed and compared.

Table 7.5 Link budget table

Range	5 m	10 m
Transmit power (P_T)	10 dBm	10 dBm
Tx. antenna gain (G_t)	30 dBi	30 dBi
Rx. antenna gain (G_r)	30 dBi	30 dBi
Center frequency (fc)	60 GHz	60 GHz
Path loss (L)	98.98 dB	105 dB
Noise floor (N)	−70.98	−70.98
Noise figure (F)	10 dB	10 dB
Implementation loss (I)	8 dB	8 dB
Signal-to-noise ratio (SNR)	14 dB	14 dB
Margin	20 dB	13.98 dB

Equalization: OFDM modulation is well suited for operation in multipath channels. Essentially, a frequency selective channel is divided into a number of flat-faded channels, simplifying the equalization function [14]. More specifically, the equalizer degenerates to simple scaling. On the other hand, typical time domain equalization for a single carrier system is computationally complex. However, a technique known as single carrier block transmission (SCBT) can take advantage of frequency domain equalization similar to OFDM [15]. As for constant envelope modulations, a complex equalization scheme is required.

PAPR: Constant envelope modulation systems have no PAPR. The PAPR of single carrier modulation is a function of constellation size and pulse shaping. Larger constellation sizes end up with larger PAPR. Pulse shaping impacts PAPR as well. Lower excess bandwidths of root raised cosine pulse shapes result in higher PAPR. The differential PAPR between QPSK and 64QAM could be in the range of 2–3 dB based on the pulse shaping excess bandwidth [16]. On the other hand, the PAPR of OFDM is not a function of constellation size, when the number of subcarriers is large. It is typically in the 12–14 dB range. The PAPR associated with small constellation size single carrier systems (such as BPSK and QPSK) is much less than that of OFDM systems. However, PAPR differential between a single carrier with large constellation size and OFDM would be much less. While PAPR associated with OFDM is fixed, single carrier transmission offers a wider range of PAPRs (with varying data transmission rates) for the designer to work with.

Amplifier efficiency is a function of the operating point which in itself is impacted by PAPR. The lower the PAPR the higher the operating point of the amplifier will be. As such, the battery life would be longer compared to the case where operating point is lower. Constant envelope modulations can utilize class C power amplifiers. OFDM and SC systems utilize class A, B, or AB amplifiers with lower efficiency ratings.

Back off is the difference between the amplifier output power and the maximum possible output power and it is a function of PAPR. Back off must be selected judiciously, otherwise nonlinear distortion is generated. Nonlinear distortion results in spectral regrowth that interferes with other spectrum users.

PAPR also impact the number of required A/D bits. Clearly, more bits of accuracy are needed when a system has a larger PAPR. Consequently, single carrier modulation schemes utilize fewer bits in their A/D compared to OFDM systems.

Spectral Efficiency: in terms of spectral efficiency, OFDM is superior to single carrier transmission. Among the three systems, constant envelope modulation schemes are the least spectrally efficient system.

Timing, **Phase, and Frequency Errors**: Timing, frequency estimation, and phase noise influence the performance of both OFDM and single carrier systems. While OFDM is more sensitive to frequency offset, single carrier systems are more sensitive to timing errors. Both modulations are influenced by phase noise, but OFDM is more impacted. Of the three modulation schemes, constant envelope schemes are the least sensitive to phase noise.

Phase noise at 60 GHz could significantly degrade the system performance. The relative phase noise at 60 GHz is

$$20\log\left(\frac{60e0}{2.5e9}\right) = 27.6 \text{ dB}$$

larger compared to that of 2.5 GHz. One way to avoid excessive phase noise is to use higher quality crystals which impact the material cost. The other technique is to transmit the reference oscillator [17]. However, extra bandwidth is required to transmit the reference oscillator. Additionally, both multipath and noise deteriorate the reference quality.

Complexity: In an OFDM system, IFFT and FFT are deployed in OFDM transmitter and receivers, respectively. SCBT, on the other hand, deploys both FFT and IFFT blocks at the receiver. As such, SCBT transmitter will be simpler compared to OFDM. On the other hand, SCBT receiver will be more complex in comparison to OFDM.

There is no best solution for every possible application. However, for a given application one can find the best choice. If an application requires the most resilient performance in multipath channels and transmitter power efficiency is not very critical, then OFDM emerges as the best solution. On the other hand, if both battery life and support of higher data rates are equally important and channels are either LOS or NLOS with lower delay spread then SC is the preferred solution. Finally, if the transceiver system cost and battery life are equally important and very high data rates are not necessary, then constant envelope modulation would be the solution of choice. For instance OFDM, SC and constant envelope modulation are suitable for wireless HDMI, desktop environment, and hand-held consumer electronic applications, respectively.

7.7 Application Scenarios

A review of future application of WPAN shows that there is a need for communication systems that can go well beyond 1 Gbps. It turns out that the majority of application scenarios involve high-definition (HD) video transmission. HD 1,080 p format has a resolution of 1,920 × 1,080 with a refresh rate of 60 frames per second. The data rate requirements for some existing and upcoming HD signals as color depth and frame refresh rates increase are shown in Fig. 7.4 [18]. It is seen that wireless transmission of uncompressed HDTV signal requires data rates about or exceeding 3 Gbps.

The high throughput and promising link budget of 60 GHz band enable a number of indoor applications scenarios. Among them, the following application scenarios seem to be more appealing [19]:

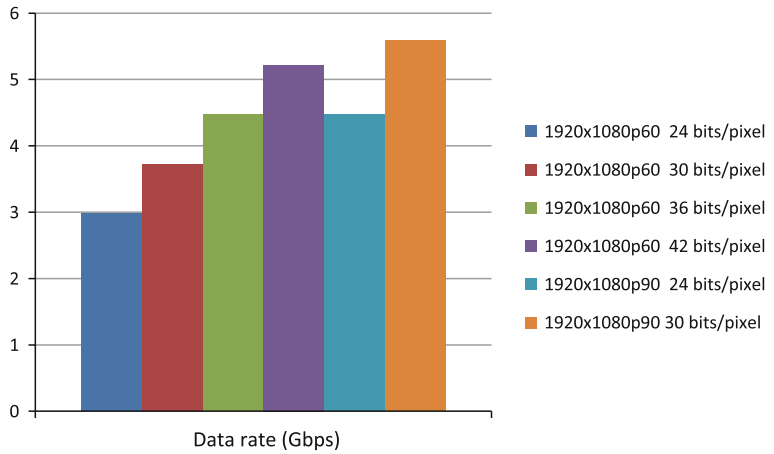

Fig. 7.4 Data rate requirements for some current and upcoming HDTV signal

– Uncompressed HD content delivery in living room requires a range of up to 10 m and data rates of up to 4 Gbps (Fig. 7.5). The transmission channel could be either LOS or NLOS depending on the geometry. System should be able to deal with temporary signal blockage by people. HD content could originate from a Blu-Ray player, set-top box, DVD player, or cable box. The link is highly asymmetric, indicating that significant part of communication is from the source to the display unit. A very low bit error rate (BER) is expected.
– Audio/video/text file transfer from kiosks set up inside or outside stores typically require data rates of up to couple of Gbps. A range of 1–2 m should be adequate. Communication channel can be assumed to be mostly LOS and it is typically highly asymmetric.
– Conference room networking allows laptops to communicate with each other or the slide projector (Fig. 7.6). Expected range, data rates, and channel type are 1–5 m, up to 2 Gbps and LOS, respectively. In this case, communication channel could be symmetric or asymmetric.
– Wireless office connectivity is a scenario in which laptops/desktops are connected to the backhaul (Fig. 7.7). Other devices on or around the desk such as a wireless hard drive, an electronic tablet, or a digital camera could also

Fig. 7.5 Wireless HD content delivery

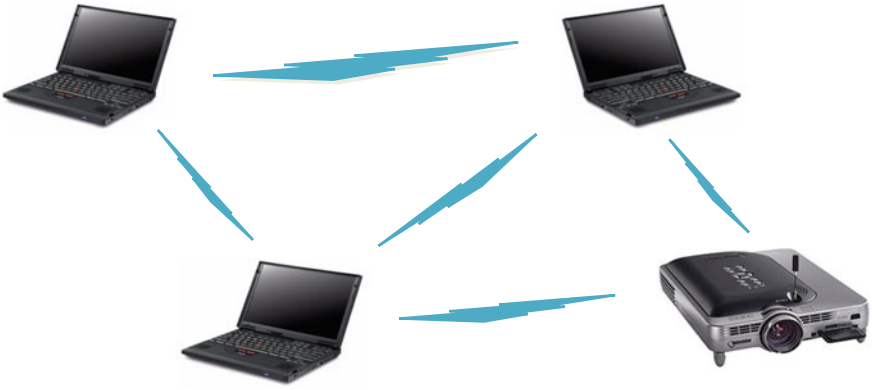

Fig. 7.6 Conference room network

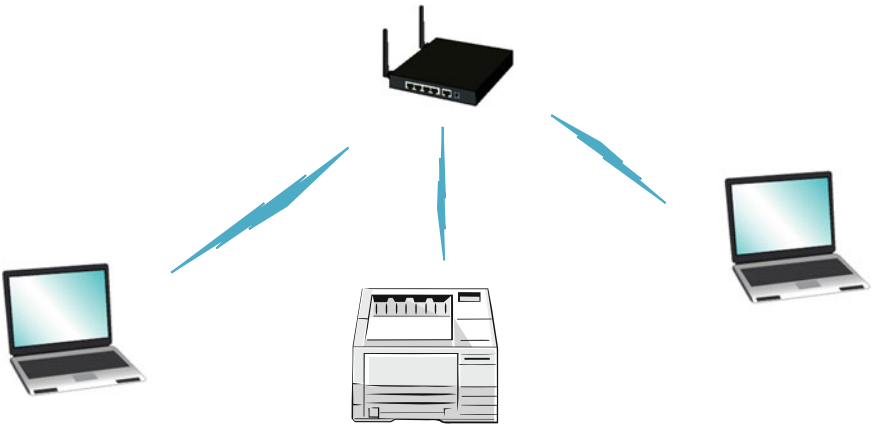

Fig. 7.7 Wireless office scenario

connected to the laptop. Range of up to 5 m and data rates of up to 3.5 Gbps are expected. Communication link would be mostly asymmetric.

7.8 Antennas

Per our earlier analysis, the use of directional antennas is a necessity for 60 GHz radios to obtain gigabit rates. In this section, we review the antenna types and define antenna gain and antenna pattern. Beamforming concept is explained and the corresponding mathematical frame is established. We then introduce smart antennas as an enabler technology for robust and low cost radios. Finally, switched

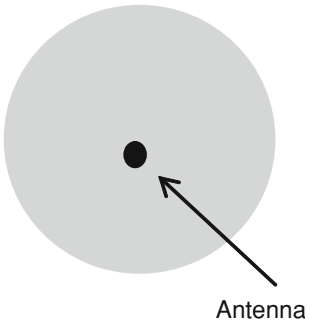

Fig. 7.8 Isotropic antenna pattern

beam antennas and adaptive antennas are presented and their attributes are highlighted. Interested reads are encouraged to look into [20, 21] for detailed treatment of the topics.

7.8.1 Antenna Types

From directivity point of view, there are three types of antennas, namely isotropic, omnidirectional and directional antennas. While isotropic antennas radiate (or receive) equally well in all directions in the space as shown in Fig. 7.8, omnidirectional antennas radiate (or receive) equally well in all directions only in the horizontal plane as seen in Fig. 7.9. Directional antennas radiate (or receive) in a particular direction in the space (Fig. 7.10).

Omnidirectional and isotropic antennas are intended for the scenarios when the user's location is not known to the transmitter. However, if the user's location in the space is known, power propagated in directions other than the intended user is wasted. This wasted power turns to an interference source for other spectrum users. Directional antennas should be used instead to deliver power to the intended user.

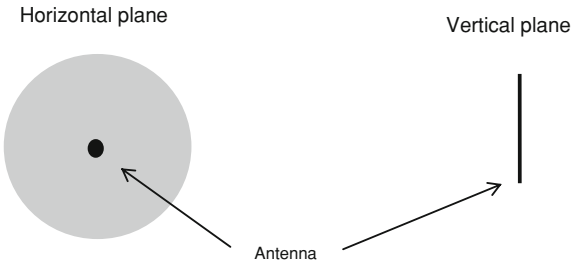

Fig. 7.9 Omnidirectional antenna patterns

Fig. 7.10 Directional antenna

7.8.2 Antenna Gain and Antenna Pattern

The antenna gain in a certain direction $\vec{d}$ in the three-dimensional space is defined by

$$G\left(\vec{d}\right) = \rho \frac{U\left(\vec{d}\right)}{U_{\text{ave}}}$$

where $U(\vec{d})$, U_{ave} and ρ denote the power spectral density in direction d, average power density, and antenna efficiency. Typically, antenna gain is expressed in dBi

$$G_{\text{dB}i} = 10\log G_{\text{abs}}$$

where G_{abs} is the absolute value of the antenna gain. Note that the i in dBi denotes isotropic.

Antenna pattern is a three-dimensional object indicating the antenna gains in different directions in the space. Oftentimes, instead of the three-dimensional antenna pattern, the projections of it onto the horizontal (azimuthal) and vertical (elevation) planes are provided.

7.8.3 Beamforming

Beamforming is a technique to generate various radiation pattern through the use of antenna elements. A uniform linear array (ULA) is a collection of N antenna elements with equal spacing of d along a straight line as shown in Fig. 7.11.

The transmitted signal from the source is a complex tone such as

$$x(t) = ae^{j\omega t}$$

Let us assume that this signal impinges on ULA with an angle θ_0. A delayed version of the signal is received at the ith antenna element

$$x(t - t_i) = e^{-j\omega t_i} ae^{j\omega t} = e^{-j\omega t_i} x(t)$$

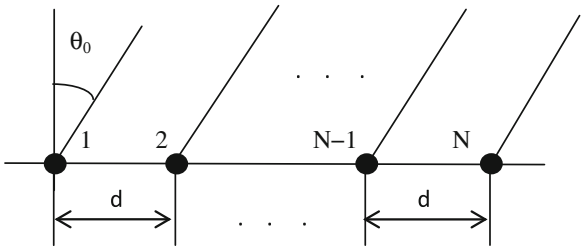

Fig. 7.11 Beamforming illustration

where $t_i = \frac{(i-1)d\ \sin\theta_o}{c}$ and c is the speed of light. Note that $t_1 = 0$.

Delay-sum beamformer (or phase array) undoes the delay associated with each received component such that received signals line up. As such, the received signals are combined in the following fashion:

$$y(t) = \sum_{i=1}^{N} w_i^* x(t - t_i)$$

where weights are.

$$w_{i=} e^{-j\omega\frac{(i-1)d\ \sin\theta}{c}}$$

Let us compute the beamformer output at incidence angle θ_0

$$y(t) = \sum_{i=1}^{N} e^{j\omega\frac{(i-1)d[\sin\theta - \sin\theta_0)}{c}} x(t) = \sum_{i=1}^{N} x(t) = Nx(t).$$

At angle θ_0, the output is increased N times compared to a single antenna element. At other angles, due to incoherent addition the output is not attenuated. The beamformer pattern, by definition, is given by

$$G(\theta) = \left| \sum_{i=1}^{N} e^{j\omega\frac{(i-1)d[\sin\theta - \sin\theta_0)}{c}} \right|$$

as a function of signal arrival angle θ.

The beam forming patterns for incidence angles of 0 and 30 degrees and array spacing of d = $\lambda/2$ are shown in Fig. 7.12a–b. Beamwidth is a function of the number of antenna elements N. A comparison is provided in Fig. 7.12c. Clearly, beamwidth becomes narrower as the number of the antenna elements increases from $N = 5$ to 10.

Beamforming can be done entirely in digital. To do so, each and every path is sampled upfront right after each antenna element at the receiver. Since each and every RF path requires a data converter (A/D), design cost would be high. Alternatively, beamforming can be implemented in analog hardware. At the receiver, once all the manipulations are performed, signal can be digitized. In this way, only a single data converter (A/D) would suffice lowering the implementation cost.

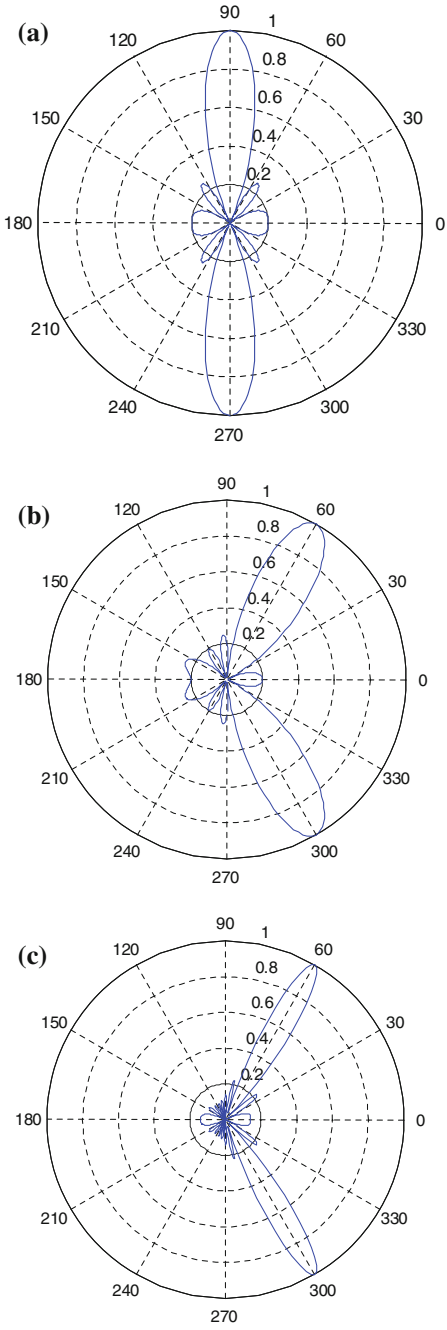

Fig. 7.12 Beamforming patterns for (a) $\theta_0 = 0°$, N = 5, (b) $\theta_0 = 30°$, N = 5, and (c) $\theta_0 = 30°$, N = 10

7.8.4 Smart Antennas

Smart antennas are antenna systems capable of generating various radiation and reception antenna patterns. This capability is reached through the introduction of a control loop and signal processing techniques to an antenna array such that the combined outputs of antenna array produce desirable antenna patterns. System capacity and coverage area can be both increased due to utilization of smart antennas.

Smart antenna concept has been around for a quite a while. However, these systems were only built for defense system due to their high implementation cost in the past. Advances in signal processing, SDR, and ASIC technology has made affordable implementation of smart radios in wireless applications possible.

Block diagram of a smart antenna is depicted in Fig. 7.13. It consists of antenna elements, a combiner, control loop, and signal processing algorithms. The use of DSP algorithms and added software makes the system smart.

7.8.4.1 Smart Antennas Categories

Smart antennas can be classified into two main categories, namely switched beam antennas and adaptive array antennas. Switched beam antennas generate only a finite number of fixed antenna patterns (Fig. 7.14), while adaptive antenna arrays present an infinite number of antenna patterns to choose from as depicted in Fig. 7.15.

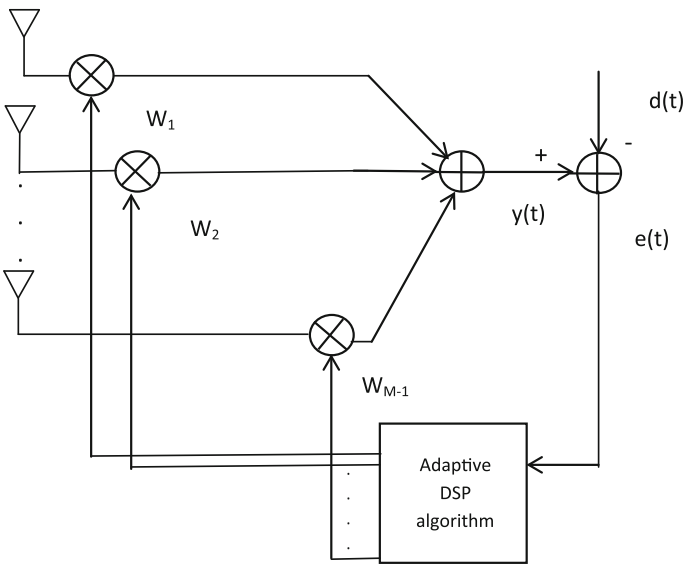

Fig. 7.13 Smart antenna

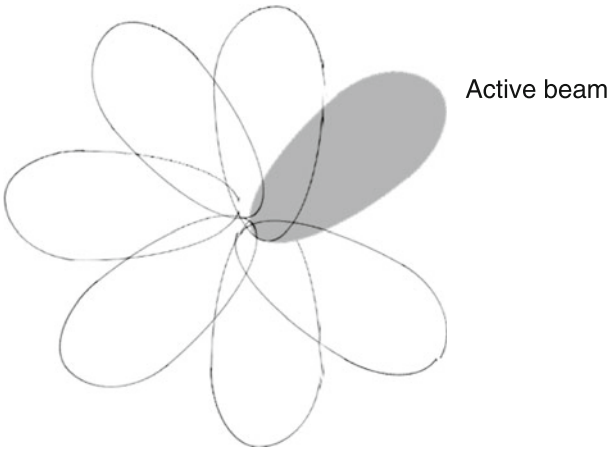

Fig. 7.14 Switched beam antenna

Fig. 7.15 Adaptive antenna array

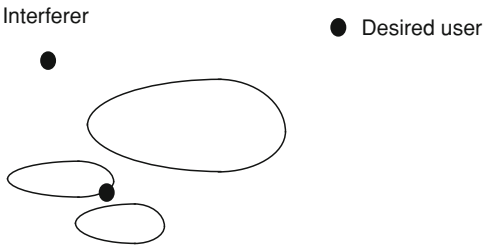

Switched beam antenna systems choose from all the available settings the one that yields the best performance. The performance metric could be signal-to-noise ratio or signal-to-noise plus interference ratio. The interference rejection capability of switched beam antennas is limited as the number of supported antenna patterns is limited. In general, the effectiveness of switched beam antennas is a function of relative location of the desired user and interference as well as the available antenna patterns.

With the aid of measurements and signal processing algorithms, adaptive antenna arrays determine the direction of the desired user and interference. Complex weights are then assigned to the outputs of the antenna elements and the weighted sum is computed. An adaptive algorithm adjusts the weights in accordance to an objective function such as signal-to-noise ratio or probability of error. In the resulting antenna pattern, maximal gain is allocated to the desired signal, while the interference is optimally suppressed.

Adaptive antenna arrays are more complex compared to the switched beam systems and are consequently more costly. In terms of performance, however, adaptive antennas provide the optimum pattern while the switched beam systems do not typically provide the optimum pattern.

Smart antennas, from the hardware perspective, require multiple antenna elements. These antennas can have different arrangements such as linear, circular, or grid. For instance, phase arrays have a linear arrangement.

In adaptive antenna arrays a cost function comparing the array output with a locally generated version of the desired output is initially formed. Then array weights are computed subject to some sort of criterion such as minimum mean square error (MMSE) or least squares (LS). This approach leads to a direct solution. However, in practice iterative solutions are preferred as they not only entail a lower computational complexity but they are capable of tracking non-stationary channels as well. LMS (least mean square) and recursive least squares (RLS) are two of the popular iterative techniques.

7.9 Antenna Training Procedure

The objective of antenna training procedure is to determine the best antenna beam pair when two devices are communicating with each other. Blind search over all possible combinations of transmitter/receiver beams is certainly a possible solution. This approach, however, could be quite complex. A divide and conquer strategy is preferred as it is less costly to implement. In this solution, initially the best sector pair is found. The best beam pair is determined next.

Two Antenna system arrangements, known as symmetric antenna system (SAS) and asymmetric antenna system (AAS), can occur in practice. In a SAS transmission and reception modes of each node utilize the same antenna system. If one or both nodes use different antenna systems for transmission and reception modes, one ends up with an AAS. IEEE 802.15.3c's antenna training procedures are based on divide and conquer strategy [22]. Two antenna system arrangements namely SAS and AAS are considered and procedures for each are listed. The training procedure for SAS, is simpler compared to AAS, as training in one direction is sufficient. In the remainder of this section sector level training, beam level training, high resolution (HRS) beam level training, as well as beam tracking are described.

Let us consider the scenario in which two devices namely DEV1 and DEV2 are being trained. Both devices use different sets of antennas for transmission and reception. Two levels of training, namely sector and beam levels, are conducted. Sector training in itself is composed of two parts, DEV1 (Tx) to DEV2 (Rx) training followed by DEV2 (Tx) to DEV1 (Rx) training.

By convention $J(n,u)$ denotes the number of transmit or receive antennas belonging to DEVn. Parameter n is the device number and $n = 0, 1, 2,\ldots, N-1$. Parameter u is set to either transmit or receive modes. As such

$J(1,t)$ number of transmit sectors of DEV1
$J(1,r)$ number of receive sectors of DEV1
$J(2,t)$ number of transmit sectors of DEV2
$J(2,r)$ number of transmit sectors of DEV2.

DEV1 to DEV2 sector training is made of $J(1,t)$ cycles. Each cycle is repeated $J(2,r)$ to allow DEV2 to receive each transmission through a different receive antenna. Upon the completion of the cycle, DEV2 selects the best transmit sector/receive sector based on a suitable metric such as SNR or SINR.

Then the roles are reversed, DEV2 transmits and DEV1 receives. DEV2 to DEV1 sector training consists of $J(2,t)$ cycles. Each cycle is repeated $J(1,r)$ to allow DEV1 to receive each transmission through a different receive antenna. At the end of cycle the best performing transmit sector/receive sector is selected.

Beam level training can start at the conclusion of the sector training. By convention $K(n,u)$ denotes the number of transmit or receive fine beams relevant to DEVn. Parameter n is the device number and $n = 0,1,2,\ldots, N-1$. Parameter u is set to either transmit or receive modes. As such

$K(1,t)$ number of DEV1's transmit fine beams
$K(1,r)$ number of DEV1's receive fine beams
$K(2,t)$ number of DEV2's transmit fine beams
$K(2,r)$ number of DEV2's receive fine beams.

Similar to sector training, beam level training consists of two parts as well. Initially DEV1 transmits and DEV2 receives. Then, DEV2 transmits and DEV1 receives. DEV1 to DEV2 beam training has $K(1,t)$ cycles. Each cycle is repeated $K(2,r)$ times to allow DEV2 to listen from different directions. DEV2 picks the best beam pair. After role reversal, DEV2 transmits and DEV1 receives. DEV2 to DEV1 sector training consists of $K(2,t)$ cycles. Each cycle is repeated $K(1,r)$ to allow DEV1 to receive each transmission through a different receive antenna. At the end, best beam pair is selected by DEV1.

If high resolution beam training is supported, then another procedure similar to sector and beam training is performed to determine the best HRS beam pair.

Since communication channel between a device and another slowly changes over time, tracking becomes necessary. The goal of tracking procedure is to have the best pair of beams at all times. The best cluster consisting of the best beam and its neighbors and second best cluster consisting of second best beam and its neighbors are formed. A search is conducted to obtain the best beam.

7.10 Unequal Error Protection

One of the unique features of 60 GHz standards such as IEEE 802.15.3c or ECMA 387 is support for unequal error protection (UEP). It essentially means that MSB and LSB bits are treated differently. The main approaches to UEP have been elaborated in the previous chapter.

To evaluate UEP, HD video frames were transmitted with the aid of 802.15.3c and the quality of EEP and UEP encoded sequences were compared at the receive end [23]. In terms of BER performance, MSB bits are somewhat superior to EEP bits (1.5–2 dB) and LSB bits are somewhat inferior to EEP bits (1–2 dB).

However, the BER performance does not reflect the advantages of UEP. To witness that, we need to resort to performance metrics such as peak signal-to-noise ratio (PSNR) and video quality metric (VQM) [24]. Both metrics point to the same conclusion. At high error rates UEP outperforms EEP, while at lower error rates EEP is superior. Moreover, both PSNR and VQM metrics have a crossover point. The crossover point appears to be somewhat larger for VQM metric though.

The variance of PSNR subject to a fixed BER was computed as well. It turns out that the variance of UEP is much smaller than that of EEP, indicating superior visual quality of UEP scheme. To have the best performance over the entire BER range, an adaptive scheme can be deployed to deploy EEP at low error rates and UEP at high error rates.

There are also a couple of other strategies in IEEE 802.15.3c that take advantage of UEP to improve performance. For instance, adjacent image pixels are placed on different packets. In this way if one packet is corrupted, other packets carrying adjacent pixels can be used to recover the lost pixel. The other strategy is to divide a packet into MSB and LSB sections with individual CRCs for each piece. If the CRC associated with MSB indicates no checksum error, no retransmission is requested. Otherwise, retransmission is requested and this time only the MSB section is retransmitted.

7.11 IEEE 802.15.3c Channel Model

This model has been developed by IEEE 802.15.3c channel modeling subcommittee for high throughput applications in different operating environments. The findings have been captured in [25]. A summary of the approach is presented in this section.

7.11.1 Large-Scale Fading

Large-scale path loss is expressed as

$$\overline{\mathrm{PL}} = \mathrm{PL}_0 + 10\, n \log\left(\frac{d}{d_0}\right) + s$$

where, d_0, PL_0, n, and s are reference distance, path loss at reference distance, path loss exponent, and shadowing, respectively. Path loss exponent in LOS and NLOS are in (1.16–1.53) and (2.44–3.74) ranges, respectively. Shadowing is lognormally distributed with mean of zero and standard deviation of σ_s. σ_s could be as low as 1.5 (in LOS) and as high as 8.6 dB (in NLOS) depending on the specific environment.

7.11.2 The Channel Model

The channel model, known as directional Saleh-Valenzuela (S-V),[9] is given by

$$h(t,\theta) = \sum_{l=0}^{L} \sum_{k=0}^{K_l} a_{k,l}\delta\big(t - T_l - \tau_{k,l}\big)\delta\big(\theta - \Psi_l - \psi_{k,l}\big)$$

where

L	number of clusters
K_l	number of multipath components (number of rays) in the lth cluster
$a_{k,l}$	multipath gain coefficient of the kth ray in the lth cluster
T_l	arrival time of the first ray of the lth cluster
$\tau_{k,l}$	delay of the kth ray within the lth cluster relative to the first path arrival time, T_l
Ψ_l	mean angle of arrival of lth cluster
$\psi_{k,l}$	angle of arrival of the kth ray within the lth cluster.

Measurement campaigns at 60 GHz have verified the presence of a strong LOS component in addition to the clustering phenomenon. As such the channel can be obtained by merging of two-path and the directional (S-V) model. Since the two-path model components are spaced much less than sampling period, then two-path model components are lumped together into a single components. We then have

$$h(t,\theta) = \beta\ \delta(\tau) + \sum_{l=0}^{L} \sum_{k=0}^{K_l} a_{k,l}\delta\big(t - T_l - \tau_{k,l}\big)\delta(\theta - \Psi_l - \psi_{k,l})$$

The LOS component can be computed deterministically or modeled statistically. The statistical modeling follows:

$$\beta = 20\ \log_{10}\left[\frac{\mu_d}{d}\left|\sqrt{G_{t_1}G_{r_1}} + \sqrt{G_{t_2}G_{r_2}}\Gamma_0 e^{j\frac{4\pi h_1 h_2}{\lambda d}}\right|\right] - \mathrm{PL}_d(\mu_d)$$

where

$$\mathrm{PL}_d(\mu_d) = 20\log_{10}\left(\frac{4\pi d_0}{\lambda}\right) + A_{\mathrm{NLOS}} + 10 n_d \log_{10}\left(\frac{d}{d_0}\right).$$

and

A_{NLOS}	Constant attenuation for NLOS
μ_d	Mean distance
Γ_0	Reflection coefficient
h_1	Height of the transmit antenna (uniform distributions in [0 0.3] range)
h_2	Height of the receive antenna (uniform distributions in [0 0.3] range)

[9] Directional S–V is also known as TSV model [26].

G_{t1} Gain of transmit antenna for path 1
G_{t2} Gain of transmit antenna for path 2
G_{r1} Gain of receive antenna for path 1
G_{r2} Gain of receive antenna for path 2.

The cluster and ray arrival times both follow Poisson distributions. In other words,

$$p(T_l|T_{l-1}) = \Lambda e^{-\Lambda(T_l - T_{l-1})}$$

$$p\left(\tau_{k,l}|\tau_{k-1,l}\right) = \lambda e^{-\lambda(\tau_{k,l} - \tau_{k-1,l})} \quad k > 0.$$

The number of clusters follows a uniform distribution and utilizes mean number of clusters. The mean number of clusters is scenario dependent and varies from 3 to 14. The ray AOA within each cluster can be modeled as either a zero mean Laplacian or a zero mean Gaussian random variable. The mean angle of arrival (AOA) is modeled as having a uniform distribution conditioned on the first cluster mean AOA.

7.11.3 Small-Scale Fading

Ray and cluster amplitudes are adequately modeled by lognormal distributions.

7.11.4 Model Parameters

The model parameters are listed below:

Λ Cluster arrival rate (1/ns)
λ Ray arrival rate (1/ns)
Γ Cluster decay rate (ns)
γ Ray decay rate (ns)
σ_c Cluster lognormal standard deviation (dB)
σ_r Ray lognormal standard deviation (dB)
σ_ϕ Angle spread (deg)
$\bar{L}$ Average number of clusters
Δk Ray Rician factor (dB)
Ω Average power of the first ray of the first cluster (for combined two path and S-V model) (dB)
n_d Path loss exponent
A_{NLOS} Constant attenuation for NLOS.

Table 7.6 Model parameters for CM1 [25]

Parameter	TX 360° RX 15°	TX 60° RX 15°	TX 30° RX 15°	TX 15° RX 15°	TX 360° RX 15°
Λ (1/ns)	0.191	0.194	0.144	0.045	0.21
λ (1/ns)	1.22	0.9	1.17	0.93	0.77
Γ (ns)	4.46	8.98	21.5	12.6	4.19
γ (ns)	6.25	9.17	4.35	4.98	1.07
σ_c (dB)	6.28	6.63	3.71	7.34	1.54
σ_r (dB)	13	9.83	7.31	6.11	1.26
σ_ϕ (degree)	49.8	119	46.2	107	8.3
$\bar{L}$	9	11	8	4	4
Δk (dB)	18.8	17.4	11.9	4.6	NA
Ω (dB)	−88.7	−108	−111	−110.7	NA
n_d	2	2	2	2	NA
A_{NLOS}	0	0	0	0	NA

Columns 1 and 5 parameters have been reported by two different entities

7.11.5 Environments

The eight channel models are as follows:
CM1 Residential (LOS)
CM2 Residential (NLOS)
CM3 Office (LOS)
CM4 Office (NLOS)
CM5 Library (LOS)
CM6 Library (NLOS)
CM7 Desktop (LOS)
CM8 Desktop (NLOS).

Channel models CM1, CM3, CM4, CM5, and CM7 consist of 5, 2, 3, 1, and 3 transmit/receive antenna configurations, respectively. The channel model parameters for CM1, CM3, CM4, CM5, and CM7 are provided in Tables 7.6, 7.7, 7.8, and 7.9. The NLOS models CM2, CM6, and CM8 can be obtained by removing the LOS component from CM1, CM5, and CM7, respectively.

7.12 MAC

IEEE 802.15.3c MAC is based on 802.15.3 MAC that combines CSMA/CA and TDMA access schemes [22]. While CSMA/CA is used for signaling, data transmission is accomplished with TDMA. IEEE 802.15.3 MAC was described in some detail in Chap. 4. Here, we briefly review the new features of the IEEE 802.15.3c MAC.

Table 7.7 Model parameters for CM3 and CM4 [25]

	CM3	CM3	CM4	CM4	CM4
Parameter	TX 30° RX 30°	TX 60° RX 60°	TX 360° RX 15°	TX 30° RX 15°	TX omni RX 15°
Λ (1/ns)	0.041	0.027	0.032	0.028	0.07
λ (1/ns)	0.971	0.293	3.45	0.76	1.88
Γ (ns)	49.8	38.8	109.2	134	19.4
γ (ns)	45.2	64.9	67.9	59	0.42
σ_c (dB)	6.6	8.04	3.24	4.37	1.82
σ_r (dB)	11.3	7.95	5.54	6.66	1.88
σ_ϕ (degree)	102	66.4	60.2	22.2	9.1
$\bar{L}$	6	5	5	5	6
Δk (dB)	21.9	11.4	19	19.2	NA
Ω (dB)	$-3.27d$-85.8	$-0.303d$-90.3	-109	-107.2	NA
n_d	2	2	3.35	3.35	NA
A_{NLOS}	0	0	5.56@3 m	5.56@3 m	NA

Table 7.8 Model parameters for CM5 [25]

Parameter	CM5
Λ (1/ns)	0.25
λ (1/ns)	4
Γ (ns)	12
γ (ns)	7
σ_c (dB)	5
σ_r (dB)	6
σ_ϕ (degree)	10
$\bar{L}$	9
K_{LOS} (dB)	8

A couple of new acknowledgment types known as block acknowledgment (Blk-ACK) and block negative acknowledgment (Blk-NAK) is defined. A Blk-ACK is sent from the receiver to the transmitter after short interframe space (SIFS), in the event the receiver is asked to acknowledge an aggregated frame of many subframes. To minimize transmission overhead when the channel is clear, the receiver can instead send a (Blk-NAK) in which only the erroneous subframes are listed.

To facilitate UEP, MAC service data units (MSDU) are divided into MSB and LSB subframes. Lower order modulation and FEC are applied by PHY to the MSB subframes compared to LSB subframes. Upon aggregation of MSB and LSB subframes, one PPDU frame is formed and the required side information such as UEP method is specified in the subheader corresponding to each subframe.

Table 7.9 Model parameters for CM7 [25]

	CM7	CM7	CM7
Parameter	TX 30° RX 30°	TX 60° RX 60°	TX omni RX 21 dBi
Λ (1/ns)	0.037	0.047	1.72
λ (1/ns)	0.641	0.373	3.14
Γ (ns)	21.1	22.3	4.01
γ (ns)	8.85	17.2	0.58
σ_c (dB)	3.01	7.27	2.7
σ_r (dB)	7.69	4.42	1.9
σ_ϕ (degree)	34.6	38.1	14
$\bar{L}$	3	3	14
Δk (dB)	11	17.2	NA
Ω (dB)	4.44*d*-105.4	3.46*d*-98.4	NA
h_1	Ud1*	Ud1	NA
h_2	Ud1	Ud1	NA
D	Ud2+	Ud2	NA
G_{T1}	GSS−	GSS	NA
G_{R1}	GSS	GSS	NA
G_{T2}	GSS	GSS	NA
G_{R2}	GSS	GSS	NA
n_d	2	2	NA
A_{NLOS}	0	0	NA

*uniform distribution in [0 0.3] range
+uniform distribution in [*d*-0.3 *d*+0.3] range
−Gaussian antenna model as defined in [35]

7.13 IC Process Technology

The three main Integrated Circuit (IC) process technologies for the 60 GHz band are compound semiconductor technology such as Indium Phosphide (InP) and Gallium Arsenide (GaAs), Complementary Metal Oxide Semiconductor (CMOS), and Silicon Germanium (SiGe) technology such as BiCMOS. A comparison of these technologies is provided in Table 7.10.

InP and GaAs processes are bulky, power hungry, and expensive and as such are not fit for consumer electronics market. A number of different groups are working on the process technologies for 60 GHz. In particular, a great deal of momentum is behind CMOS research and development. IBM is pursuing SiGe, while the

Table 7.10 A comparison of IC process technologies

Process	Pros	Cons
InP and GaAs	Fast, high gain, low noise	Bulky, expensive, poor integration, power hungry
CMOS	High level of integration, low cost	Low gain, low linearity, poor noise
SiGe	High gain, low noise, high thermal conductivity	Lower integration and higher manufacturing cost than CMOS

Wireless Research Center at UC Berkeley and Georgia Electronic Design Center of Georgia Tech are working independently on CMOS. Performance related figures of merit such as f_T (cut-off frequency) and f_{max} (maximum oscillation frequency) have improved for both CMOS and SiGe [27]. The performance roadmap of CMOS indicates that CMOS transistors are competitive with InP and GaAs and will remain so in the near future [28]. In terms of cost, ease of manufacturing and integration level CMOS is at an advantage compared to the other process technologies. Although the 60 GHz front-runner process technology appears to be CMOS, it is not clear what the market share of each technology will be.

7.14 Chipsets Providers

Sibeam[10] has produced three generations of CMOS chipsets based on WirelessHD spec for 60 GHz market [29]. They are implemented in CMOS 90 nm and an antenna array of 32 elements is part of the beamforming engine. Each chipset consists of two chips, namely baseband/MAC and RFIC. While the second generation chipsets support WirelessHD 1.0 only, the third generation chipsets support both WirelessHD 1.0 and WirelessHD 1.1. A hybrid WirelessHD/WiGig capable silicon is in the works.

IBM and Media Tek of Taiwan have jointly developed chipsets per IEEE 802.15.3c and IEEE 802.11ad draft for 60 GHz space [30]. The developed silicon utilizes SiGe BiCMOS process and incorporates 16 antenna elements, utilizes a super heterodyne receiver, and delivers a speed of upto 5 Gbps.

Japanese manufacturers namely Toshiba, Panasonic, and Hitachi are also developing chipsets for the 60 GHz market [31]. A few fabless semiconductor developers, such as Perasotech [32], are pursuing standard-based silicon as well.

7.15 60 GHz Products

The first wave of standard-based 60 GHz consumer electronics products has already hit the market [33]. WirelessHD is the first and only standard to reach the consumer. Wireless HDMI extenders (also known as wireless HD kites) manufactured by Gefen, Cables To Go, BEST BUY, ABOCOM, and TrueLink are already on the shelves. They consist of a transmitter and a receiver unit implementing WirelessHD protocol. The kit can provide a wireless link between a source such as Blue-Ray player, DVD player, or a satellite receiver and a display unit. A number of resolutions up to 1,080 p with 60 frames per second are

[10] SiBeam was acquired by Silicon Image in 2011. It is now a subsidiary of Silicon Image (http://www.siliconimage.com).

supported. Between the transmitter and receiver units, LOS and no obstructions is expected. The typical system range is about 10 m.

Aside from Wireless HDMI Extenders, Dell offers Alienware gaming laptop with 60 GHz link in two models M17x and M14x. There are also a few TV sets with WirelessHD capability. They include a 54″ Panasonic class Viera Z1 series Plasma, a 55″ LG model 55LH95-UA, and a 46″ Sony BRAVIA XBR 10 series.

7.16 A Comparison Between Conventional and 60 GHz UWB Technologies

Earlier in this chapter, we established that there are a number of applications that require the ability to communicate huge amount of information (1 Gbps or more). The need for high throughput communication systems and inability of the existing wireless solutions has led to examination of alternatives such as UWB.

UWB communications consist of conventional and 60 GHz UWB. Compared to the earlier communication systems, both 60 GHz and UWB deploy huge system bandwidths larger than half a GHz. To compare these technologies a number of features such as offered data rates, transmission range, availability of standards, international regulatory climate, and maturity of silicon technology are selected. In the remainder of this section, these technical features will be reviewed.

International regulations: Lawful unlicensed operation of UWB devices in the US started in 2002. From the very start, UWB was well received in the US. The regulations were mostly favorable to the promising technology. Then a standard for high throughput UWB communications known as ECMA-368 was established. A significant amount of investment was mode on developing silicon and a number of companies in the US and other countries worked on developing chipset for UWB market. While some were proprietary solutions most of them were standard based.

Unfortunately, UWB has not gained that level of acceptance outside the US. It has been long argued that UWB, being an underlay[11] technology, could interfere with the operation of the existing services such as IEEE 802.11a. Consequently, regulators in Europe, Japan, China, and Korea have either banned UWB operation in some bands, have established extremely low emission profiles, or have required detect and avoid (DAA) functionality in some bands.[12] With DAA, a UWB device can only operate when the incumbents are not using the band. As such quality of service (QoS) cannot be guaranteed. Above and beyond that providing DAA

[11] The power spectral density of the underlay system is significantly lower than the incumbent users, but the underlay is present at all times.

[12] UWB devices can optionally lower their emissions by 30 dB in Far East (40 dB in Europe) to avoid DAA. However, given the original range of 10 m, this level attenuation limits the range to 0.3 m (0.1 m in Europe).

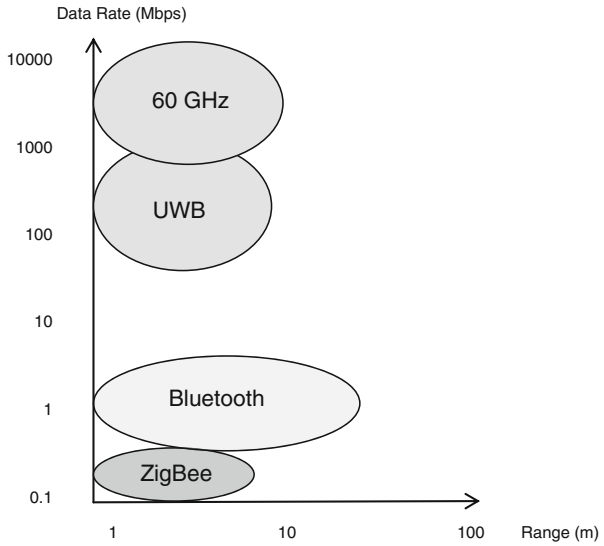

Fig. 7.16 A comparison of WPAN technologies and standards

functionality may not be too complex to implement, but it certainly adds to the cost of the UWB products.

Data Rate: A number of WPAN technologies with different capabilities have been introduced over the past 15 years. While Bluetooth, ZigBee[13] address low data rate application, UWB can be applied to both low data rate and high throughput applications as we saw in Chap. 1. One of the interesting features of the conventional UWB technology was the ability to provide extremely large data rates at short ranges. This was mainly due to bandwidth availability in 3.1–10.6 GHz range. However, recent regulations outside the US have limited the available bandwidth. Consequently, a couple of Gbps is perhaps all that can be achieved with UWB. The 60 GHz UWB standards, on the other hand, easily achieve 6 Gbps. WirelessHD can reportedly can achieve a theoretical throughput of 28 Gbps. A comparison between WPAN technologies is shown in Fig. 7.16.

Range: Both conventional and 60 GHz are expected to be used for indoor delivery of multimedia within home environment. The achievable range for each is in the order of 10 m. However, in Europe and Far East, UWB devices can only operate in upper band groups of ECMA band plan with no DAA. For instance, in Japan and Korea UWB devices can operate in bands 9 through 13. A simple application of Friis law reveals that WiMedia band group 6 (consisting of bands 9

[13] ZigBee is based on PHY and MAC defined by IEEE 802.15.4 and consists of a suite of higher level protocols enabling low power low cost WPAN networking for control and sensor network applications (http://www.zigbee.org/).

Table 7.11 Technical features of conventional and 60 GHz UWB

Technology	Data rate	DAA requirement	QoS	Range	Chipset maturity	Products	Available standards
Conventional UWB	++	–	−#	+*	++	+	+
60 GHz UWB	+++	+	+	+	+	+	++

*only in the US, can be considerably shorter elsewhere
#outside the US in bands requiring DAA

through 11) achieves only 23 % of the range associated with band group 1.[14] Given that band group 1 can support a range of 10 m, band group 6 can only support a range of 2.3 m. This operating range is far shorter than the required 10 range.

Chipset maturity: We examined the chipset evolution path for UWB in Chap. 5. The most recent UWB chipsets combine RF, MAC, PHY into a single die. Two chip solutions for 60 GHz are in the market, but single chip solution is in the works. As such the state of art in chipset technology for 60 GHz UWB is not quite in par with UWB. However, with all the momentum behind 60 GHz, it is just a matter of time before single chip solution becomes reality.

Availability of standards: The only established UWB standard for high speed communications is WiMedia. On the other hand, five standards for 60 GHz communications have been released so far. If one standard is not suitable, there are a few others to utilize.

Products: The availability of chipset for both technologies has led to commercial products. Products for conventional and 60 GHz technologies are listed in Chaps. 5 and 7.

A summary of the technical features of the two standards is provided in Table 7.11. The availability of large swaths of spectrum in 60 GHz band, higher data rate capability of it, and lack of DAA requirement tip the scale in favor of 60 GHz UWB. Above and beyond, the 60 GHz band power limits are not as severe as that of UWB and the band is not nearly as crowded as lower frequencies like 2.4 GHz and UNII. Due to smaller antenna sizes, multiple antenna techniques such as diversity and phase arrays can be deployed to improve the link quality. In conclusion, 60 GHz UWB appears to be in a better position for delivering multi-gigabit data rates in WPAN applications. However, conventional UWB is suitable for other applications such as ranging and sensor networks.

What We Learned

- 60 GHz band definition, spectrum allocations, regulations, and restrictions;
- Characteristics of 60 GHz UWB
- Capacity and link budget evaluation for 60 GHz UWB

[14] The ratio of transmission ranges associated with band groups 6 and 1 is given by $(f_1/f_6)^2 = 0.23$ where $f_1 = 3{,}960$ MHz and $f_6 = 8{,}184$ MHz are the center frequencies of band groups 1 and 6, respectively.

- Smart antenna component of the technology;
- Antenna training procedure;
- UEP component of the technology;
- IEEE 802.15.3c channel model and differences with other UWB channel models;
- IC process technology evaluation, chipsets, and providers;
- Existing products in the markets;
- Comparison between UWB and 60 GHz UWB.

Problems

1. A certain 60 GHz product with a 2 GHz of bandwidth can only afford transmit/receive antennas with 10 dB of gain. What is the maximum rate that this product can deliver in WPAN environment?
2. If a clinic medical staff is planning to utilize tablets that can wirelessly download images and video from a server. Propose a technology to achieve this vision and justify your proposed solution.
3. Are there any other wireless technologies that can compete with 60 GHz UWB for WPAN applications? Research the issue and compare any technology you find to 60 GHz UWB.

References

1. J.D. Kraus, R.J. Marhefka, *Antennas for All Applications*, 3rd edn. (McGraw-Hill, New York, 2002)
2. Online. Available at: http://en.wikipedia.org/wiki/Microwave
3. Japan Ministry of Public Management, Home Affairs, Posts and Telecommunication, Regulations for the Enforcement of Radio Law, 6-4.2 Specified Low Power Radio Station (17) 59–66 GHz band, 2000
4. Federal Communications Commission (FCC), Code of Federal Regulation title 47 Telecommunication, Chapter 1, part 15.255, Oct, 2004
5. Industry Canada Spectrum Management Telecommunications, Radio Standard Specification-210, Issue 6, Low-Power Licensed-Exempt Radio Communication Devices (All Frequency Bands): Category1 Equipment, Sept 2005
6. Australian Communications and Media Authority (ACMA), Radiocommunications (Low Interference Potential Devices) Class License Variation 2005 (No. 1), Aug 2005
7. Ministry of Information and Communication of Korea, *Frequency Allocation Comment of* 60 GHz *Band*, Apr 2006
8. ETSI DTR/ERM-RM-049, Electromagnetic Compatibility and Radio Spectrum Matters (ERM): System Reference Document: Technical Characteristics of Multiple Gigabit Wireless Systems in the 60 GHz Range, Mar 2006
9. ofcom, Release of the 59–64 GHz band- A Statement on ofcom's decision for a licence expempt approach for Fixed Wireless Systems in the 60 GHz Band, Dec 2009
10. iDA Singapore, Proposed Regulatory Framework for 60 GHz Frequency Band, Feb 2010
11. J. Howarth, A.P. Lauterbach, M.J. Boers, L.M. Davis, A. Parker, J. Harrison, J. Rathmell, M. Batty, W. Cowley, C. Burnet, L. Hall, D. Abbott, N. Weste, 60 GHz Radios: Enabling Next-Generation Wireless Applications. EURASIP J. Wireless Commun. Networking. Vol. **2007** (2007)

12. C. Anderson, T.S. Rappaport, In-building Wideband Partition loss measurements at 2.5 and 60 GHz. IEEE Trans. Wireless Commun. **3**(3), 922–928 (2004)
13. H. Xu, V. Kukshya, T.S. Rappaport, Spatial and temporal characteristics of 60 GHz indoor channels. IEEE J. Sel. Areas Commun. **20**(3), 620–630 (2002)
14. R. Van Nee, R. Prasad, *OFDM for Wireless Multimedia Communications* (Artech House, Boston, 1999)
15. F. Pancaldi et al., Single-Carrier Frequency Domain Equalization. IEEE Signal Process. Mag. (2008)
16. S.K. Yong, P. Xia, A. Valdes-Garcia, *60 GHz Technology for Gbps WLAN and WPAN* (Wiley, New York, 2011)
17. Y. Shoji, K. Hamaguchi, H. Ogawa, Millimeter-wave remote self-heterodyne system for extremely stable and low-cost broad-band signal transmission. IEEE Trans. Microwave Theory Tech. **50**(6), 1458–1468 (2002)
18. S.K. Yong, C.C. Chong, An overview of multigigabit wireless through millimeter wave technology: potentials and technical challenges, EURASIP J. Wireless Commun. Networking, Vol. **2007**, (2007)
19. A. Sadri, 802.15.3c Usage Model Document (UMD), Draft, IEEE 802.15.3 TG3c document: 15-06-0055-14-003c, Jan 2006
20. J.C. Liberti, T.S. Rappaport, *Smart Antennas for Wireless Communications: IS-95 and Third Generation CDMA Applications* (Prentice Hall, Upper Saddle River, 1999)
21. R. Kawitkar, D.G. Wakde, Advances in smart antenna system. J. Sci. Ind. Res. **64**, 660–665 (2005)
22. IEEE 802.15.3c, Wireless Medium Access Control (MAC) and Physical Layer (PHY) Specification for High Rate Wireless Personal Area Networks (WPAN) Amendment 2: Millimeter-wave-based Alternative Physical Layer Extension, 2009
23. H. Singh et al., Principles of IEEE 802.15.3c: multi-gigabit millimeter-wave wireless pan. IEEE Commun. Mag. **46**, 71–78 (2009)
24. M.H. Pinson, S. Wolf, A new standardized method for objectively measuring video quality. IEEE Trans. Broadcast. **50**, 312–322 (2004)
25. S.K. Yong, TG3c Channel Modeling Sub-committee Final Report IEEE 802.15-07- 0584-01-003c. Mar 2007
26. K. Sato, H. Sawada, Y. Shoji, S. Kato, Channel Model for Millimeter Wave WPAN, *PIMRC'07 Proceedings*. 2007
27. Online. Available at: http://www.itrs.net/
28. Online. Available at: http://www.itrs.net/Links/2006Update/2006UpdateFinal.htm
29. Online. Available at: http://www.wirelesshd.org/consumers/product-listing/. Accessed 11 June 2011
30. A. Valdes-Garcia et al., Single –Element and Phased-Array Transceiver Chipsets for 60 GHz Communications, *IEEE Commun. Mag.* Apr 2011
31. Online. Available at: http://telematicsnews.info/2010/01/31/hitachi-panasonic-and-toshiba-developing-60ghz-transceiver-chips/
32. Online. Available at: http://www.perasotech.com/. Accessed 11 June 2011
33. Online. Available at: http://www.siliconimage.com/products/family.aspx?id=11. Accessed 11 June 2011
34. J. Wells, *Multi-Gigabit Microwave and Millimeter-Wave Wireless Communications* (Artech House, Boston, 2010)
35. I. Toyoda, Reference antenna model with side lobe level for TG3c Evaluation. IEEE 802.15.06-0474-00-003c. Oct 2006

Chapter 8
IEEE 60 GHz Standards

Over the past few years at least five standards for data communication via 60 GHz have been established by standard setting bodies and industrial forums. Two standards have emerged from IEEE 802 forums. They are IEEE 802.15.3c [1] and IEEE 802.11 ad [2]. IEEE 802.15.3c addresses wireless personal area communications (WPAN) space, while IEEE 802.15 ad is intended for wireless local area networks (WLAN) and is an extension to the existing IEEE 802.11 family. The third standard has been established by the European computer manufacturing association (ECMA) under ECMA 387 [3, 4]. ECMA 387, WiGig [5], and WirelessHD [6] will be covered in Chap. 9. A summary of IEEE 802.15.3c, IEEE 802.11 ad, and ECMA 387 attributes is provided in Table 8.1. In the remainder of this chapter, IEEE 802.15.3c and IEEE 802.11 ad standards will be introduced and their attributes will be described.

8.1 IEEE 802.15.3c

The physical (PHY) layer supports three modes known as single carrier (SC), high-speed interface (HSI), and audio-visual (AV) modes. The single carrier (SC) mode is designed for low power and low complexity applications such as video download at a kiosk. The high-speed interface (HSI) mode is intended for low latency bi-directional data transfer connecting laptops and handheld electronic devices around a conference table. The AV mode can be used to transmit uncompressed HD content. The AV low-rate PHY (LRP) sets up connections through its omnidirectional coverage. Then, the high-rate PHY (HRP) transmits HD video and audio.

The SC mode uses either Reed-Solomon (RS) or LDPC codes. RS codes are mandatory, but LDPC codes are optional. Both HSI and AV modes employ OFDM. As for FEC, HSI utilizes low density parity-check (LDPC) codes, while the AV mode uses Reed-Solomon (RS) and convolutional codes (CC).

A comparison between the PHY attributes of the three modes of IEEE 802.15.3c is presented in Table 8.2. Among the three modes SC has the least

S. Emami, *UWB Communication Systems: Conventional and 60 GHz*,
DOI: 10.1007/978-1-4614-6753-3_8,

Table 8.1 60 GHz standards

Standard	Modulation	FEC	Data rate (Mbps)
IEEE 802.15.3c SC	$\pi/2$ BPSK, GMSK, $\pi/2$ QPSK, $\pi/2$ 8-PSK, $\pi/2$ 16-QAM	RS, LDPC	25.8–5,280
HSI	OFDM/QPSK, OFDM/16-QAM, OFDM/64-QAM	LDPC	32.1–5,775
AV	OFDM/BPSK, OFDM/QPSK, OFDM/16-QAM	Concatenated codes: RS+Convolutional codes	2.5–3,807
ECMA 387			
Class A-SCBT	BPSK, QPSK, NS8QAM, 16QAM, TCM16QAM, UEP-QPSK, UEP-16QAM	Concatenated codes: RS+Convolutional codes	397–6,350
Class A-OFDM	QPSK, 16QAM, UEP-QPSK, UEP-16QAM	Concatenated codes: RS+Convolutional codes	1,008–4,032
Class B	DBPSK, DQPSK, UEP-QPSK, DAMI	RS	794–3,175
Class C	OOK, 4-ASK	RS	800–3,200
IEEE 802.11ad LP SC	$\pi/2$-BPSK, $\pi/2$-QPSK	RS, block code	626–2,502
SC	$\pi/2$-BPSK, $\pi/2$-QPSK, $\pi/2$-16-QAM	LDPC	385–4,620
OFDM	QPSK, SQPSK, 16-QAM, 64-QAM	LDPC	693–6,756

implementation complexity. SC could utilize less-expensive power amplifiers and ADC/DAC. Between HSI and AV modes, HSI could be somewhat more complex due to use of LDPC codes instead of concatenated codes. On the other hand, HSI achieves a higher operating range than AV [7].

8.1.1 SC PHY

There are three classes of coding and modulation, known as classes 1, 2, and 3. These classes are devised to address the needs of various market sectors. While class 1 is intended for lower cost applications, class 3 supports high end applications. Classes 1 and 2 achieve data rates up to 1.5 and 3 Gbps, respectively. Data rates between 3 and 5 Gbps are reached by class 3.

8.1.1.1 Transmitter

An IEEE 802.15.3c compliant SC transmitter block diagram is depicted in Fig. 8.1.

Table 8.2 IEEE 802.15.3c attributes

Mode	Modulation	FEC	Data rate (Mbps)
SC Class 1	$\pi/2$ BPSK, GMSK	RS (255, 239), LDPC (672, 504), LDPC(672, 504)	28.5, 412, 825, 1650, 1320, 440, 880
SC Class 2	$\pi/2$ QPSK	LDPC (672, 336), LDPC (672, 504), LDPC (672, 588), LDPC (1,440, 1,344), RS (255, 239)	1,760, 2,640, 3,080, 3,290, 3,300
SC Class 3	$\pi/2$ 8-PSK, $\pi/2$ 16-QAM	LDPC (672, 504)	3,960, 5,280
HSI	OFDM/QPSK, OFDM/16-QAM, OFDM/64-QAM	LDPC (672, 336), LDPC (672, 420), LDPC (672, 504), LDPC (672, 588)	32.1, 1,540, 2,310, 2,695, 3,080, 4,620, 5,390, 5,775, 1,925, 2 503, 3,850, 5,005
AV LRP	OFDM/BPSK	Convolutional codes rates ½,1/3,2/3	2.5, 3.8, 5.1, 10.2
AV HRP	OFDM/QPSK, OFDM/16-QAM	Concatenated codes: RS (224, 216) + Convolutional codes rates 1/3, 2/3, 4/5, 4/7	952, 1,904, 3,807

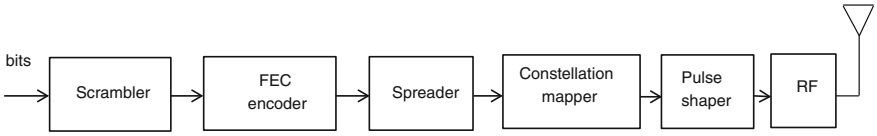

Fig. 8.1 SC transmitter block diagram

8.1.1.2 Preamble

The SC PHY frame consists of preamble, header, and payload fields. The purpose of preamble is to help with AGC, frame synchronization, timing acquisition, and channel estimation. Header contains information necessary for decoding the payload. Preamble itself consists of SYNC, SFD (start frame delimiter), and CES (channel estimation sequence).

The goal of SYNC is to help with the frame detection and it consists of 14 repetition of a_{128}. SFD helps with the frame timing. Two different SFD sequences are used for MR (medium rate) and HR (high rate). The SFD for MR and HR are $[a_{128}\ -a_{128}\ a_{128}\ -a_{128}]$ and $[a_{128}\ a_{128}\ -a_{128}\ -a_{128}]$, respectively.

CES is used for CIR (channel impulse response) estimation and is made up of $[b_{128}\ b_{256}\ a_{256}\ b_{256}\ a_{256}]$ where a_{256} is first in time. CMS preamble is somewhat different. The SYNC, SFD, and CES consist of 48 repetitions of b_{128}, $[b_{128}\ -b_{128}\ b_{128}\ b_{128}\ -b_{128}\ -b_{128}\ -b_{128}]$ and $[b_{128}\ b_{256}\ a_{256}\ b_{256}\ a_{256}\ a_{128}]$ (a_{128} is first in time).

The Golay complementary sequences of length 128 and 256 are

$$a_{128} = [0x0536635005C963AFFAC99CAF05C963AF]$$
$$b_{128} = [0x0A396C5F0AC66CA0F5C693A00AC66CA0]$$

$$a_{256} = [a_{128} b_{128}]$$
$$b_{256} = [a_{128} \underline{b}_{128}].$$

Complement of a sequence is denoted by the underline. The sequence on the right side (b_{128} and $\underline{b}_{128}$ is first in time.

8.1.1.3 Data Rate

The supported data rates (rounded to three significant digits) for the three classes of SC mode are listed in Table 8.3. A subblock consists of 512 chips and chipping rate is 1,750 Mchips/s.

For single carrier system, data rate can be determined using the following formula:

$$\text{Data Rate} = \frac{1}{T_c} \times \text{FEC rate} \times \text{Number of constellation bits} \times \frac{1}{\text{Spreading factor}}.$$

For class 1 with no pilot word, the supported data rates are computed as follows:

Table 8.3 SC supported data rates

Data rate (Mbps) (no pilot word)	Spreading factor	Modulation	Coding	Class
25.8 (CMS)	64	$\pi/2$ BPSK/(G)MSK	RS (255, 239)	1
412	4	$\pi/2$ BPSK/(G)MSK	RS (255, 239)	1
825	2	$\pi/2$ BPSK/(G)MSK	RS (255,239)	1
1,650	1	$\pi/2$ BPSK/(G)MSK	RS (255, 239)	1
1,320	1	$\pi/2$ BPSK/(G)MSK	LDPC (672, 504)	1
440	2	$\pi/2$ BPSK/(G)MSK	LDPC (672, 336)	1
880	1	$\pi/2$ BPSK/(G)MSK	LDPC (672, 336)	1
1,760	1	$\pi/2$ QPSK	LDPC (672, 336)	2
2,640	1	$\pi/2$ QPSK	LDPC (672, 504)	2
3,080	1	$\pi/2$ QPSK	LDPC (672, 588)	2
3,290	1	$\pi/2$ QPSK	LDPC (1,440, 1,344)	2
3,300	1	$\pi/2$ QPSK	RS (255, 239)	3
3,960	1	$\pi/2$ 8-PSK	LDPC (672, 504)	3
5,280	1	$\pi/2$ 16-QAM	LDPC (672, 504)	3

Data rate = (1760e6) × (239/255) × 1 × (1/64) ∼25.8 Mbps
Data rate = (1760e6) × (239/255) × 1 × (1/4) ∼412 Mbps
Data rate = (1760e6) × (239/255) × 1 × (1/2) ∼825 Mbps
Data rate = (1760e6) × (239/255) × 1 × (1) ∼1,650 Mbps
Data rate = (1760e6) × (504/672) × 1 × (1) = 1,320 Mbps
Data rate = (1760e6) × (336/672) × 1 × (1/2) = 440 Mbps
Data rate = (1760e6) × (336/672) × 1 × (1) = 880 Mbps.

Subject to a pilot word of length 64, data rate is determined by

$$\text{Data Rate} = \frac{512-64}{512} \times \frac{1}{T_c} \times \text{FEC rate} \times \text{Number of constellation bits}$$

For class 1, data rate with pilot word of length 64, data rates will change to

Data rate = [(512-64)/512] × (1760e6) × (239/255) × 1 × (1/4) ∼361 Mbps
Data rate = [(512–64)/512] × (1760e6) × (239/255) × 1 × (1/2) ∼722 Mbps
Data rate = [(512-64)/512] × (1760e6) × (239/255) × 1 × (1) ∼1,440 Mbps
Data rate = [(512-64)/512] × (1760e6) × (504/672) × 1 × (1) ∼1,160 Mbps
Data rate = [(512-64)/512] × (1760e6) × (336/672) × 1 × (1/2) ∼385 Mbps
Data rate = [(512-64)/512] × 1760e6) × (336/672) × 1 × (1/2) ∼770 Mbps.

The results are tabulated below. Note that pilot word of 64 cannot be used with the lowest rate.

Pilot word length	Data rate (Mbps)	Data rate (Mbps)	Data rate (Mbps)	Data rate (Mbps)	Data rate (Mbps)	Data rate (Mbps)	Data rate (Mbps)
0	25.8	412	825	1,650	1,320	440	880
64	–	361	722	1,440	1,160	385	770

8.1.1.4 Scrambler

An industry standard scrambler with the following generator polynomial

$$g(D) = 1 + D^{14} + D^{15}$$

is utilized where D is a single bit delay element. Both scrambler and descrambler should start from the same 15 bit state. The initial state of the LFSR is communicated to the receiver via the PHY header. Note that pilot word and pilot channel estimation are not scrambled.

8.1.1.5 FEC

The SC PHY employs Reed-Solomon (RS) or LDPC codes. The two RS codes are RS (255, 239) and shortened RS (33, 17) and their implementation is mandatory. The systematic LDPC codes used in the standard are LDPC (672, 336), LDPC (672, 504), LDPC (672, 588), and LDPC (1,440, 1,344). Support for LDPC codes is optional. The rate associated with either RS (m, n) or LDPC (m, n) is n/m.

The generator polynomial for the systematic RS (255,239) is given by

$$g(x) = \prod_{k=1}^{16} \left(x + \alpha^k\right)$$

where $\alpha = 0x02$ is a root of the primitive polynomial $p(x) = 1 + x^2 + x^3 + x^4 + x^8$. The shortened version of the code is denoted by RS (16 + L, L). To shorten the code, instead of 239 octets L octets are concatenated with (239-L) zeros and are encoded. These concatenated zeros are not transmitted. As such, the code word becomes 16 + L octets long. Upon selection of L = 17 one ends up with RS (33, 17).

8.1.1.6 Spreader

The spreading factor 2 (or 4) is implemented by XORing every 2 (or 4) bits of the scrambler LFSR with the incoming information. Clearly, the LFSR circuit runs 2 (or 4) times faster than the incoming data, respectively.

If the spreading factor is 64, then the output of an LFSR defined by

$$g(D) = 1 + D^{14} + D^{15}$$

selects one of the two 64 bit Golay codes to be XORed with the incoming data. In other words, if the LFSR output is one of the two 64 bit Golay code that is XORed with the incoming bit. Otherwise, the incoming bit is XORed with the other 64 bit Golay code. The two 64 bit Golay codes in HEX form are 63AF05C963500536 and 6CA00AC66C5F0A39.

8.1.1.7 Modulation

IEEE 802.15.3c supports a number of modulation schemes such as $\pi/2$ BPSK, $\pi/2$ QPSK, $\pi/2$ 8-PSK, and $\pi/2$ 16-QAM as shown in Fig. 8.2. The stream is divided into 1, 2, 3, or 4 bits in case of BPSK, QPSK, 8-PSK, and 16-QAM, respectively. Then, a constellation point is selected. For BPSK $d_n = 2g_n - 1$ where g_n is either 1 or 0. Then d_n is mapped into z_n through

$$z_n = d_n j^n$$

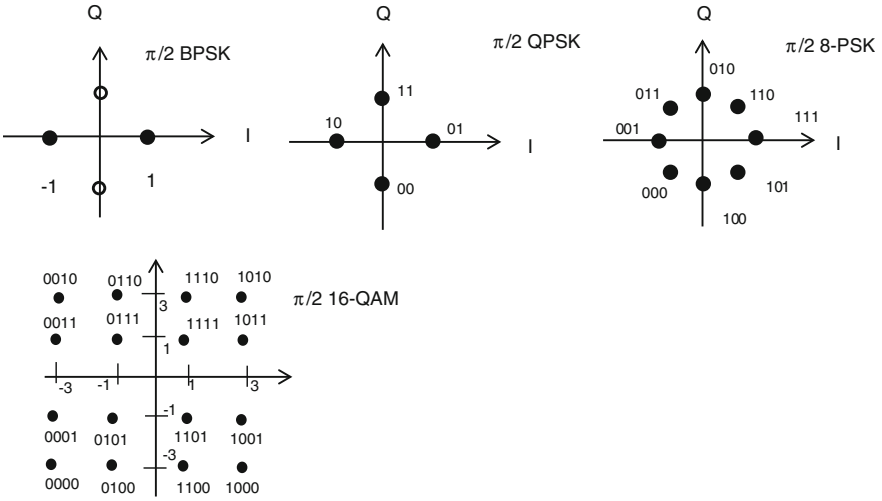

Fig. 8.2 SC constellations

where $n = 1, 2, 3, \ldots, N$. In case of $\pi/2$ BPSK, the $\pi/2$ rotation lowers the resulting PAPR. For other modulations, the rotation was included to simplify the implementation.

The differentially encoded bits are fed into GMSK encoder to obtain GMSK signal. With proper pulse shape $\pi/2$ BPSK and GMSK are roughly equivalent. Pulse shaping filtered signal must honor the transmit mask for each and every modulation.

8.1.1.8 Equalization

Pilot words are placed in between data chunks to act as known cyclic prefix and facilitate equalization. The receiver converts the temporal signal into frequency domain through the use of FFT. Then the equalization is conducted in the frequency domain. Finally, the spectral domain signal is taken back into time domain with the aid of IFFT operation. The pilot word in each subblock is used for channel estimation. The estimation results are then used in the frequency domain equalization (FDE).

As for the equalization scheme, there are some options [8]. Zero forcing (ZF) equalizer simply inverts the channel or

$$C_{\mathrm{ZF}}(k) = \frac{1}{H(k)}$$

where *H(k)* is the estimated channel. Unfortunately, ZF leads to noise enhancement in the presence of spectral nulls. Another option is to use minimum mean-square error (MMSE)

$$C_{\mathrm{MMSE}}(k)=\frac{H^{*}(k)}{|H(k)|^{2}+1/\mathrm{SNR}}$$

where * denotes the conjugate transpose operation. MMSE minimizes the combined ISI and noise contributions. Performance wise, MMSE is significantly superior to ZF in frequency selective channels. However, a signal-to-noise ratio estimate is required.

8.1.1.9 Common Mode Signaling

Through the use of Common Mode Signaling (CMS), interoperability among different PHY modes is provided. Beacon frame, sync frame, and training sequence in beam forming procedure are all transmitted using CMS. The transmitter consists of three blocks namely a scrambler, an RS encoder, and a spreader. The modulation/coding parameters of CMS are given in Table 8.3.

8.1.1.10 UEP

When information signals, such as images, video, or audio are source encoded, some bits turn out to be more important than the others. For instance, an error in MSB of a word is far more costly compared to an error in the LSB of the same word. IEEE 802.15.3c accommodates unequal error protection as an option and it is implemented using one (or both) of the two approaches.

In the first approach, the incoming bits are classified into MSB and LSB streams, then these two streams are encoded with different FEC codes. Heavier coding is applied to the MSB stream. Then the coded bits are multiplexed. The multiplexing pattern depends on the utilized FECs. Let us take an example. In our example, the MSB and LSB groups are FEC coded using LDPC (672, 336) and LDPC (672, 504), respectively. Note that MSB group benefits from a lower code rate and heavier protection. Then, six MSB bits (A1, A2, A3, A4, A5, and A6) and four LSB bits (B1, B2, B3, and B4) are multiplexed and interleaved as illustrated in Fig. 8.3 to form a single stream.

A6	B4	**A5**	B3	**A4**	**A3**	B2	**A2**	B1	**A1**

Fig. 8.3 An UEP multiplexing pattern

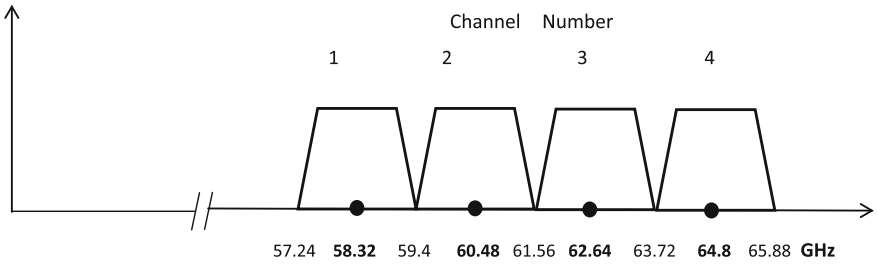

Fig. 8.4 mmW channels

In the second approach, the MSB and LSB bits are mapped into a skewed constellation where the horizontal distance between the points is larger compared to the vertical distance. The MSBs are mapped into horizontal axis points, while LSBs are mapped into vertical axis. The scaling factor of 1.25 is specified in the standard for the horizontal axis.

8.1.1.11 Band Plan

The millimeter wave band is divided into four channels, where each channel is 2.16 GHz wide. The upper, the lower (start and stop), and the center frequencies of each channel are shown in Fig. 8.4. The center frequencies can be generated from affordable crystals through the use of a PLL.

8.1.1.12 Emission Mask

The occupied bandwidth is 1.782 GHz. The emission mask per channel is shown in Fig. 8.5.

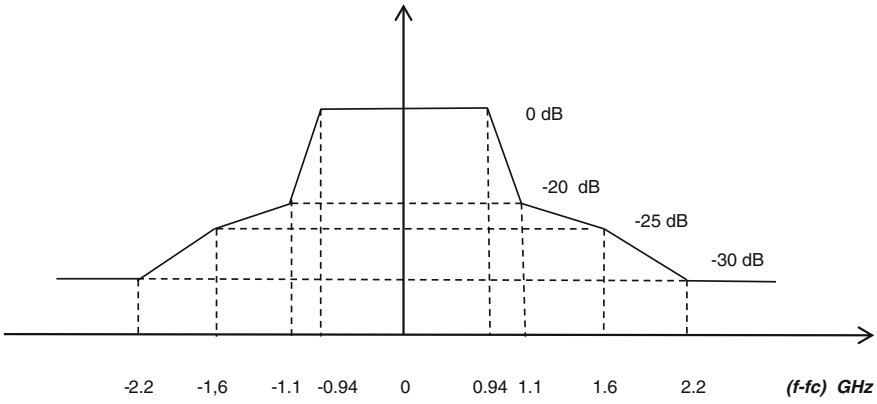

Fig. 8.5 mmW spectral mask

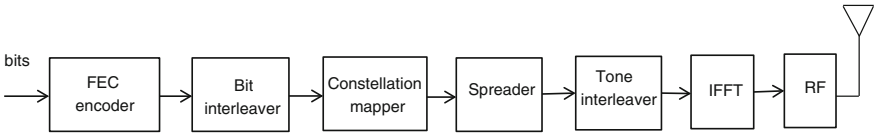

Fig. 8.6 HSI Transmitter block diagram

8.1.2 HSI PHY

8.1.2.1 Transmitter

The HSI OFDM transmitter is depicted in Fig. 8.6.

8.1.2.2 Preamble

In HSI mode, there are two preamble types, namely short preamble and long preamble. Short preamble is only used for the HSI lowest data rate (32.1 Mbps). From the structure point of view long and short preambles are identical to CMSSC and SC preambles. In other words, preamble components SYNC, SFD, and CES have the same structure as those of SC and CMSSC. However, both types use HSI chip rate (2640 MHz).

8.1.2.3 Data Rate

The modulation, FEC coding, and spreading factors for the 12 HSI data rates are listed in Table 8.4. Only the lowest data rate utilizes a spreading factor other than one. The UEP applies only to the past four data rates, namely 1,925, 2,503, 3,850, and 5,005 Mbps. The codes applied to MSB and LSB portions are listed in Table 8.4.

The OFDM parameters are listed in Table 8.5. There are five types of subcarriers: data, pilot, DC, guard, and reserved subcarriers. The number of used subcarriers (N_u) consists of the data (N_{dsc}), pilot (N_P), and DC subcarriers (N_{dc}). In other words,

$$N_u = N_{\text{dsc}} + N_P + N_{\text{dc}}$$

The used bandwidth is defined as

$$\text{BW} = N_u \Delta f_{\text{sc}}$$

where Δf_{sc} is the subcarrier spacing.

Table 8.4 HSI supported data rates

Data rate (Mbps)	Spreading factor	Modulation	FEC
32.1	48	OFDM/QPSK	LDPC (672, 336)
1,540	1	OFDM/QPSK	LDPC (672, 336)
2,310	1	OFDM/QPSK	LDPC (672, 504)
2,695	1	OFDM/QPSK	LDPC (672, 588)
3,080	1	OFDM/16-QAM	LDPC (672, 336)
4,620	1	OFDM/16-QAM	LDPC (672, 504)
5,390	1	OFDM/16-QAM	LDPC (672, 588)
5,775	1	OFDM/64-QAM	LDPC (672, 420)
1,925	1	OFDM/QPSK	MSB: LDPC (672, 336) LSB: LDPC (672, 504)
2,503	1	OFDM/QPSK	MSB: LDPC (672, 504) LSB: LDPC (672, 588)
3,850	1	OFDM/16-QAM	MSB: LDPC (672, 336) LSB: LDPC (672, 504)
5,005	1	OFDM/16-QAM	MSB: LDPC (672, 504) LSB: LDPC (672, 588)

Table 8.5 OFDM parameters

Parameter	Value
Number of subcarriers (N_{sc})	512
Number of data subcarriers (N_{dsc})	336
Number of pilot subcarriers (N_p)	16
Number of guard subcarriers (N_g)	141
Number of DC subcarriers (N_{dc})	3
Number of reserved subcarriers (N_r)	16
Number of used subcarriers (Nu)	355
IFFT and FFT period (T_{FFT})	~193.94 ns
Guard interval duration (T_{GI}) (in samples)	~24.24 (64) ns
OFDM Symbol duration ($Ts = T_{FFT} + T_{GI}$)	~218.18 ns
Number of samples per OFDM symbol ($Ncps = Nsc + N_{GI}$)	576
Subcarrier frequency spacing ($\Delta f_{sc} = 1/T_{FFT}$)	5.15625 MHz
Used bandwidth ($BW = N_u$ dfsc)	1,831 MHz
Sampling rate ($f_s = N^*\Delta f_{sc}$)	2,640 MHz

The data rates are determined by

$$\text{Data Rate} = \frac{1}{(T_{\text{FFT}} + T_{\text{GI}})} \times \text{FEC rate} \times N_{\text{sd}} \times \text{Number of} \frac{\text{bits}}{\text{subcarrier}} \times \frac{1}{\text{Spreading factor}}.$$

The first 8 rates of Table 8.4 are computed as follows:

Data rate = (1/218.18e-9) × (1/2) × 336 × 2 × (1/48) ~32 Mbps
Data rate = (1/218.18e-9) × (1/2) × 336 × 2 ~1,540 Mbps

Data rate = (1/218.18e-9) × (3/4) × 336 × 2 ~2,310 Mbps
Data rate = (1/218.18e-9) × (7/8) × 336 × 2 ~2,695 Mbps
Data rate = (1/218.18e-9) × (1/2) × 336 × 4 ~3,080 Mbps
Data rate = (1/218.18e-9) × (3/4) × 336 × 4 ~4,620 Mbps
Data rate = (1/218.18e-9) × (7/8) × 336 × 4 ~5,390 Mbps
Data rate = (1/218.18e-9) × (5/8) × 336 × 6 ~5,775 Mbps.

8.1.2.4 FEC

Unlike SC mode, HSI mode employs LDPC codes only. Four LDPC codes namely LDPC (672, 336) (rate 1/2), LDPC (672, 504) (rate 3/4), LDPC (672, 588) (rate 7/8), and LDPC (672, 420) (rate 5/8) provide error protection in this mode.

8.1.2.5 Interleaving

HSI transmitter deploys a turbo-based bit interleaver (which is optional) and a tone interleaver. While the bit interleaver operates on FEC encoded bit stream, tone interleaver permutes the modulated symbols. Bit interleaver has an iterative structure and it is best implemented using a lookup table approach. More information is provided in [1].

Tone interleaver makes sure that neighboring symbols are not mapped into adjacent subcarriers. The index associated with each subcarrier is bit reversed. In Fig. 8.7 bit reversed indices are plotted against the original indices. The jagged nature of the plot indicates that adjacent subcarriers are not nearby each other, after the interleaving operation.

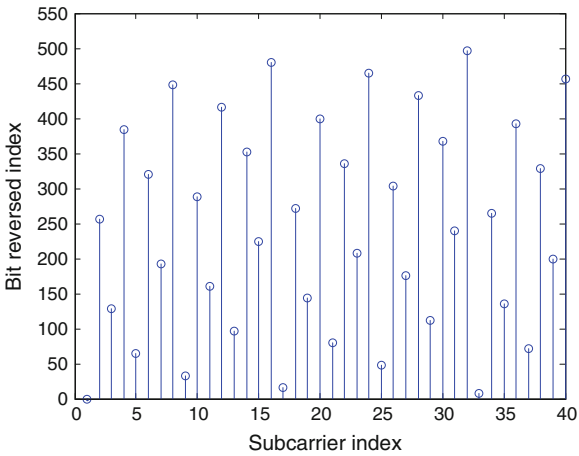

Fig. 8.7 Bit reversed indexing for the first 40 subcarriers

8.1.2.6 Multiplexing

For UEP rates multiplexing pattern depends on the utilized FEC rates. When code rates ½ (MSB) and ¾ (LSB) are deployed, then MSB streams $a_0\ a_1\ a_2$ and LSB streams $b_0 b_1$ will be multiplexed as in $a_0 b_0 a_1 b_1 a_2$. On the other hand, when code rates 3/4 (MSB) and 7/8 (LSB) are deployed, then MSB streams $a_0 a_1 a_2 a_3 a_4 a_5 a_6 a_7$ and LSB stream $b_0 b_1 b_2 b_3 b_4 b_5 b_6$ will be multiplexed as in $a_0 b_0 a_1 b_1 \ldots a_6 b_6 a_7$.

8.1.2.7 Modulation

Subcarrier constellations consist of QPSK, 16-QAM, and 64-QAM. The QPSK as well as 16-QAM constellation are shown in Fig. 8.8. A skewed constellation is constructed by scaling the horizontal axis by 1.25 ($d = 1.25$).

8.1.2.8 UEP

In UEP (unequal error protection) the MSB and LSB bit streams are encoded using two different rate FECs. Then they are multiplexed and the multiplexing pattern is a function of FEC rates. In the case of EPP (equal error protection) multiplexing pattern degenerates into conventional multiplexing. The details of multiplexing pattern for these rates are elaborated below.

Data rates 1,925 and 3,850 Mbps utilize codes LDPC (672, 336) and LDPC (672, 504) for MSB and LSB bit groups, respectively. Then three bits from the first encoder, $a_0\ a_1\ a_2$, and 2 bits from the second encoder, $b_0\ b_1$, are multiplexed to form the 5 bit pattern $a_0\ b_0\ a_1\ b_1\ a_2$.

Data rates 2,503 and 5,005 Mbps utilitize codes LDPC (672, 504) and LDPC (672, 588) for MSB and LSB bit groups, respectively. Then 7 bits from the first encoder, $a_0\ a_1\ a_2 \ldots\ a_7$, and 6 bits from the second encoder, $b_0\ b_1\ b_2 \ldots\ b_6$, are multiplexed to form the 13 bit pattern $a_0\ b_0\ a_1\ b_1 \ldots\ a_6\ b_6\ a_7$.

8.1.3 AV PHY

Two options known as high-rate PHY (HRP) and low-rate PHY (LRP) are supported in audio-visual (AV) mode.

8.1.3.1 Transmitter

The transmitter block diagrams for the two AV options are drawn in Fig. 8.9. Since serial implementation of a single convolutional code could be stretching

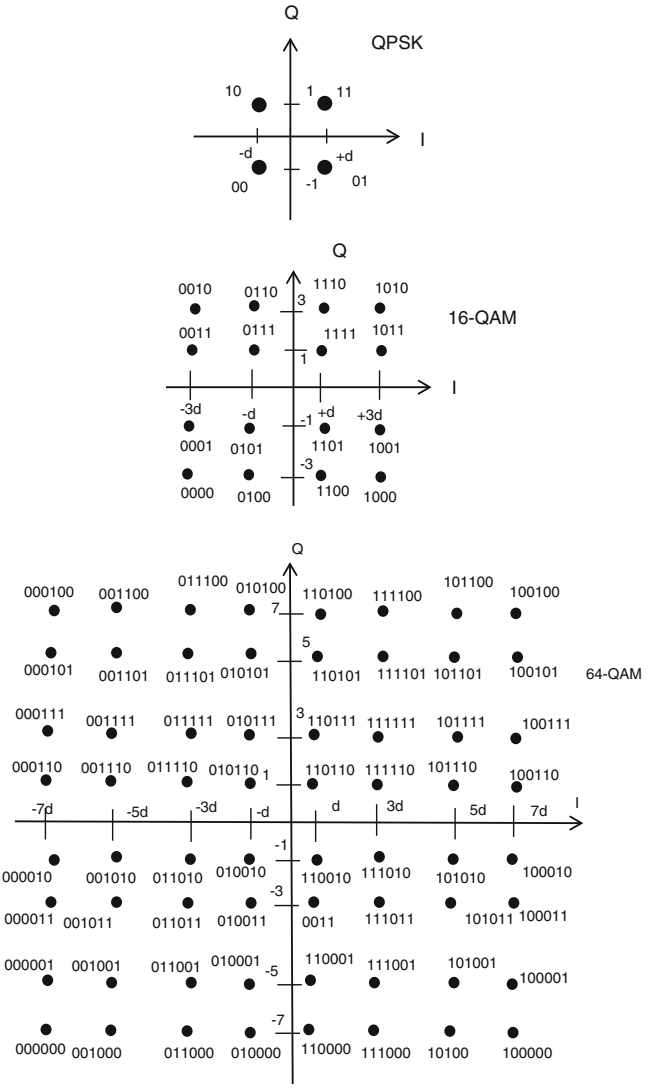

Fig. 8.8 Signal constellations

today's implementation speeds, parallel bank of convolutional encoder/decoders instead have been utilized.

The data rate, modulation, and FEC choices for both HRP and LRP are provided in Tables 8.6 and 8.7. Both options are OFDM based. The subcarrier modulation for LRP is BPSK, while both QPSK and 16-QAM modulations are supported in HRP. EEP applies only to the first three rates in Table 8.6. In UEP, convolutional codes (CC) rates 4/7 and 4/5 provide protection for MSB and LSB streams, respectively. The last two rates of Table 8.6 are used for retransmission.

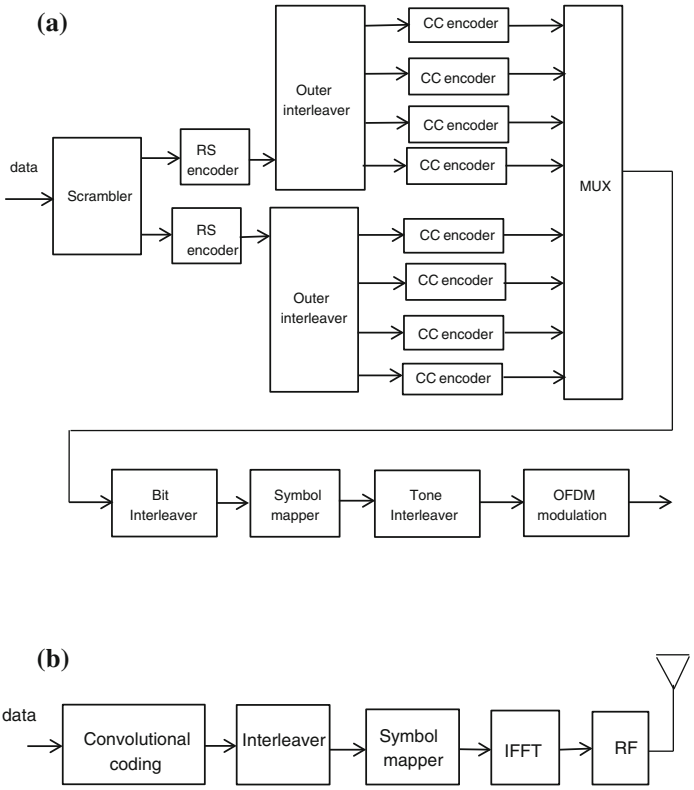

Fig. 8.9 Transmitter block diagrams for (**a**) HRP and (**b**) LRP

Table 8.6 AV-HRP data rates

Data rate (Gbps)	Modulation	FEC (inner code)	FEC (outer code)	Protection type
0.952	OFDM/QPSK	1/3	RS (224, 216)	EEP
1.904	OFDM/QPSK	2/3	RS (224, 216)	EEP
3.807	OFDM/16-QAM	2/3	RS (224, 216)	EEP
1.904	OFDM/QPSK	4/7 4/5	RS (224, 216)	UEP
3.807	OFDM/16-QAM	4/7 4/5	RS (224, 216)	UEP
0.952	OFDM/QPSK	1/3	RS (224, 216)	MSB only retransmission
1.904	OFDM/QPSK	2/3	RS (224, 216)	MSB only retransmission

Table 8.7 AV-LRP data rates

Data rate (Mbps)	Modulation	FEC (inner code)	Repetition
2.5	OFDM/BPSK	1/3	8×
3.8	OFDM/BPSK	1/2	8×
5.1	OFDM/BPSK	2/3	8×
10.2	OFDM/BPSK	2/3	4×

Note that HRP has enough bandwidth to carry 1,080p[1] format since 1,920 × 1,080 × 60 × 24 ~3 Gbps.

In the omni LRP mode, each OFDM symbol and its cyclic prefix are repeated 4 or 8 times based on data rate. Each symbol is sent using a different antenna direction or pattern. If there is only one transmit antenna, the same pattern is used for all repetitions. In the directional mode initially the best direction is determined through examination of the received pattern. Then the repetition coding for the selected direction (or pattern) is accomplished by adding one OFDM symbol as cyclic prefix to the 4 or 8 times repeated OFDM symbols. As such, in the case of eight times (×) directional repetition, each OFDM symbol is repeated nine times. Similarly, in case of four times (×) directional repetition, each OFDM symbol is repeated five times.

8.1.3.2 OFDM Parameters

The OFDM parameters for HRP and LRP options of AV are listed in Tables 8.8 and 8.9.

8.1.3.3 Data Rate

- The data rates AV-HRP option are given by

$$\text{Data Rate} = \frac{1}{(T_{\text{FFT}} + T_{\text{GI}})} \times \text{FEC rate} \times N_{\text{sd}} \times \text{Number of bits/subcarrier}$$

Upon substitution we get

Data rate = (1/227e-9) × (1/3) × (216/224) × 336 × 2 ~ 952 Mbps
Data rate = (1/227e-9) × (2/3) × (216/224) × 336 × 2 ~ 1,904 Mbps
Data rate = (1/227e-9) × (2/3) × (216/224) × 336 × 4 ~ 3,807 Mbps.

[1] Implies a resolution of 1,920 × 1,080, 24 bit color with rate of 60 frames per second.

Table 8.8 HRP OFDM parameters

Parameter	Value
Number of subcarriers (N_{sc})	512
Number of data subcarriers (N_{dsc})	336
Number of pilot subcarriers (N_p)	16
Number of null subcarriers (N_g)	157
Number of DC subcarriers (N_{dc})	3
Number of used subcarriers (N_u)	352
IFFT and FFT period (T_{FFT})	~202 ns
Guard interval duration (T_{GI}) (in samples)	~25.2 (64) ns
OFDM Symbol duration ($Ts = T_{FFT} + T_{GI}$)	~227 ns
Number of samples per OFDM symbol ($N_{cps} = N_{sc} + N_{GI}$)	576
Subcarrier frequency spacing ($\Delta f_{sc} = 1/T_{FFT}$)	4.957 MHz
Used bandwidth ($BW = N_u \Delta f_{sc}$)	1,760 MHz
Sampling rate ($f_s = N^*\Delta f_{sc}$)	2,538 MHz

Table 8.9 LRP OFDM parameters

Parameter	Value
Number of subcarriers (N_{sc})	128
Number of data subcarriers (N_{dsc})	30
Number of pilot subcarriers (N_p)	4
Number of null subcarriers (N_g)	91
Number of DC subcarriers (N_{dc})	3
Number of used subcarriers (Nu)	37
IFFT and FFT period (T_{FFT})	~403 ns
Guard interval duration (T_{GI}) (in samples)	~88.3 (28) ns
OFDM Symbol duration ($Ts = T_{FFT} + T_{GI}$)	~492 ns
Number of samples per OFDM symbol ($N_{cps} = N_{sc} + N_{GI}$)	576
Subcarrier frequency spacing ($\Delta f_{sc} = 1/T_{FFT}$)	2.48 MHz
Used bandwidth ($BW = N_u \Delta f_{sc}$)	92 MHz
Sampling rate ($f_s = N^*\Delta f_{sc}$)	317.25 MHz

- The data rates for AV-LRP option can be found using

$$\text{Data Rate} = \frac{1}{(T_{FFT}+T_{GI})} \times \text{FEC rate} \times N_{sd} \times \text{Number of} \frac{\text{bits}}{\text{subcarrier}} \times \frac{1}{\text{repetition rate}}$$

The computed rates upon substitution are

Data rate = (1/492e-9 × (1/3) × 30 × 1 × (1/8) ~ 2.5 Mbps
Data rate = (1/492e-9) × (1/2) × 30 × 1 × (1/8) ~ 3.8 Mbps
Data rate = (1/492e-9) × (2/3) × 30 × 1 × (1/8) ~ 5.1 Mbps
Data rate = (1/492e-9) × (2/3) × 30 × 1 × (1/4) ~ 10.2 Mbps.

8.1.3.4 Preamble

The first four symbols of HRP preamble are obtained in the following way. The generator polynomial $g(x) = 1 + D + D^2 + D^7 + D^8$ with all ones initial conditions generates the m-sequence five consecutive times. Then a flipped version of m-sequence is appended to the stream and enough zeros are added to occupy a time interval equal to that of 5 OFDM symbols. Finally, the resulting stream is resampled 3/2 times.

The definitions of symbol 5 through 8 in frequency domain are given in [1]. Before taking the 512 point IFFT to convert symbols 5 through 8 into time domain, symbols 5, 6, 7, and 8 are multiplied by 1, 1,−1, and −1, respectively. Continuous phase transitions are provided for symbols 5–6 as well as symbols 7–8. Finally, the last 2 × 64 samples of each IFFT are repeated.

Long omni LRP preamble is depicted below. FOE stands for frequency offset estimation. The content of each field is

CES	AGC2	Rx diversity	Fine FOE	Coarse FOE	AGC

AGC	(−1,−1,1) repeated 26 times and spread with Barker 13 sequence modulated via OQPSK or π/4QPSK
Coarse FOE	(−1,1,−1,1,1,1,−1,−1,1) repeated 9 times and spread with Barker 13 sequence modulated via π/4QPSK or OQPSK
Fine FOE	1,440 chips generated by $m = 12$ m-sequence modulated via π/4QPSK or OQPSK
AGC2	20 repetitions of long OFDM training symbol defined in []
Rx Diversity	2,560 chips generated through the use of $m = 6$ m-sequence modulated via OQPSK
AGC2	20 repetitions of OFDM (32 sample) training symbol defined in []
CES	32 OFDM training symbols (IFFT 128 samples + CP 28 samples = 156 samples long).

Short omni preamble is shown below. The content of each field is

CES	AGC	Rx diversity	Signal detect	AGC2	AGC1

AGC1	368 chips, uses $m = 6$ m-sequence modulated via π/4QPSK or OQPSK
AGC2	264 chips, uses $m = 6$ m-sequence modulated via π/4QPSK or OQPSK
Signal detection	720 chips, uses $m = 6$ m-sequence modulated via π/4QPSK or OQPSK
Rx Diversity	2,560 chips generated through the use of $m = 6$ m-sequence modulated via OQPSK

AGC	(−1,−1,1) repeated 26 times and spread with Barker 13 sequence modulated via OQPSK or π/4QPSK
CES	32 OFDM symbols (IFFT 128 samples + CP 28 samples = 156 samples long)

Directional LRP preamble is made of 5 repetitions of 128 point OFDM training symbol defined in [].

The AV mode employs m-sequences with the generator polynomials

$$g(D) = 1 + D^5 + D^6$$

and

$$g(D) = 1 + D^6 + D^8 + D^{11} + D^{12}.$$

The initial conditions for $m = 6$ and $m = 12$ m-sequences are 0b010111 and 0xB50, respectively. Barker 13 sequence is given by $\{-1\ -1\ -1\ -1\ -1\ 1\ 1\ -1\ -1\ 1\ -1\ 1\ -1\}$. In phase and quadrature components of QPSK utilize the same PN sequence. Q component is delayed by half a chip in case of OQPSK modulation.

8.1.3.5 Scrambler

The scrambler in HRP is identical to the one used in the SC mode. In contrast to HRP, data in LRP option is not scrambled.

8.1.3.6 FEC

Error protection for LRP and HRP are provided through the use of convolutional codes and concatenated codes, respectively. The concatenated codes consist of RS (224, 216, t = 4) as the outer code and a convolutional code as the inner code.

The RS (224, 216), the outer component of the concatenated code, is obtained by shortening RS (255, 247). The generator polynomial for RS (255, 247) is given by

$$g(x) = \prod_{k=1}^{8} (x + \alpha^k)$$

where $\alpha = 0x02$ is a root of the primitive polynomial $p(x) = 1 + x^2 + x^3 + x^4 + x^8$.

As for the convolutional code component of the concatenated code, the mother code is a rate 1/3 constraint length 7 convolutional code with generator polynomial

$$g_0 = 133 \quad g_1 = 171 \quad g_2 = 165.$$

This happens to be the same rate 1/3 convolutional code used in ECMA 368 standard.

Rates 1/2, 4/7, 2/3, and 4/5 are obtained through puncturing with the following puncturing patterns:

½ $\boldsymbol{b_0}\ \boldsymbol{b_1}\ b_2$
4/7 $\boldsymbol{b_0}\ \boldsymbol{b_1}\ b_2|\boldsymbol{b_3}\ b_4\ b_5|\boldsymbol{b_6}\ \boldsymbol{b_7}\ b_8|\boldsymbol{b_9}\ \boldsymbol{b_{10}}\ b_{11}$
2/3 $\boldsymbol{b_0}\ \boldsymbol{b_1}\ b_2|\boldsymbol{b_3}\ b_4\ b_5$
4/5 $\boldsymbol{b_0}\ \boldsymbol{b_1}\ b_2|\boldsymbol{b_3}\ b_4\ b_5|\boldsymbol{b_6}\ b_7\ b_8|\boldsymbol{b_9}\ b_{10}\ b_{11}$.

For instance, rate 2/3 is obtained by using $\boldsymbol{b_0}\boldsymbol{b_1}b_2|\boldsymbol{b_3}b_4b_5$ pattern. As seen, we end up with 3 output bits for every 2 input bits.

8.1.3.7 Bit Reversal Tone Interleaver

OFDM Subcarrier indices range from 0 to N − 1, where N is the number of subcarriers in an OFDM symbol. To make sure that neighboring symbols are not mapped into adjacent subcarriers, the index associated with each subcarrier is bit reversed. For instance, subcarrier number 6 (or 110 in binary notation) is mapped into subcarriers number 011 (or subcarrier number 3). Pilot, null, and DC subcarriers contents will be placed in the bit-reversed position ahead of time. As such they will end up in their known positions after the interleaving is done.

8.1.3.8 Outer Interleaver

This type of interleaving applies to HRP mode only. RS codewords are interleaved so that the error correction capability of the code is not used up by one or two error bursts from the convolutional decoder.

Let N be the number of output octets of the RS code. The output octets will be written row-wise into a rectangle of size $N \times d$ where parameter d is the depth of the interleaver. Once the rectangular box is filled, it is read column wise. The first row is fed into the first parallel convolutional encoder, the second row is fed into the second convolutional encoder, …, the Mth row is fed into the Mth parallel encoder. This operation is repeated N/M times until the entire box is read out. For HRP data field $d = 4$ and $M = 4$ are used, other fields such as HRP header, MAC header, and HCS utilize $d = 4$ and $M = 4$.

8.1.3.9 Modulation

The QPSK and 16QAM constellations in the EEP option are identical to the constellations in Fig. 8.7 when $d = 1$. Skewed constellations for UEP support are obtained by setting $d = 1.25$.

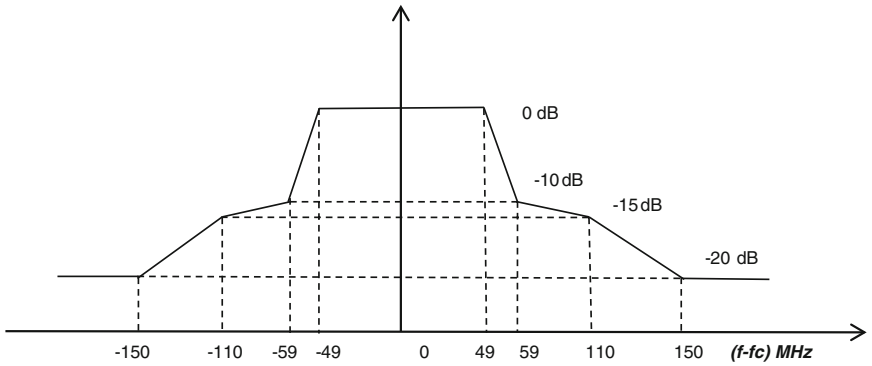

Fig. 8.10 AV-LRP transmit mask

Table 8.10 LRP channels

LPR channel #	Start frequency (MHz)	Center frequency (MHz)	Stop frequency (MHz)
1	fc[a] − 207.625	fc − 158.625	fc − 109.625
2	fc − 49	fc	fc + 49
3	fc + 109.625	fc + 158.626	fc + 207.625

[a] fc is the center frequency of an HRP channel

8.1.3.10 Emission Mask

The emission mask and band plan for HRP are identical to that of SC mode. The LRP emission mask is shown in Fig. 8.10. Within each HRP channel three LRP channels are fitted. The details of the LRP channels in reference to the center frequency of the HRP channel are given in Table 8.10.

8.2 IEEE 802.11ad

The standard offers three operational modes known as low power single carrier (SC), single carrier (SC), and OFDM modes. The main attributes of each mode are summarized in Table 8.11. While the SC mode accommodates handheld power constrained devices, OFDM mode is suitable for high-throughput devices.

8.2.1 Modes

- Data rates as well as modulation/coding options for the optional low power single carrier (SC) mode are provided in Table 8.12.

Table 8.11 IEEE 802.11ad modes

Mode	Modulation	FEC	Data rates (Mbps)
Low power SC	π/2-BPSK, π/2-QPSK	RS (224, 208) block code (8,8) block code (9,8) block code (12,8) Block code (16, 8)	626, 834, 1112, 1251, 1668, 2224, 2503

SC	π/2-BPSK, π/2-QPSK, π/2-16-QAM	LDPC (672, 336)
		LDPC (672, 504)
		LDPC (672, 546)
		LDPC (672, 420)
			385, 770, 962.5, 1,155, 1,251.5, 1,540, 1,925, 2,310, 2,502.5, 3,080, 3,850, 4,620

OFDM	QPSK, SQPSK, 16-QAM, 64-QAM	LDPC (672, 336)
		LDPC (672, 504)
		LDPC (672, 546)
		LDPC (672, 420)
			693, 866.25, 1,386, 1,732.5, 2,079, 2,772, 3,465, 4,158, 4,504.5, 5,197.5, 6,237, 6,756.75

Table 8.12 Data rate, modulation, and coding for low power SC mode

Rate (Mbps)	Modulation	Effective code rate	FEC coding
626	π/2-BPSK	13/28	RS (224, 208) + Block Code (16, 8)
834	π/2-BPSK	13/21	RS (224, 208) + Block Code (12, 8)
1112	π/2-BPSK	52/63	RS (224, 208) + SPC (9, 8)
1251	π/2-QPSK	13/28	RS (224, 208) + Block Code (16, 8)
1668	π/2-QPSK	13/21	RS (224, 208) + Block Code (12, 8)
2224	π/2-QPSK	52/63	RS (224, 208) + SPC (9, 8)
2503	π/2-QPSK	13/14	RS (224, 208) + Block Code (8, 8)

- The SC mode utilizes π/2-BPSK, π/2-QPSK, and π/2-16QAM modulations together with LDPC codes for error protection. It can be shown that with proper filtering, π/2-BPSK is equivalent to differentially coded GMSK. Data rates as low as 385 Mbps and as high as 4620 Mbps is supported (Table 8.13).
- OFDM subcarriers are modulated with the aid of SQPSK, QPSK, 16-QAM, and 64-QAM schemes. The same LDPC codes used in SC mode provide error protection for this OFDM mode as well. Data rates up to the maximum of almost 7 Gbps are offered (Table 8.14).

8.2.2 System Parameters

The OFDM and SC system parameters are listed in Tables 8.15 and 8.16.

There is a great deal of similarity between the OFDM mode and HSI of IEEE 802.15.3c such as number of data subcarriers, pilot subcarriers, DC subcarriers, etc. However, IEEE 802.11 ad is a WLAN standard in contrast to WPAN-based 802.15.3c. As such, one expects longer ranges and larger delay spreads.

Table 8.13 Data rate, modulation, and coding for SC mode

Data rate (Mbps)	Modulation	Repetition	LDPC code	Code rate
385	π/2-BPSK	2	(672, 336)	1/2
770	π/2-BPSK	1	(672, 336)	1/2
962.5	π/2-BPSK	1	(672, 420)	5/8
1,155	π/2-BPSK	1	(672, 504)	3/4
1,251.25	π/2-BPSK	1	(672, 546)	13/16
1,540	π/2-QPSK	1	(672, 336)	1/2
1,925	π/2-QPSK	1	(672, 420)	5/8
2,310	π/2-QPSK	1	(672, 504)	3/4
2,502.5	π/2-QPSK	1	(672, 546)	13/16
3,080	π/2-16QAM	1	(672, 336)	1/2
3,850	π/2-16QAM	1	(672, 420)	5/8
4,620	π/2-16QAM	1	(672, 504)	3/4

Table 8.14 Data rate, modulation, and coding for OFDM mode

Data rate (Mbps)	Modulation	LDPC code	Code rRate
693.00	SQPSK	(672, 336)	1/2
866.25	SQPSK	(672, 420)	5/8
1,386.00	QPSK	(672, 336)	1/2
1,732.50	QPSK	(672, 420)	5/8
2,079.00	QPSK	(672, 504)	3/4
2,772.00	16-QAM	(672, 336)	1/2
3,465.00	16-QAM	(672, 420)	5/8
4,158.00	16-QAM	(672, 504)	3/4
4,504.50	16-QAM	(672, 546)	13/16
5,197.50	64-QAM	(672, 420)	5/8
6,237.00	64-QAM	(672, 504)	3/4
6,756.75	64-QAM	(672, 546)	13/16

Table 8.15 OFDM parameters

Parameter	Value
Number of subcarriers (N_{sc})	512
Number of data subcarriers (N_{sd})	336
Number of pilot subcarriers (N_{sp})	16
Number of DC subcarriers (N_{dc})	3
Number of used subcarriers ($N_{st} = N_{sd} + N_{sp} + N_{dc}$)	355
Subcarrier frequency spacing ($\Delta f_{sc} = 1/T_{FFT}$)	5.15625 MHz
Nominal used bandwidth BW = Nst x Δf_{sc}	1,830.5 MHz
IFFT and FFT period (T_{FFT})	$\sim$194 ns
Guard interval duration (T_{GI}) ($T_{GI} = T_{FFT}/4$)	$\sim$48.4 ns
OFDM Symbol duration ($Ts = T_{FFT} + T_{GI}$)	$\sim$242 ns
Number of samples per OFDM symbol	576
Sampling rate ($f_s = N/T_{FFT}$)	2,640 MHz

Table 8.16 SC parameters

Parameter	Value
Chipping rate (F_c)	1,760 MHz
Chip duration ($T_c = 1/F_c$)	0.57 ns

Consequently, the OFDM option of 802.11ad is designed based on guard interval length of 48.4 ns as opposed to GI duration of 24.24 ns for HSI.

8.2.3 Data Rate

- The data rates for various combinations of modulation/FEC coding for the OFDM mode can be computed using

$$\text{Data Rate} = \frac{1}{(T_{\text{FFT}} + T_{\text{GI}})} \times \text{FEC rate} \times N_{\text{sd}} \times \text{Number of bits/subcarrier}$$

Data rate = (1/242.4e-9) × 336 × (1/2) ~ 693 Mbps
Data rate = (1/242.4e-9) × 336 × (5/8) ~ 866 Mbps
Data rate = (1/242.4e-9) × 336 × (1/2) × 2 ~ 1,386 Mbps
Data rate = (1/242.4e-9) × 336 × (5/8) × 2 ~ 1,732 Mbps
Data rate = (1/242.4e-9) × 336 × (3/4) × 2 ~ 2,079 Mbps
Data rate = (1/242.4e-9) × 336 × (1/2) × 4 ~ 2,772 Mbps
Data rate = (1/242.4e-9) × 336 × (5/8) × 4 ~ 3,465 Mbps
Data rate = (1/242.4e-9) × 336 × (3/4) × 4 ~ 4,158 Mbps
Data rate = (1/242.4e-9) × 336 × (13/16) × 4 ~ 4,504 Mbps
Data rate = (1/242.4e-9) × 336 × (5/8) × 6 ~ 5,197 Mbps
Data rate = (1/242.4e-9) × 336 × (3/4) × 6 ~ 6,237 Mbps
Data rate = (1/242.4e-9) × 336 × (13/16) × 6 ~ 6,756 Mbps

- In the SC mode data blocks of N_d symbols are formed. Between consecutive data blocks, guard intervals of N_{GI} symbols are inserted. The data transmission efficiency is therefore reduced by $N_d/(N_d + N_{GI})$ factor. The guard interval is a 64 point Golay sequence. The number of data symbols in a block are 448, 896, and 1,792 symbols for $\pi/2$-BPSK, $\pi/2$-QPSK, and $\pi/2$-16-QAM, respectively. Thus, the SC data rates for various modulation/FEC combinations are given by

$$\text{Data Rate} = \frac{N_d}{(N_d + N_{\text{GI}})} \times \frac{1}{\text{T}_\text{c}} \times \text{FEC rate} \times \text{Number of bits/constellation} \times \frac{1}{\text{speading factor}}$$

where T_c = 1/1760e6 s.

Data rate = (448/[448 + 64]) × (1760e6) × (1/2) × (1/2) = 385 Mbps
Data rate = (448/[448 + 64]) × (1760e6) × (1/2) = 770 Mbps
Data rate = (448/[448 + 64]) × (1760e6) × (5/8) = 962.5 Mbps
Data rate = (448/[448 + 64]) × (1760e6) × (3/4) = 1,155 Mbps
Data rate = (448/[448 + 64]) × (1760e6) × (13/16) ~ 1,251 Mbps
Data rate = (448/[448 + 64]) × (1760e6) × (1/2) × 2 = 1,540 Mbps
Data rate = (448/[448 + 64]) × (1760e6) × (5/8) × 2 = 1,925 Mbps
Data rate = (448/[448 + 64]) × (1760e6) × (3/4) × 2 = 2,310 Mbps
Data rate = (448/[448 + 64]) × (1760e6) × (13/16) × 2 = 2,502.5 Mbps
Data rate = (448/[448 + 64]) × (1760e6) × (1/2) × 4 = 3,080 Mbps
Data rate = (448/[448 + 64]) × (1760e6) × (5/8) × 4 = 3,850 Mbps
Data rate = (448/[448 + 64]) × (1760e6) × (3/4) × 4 = 4,620 Mbps

- The data rate associated with the low power SC is given by

$$\text{Data Rate} = \frac{N_\text{d}}{(N_d + N_{\text{GI}})} \times \frac{1}{T_c} \times \text{FEC rate} \times \text{Number of bits/constellation}$$

where T_c = 1/1760e6, $N_d = 40$, and $N_{\text{GI}} = 15$.

Data rate = (49/[49 + 15]) × (1760e6) × (104/224) ~ 626 Mbps
Data rate = (49/[49 + 15]) × (1760e6) × (208/224) ~ 1,251 Mbps
Data rate = (49/[49 + 15]) × (1760e6) × (208/224) × 2 ~ 2,502 Mbps.

8.2.4 Scrambler

Bit scrambling is accomplished by XORing each data bit with a length 127 sequence generated by the polynomial defined by

$$g(D) = 1 + D^4 + D^7.$$

Scrambling as described applies to all three modes.

8.2.5 FEC

The lowest data rate of low power SC mode utilizes concatenated codes. The outer and the inner codes are RS (224,208) and the inner code is a block code. Both RS and the block code can be implemented with very little complexity. Note that (9, 8) code is a single parity check code. The generator matrix for the block codes are the identity matrix for G_{8x8},

$$G_{8\times 9} = \begin{bmatrix} 1 & 0 & 0 & 0 & 0 & 0 & 0 & 0 & 1 \\ 0 & 1 & 0 & 0 & 0 & 0 & 0 & 0 & 1 \\ 0 & 0 & 1 & 0 & 0 & 0 & 0 & 0 & 1 \\ 0 & 0 & 0 & 1 & 0 & 0 & 0 & 0 & 1 \\ 0 & 0 & 0 & 0 & 1 & 0 & 0 & 0 & 1 \\ 0 & 0 & 0 & 0 & 0 & 1 & 0 & 0 & 1 \\ 0 & 0 & 0 & 0 & 0 & 0 & 1 & 0 & 1 \\ 0 & 0 & 0 & 0 & 0 & 0 & 0 & 1 & 1 \end{bmatrix},$$

$$G_{8\times 12} = \begin{bmatrix} 1 & 0 & 0 & 0 & 0 & 0 & 0 & 0 & 1 & 1 & 0 & 0 \\ 0 & 1 & 0 & 0 & 0 & 0 & 0 & 0 & 1 & 0 & 1 & 0 \\ 0 & 0 & 1 & 0 & 0 & 0 & 0 & 0 & 0 & 1 & 0 & 1 \\ 0 & 0 & 0 & 1 & 0 & 0 & 0 & 0 & 0 & 0 & 1 & 1 \\ 0 & 0 & 0 & 0 & 1 & 0 & 0 & 0 & 1 & 0 & 1 & 1 \\ 0 & 0 & 0 & 0 & 0 & 1 & 0 & 0 & 1 & 1 & 0 & 1 \\ 0 & 0 & 0 & 0 & 0 & 0 & 1 & 0 & 1 & 1 & 1 & 0 \\ 0 & 0 & 0 & 0 & 0 & 0 & 0 & 1 & 0 & 1 & 1 & 1 \end{bmatrix},$$

and

$$G_{8\times 16} = \begin{bmatrix} 1 & 0 & 0 & 0 & 0 & 0 & 0 & 0 & 0 & 1 & 1 & 0 & 1 & 0 & 1 & 0 \\ 0 & 1 & 0 & 0 & 0 & 0 & 0 & 0 & 0 & 0 & 1 & 1 & 0 & 1 & 0 & 1 \\ 0 & 0 & 1 & 0 & 0 & 0 & 0 & 0 & 1 & 0 & 0 & 1 & 1 & 0 & 1 & 0 \\ 0 & 0 & 0 & 1 & 0 & 0 & 0 & 0 & 0 & 1 & 0 & 0 & 1 & 1 & 0 & 1 \\ 0 & 0 & 0 & 0 & 1 & 0 & 0 & 0 & 1 & 0 & 1 & 0 & 0 & 1 & 1 & 0 \\ 0 & 0 & 0 & 0 & 0 & 1 & 0 & 0 & 0 & 1 & 0 & 1 & 0 & 0 & 1 & 1 \\ 0 & 0 & 0 & 0 & 0 & 0 & 1 & 0 & 1 & 0 & 1 & 0 & 1 & 0 & 0 & 1 \\ 0 & 0 & 0 & 0 & 0 & 0 & 0 & 1 & 1 & 1 & 0 & 1 & 0 & 1 & 0 & 0 \end{bmatrix}$$

The systematic RS (224,208) code is the shortened version of RS (255,239). To shorten RS (255,239), 208 octets are concatenated with 31 zeros and are encoded. These concatenated zeros are not transmitted. As such one ends up with RS (224,208). The RS code has the following generator polynomial

$$G(x) = \prod_{k=1}^{16} (x + \alpha^k)$$

where $\alpha = 0x02$ is a root of the primitive polynomial $p(x) = 1+x^2+x^3+x^4+x^8$. A code symbol or octets is represented by $b_0b_1b_2b_3b_4b_5b_6b_7$ where b_0 is the LSB.

The following four systematic LDPC codes:

LDPC (672, 336) rate 1/2,
LDPC (672, 504) rate 3/4,
LDPC (672, 546) rate 13/16
LDPC (672, 420) rate 5/8

provide error protection for both SC and the OFDM. Note that LDPC code rates 1/2 and 3/4 are also used in HSI mode of IEEE 802.15.3c as well.

8.2.6 Modulation

The OFDM option of the standard uses either SQPSK (Spread QPSK), QPSK, 16-QAM, or 64-QAM for subcarrier modulation. The SQPSK and QPSK are somewhat unorthodox and will be covered in this section. 64 QAM constellation is identical to the one depicted in Fig. 8.8 when $d = 1$.

The SQPSK starts by dividing the bit stream into bit pairs and bit pairs are mapped into one of the four constellation points. This process is repeated for the right half of OFDM subcarriers. The remaining subcarriers (left half of the OFDM subcarriers) are selected to be the complex conjugate of the right half. In terms of spectral efficiency, this modulation is equivalent to BPSK. However, one can benefit from frequency diversity in the demodulation process. As such, SQPSK is expected to outperform plain BPSK in multipath environments.

The QPSK modulation utilized in this standard is identical to DCM used in ECMA 368 and transmits two bits of information per subcarrier. Four back-to-back bits are converted into two complex symbols such that every other bit pair makes a complex QPSK symbol. The complex QPSK pair is then linearly mapped into two other symbols. The resulting symbols come from a 16-QAM constellation. The two 16-QAM constellations are placed 168 subcarriers apart. The performance in AWGN is equivalent to QPSK. However, it will outperform plain QPSK in fading channels since it can benefit from diversity.

Both static and dynamic pairing of subcarriers is supported in the standard. In static pairing, each subcarrier is paired with one that is 166 subcarriers away. In dynamic pairing the selection is done on the fly. The signal strength for each subcarrier on the right half of OFDM spectrum is determined. The process is repeated for the left half of the OFDM spectrum. Then the two lists are sorted and associations based on the ranking of subcarriers are made.

After modulation a spreading operation is performed defined by

$$r(n) = Ga_{32}\ (n\ mod\ 32)d\left(\left\lfloor\frac{n}{32}\right\rfloor\right)e^{j\pi\frac{n}{2}}\quad n = 0, 1, 2, \ldots$$

where *d()* is a constellation point, $\lfloor \frac{n}{32} \rfloor$ performs the floor operation on $\frac{n}{32}$ and Ga_{32} is $Ga_{32} = [+1\ +1\ +1\ +1\ +1\ -1\ +1\ -1\ -1\ -1\ +1\ +1\ +1\ -1\ -1\ +1\ +1\ +1 -1\ -1\ +1\ -1\ -1\ +1\ -1\ -1\ -1\ -1\ +1\ -1\ +1\ -1]$.

8.2.7 Preamble

The preamble, responsible for packet detection, synchronization, AGC, frequency offset estimation, and channel estimation, consists of a short training field followed by a channel estimation sequence.

Short training Field	CES

For OFDM, the short training field (STF) is made of 48 repetitions of Gb_{128} followed by $-Gb_{128}$ and $-Ga_{128}$. The mathematical definition of the transmitted signal is given by

$$S_{\mathrm{STF}}(n) = \begin{cases} \mathrm{Ga}_{128}(n \bmod 128)e^{j\pi\frac{n}{2}} & n = 0, 1, \ldots, 48 \times 128 - 1 \\ -\mathrm{Ga}_{128}(n \bmod 128)e^{j\pi\frac{n}{2}} & n = 48 \times 128, \ldots, 49 \times 128 - 1 \\ -\mathrm{Ga}_{128}(n \bmod 128)e^{j\pi\frac{n}{2}} & n = 49 \times 128, \ldots, 50 \times 128 - 1 \end{cases}$$

where Ga_{128} and Gb_{128} are Golay complementary sequences of length 128 defined by

Ga_{128} = [
1 1 -1 -1 -1 -1 -1 -1 -1 1 -1 1 1 -1 -1 1 1 -1 -1 1 -1 1 -1 1 -1 -1 -1 -1 1 1 -1 -1
1 1 -1 -1 -1 -1 -1 -1 -1 1 -1 1 1 -1 -1 1 -1 1 1 -1 1 -1 1 -1 1 1 1 1 1 -1 -1 1 1
-1 -1 1 1 1 1 1 1 1 -1 1 -1 -1 1 1 -1 -1 1 1 -1 1 -1 1 -1 1 1 1 1 -1 -1 1 1
1 1 -1 -1 -1 -1 -1 -1 -1 1 -1 1 1 -1 -1 1 -1 1 1 -1 1 -1 1 -1 1 1 1 1 -1 -1 1 1],

and

Gb_{128} = [
-1 -1 1 1 -1 -1 -1 -1 1 -1 1 -1 1 -1 -1 1 -1 1 1 -1 -1 1 -1 1 1 1 1 1 1 1 -1 -1
-1 -1 1 1 -1 -1 -1 -1 1 -1 1 -1 1 -1 -1 1 1 -1 -1 1 1 -1 1 -1 -1 -1 -1 -1 -1 -1 1 1
1 1 -1 -1 1 1 1 1 -1 1 -1 1 -1 1 1 -1 1 -1 -1 1 1 -1 1 -1 -1 -1 -1 -1 -1 -1 1 1
-1 -1 1 1 -1 -1 -1 -1 1 -1 1 -1 1 -1 -1 1 1 -1 -1 1 1 -1 1 -1 -1 -1 -1 -1 -1 -1 1 1].

For SC, the short training field (STF) consists of of 16 repetitions of Ga_{128} followed by -Ga_{128}. The mathematical definition of the transmitted signal is given by

$$S_{\mathrm{STF}}(n) = \begin{cases} \mathrm{Ga}_{128}(n \bmod 128)e^{j\pi\frac{n}{2}} & n = 0, 1, \ldots, 16 \times 128 - 1 \\ -\mathrm{Ga}_{128}(n \bmod 128)e^{j\pi\frac{n}{2}} & n = 16 \times 128, \ldots, 17 \times 128 - 1 \end{cases}$$

The channel estimation sequences for SC and OFDM are given by

$$r_{SC} = (Gu_{512}(n) + Gv_{512}(n - 512) + Gv_{512}(n - 1024))e^{j\pi\frac{n}{2}}$$
$$n = 0, 1, ...,1151$$

and

$$r_{OFDM} = (Gv_{512}(n) + Gu_{512}(n - 512) + Gv_{512}(n - 1024))e^{j\pi\frac{n}{2}}$$
$$n = 0, 1, ...,1151$$

where $Gu_{512}(n)$ and $Gv_{512}(n)$ are defined for $0 \leq n \leq 511$ and are zero elsewhere,

$$Gu_{512} = [-Gb_{128} \quad -Ga_{128} \quad Gb_{128} \quad -Ga_{128}],$$

$$Gv_{512} = [-Gb_{128} \quad Ga_{128} \quad -Gb_{128} \quad -Ga_{128}].$$

A detection mechanism can be put together to take advantage of the autocorrelation property of the Golay codes. The zero correlation zone property not only leads to accurate channel estimation, it can also simplify I/Q imbalance estimation process [6].

8.2.8 Emission Mask

The occupied bandwidth is 1.88 GHz. Channelization is identical to IEEE 892.15.3c. Spectral mask for 802.11 ad is given in Fig. 8.11.

What We Learned

- SC option of IEEE 802.15.3c: Modulation, coding, data rate, scrambler, spreader, transmitter block diagram, preamble structure, receiver equalization, band plan, and emission mask

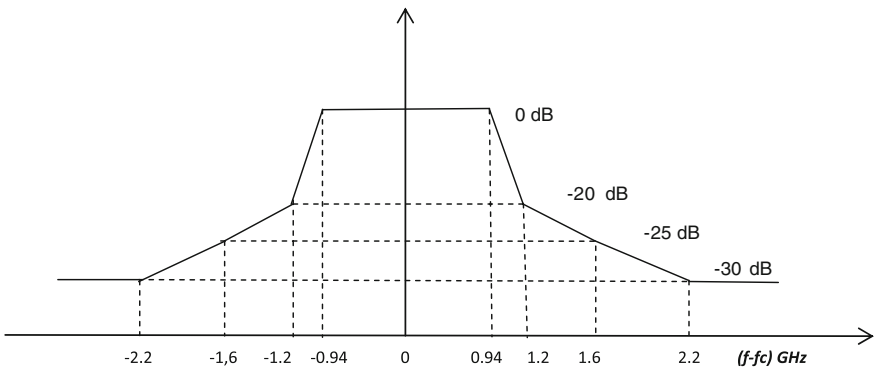

Fig. 8.11 IEEE 802.11 ad spectral mask

- HSI option of IEEE 802.15.3c: Modulation, coding, data rate, interleaving, multiplexing transmitter block diagram, and band plan
- AV option of IEEE 802.15.3c: Modulation, coding, data rate,, scrambler, bit/tone interleaving, transmitter block diagram preamble structure, and emission mask
- IEEE 802.11ad modes, modulation, coding, data rates, scrambler, preamble structure, and emission mask.

Simulation Projects

1. Simulate the BER performance of IEEE 802.15.3c SC option in AWGN as well as in CM1 channel. Operate in channel 1 of the band plan and select the lowest data rate.
2. Simulate the BER performance of IEEE 802.15.3c HSI option in AWGN as well as in CM1 channel. Operate in channel 1 of the band plan and select the lowest data rate. Determine PAPR of the transmitted signal.
3. Simulate the BER performance of IEEE 802.15.3c AV-LRP options in AWGN as well as in CM1 channel. Operate in channel 1 of the band plan and select the lowest data rate. Determine PAPR of the transmitted signal.
4. Simulate the BER performance of IEEE 802.11ad SC option in AWGN as well as in CM1 channel. Operate in channel 1 of the band plan and select the lowest data rate.

References

1. IEEE 802.15.3c, wireless medium access control (MAC) and physical layer (PHY) Specification for High Rate wireless personal area networks (WPAN) Amendment 2: Millimeter-wave-based Alternative Physical Layer Extension (2009)
2. IEEE 802.11 ad, PHY/MAC Complete Proposal Specification, May (2010)
3. European Computer Manufacturing Association, "High Rate 60 GHz PHY, MAC and HDMI PAL," Standard ECMA-387, 1st edn. December 2008. online. Available at: <http://www.ecma-international.org> Accessed 26 Dec 2010
4. European Computer Manufacturing Association, "High Rate 60 GHz PHY, MAC and PALs," Standard ECMA-387, 2nd edn. December 2010. online. Available at: <http://www.ecma-international.org> Accessed 8 May 2011
5. online. Available at: <http://wirelessgigabitalliance.org/> Accessed 26 Dec 2010
6. online. Available at: <http://www.wirelesshd.org/> Accessed 26 Dec 2010
7. X. Zhu, A. Doufexi and T. Kocak, On the Performance of IEEE 802.15.3c Millimeter Wave WPANs: PHY and MAC (2010)
8. M. Lei, I. Lakkis, H. Harada and S. Kato, MMSE-FDE Based on Estimated SNR for Single-Carrier Block Transmission (SCBT) in Multi-Gbps WPAN (IEEE 802.15.3c), ICC (2008)

Chapter 9
Other 60 GHz Standards

IEEE 802 forums have established two standards for 60 GHz communications. The first one, IEEE 802.15.3c, addresses wireless personal area communications (WPAN) space. The second standard, IEEE 802.11 ad, is intended for wireless local area networks (WLAN) and is an extension to the existing IEEE 802.11 family. These two standards were addressed in great detail in Chap. 8.

There are, however, three other standards besides IEEE standards for 60 GHz band. The first standard has been established by the European computer manufacturing association (ECMA) under ECMA 387 [1, 2]. The remaining two have been developed by WirelessHD[1] and WiGig[2] industry alliances. It is the objective of this chapter to introduce these standards and describe their individual attributes.

9.1 ECMA 387

So far two editions of ECMA 387 have been published [1, 2]. The first edition, published in Dec 2008, introduces three types of devices, namely type A, type B, and type C [1]. Type A devices employ either single carrier block transmission (SCBT) mode or OFDM mode. Rate 0.397 Gbps of SCBT is considered mandatory. All other rates are optional. Type A devices support directional antennas. As for type B, rate 0.794 Gbps employing DBPSK is considered mandatory. Other rates using DQPSK, UEP-QPSK, and DAMI are optional. Type C devices are required to support rate 0.8 Gbps employing OOK. Support for all other rates is optional.

Type A devices are required to support rate 0.794 Gbps of type B and rate 0.8 Gbps of type C. Type B devices are required to support (the transmission of) rate 0.397 Gbps of type A and rate 0.8 Gbps of type C. Type C devices are not required to support any of type A or type B rates.

A comparison between the PHY attributes of the three device types is provided in Table 9.1. Type C devices are the least complex, as their modulation and coding

[1] http://www.wirelesshd.org/
[2] http://wirelessgigabitalliance.org/

S. Emami, *UWB Communication Systems: Conventional and 60 GHz*,
DOI: 10.1007/978-1-4614-6753-3_9,

Table 9.1 ECMA 387 PHY attributes

Type	Modulation	FEC	Data rate (Mbps)
A SCBT mode	BPSK,QPSK,NS8QAM, 16QAM,TCM-16QAM,UEP-QPSK,UEP-16QAM	Concatenated codes: RS(255,239) + CC rates ½, 6/7,5/6,2/3,4/7,4/5	397,794,1588,2722,3175,4234, 4763,6350,2117
A OFDM mode	QPSK,16QAM,UEP-QPSK,UEP-16QAM	RS(255,239) + CC rates 1/3,2/3,4/7,4/5	1008,2016,4032
B	DBPSK,DQPSK,UEP-QPSK,DAMI	RS(255,239)	794,1588,3175
C	OOK,4-ASK	RS(255,239)	800,1600,3200

are quite simple. Type B devices are a bit more complex, since the lowest data rates associated with type A and C must be supported. Type A devices are the most complex. Their FEC, modulation, and beamforming are more costly to implement.

The second edition of ECMA 387 was published in 2010 [2]. Only two device types, known as A and B are supported. While type A is envisioned for high end, high throughput, and longer range uses, device type B is to serve low power, low cost, and handheld applications. Wireless desktops, access point data deliver, docking stations, and uncompressed video delivery are among the suggested applications. The second edition eliminates type C device. Additionally, it no longer supports Dual Alternate Mark Inversion (DAMI) modulation mode for type B devices. We, however, describe type C and DAMI mode of type B for the sake of completeness.

9.1.1 Type A-SCBT

Table 9.2 presents a summary of PHY features of SCBT mode.

9.1.1.1 Preamble

The preamble consists of synchronization and channel estimation sequences. The first eight symbols are the synchronization symbols and the last three symbols are the channel estimation symbols.

Table 9.2 SCBT mode

Data rate (Mbps)	Modulation	FEC	Spreading factor
397	BPSK	RS(255,239) + CC rate 1/2	2
794	BPSK	RS(255,239) + CC rate 1/2	1
1588	BPSK	RS(255,239)	1
1588	QPSK	RS(255,239) + CC rate 1/2	1
2722	QPSK	RS(255,239) + CC rate 6/7	1
3175	QPSK	RS(255,239)	1
4234	NS8QAM	RS(255,239) + TCM rate 5/6	1
4763	NS8QAM	RS(255,239)	1
4763	TCM-16QAM	RS(255,239) + CC rate 2/3	1
6350	16QAM	RS(255,239)	1
1588	QPSK	RS(255,239) + CC rate ½ MSB 0 LSB	1
4234	16QAM	RS(255,239) + CC rate 4/7 MSB CC rate 4/5 LSB	1
2117	UEP-QPSK	RS(255,239) + CC rate 2/3	1
4234	UEP-16QAM	RS(255,239) + CC rate 2/3	1

Ssync	Ssync	Ssync	Ssync	Ssync	Ssync	Ssync	-Ssync	$S_{FZ,16}$	$S_{FZ,16}$	$S_{FZ,16}$

Both these sequences are 256 samples long and are based on Frank-Zadoff sequence. The synchronization symbol is described as

$$S_{\text{sync}}(n) = S_{FZ,4}(n \, mod \, 16) S_{FZ,4}\left(\left\lfloor \frac{n}{16} \right\rfloor\right) \quad n = 0, 1, \ldots, 255.$$

The channel estimation symbol is a Frank-Zadoff (FZ)sequence of length 256.

By definition, FZ sequence with length of A^2 is defined by

$$S_{FZ,A}(n) = e^{\left(j\frac{2\pi pq}{A}\right)} \quad n = 0, 1, \ldots, A^2 - 1$$

where $p = (n \, mod \, A) + 1, q = \text{floor}\left(\frac{n}{A}\right) + 1$ and floor () function selects the largest integer smaller than or equal to its argument. Frank-Zadoff sequence of length 16, $S_{FZ,4}$, is shown in Fig. 9.1.

9.1.1.2 Data Rate

The data rate for the rates that utilize concatenated coding (RS + CC) can be found using

$$\text{Data Rate} = \frac{252}{256} \times \frac{1}{T_c} \times \text{FEC rate} \times \text{Number of constellation bits} \times \frac{1}{\text{Spreading factor}}.$$

There are four pilot symbols per block of 256 symbols and symbol frequency is 1728 MHz. Upon substitution we get

Data rate = 1728e6 × (239/255) × 1 × (252/256) × (1/2) × (1/2) ∼ 398.6 Mbps
Data rate = 1728e6 × (239/255) × 1 × (252/256) × (1/2) ∼ 797.1 Mbps
Data rate = 1728e6 × (239/255) × 1 × (252/256) ∼ 1594 Mbps
Data rate = 1728e6 × (239/255) × 2 × (252/256) × (1/2) ∼ 1594 Mbps
Data rate = 1728e6 × (239/255) × 2 × (252/256) × (6/7) ∼ 2733 Mbps
Data rate = 1728e6 × (239/255) × 2 × (252/256) ∼ 3188 Mbps
Data rate = 1728e6 × (239/255) × 3 × (252/256) ∼ 4782 Mbps
Data rate = 1728e6 × (239/255) × 4 × (252/256) ∼ 6377 Mbps
Data rate = 1728e6 × (239/255) × 2 × (252/256) × (1/2) ∼ 1594 Mbps
Data rate = 1728e6 × (239/255) × 4 × (252/256) × (2/3) ∼ 4251 Mbps
Data rate = 1728e6 × (239/255) × 2 × (252/256) × (2/3) ∼ 2125 Mbps
Data rate = 1728e6 × (239/255) × 4 × (252/256) × (2/3) ∼ 4251 Mbps.

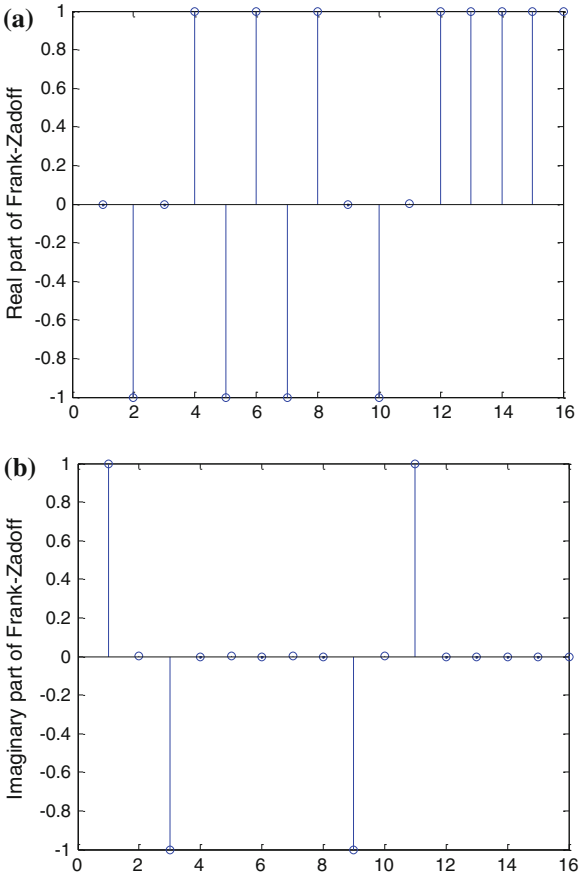

Fig. 9.1 **a** Real part of Frank-Zadoff sequence of length 16. **b** Imaginary part of Frank-Zadoff sequence of length 16

9.1.1.3 Transmitter

The transmitter block diagram is depicted in Fig. 9.2. The lowest data rate, 397 Mbps, uses a spreading factor of two. In this case, spreading operation happens right before symbol interleaving. All other rates have a spreading factor of unity.

In the case of UEP, the incoming data octets are split into MSB and LSB streams. Then each stream is passed through a baseband transmitter as shown above. At the conclusion of CC/TCM encoder block, all eight parallel paths are MUXed together to form a single stream. Afterward, bits are mapped into a constellation and symbols are interleaved.

9.1.1.4 Scrambler

An industry standard scrambler with the following generator polynomial:

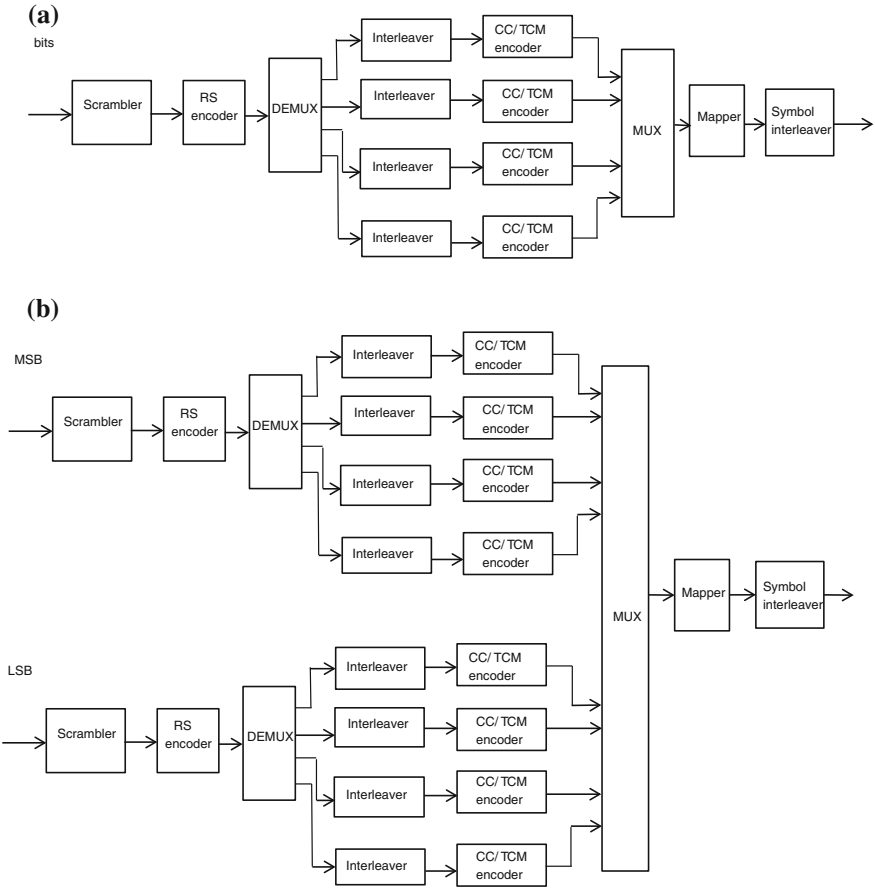

Fig. 9.2 Baseband portion of ECMA 387 SCBT transmitter. **a** EEP transmitter. **b** UEP transmitter

$$g(D) = 1 + D^{14} + D^{15}$$

is utilized where D is a single bit delay element. Scrambler and descrambler should both start from the same (15 bit) state. SC and AV modes of IEEE 802.15.3c employ the same scrambler.

9.1.1.5 Bit Interleaver

The output array is a rearranged version of the input array. The relationship between the input and output indices is defined as

$$l = \left[6\left\lfloor\frac{k}{6}\right\rfloor + 7(k \bmod 6)\right] \bmod 48$$

The following is the output array index, given that input index ranges from 0 to 47. The indices are read from left to right.

0	7	14	21	28	35	6	13	20	27	34	41	12	19	26	33	40	47	18	25
32	39	46	5	24	31	38	45	4	11	30	37	44	3	10	17	36	43	2	9
16	23	42	1	8	15	22	29												

9.1.1.6 Modulation

BPSK, QPSK, UEP-QPSK, NS8QAM, 16QAM, and UEP-16QAM constellations are shown in Fig. 9.3. The symbol indices start from 0 for constellations with odd and even symbol indices.

Both QPSK and 16QAM can provide UEP capability by deploying skewed constellations. In skewed constellations, the horizontal axis is stretched or scaled by factor of 1.25. As such, the distance between the points in horizontal direction is larger than the distance in vertical direction. The MSB and LSB bit groups are mapped into horizontal and vertical axes, respectively.

9.1.1.7 FEC

The majority of data rates utilize concatenated coding consisting of RS (255, 239) and convolutional codes. Some rates use plain RS (255,239) for error protection. A few rates combine RS (255,239) with trellis coded modulation.

Equal error protection (EPP) is applied to most data rates but not all. A few data rates apply UEP by coding MSB and LSB parts of code words with different rate convolutional codes. In a couple of cases, UEP is provided by discarding the LSB parts of the code words and providing error protection for MSP portions.

The convolutional code used in this standard is a rate ½ code with four stages of memory and generator polynomials described by $g_0 = 23$ and $g_1 = 35$. This code serves as the mother code. Rates 4/7, 2/3, 4/5, 5/6, and 6/7 are obtained through puncturing with the following puncturing patterns:

4/7 $\mathbf{b_0 b_1}|\mathbf{b_3 b_4}|\mathbf{b_5 b_6}|\mathbf{b_7} b_8$
2/3 $\mathbf{b_0 b_1}|\mathbf{b_3} b_4$
4/5 $\mathbf{b_0} b_1|\mathbf{b_2} b_3|\mathbf{b_4 b_5}|\mathbf{b_6} b_7$
5/6 $\mathbf{b_0 b_1} | b_2 \mathbf{b_3}|\mathbf{b_4} b_5|\mathbf{b_6} b_7|\mathbf{b_8} b_9$
6/7 $\mathbf{b_0 b_1} | b_2 \mathbf{b_3}|\mathbf{b_4} b_5 | b_6 \mathbf{b_7}|\mathbf{b_8} b_9 | b_{10} \mathbf{b_{11}}$.

Fig. 9.3 Signal constellation

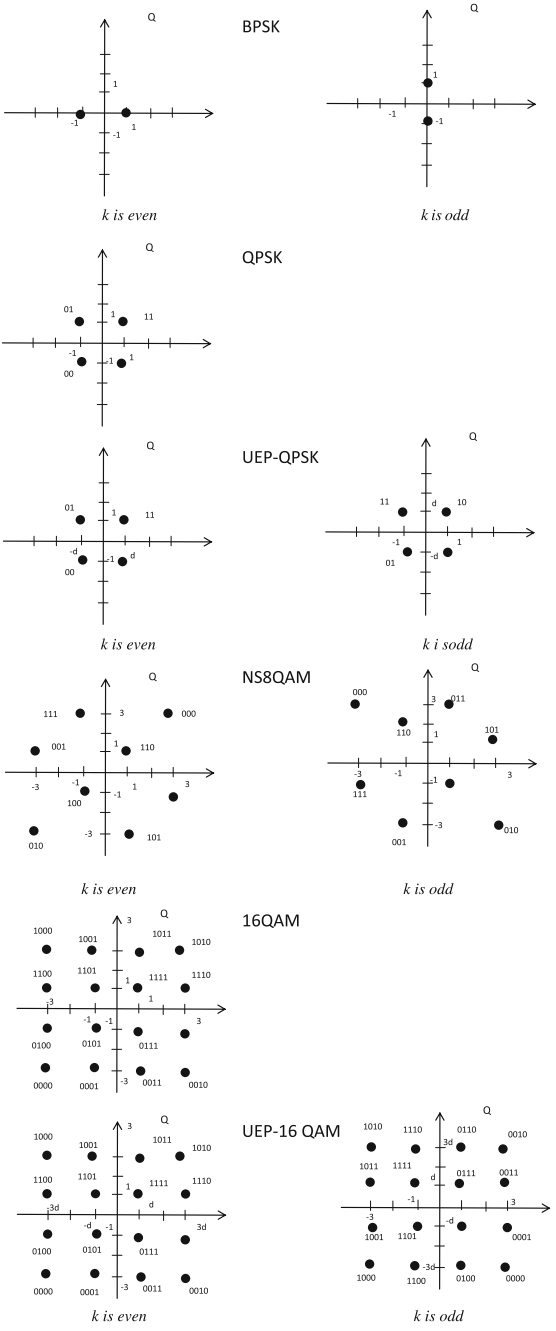

9.1.1.8 Symbol Interleaver

The symbol interleaver is a 21 by 24 double helical scan (DHS) interleaver. A block of 504 data points, u(k), is stored in a two-dimensional array, r(m,n). Then the array points are placed in another block, w(k), in a certain fashion and transmitted over the channel. The intermediate array is given by

$$r(m,n) = u(k)$$

where

$$m = \left[(k \bmod 21) + \left\lfloor \frac{k}{21} \right\rfloor\right] \bmod 24$$

and

$$n = k \bmod 21.$$

Finally, w(k) is obtained from

$$w(k) = r(m,n)$$

where

$$m = 23 - \left[(k \bmod 21) + \left\lfloor \frac{k}{21} \right\rfloor\right] \bmod 24$$

and

$$n = k \bmod 21.$$

9.1.1.9 Channel Bonding

Type A ECMA 387 SCBT devices can double, triple, or quadruple their data rates by bonding two, three, or all four channels, respectively. Channel bonding is only applicable to type A and B devices. A total of ten channels are constructed from the four channels. The band numbers are specified in Table 9.3.

9.1.2 Type A-OFDM

The supported data rates as well as modulation/coding options for the OFDM mode are summarized in Table 9.4. Here UEP-QPSK and UEP-6QAM refer to the use of skewed constellation for modulation with a scaling factor of 1.25 in horizontal direction compared to the standard constellations.

Table 9.3 ECMA 387 bands

Band Number	Channel(s)
1	1
2	2
3	3
4	4
5	1 + 2
6	2 + 3
7	3 + 4
8	1 + 2 + 3
9	2 + 3 + 4
10	1 + 2 + 3 + 4

Table 9.4 OFDM mode

Data Rate (Mbps)	Modulation	FEC
1008	QPSK	RS(255,239) + CC rate 1/3
2016	QPSK	RS(255,239) + CC rate 2/3
4032	16QAM	RS(255,239) + CC rate 2/3
2016	QPSK	RS(255,239) + CC rate 4/7 MSB CC rate 4/5 LSB
4032	16QAM	RS(255,239) + CC rate 4/7 MSB CC rate 4/5 LSB
2016	UEP-QPSK	RS(255,239) + CC rate 2/3
4032	UEP-16QAM	RS(255,239) + CC rate 2/3
2016	QPSK	RS(255,239) + CC rate 2/3 MSB 0 LSB

9.1.2.1 OFDM System Parameters

The OFDM system parameters are listed in Table 9.5.

9.1.2.2 Data Rate

The data rates for the OFDM mode can be computed using

$$\text{Data Rate} = \frac{1}{(T_{FFT} + T_{GI})} \times \text{FEC rate} \times N_{sd} \times \text{Number of bits/subcarrier.}$$

Data rate = (1/222.23e-9)*360*2*(239/255)*(1/3) $\sim$ 1008 Mbps
Data rate = (1/222.23e-9)*360*2*(239/255)*(2/3) $\sim$ 2016 Mbps
Data rate = (1/222.23e-9)*360*4*(239/255)*(2/3) $\sim$ 4032 Mbps.

Table 9.5 OFDM parameters

Parameter	Value
Number of subcarriers (N)	512
Number of data subcarriers(N_D)	360
Number of pilot subcarriers (N_P)	16
Number of null subcarriers (N_N)	133
Number of DC subcarriers (N_{DC})	3
Subcarrier frequency spacing ($\Delta fsc = 1/T_{FFT}$)	5.0625 MHz
Used bandwidth ($BW = (N_D + N_P + N_{DC})\ \Delta fsc$)	1918.7 MHz
IFFT and FFT period (T_{FFT})	197.53 ns
Guard interval duration (T_{GI}) (in samples)	24.70 (64) ns
OFDM Symbol duration ($Ts = T_{FFT} + T_{GI}$)	222.23 ns
Number of samples per OFDM symbol ($Ncps = N + N_{GI}$)	576
Sampling rate ($fs = N/T_{FFT}$)	2592 MHz

9.1.2.3 Transmitter

The OFDM block diagram is depicted in Fig. 9.4. Similar to IEE 802.15.3c, this ECMA standard takes advantage of a parallel bank of convolutional encoder/decoders. As we stated before, serial implementation of a single convolutional code could be pushing the limits of today's implementation speeds.

9.1.2.4 Preamble

The preamble consists of synchronization and channel estimation fields separated by a cyclic prefix (CP) of 64 samples. The synchronization field is made of seven short symbols (S_s). On the other hand, there are two long symbols (S_{long}) in CES field. Long and short symbols are 512 samples and 256 samples, respectively. Both symbols are specified in frequency domain and are listed in [1].

Ss	Ss	Ss	Ss	Ss	Ss	−Ss	CP	S_{long}	S_{long}

9.1.2.5 Scrambler

It is identical to the one used in A-SCBT mode.

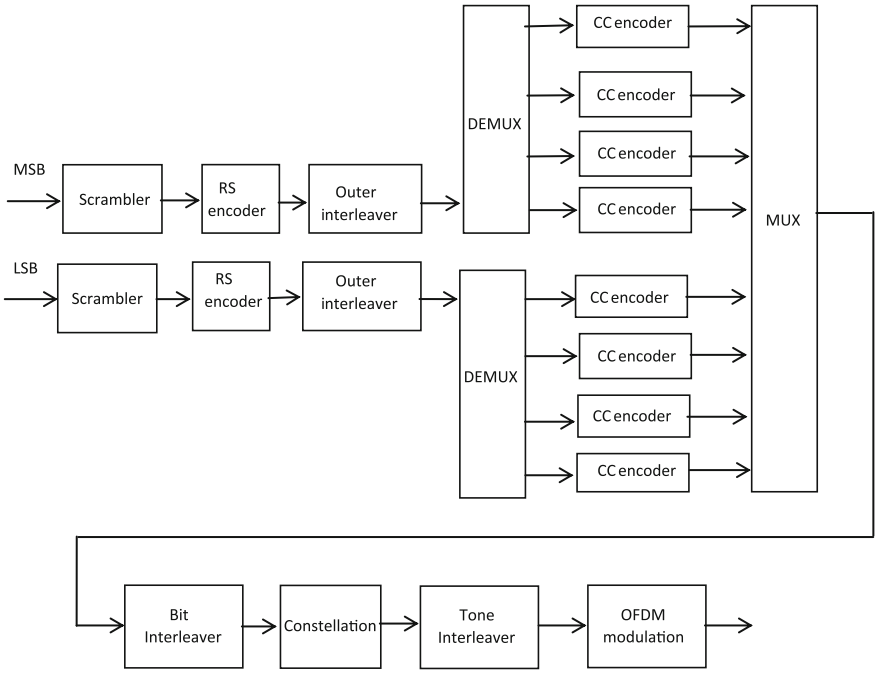

Fig. 9.4 Baseband portion of ECMA 387 OFDM transmitter

9.1.2.6 Outer Interleaver

The outer interleaver is $N_{oi} = 8064$ bits long and the ordering of the bits into the interleaver is defined by x = 0,1,2,…, $N_{oi} - 1$. The ordering of the bits leaving the interleaver is given by

$$Y = \text{prune}(\left[\frac{S(S+1)}{2}\right] \text{mode } P)$$

where $S = 0, 1, 2, \ldots, P, P = 2^{\lceil \log_2 N_{oi} \rceil}$ and *prune*() operation eliminates elements larger than $N_{oi} - 1$.

9.1.2.7 FEC

A concatenated coding scheme is used. The outer and inner codes are RS(255,239) and a convolutional code, respectively. The deployed mother convolutional code is of rate 1/3, has six memory elements ($K = 7$), and is specified by the generator polynomials $g_0 = 133, g_1 = 171,$ and $g_2 = 165$. Through puncturing, rates 4/7, 2/3, and 4/5 are obtained. These convolutional codes are identical to the ones used in IEEE 802.15.3c AV-HRP mode.

9.1.2.8 Bit Interleaver

An interleaver of size 48 bits is deployed and the index of bit stream entering the interleaver is specified by $x = 0,1, 2,\ldots, 47$. Then, the index of bit stream coming out of the interleaver is given by $y = 0,1,2,\ldots, 47$, where

$$y = \left[6\left\lfloor\frac{x}{6}\right\rfloor - 5(x \; mod \; 6)\right] mod \; 48.$$

A different interleaver of size 48 is defined for the UEP mode. The input output relationship is given by

$$y = \begin{bmatrix} 2\left(\left[6\left\lfloor\frac{x}{6}\right\rfloor - 5(x \; mod \; 6)\right] mod \; 24\right) & 0 \le x \le 23 \\ 2\left(\left[6\left\lfloor\frac{x}{6}\right\rfloor - 5(x \; mod \; 6)\right] mod \; 24\right) + 1 & 24 \le x \le 47 \end{bmatrix}$$

9.1.2.9 Tone Interleaver

Within a given OFDM symbol, adjacent symbols are mapped into different subcarriers. The tone interleaver reverses the binary bit order associated with each subcarrier.

9.1.2.10 Antenna Training Sequence

The antenna training sequence consists of N_{TXTS} repetitions of Frank-Zadoff sequences of length 256 to train transmitter antennas followed by N_{RXTS} repetitions of Frank-Zadoff sequences of length 256 to train receiver antennas.

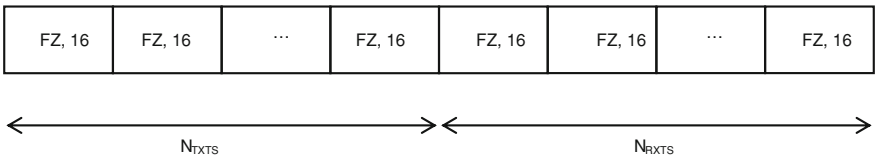

9.1.3 Type B

The modulation/coding attributes of type B system are given in Table 9.6. The last mode was defined in the first edition, but it not part of the second edition.

9.1.3.1 Transmitter

The type B transmitter block diagram for both EEP and UEP are depicted in Fig. 9.5.

Table 9.6 Type B data rates

Data rate (Gbps)	Modulation	FEC	Spreading factor
0.794	DBPSK	RS(255,239)	2
1.588	DBPSK	RS(255,239)	1
3.175	DQPSK	RS(255,239)	1
3.175	UEP-QPSK	RS(255,239)	1
3.175	DAMI	RS(255,239)	1

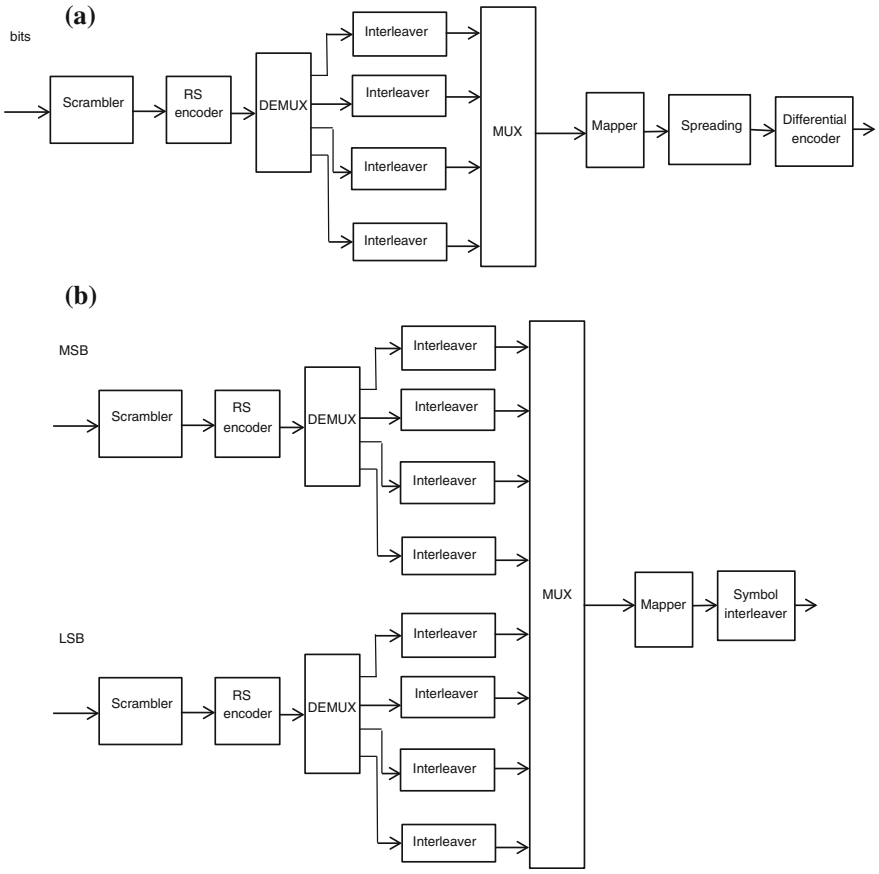

Fig. 9.5 Baseband portion of ECMA 387 type B transmitter. **a** EEP. **b** UEP

Table 9.7 Type B PHY parameters

Parameter	Value
Symbol duration in ns (T_{sym})	0.5787*
Number of data symbols per block (N_D)	252
Number of pilot symbols per block (N_P)	4

* For DAMI mode $T_{sym} = 0.2894$ ns

9.1.3.2 Data Rate

The PHY layer parameters of type B are summarized in Table 9.7. Type B systems are single carrier transmitters. As such, the data rate can be computed as follows:

$$\text{Data Rate} = \frac{252}{256} \times \frac{1}{T_{\text{sym}}} \times \text{FEC rate} \times \text{Number of constellationbits} \times \frac{1}{\text{Spreading factor}}$$

where (252/256) ratio reflects the ratio of data symbols to the total symbols.

Data rate = (252/256) × (1/(0.5787e-9)) × (239/255) × (1/2) ∼ 0.79 Gbps
Data rate = (252/256) × (1/(0.5787e-9)) × (239/255) ∼ 1.58 Gbps
Data rate = (252/256) × (1/(0.5787e-9)) × (239/255) × 2 ∼ 3.19 Gbps
Data rate = (252/256) × (1/(0.2894e-9)) × (239/255) ∼ 3.19 Gbps (DAMI)

9.1.3.3 Preamble

There are eight synchronization symbols and three channel estimation symbols in the preamble as shown below.

Ssync	Ssync	Ssync	Ssync	Ssync	Ssync	Ssync	-Ssync	S_{CES}	S_{CES}	S_{CES}

The synchronization symbol is described as

$$S(n) = S_{FZ,4}(n \bmod 16) S_{FZ,4}\left(\left\lfloor \tfrac{n}{16} \right\rfloor\right) \quad n = 0, 1, \ldots, 255$$

$$S_{\text{sync}}(n) = Re\{S(n)\} + Im\{S(n)\} \quad n = 0, 1, \ldots, 255.$$

where $S_{FZ,4}$ is 16 point Frank-Zadoff sequence.

To find CES symbol, one starts off with a Frank-Zadoff sequence of length 256. If both real and imaginary components are positive or if real part is larger than imaginary part then $S_{CES}(n) = +1$. Otherwise, if both real and imaginary components are negative or if real part is smaller than imaginary part, then $S_{CES}(n) = -1$.

9.1.3.4 Scrambler

It is identical to the one used in type A-SCBT mode.

9.1.3.5 Interleaver

It is identical to the one used in type A-SCBT mode.

9.1.3.6 Spreading

The output index in determined by

$$z(n) = y(\frac{n}{N_{\text{TDS}}})$$

where $y(n)$ is the input data stream and N_{TDS} is the spreading factor.

9.1.3.7 Symbol Interleaver

It is identical to the one used in type A-SCBT mode.

9.1.3.8 Modulation

Signal constellations for both DBPSK and DQPSK are shown in Fig. 9.6. Bits or a pair of bits (in the case of DQPSK) are mapped into constellation points.

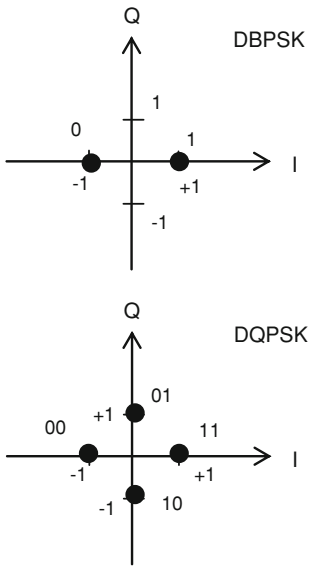

Fig. 9.6 DBPSK and DQPSK constellations

Table 9.8 DAMI encoder table

b(n-2) b(n)	I(n)
00	0
01	1
10	−1
11	0

Fig. 9.7 DAMI constellation

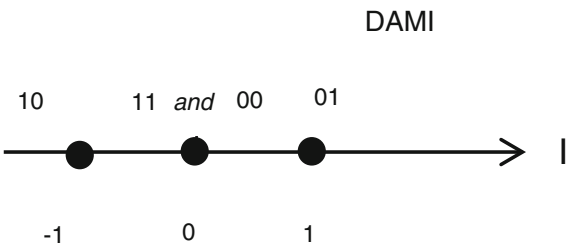

9.1.3.9 DAMI

The encoder table and signal constellation for Dual Alternate Mark Inversion (DAMI) are presented in Table 9.8 and Fig. 9.7, respectively. The two initial bits of the stream can be assumed to be zero. A Reed–Solomon (RS) coding is applied to the bit stream prior to DAMI encoding. The second edition of ECMA standard drops this mode.

9.1.3.10 Emission Mask

The spectral emission mask for types A and B devices of ECMA-387 is provided in Fig. 9.8.

9.1.4 Type C

The main attributes of type C are summarized in Table 9.9.

9.1.4.1 Transmitter

The block diagram representation of type C transmitter is shown in Fig. 9.9.

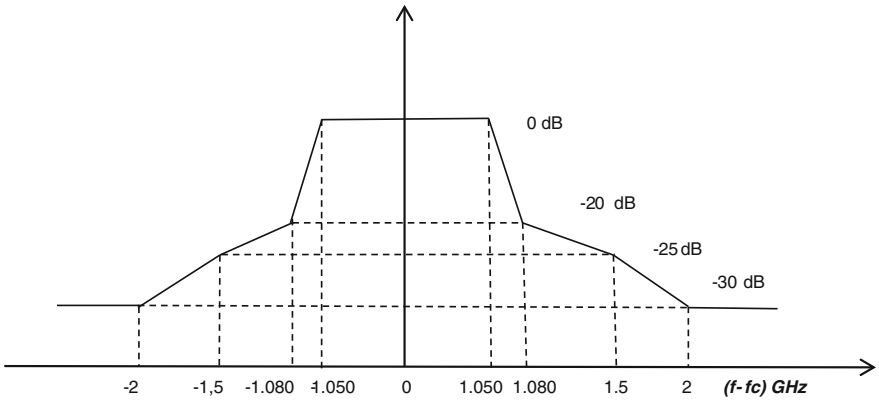

Fig. 9.8 Transmit spectral mask

Table 9.9 Type C data rates

Data Rate (Gbps)	Modulation	FEC	Spreading Factor
0.8	OOK	RS(255,239)	2
1.6	OOK	RS(255,239)	1
3.2	4-ASK	RS(255,239)	1

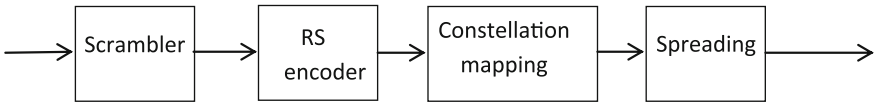

Fig. 9.9 Baseband portion of ECMA 387 type C transmitter

Table 9.10 Type C PHY parameters

Parameter	Value
Symbol duration (T_{sym})	0.5787
Number of data symbols per block (N_D)	508
Number of pilot symbols per block (N_P)	4

9.1.4.2 Data rate

PHY layer parameters for type C are given in Table 9.10. The expression for data rate is given by

$$\text{Data Rate} = \frac{508}{512} \times \frac{1}{T_{sym}} \times \text{ FEC rate } \times \text{ Number of constellationbit}s \times \frac{1}{\text{Spreading factor}}$$

where (508/512) factor reflects the ratio of data symbols to the total symbols.

Data rate = (508/512) × (1/(0.5787e-9)) × (239/255) × (1/2) ∼ 0.8 Gbps
Data rate = (508/512) × (1/(0.5787e-9)) × (239/255) ∼ 1.6 Gbps
Data rate = (508/512) × (1/(0.5787e-9)) × (239/255) × 2 ∼ 3.2 Gbps.

9.1.4.3 Preamble

There synchronization and channel estimation fields are 4096 and 1536 samples long, respectively.

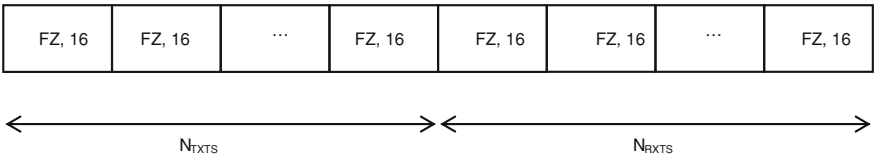

The synchronization content is determined as follows:

$$S(n) = S_{FZ,4}(n \bmod 16) S_{FZ,4}\left(\left\lfloor \frac{n}{16} \right\rfloor\right) \quad n = 0, 1, \ldots, 255$$

$$S_1(n) = Re\{S(n)\} + Im\{S(n)\} \quad n = 0, 1, \ldots, 255.$$

$$S_2(n) = \begin{cases} 1 & S_1(n) < 0 \\ 0 & S_1(n) > 0 \end{cases}$$

$$\bar{S}_2(\mathrm{n}) = 1 - S_2(n)$$

$$\bar{S}_{syn}(n) = \begin{cases} S_2(n \bmod 256) & n = 0, \ldots, 1791 \\ \bar{S}_2(n \bmod 256) & n = 1792, \ldots, 2047 \end{cases}$$

$$S_{syn}(n) = \bar{S}_{syn}\left(\mathrm{floor}\left(\frac{n}{\text{spreading factor}}\right)\right). \quad n = 0, 1, \ldots, 4095$$

To find CES content, one starts off with Frank-Zadoff sequence of length 256. If both real and imaginary components are positive or if real part is larger than imaginary part, then $S_{CES}(n) = +1$. Otherwise, if both real and imaginary components are negative or if real part is smaller than imaginary part, then $S_{CES}(n) = -1$. The resulting sequence is denoted by $S_C(n)$. Then

$$S_{C1}(n) = (S_C(n) + 1)/2$$

$$S_{C2}(n) = (-S_C(n) + 1)/2$$

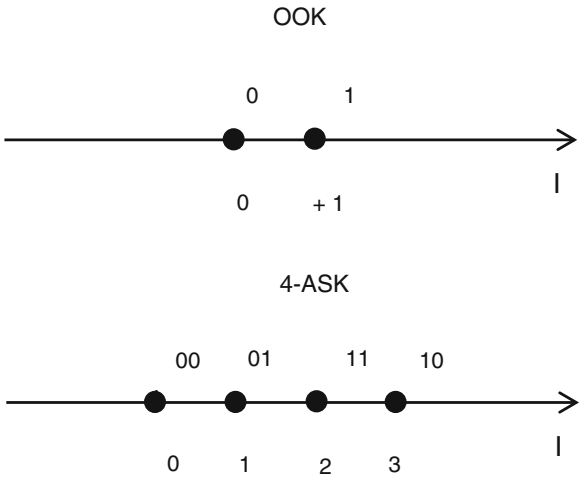

Fig. 9.10 OOK and 4-ASK constellations

$$\bar{S}(n) = \begin{cases} S_{C1}(n \bmod 256) & n = 0, \ldots, 255 \, and \, 512, \ldots, 767 \\ S_{C2}(n \bmod 256) & n = 256, \ldots, 511 \end{cases}$$

$$S_{CES}(n) = \bar{S}_n\left(\text{floor}\left(\frac{n}{\text{spreading factor}}\right)\right). \quad n = 0, 1, \ldots, 1535$$

9.1.4.4 Modulation

Both OOK and 4-ASK are essentially one-dimensional signal constellations as depicted in Fig. 9.10.

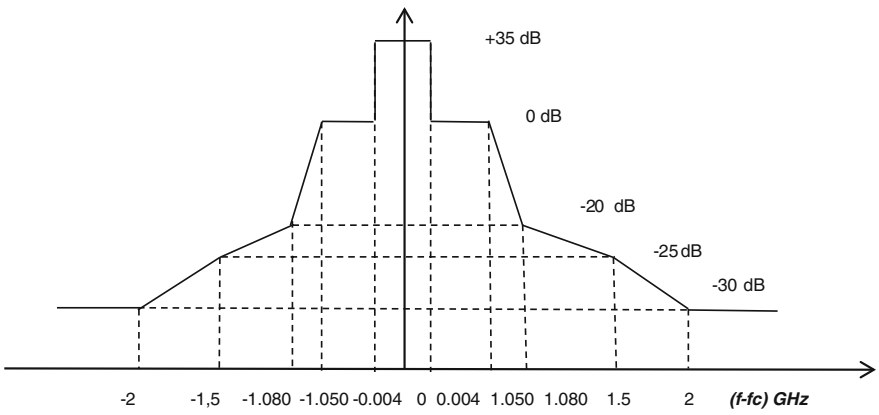

Fig. 9.11 Transmit spectral mask

Table 9.11 HRP data rates

Data rate (Gbps)	Modulation	FEC (inner code)	FEC (outer code)	Protection type
0.952	OFDM/QPSK	1/3	RS (224,216)	EEP
1.904	OFDM/QPSK	2/3	RS (224,216)	EEP
3.807	OFDM/16-QAM	2/3	RS (224,216)	EEP
1.904	OFDM/QPSK	4/7 4/5	RS (224,216)	UEP
3.807	OFDM/16-QAM	4/7 4/5	RS (224,216)	UEP
1.904	OFDM/QPSK	2/3	RS (224,216)	UEP
3.807	OFDM/16-QAM	2/3	RS (224,216)	UEP
0.952	OFDM/QPSK	1/3	RS (224,216)	MSB only Trans
1.904	OFDM/QPSK	2/3	RS (224,216)	MSB only Trans
1.428	OFDM/QPSK	1/2	RS (224,216)	EEP
2.379	OFDM/QPSK	5/6	RS (224,216)	EEP
2.855	OFDM/16-QAM	1/2	RS (224,216)	EEP
4.759	OFDM/16-QAM	5/6	RS (224,216)	EEP
5.711	OFDM/64-QAM	2/3	RS (224,216)	EEP
7.138	OFDM/64-QAM	5/6	RS (224,216)	EEP
1.428	OFDM/QPSK	2/5 2/3	RS (224,216)	UEP
2.855	OFDM/16-QAM	2/5 2/3	RS (224,216)	UEP
5.711	OFDM/64-QAM	4/7 4/5	RS (224,216)	UEP
1.428	OFDM/QPSK	1/2	RS (224,216)	UEP
2.855	OFDM/16-QAM	1/2	RS (224,216)	UEP
5.711	OFDM/64-QAM	2/3	RS (224,216)	UEP

9.1.4.5 Scrambler

It is identical to the one used in type A devices.

9.1.4.6 Spreading

It is identical to the one used in type B devices.

9.1.4.7 Emission Mask

The spectral emission mask for types C devices of ECMA 387 is provided below in Fig. 9.11.

Table 9.12 MRP data rates

Data rate (Gbps)	Modulation	FEC (inner code)	FEC (outer code)	Protection type
0.476	OFDM/QPSK	1/3	RS (224,216)	EEP
0.952	OFDM/QPSK	2/3	RS (224,216)	EEP
1.904	OFDM/16-QAM	2/3	RS (224,216)	EEP
0.952	OFDM/QPSK	4/7 4/5	RS (224,216)	UEP
1.904	OFDM/16-QAM	4/7 4/5	RS (224,216)	UEP
0.952	OFDM/QPSK	2/3	RS (224,216)	UEP
1.904	OFDM/16-QAM	2/3	RS (224,216)	UEP
0.476	OFDM/QPSK	1/3	RS (224,216)	MSB only Trans
0.952	OFDM/QPSK	2/3	RS (224,216)	MSB only Trans
0.714	OFDM/QPSK	1/2	RS (224,216)	EEP
1.190	OFDM/QPSK	5/6	RS (224,216)	EEP
1.428	OFDM/16-QAM	1/2	RS (224,216)	EEP
0.714	OFDM/QPSK	2/5 2/3	RS (224,216)	UEP
1.428	OFDM/16-QAM	2/5 2/3	RS (224,216)	UEP
0.714	OFDM/QPSK	1/2	RS (224,216)	UEP
1.428	OFDM/16-QAM	1/2	RS (224,216)	UEP

9.2 WiGig [9]

The alliance, founded in 2009, develops and promotes specifications for wireless air interface in 60 GHz band. The Board of directors consist of AMD, Broadcom, Dell, Huawei, Marvell, MediaTek, Cisco, Intel, Microsoft, Samsung, Toshiba, and Wilocity.

Similar to IEEE 802.15.3c and ECMA 387, WiGig alliance spec offers single carrier and OFDM modulation options for low power/low cost and higher speed communications, respectively [6]. While OFDM supports data rates up to 7 Gbps, single carrier modulation throughput is limited to 4.6 Gbps. Both modulations use the same preamble and channel coding scheme. The 802.11b/g/n/ac/ad PHY are incorporated into WiGig. Lower MAC is similar to that of 802.11b/g/n/ac/ad. Upper MAC is devised to enable multi-band operation. A number of protocol adaptation layers (PALs) such as IP, WiGig Display Extension (WDE), WiGig Bus Extension (WBE), and WiGig Serial Extension (WSE) are also defined for WiGig.

WiGig envisions tri-band devices supporting seamless operation among 2.4, 5, and 60 GHz. It enables far faster speeds compared to WiFi devices. In the absence of 60 GHz availability, the WiGig capable device will switch to lower (2.4 or 5 GHz WiFi) frequencies. Certification of tri-band devices requires the cooperation of both WiGig and WiFi. As per a cooperation agreement established in May

Table 9.13 LRP data rates

Omni data rate (Mbps)	Beam formed data rate (Mbps)	Modulation	FEC (inner code)	Omni repetition	Beam formed repetition
2.542	20.337	OFDM/BPSK	1/3	8x	1x
3.813	30.505	OFDM/BPSK	1/2	8x	1x
5.084	40.673	OFDM/BPSK	2/3	8x	1x
10.168	NA	OFDM/BPSK	2/3	4x	NA

Table 9.14 General parameters for the three modes

Parameter	LRP	MRP	HRP
Bandwidth	92 MHz	890 MHz	1.76 GHz
Reference sampling rate	317.25 Msamples/s	1.269 Gsamples/s	2.538 Gsamples/s
Number of subcarriers	128	256	512
FFT period	403.47 ns	201.73 ns	201.73 ns
Subcarrier spacing	2.4785 MHz	4.957 MHz	4.957 MHz
Guard interval	88.26 ns	25.22 ns	25.22 ns
Symbol duration	491.73 ns	226.95 ns	226.95 ns
Number of data subcarriers	30	168	336
Number of DC subcarriers	3	3	3
Number of pilots	4	8	16
Number of null subcarriers	91	77	157

2010, next generation WiFi alliance certification program will be jointly set up by WiFi and WiGig alliances [10]. However, it appears that WiGig alliance will eventually be absorbed by WiFi.

9.3 WirelessHD [7]

WirelessHD is a consortium of 40 companies including Broadcom, Intel, LG, Panasonic, NEC, Samsung, SiBEAM, Sony, Philips, and Toshiba. The consortium develops wireless digital interface for 60 GHz band. The first version of the spec, published in 2008, combines HD signal, multichannel audio, and control signals. The physical layer of the WirelessHD is very similar to the AV option in the IEEE 802.15.3c spec. Other features of the technology are support for smart antennas, QoS and secure communications through the use of DTCP (Digital Transmission Content Protection). The first and second generation spec support data rates up to 4 Gbps and 7 Gbps, respectively. Standard's theoretical data rate is, however, 25 Gbps. The latest version of the spec, version 1.1, was released in May 2010. The new features in 1.1 release include:

– Support for 3D frame video
– Support for 4 k (four times the HD resolution)
– Refresh rates up to 240 Hz,

– Increased HRP data rates rates up to 7.1 Gbps,
– A low power medium rate PHY,
– Additional LRP rates.

The HRP (High Rate PHY), MRP (Medium Rate PHY), and LRP (Low Rate PHY), both omni and beam formed, data rate details are provided in Tables 9.11, 9.12, 9.13. The general parameters for each PHY are listed in Table 9.14.

What We Learned

- Type A-SCBT of ECMA 387:Modulation, coding, data rates, scrambler, bit/symbol interleaver, transmitter block diagram, preamble structure, channel bonding;
- Type A-OFDM of ECMA 387:Modulation, coding, data rates, scrambler, bit/tone interleaver, transmitter block diagram, preamble structure, channel bonding;
- Type B of ECMA 387:Modulation, data rates, spreader, scrambler, bit/tone interleaver, transmitter block diagram, preamble structure, DAMI and emission mask;
- Type C of ECMA 387:Modulation, data rates, spreader, scrambler, transmitter block diagram, preamble structure, and the emission mask
- WiGig and WirelessHD

Simulation Project

1. Simulate the BER performance of ECMA 387 A-OFDM option in AWGN as well as in CM1 channel. Operate in channel 1 of the band plan and select the lowest data rate. Determine PAPR of the transmitted signal.

References

1. European Computer Manufacturing Association, High Rate 60 GHz PHY, MAC, and HDMI PAL, Standard ECMA-387, 1st edn. December (2008), [online] Available at: http://www.ecma-international.org. Accessed 26 Dec 2010
2. European Computer Manufacturing Association, High Rate 60 GHz PHY, MAC, and PALs, Standard ECMA-387, 2nd edn. December (2010), [online] Available at: http://www.ecma-international.org. Accessed 8 May 2011
3. [online] Available at: http://en.wikipedia.org/wiki/Wireless_Gigabit_Alliance. Accessed 26 Dec 2010
4. [online] Available at: http://www.prnewswire.com/news-release/wi-fi-alliancer-and-wigigtm-alliance-to-cooperate-on-expansion-of-wi-fi-technologies-93250859.html. Accessed 26 Dec 2010
5. WiGig White Paper, Defining the Future of Multi-Gigabit Wireless Communications, July (2010), [online] Available at: http://wirelessgigabitalliance.org/specifications/. Accessed 26 Dec 2010
6. [online] Available at: http://en.wikipedia.org/wiki/WirelessHD. Accessed 26 Dec 2010
7. [online] Available at: http://www.wirelesshd.org/. Accessed 26 Dec 2010

Index

S. Emami, *UWB Communication Systems: Conventional and 60 GHz*,
DOI: 10.1007/978-1-4614-6753-3,